universität wien

DISSERTATION / DOCTORAL THESIS

Titel der Dissertation / Title of the Doctoral Thesis

Gupta–Bleuler Quantization of the Electromagnetic Field in Curved Space-Times with Applications to Gravitational Photon Interferometry

verfasst von / submitted by

Thomas B. Mieling

angestrebter akademischer Grad / in partial fulfilment of the requirements for the degree of

Doktor der Naturwissenschaften (Dr. rer. nat.)

Wien, 2023 / Vienna, 2023

Studienkennzahl laut Studienblatt / degree programme code as it appears on the student record sheet	UA 796 605 411
Studienrichtung laut Studienblatt / degree programme as it appears on the student record sheet	Physik
Betreut von / Supervisor	Univ.-Prof. Piotr T. Chruściel, MSc PhD Univ.-Prof. Dipl.-Ing. Dr. Philip Walther

Abstract

Unlike Newton's theory of gravitation, Einstein's theory of general relativity predicts that Earth's gravitational field induces phase shifts not only in massive particles but also in single photons. Whereas gravitationally induced interference in massive particles has been demonstrated multiple times, experiments have yet to reach the sensitivities required to measure the analogous effect on light. While the GRAVITES project aims to demonstrate this effect in an optical fiber interferometer in the coming years, rigorous theoretical models of such experiments are still lacking.

Despite the fact that quantum field theory in curved space-times is a fully developed theoretical framework, previous descriptions of such effects of gravity on single photons have relied mainly on hybrid models combining the theory of quantum optics in flat space-time with semi-classical models of light propagation in curved space-times. This thesis develops a comprehensive theory of quantum optics in curved space-times, superseding these simplified models, and demonstrates its capability of modeling experiments on gravitational effects in single-photon interferometry.

Specifically, this thesis introduces a set of gauge-fixed Maxwell equations modeling light propagation in dielectrics that are located in an arbitrarily curved space-time. For stationary gravitational fields, a Gupta–Bleuler quantization scheme, based on these equations, is developed using the algebraic formulation of quantum field theory. Explicit solutions to the field equations are then obtained for arbitrarily curved step-index optical fibers in arbitrary stationary gravitational fields using a perturbative multiscale method. The combination of these results yields a consistent description of the interference of single photons and pairs of entangled photons in non-inertial systems that takes into account, in particular, the rotation and gravity of Earth.

Whereas previous work on this subject was limited to weak gravity and a small class of optical fiber geometries, the model developed here applies to arbitrarily strong gravitational fields and allows for arbitrary fiber geometries. The GRAVITES experiment is planned to test the predictions made here, thus performing the first test of quantum field theory in curved space-times on the laboratory scale.

Zusammenfassung

Im Gegensatz zur Newtonschen Gravitationstheorie sagt Einsteins allgemeine Relativitätstheorie vorher, dass das Schwerefeld der Erde nicht nur Phasenschübe in massiven Teilchen, sondern auch in Photonen hervorruft. Gravitative Phasenschübe in der Interferenz massiver Teilchen wurden bereits mehrfach nachgewiesen, doch haben Experimente bisher nicht die nötige Empfindlichkeit erreicht, um den entsprechenden Einfluss auf Licht zu messen. Während das GRAVITES-Projekt plant, diesen Effekt in den kommenden Jahren mit optischen Faserinterferometern nachzuweisen, sind rigorose theoretische Modelle solcher Experimente nach wie vor ausständig.

Obwohl die Quantenfeldtheorie in krummen Raumzeiten vollständig entwickelt ist, wurde der Einfluss des Gravitationsfeldes auf einzelne Photonen bisher meist mit Hybridmodellen beschrieben, die den Formalismus der Quantenoptik in der flachen Raumzeit mit semiklassischen Modellen für Lichtausbreitung in krummen Raumzeiten kombinieren. In dieser Arbeit wird anstelle vereinfachter Modelle eine umfassende Theorie der Quantenoptik in krummen Raumzeiten entwickelt und ihre Fähigkeit demonstriert, Experimente zum Nachweis von gravitativen Effekten in der Interferenz einzelner Photonen zu modellieren.

Konkret werden in dieser Arbeit eichfixierte Maxwell-Gleichungen aufgestellt, welche die Lichtausbreitung in Dielektrika modellieren, die sich in beliebig gekrümmten Raumzeiten befinden. Für stationäre Gravitationsfelder wird mithilfe dieser Gleichungen ein Gupta–Bleuler-Quantisierungsschema entwickelt, das auf der algebraischen Formulierung der Quantenfeldtheorie beruht. Anschließend werden mit einer störungstheoretischen Mehrskalenmethode explizite Lösungen der Feldgleichungen für beliebig gekrümmte optische Stufenindexfasern in beliebigen stationären Gravitationsfeldern ermittelt. Aus der Kombination dieser Ergebnisse ergibt sich eine konsistente Beschreibung der Interferenz einzelner Photonen und verschränkter Photonenpaare in Nicht-Inertialsystemen unter Berücksichtigung der Rotation und Gravitation der Erde.

Während bisherige Arbeiten zu diesem Thema auf schwache Gravitationsfelder und eine geringe Anzahl an Fasergeometrien beschränkt war, ist das hier entwickelte Modell auch bei starken Gravitationsfeldern gültig und lässt gleichzeitig beliebige Fasergeometrien zu. Das GRAVITES-Experiment soll die hier getätigten Vorhersagen überprüfen und damit den ersten Labortest der Quantenfeldtheorie in krummen Raumzeiten durchführen.

Contents

Chapter 1

Introduction

This thesis is concerned with the formulation of a theory of gravitational quantum optics. More specifically, it extends the standard theory of quantum optics to include effects of gravity, as described by the general theory of relativity, using methods of quantum field theory in curved space-times, with the specific aim of providing a comprehensive model of future experiments on the influence of gravity on single photons.

Both the theory of general relativity and quantum theory provide well-established frameworks for describing experiments at large and small scales, respectively. However, experimental tests of their interplay are still lacking: to date, no experiment has been realized that requires for the theoretical explanation of its observations both general relativity and quantum theory in the sense of not being otherwise explicable using either a model based on quantum mechanics in a Newtonian gravitational field or classical physics in curved space-time [1–5].

Even though some experimental tests of general relativity used quantum systems in their measurement schemes and experiments on gravitational effects in quantum systems can be explained by theories of quantum physics in curved space-times, the hitherto-conducted experiments are generally not regarded as directly testing the interplay of quantum theory and general relativity [2; 6; 7].

On the one hand, classical tests of general relativity, in particular those concerned with the gravitational redshift, commonly used quantum-mechanical effects in their measurement or detection schemes. However, the systems being measured did not exhibit quantum phenomena without which the experimental result would be inexplicable [2]. For example, the Pound–Rebka experiment measured the gravitational redshift of γ-rays emitted in the process of radioactive decay of ^{57}Co to ^{57}Fe [8] and relied on the Mössbauer effect to obtain recoil-free emission and absorption of the photons whose redshift was being measured [9; 10]. Despite making use of such quantum-mechanical processes, the Pound–Rebka experiment is not considered a test of the interface of quantum physics and general relativity since the primary observable, the redshift occurring in the emission and absorption of electromagnetic radiation at different altitudes, does not require quantum-mechanical properties of the electromagnetic field for its explanation. Similarly, large-scale experiments

on the gravitational redshift using either the *Gravity Probe A* satellite [11–13] or *Galileo* satellites on elliptical orbits [14] relied on optical clocks as frequency standards but did not demonstrate quantum interference that is sensitive to the gravitational redshift [2, Sect. 5.1].

On the other hand, experiments have demonstrated gravitationally induced phase shifts in the quantum interference of massive particles. The first experiment of this kind was carried out by Colella, Overhauser, and Werner, and demonstrated a phase shift imprinted by Earth's gravitational field on single neutrons as they traversed a Mach–Zehnder interferometer that could be rotated as to vary the height difference, and thus the difference in gravitational potential, between its two interferometer arms [15]. Whereas this experiment and its many successors, see, e.g., Ref. [16] and references therein, demonstrate signatures of quantum physics and gravity simultaneously, the gravitational aspects of these experiments do not require general relativity for their explanation. Even though these experiments can be explained in the framework of general relativity or, more generally, by metric theories of gravity in the weak-field regime, they can also be explained using the Schrödinger equation for non-relativistic particles, coupled to a Newtonian gravitational potential [2; 17; 18]. For this reason, they are generally not regarded as experiments testing the interplay of quantum theory and general relativity either.

This state of affairs has inspired searches for new experimental setups that could directly test the interplay of quantum theory and general relativity. Different mechanisms that could shed light on this issue have been identified: (i) gravitationally induced phase shifts in single-photon or multi-photon interferometry [19–22], (ii) gravitationally induced decoherence in quantum interferometry [23; 24], and (iii) gravitationally mediated entanglement of massive particles [25; 26]. Experiments of type (i) provide an advantage over the aforementioned interference experiments of massive particles since the fact that photons are massless rules out any Newtonian model of such experiments [27, p. 60]. Moreover, using multi-photon states that exhibit non-classical detection statistics, one can construct setups where both general relativity and quantum theory are necessary to explain the expected interference signals. Whereas the quantum aspect of such experiments mainly consists of effects arising from the deviation of quantum statistics from classical statistics, experiments of type (ii) could provide further insights into the interplay of gravity and quantum physics by testing how the dynamics of external degrees of freedom of a particle influence the rate of evolution in its internal degrees of freedom. Furthermore, experiments of type (iii) on gravitationally mediated entanglement could provide information about possible quantum theories of gravity [28–30].

At the time of writing, only experiments of type (i), i.e., photon interferometry in which the interferometric phase shift is induced by Earth's gravitational field, appear to be feasible with present-day technology [4; 7; 19; 31]. The GRAVITES project at the University of Vienna aims to realize such an experiment. Feasibility studies of alternative experimental setups with similar aims can be found in Refs. [32–34].

A schematic drawing of the GRAVITES setup is shown in Fig. 1.1. The basic scheme is as

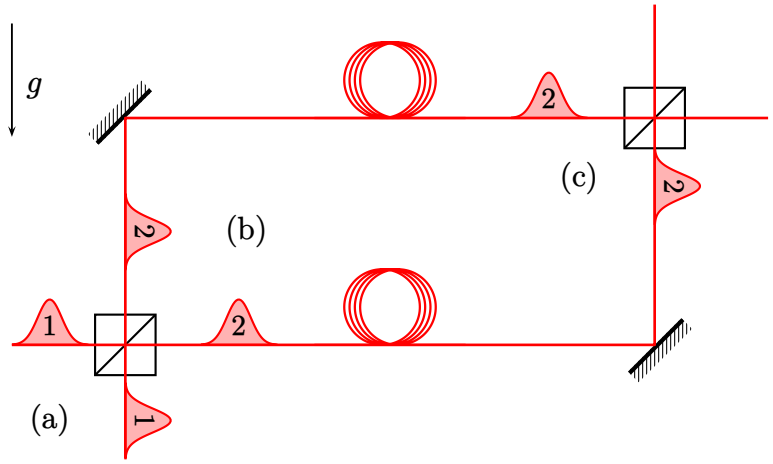

Figure 1.1: Schematic drawing of gravitationally induced interference of path-entangled two-photon states in a Mach–Zehnder interferometer. The insets in the Gaussian wave packets indicate the photon occupation numbers: two indistinguishable photons are sent into the two inputs of the first beam splitter (a) where the Hong–Ou–Mandel effect leads to the generation of an entangled two-photon state (b). This state acquires twice the single-photon phase shift, thus producing non-classical output probabilities at the second beam splitter (c).

follows: by sending two indistinguishable photons into separate input ports of a symmetric beam-splitter (a), the Hong–Ou–Mandel effect causes photons to "bunch," i.e., the two photons always exit the beam-splitter at identical output ports. This means that both photons either enter the lower interferometer arm or both enter the upper arm, but never is any interferometer arm occupied by a single photon (b). The difference in gravitational potentials between the two interferometer arms then induces a phase shift on the photons, and, as a calculation shows, the relative phase shift in the two-photon state is twice as large as that for a single-photon state or classical light rays (c). At the second beam splitter, the output probabilities of the photons depend on the quantum phase shift accumulated in the interferometer.

The interference pattern obtained by measuring these output probabilities for various values of the height difference between the two interferometer arms then demonstrates signatures of general relativity and quantum physics simultaneously: the general-relativistic aspect is that metric theories of gravity predict an influence of Earth's gravitational field on light that is absent in Newtonian gravity, and the quantum-mechanical aspect is that the expected fringe frequency of two-photon states is twice as large as that for classical light. For comparison: an analogous experiment involving non-relativistic massive particles would be explicable using quantum mechanics coupled to Newtonian gravity, and if one were to perform an analogous experiment with single photons instead of pairs of entangled photons, then the output statistics at the second beam splitter would follow a pattern indistinguishable from that corresponding to the intensities of classical light pulses propagating through the interferometer.

1.1 Previous Theoretical Models

So far, experimental proposals on gravitational photon interferometry were analyzed using a variety of models that can be distinguished by their description of light propagation (ray optics, scalar optics, or wave optics) and their description of quantum properties of light (classical theory, semi-classical theory, or quantum field theory), cf. Table 1.1. All such models are restricted to weak gravitational fields and are thus based on perturbative schemes.

	Classical theory	Semi-classical theory	Quantum field theory
Ray optics	Refs. [20; 35–37]	Refs. [2; 21; 38; 39]	Ref. [5]
Scalar optics			Refs. [22; 40–45]
Wave optics			Ref. [46]
Fiber optics	Refs. [47; 48]	Ref. [4]	Ref. [49]

Table 1.1: Overview of theoretical models of gravitational effects in the interferometry of light, all of which are restricted to linearized gravity.

Ray-Optics Models In ray-optics models, gravitational effects on light propagation are studied using methods of geometrical optics [2; 5; 20; 21; 35–39]. As such models describe the influence of gravity on classical light rays, further considerations are necessary to infer the effect of gravity on single photons. Despite identifying light rays with world-lines of photons, Refs. [20; 35–37] did not embed their results into a quantum-theoretical framework, as can be seen, e.g., by noting that none of the referenced papers give explicit formulas for photon detection probabilities. The connection between classical and quantum phase shifts was studied in more detail in Refs. [2; 21; 38; 39]. These articles, however, relied on semi-classical models in which the quantum-mechanical aspects of photon interference were described in a framework closely resembling that of quantum mechanics or quantum optics in flat space-time: Contrary to studies based on quantum field theory in curved space-time (discussed below), these models did not relate the inner products of quantum states to relativistic products of classical solutions in curved space-time manifolds. Instead, the models can be regarded as ad-hoc modifications of quantum optics in flat space-time to incorporate gravitational phase shifts. Such ad-hoc corrections to non-gravitational theories are, however, insufficient for providing logically consistent theoretical models as they generally cannot ensure the corrections to be complete and independent in the sense of Ref. [50], which criticized analogous modifications of the non-relativistic Schrödinger equation for massive particles to account for relativistic effects. Similar criticism of describing the gravitational redshift on light by introducing ad-hoc corrections into non-relativistic equations, such as ascribing an "effective gravitational mass" to photons, as was done, i.a., in Refs. [2; 27, Sect. 5.3], was raised in Ref. [51]. A more consistent method of using ray-optics results in the framework of quantum field theory in curved space-times was developed in Ref. [5] by extending the optical phases along single light rays to eikonal

functions of approximately plane waves. The resulting theory can be regarded as a high-frequency limit of scalar-optics models, which are discussed below. Although presenting a more rigorous quantization scheme, the analysis in Ref. [5] is not fully consistent as the mathematical model developed there is applied to light propagation in optical fibers despite being based on the massless Klein–Gordon equation that describes wave propagation in free space.

Scalar-Optics Models Models of quantum interferometry in Earth's gravitational field that are based on the principles of quantum field theory in curved space-times were developed in Refs. [22; 40–45]. These articles, however, did not quantize the full electromagnetic field but rather considered a massless scalar field to simplify the model. In particular, all aforementioned papers except for Ref. [22] studied the massless Klein–Gordon equation and were thus limited to describing light propagation in vacuo. Ref. [22], on the other hand, allowed for light propagation in dielectric materials, such as optical fibers, by formulating a wave equation based on Gordon's optical metric [52]. However, all such models fall short of accurately describing future experiments on gravitational photon interferometry since the scalar field equation is insufficient for describing optical fiber modes even in flat space-time. Instead, consistent descriptions of fiber optics in a gravitational field must take the tensorial character of the electromagnetic field into account.

Wave-Optics Models Compared to models based on ray optics or scalar optics, wave-optics descriptions of light propagation in external gravitational fields are based on Maxwell's equations in curved space-times. As the latter constitute tensorial partial differential equations, their analysis is more involved than that of ray-optics or scalar-optics models. The first analysis of Maxwell's equations for optical fibers in a weak gravitational field was provided in Ref. [47], where the gravitationally induced phase shift was inferred from the wave equation satisfied by the longitudinal component of the electric and magnetic fields. This result was later confirmed by a more comprehensive analysis that computed all components of the electromagnetic field in such fibers [48]. However, both these papers restricted the discussion to classical considerations and did not consider quantum properties of the electromagnetic field. The results of Ref. [48] were used in Ref. [4, Chap. 9] to model the GRAVITES experiment at the single-photon level using the formalism of quantum optics in flat space-time with the gravitational phase shift inserted where found appropriate. Such methods, however, are subject to the same criticism as the semi-classical ray-optics models discussed above. The necessity of describing gravitational photon interferometry experiments using models based, instead, on quantization schemes for Maxwell's equations in curved space-times was recognized in Ref. [46]. However, the model developed there is limited to electromagnetic plane waves in free space and is thus not applicable to fiber optics. A quantum theory of electromagnetic fiber modes in weak gravitational fields was developed by the present author in Ref. [49]. However, whereas ray-optics models allow for light propagation along arbitrary spatial trajectories (which can be realized by

sending light through arbitrarily bent optical fibers), the wave-optics models in Ref. [49] and Ref. [48] are limited to straight optical fibers at a constant gravitational potential or specially aligned fiber spools, respectively. This limits the applicability of such models to concrete experimental setups as the fiber geometries used there do not fall within this limited class.

1.2 This Work

To overcome the aforementioned shortcomings of previous theoretical models for photon interferometry in external gravitational fields, this thesis develops a comprehensive model of gravitational quantum optics that is based on the general framework of quantum field theory in curved space-times. Specifically, this model describes gravitational effects on light propagation in optical fibers and thus applies to current experimental proposals for demonstrating gravitationally induced phase shifts in photon interferometry, which rely on such waveguides to achieve sufficiently long interaction times of light with Earth's gravitational field.

The main two results of this thesis are the following: First, a general quantization scheme for the electromagnetic field is developed that takes into account both dielectric properties of optical fibers (in particular, allowing for discontinuous refractive indices in order to model commonly used step-index fibers) and external gravitational fields (which are assumed to be stationary). Second, a perturbative scheme for solving the field equations of this theory is developed that allows for a complete and systematic description of gravitational effects in fiber optics. This leads to an explicit formula for the optical phase shifts caused by the gravitational redshift and the Sagnac effect, which is valid for arbitrarily bent optical fibers in arbitrary stationary gravitational fields. Additionally, a transport law for the polarization of light in such fibers is derived. This leads to concrete predictions for future experiments on gravitational photon interferometry. Contrary to previous work on this subject, the present methods are not limited to weak gravitational fields. Instead, the main results apply to arbitrary stationary gravitational fields.

The results of this thesis thus improve upon previous theoretical models of gravitational photon experiments in the following aspects:

- The field equations considered here account both for dielectric media (with potentially discontinuous permeability and permittivity functions) and arbitrary gravitational fields that need not be weak, nor satisfy Einstein's field equations.

- The quantization scheme developed here applies to all strictly stationary configurations, i.e., to space-times admitting a time-like Killing vector field and dielectrics whose four-velocity is proportional to that Killing field and whose electromagnetic properties do not change in time. In particular, the scheme is not restricted to static configurations where the Killing vector field is hypersurface-orthogonal.

- As the quantization scheme used here is based on the algebraic approach to quantum field theory, it does not require the computation of the full spectrum of the field equations, as was the case in previous models that used formal mode expansions of quantum field operators.
- Finally, the model developed here directly applies to future experiments on fiber optics in Earth's gravitational field at the single-photon level without relying on heuristics to relate phase shifts computed from ray-optics or scalar-wave optics to those arising from Maxwell's equations, or ad-hoc insertions of gravitational correction terms into the formalism of quantum optics in flat space-time.

1.3 Outline

Chapter 2 describes the general framework of metric theories of gravity with emphasis on the description of Earth's gravitational field in earthbound coordinate systems.

Chapter 3 introduces classical formulations of optics in curved space-time, based both on geometrical optics and wave optics. The latter subject is described both at the level of field strengths and at the level of the electromagnetic potential. As the time evolution of the potential is not fully determined by Maxwell's equations, gauge-fixed equations are needed to describe the propagation of light in this framework. Here, this is done using a new generalization of the Lorenz gauge to linear isotropic dielectrics that provides consistent equations even for discontinuous refractive indices (which arise, for example, in step-index optical fibers).

A quantization scheme of these gauge-fixed equations is described in Chapter 4. This scheme is formulated within the framework of algebraic quantum field theory and based on the Gupta–Bleuler quantization method. In this way, one obtains a quantum theory of electromagnetic radiation that applies to general linear isotropic dielectrics (in particular, optical fibers) and general stationary gravitational fields without relying on approximation methods.

Explicit perturbative solutions to the gauge-fixed field equations for optical fibers in a gravitational field are derived in Chapter 5. The perturbative scheme is based on the multiple-scales method and applies whenever the characteristic length scales of the fiber bending and the external gravitational field far exceed the wavelength of light propagating inside the fiber. For physically plausible setups, this assumption constitutes no significant restriction to the range of applicability of the perturbative solution derived here.

Chapter 6 combines the results of the previous sections to provide a consistent description of photon interferometry in non-inertial systems. This yields explicit predictions for single-photon and multi-photon interferometry that is sensitive to Earth's rotation (Sagnac effect) and its gravitational field (gravitational redshift).

Chapter 7 concludes with a summary of the main results and an outlook on open questions in the context of this work.

Chapter 2

Gravitation

To model gravitational effects on light propagation, one is required to formulate a model of the gravitational field. This chapter describes the basic tools needed for that purpose within the framework of metric theories of gravity, where the gravitational field is described in the language of space-time geometry. As experiments are commonly interpreted in a language that treats space and time as separate concepts, Sections 2.2 and 2.3 describe the relations between space-time geometry (as a whole) and geometric aspects of space and time (considered separately). Section 2.4 describes concrete models for the gravitational field, based on Einstein's field equations and the parameterized post-Newtonian formalism. Finally, Sections 2.5 and 2.6 discuss the concrete form of the metric tensor in such models when expressed in coordinates adapted to laboratories on Earth's surface, as will be considered in later chapters.

2.1 Metric Theories of Gravitation

Since the development of Einstein's theory of gravity, the gravitational field is modeled by a Lorentzian metric ${}^{(4)}g_{\mu\nu}$ on a four-dimensional manifold $\mathscr{M}$. A motivation for modeling gravity using metric theories, starting from Einstein's equivalence principle, can be found, e.g., in Ref. [53, Sect. 2.2].

Any such space-time metric ${}^{(4)}g_{\mu\nu}$ gives rise to various derived mathematical quantities, such as the Levi-Civita covariant derivative ${}^{(4)}\nabla_\mu$, the Riemann curvature tensor ${}^{(4)}R^\mu{}_{\nu\rho\sigma}$, the Ricci curvature tensor ${}^{(4)}R_{\mu\nu} = {}^{(4)}R^\sigma{}_{\mu\sigma\nu}$, and the Ricci curvature scalar ${}^{(4)}R = {}^{(4)}R^\mu{}_\mu$. These quantities are essential to the mathematical study of gravitational fields.

The gravitational aspects of matter are described by a stress-energy-momentum tensor $T^{\mu\nu}$ that is required to be symmetric, $T^{\mu\nu} = T^{\nu\mu}$, and divergence-free, ${}^{(4)}\nabla_\mu T^{\mu\nu} = 0$. The precise details of the tensor $T^{\mu\nu}$ depend on the matter model under consideration. For the present purposes, however, no concrete matter model is needed, as only general properties of $T^{\mu\nu}$ will be used.

The paradigmatic example of this kind of gravitational theory is Einstein's theory of

general relativity, in which ${}^{(4)}g_{\mu\nu}$ is assumed to satisfy Einstein's field equation

$$ {}^{(4)}R_{\mu\nu} - \tfrac{1}{2}{}^{(4)}R\,{}^{(4)}g_{\mu\nu} + \Lambda\,{}^{(4)}g_{\mu\nu} = 8\pi T_{\mu\nu} \,, \tag{2.1} $$

where Λ is the cosmological constant. In the following, this equation will not be assumed. Even though Einstein's field equations are experimentally well tested, one might search for deviations from general relativity. A well-established method for doing so is to consider a wide-range class of gravitational theories, parameterized by a set of constants, that includes general relativity as a special case. Experiments can then produce bounds on the possible range of these parameters and thus quantify the "goodness of fit" of general relativity, or its alternatives, to experimental observations. Such a scheme is provided by the parameterized post-Newtonian formalism, which is described in Section 2.4.4 after the introduction of some mathematical notions.

2.2 Geometry of Space

Spacelike hypersurfaces provide a theoretical model for describing the geometry of "space at an instant of time" within the four-dimensional geometry of space-time. This section considers the general case of space being immersed in space-time. The more common case of space-time being foliated by embedded hypersurfaces is considered in the next section.

Immersed Submanifolds One of the most general ways in which a three-dimensional manifold $\mathscr{S}$ may "lie within" a four-dimensional manifold $\mathscr{M}$ (which is here taken to be the space-time manifold) is via an immersion

$$ \iota : \mathscr{S} \to \mathscr{M} \,, \tag{2.2} $$

i.e., a smooth map whose differential is everywhere injective [54, Chap. 4]. One of the main objects of interest in the study of immersions is the description of how the tangent bundle $\mathrm{T}\mathscr{S}$ can be regarded as "being contained" in $\mathrm{T}\mathscr{M}$. To examine this, one defines the pull-back [55, Def. 5.3; 56, Sect. 5.1.7] of the tangent bundle $\mathrm{T}\mathscr{M}$ along the immersion ι as

$$ \iota^*(\mathrm{T}\mathscr{M}) = \{(p, v^\mu) \in \mathscr{S} \times \mathrm{T}\mathscr{M} \mid \iota(p) = \pi(v^\mu)\} \,, \tag{2.3} $$

where $\pi : \mathrm{T}\mathscr{M} \to \mathscr{M}$ is the canonical projection of $\mathscr{M}$'s tangent bundle. As the differential $\mathrm{d}\iota : \mathrm{T}\mathscr{S} \to \mathrm{T}\mathscr{M}$ is everywhere injective, it defines a soldering

$$ \theta : \mathrm{T}\mathscr{S} \to \iota^*(\mathrm{T}\mathscr{M}) \qquad\qquad \theta|_p(v^i) = (p, \theta^\mu{}_i|_p v^i) \,, \tag{2.4} $$

where $\theta^\mu{}_i$ is the solder form

$$ \theta^\mu{}_i = (\mathrm{d}\iota)^\mu{}_i \,. \tag{2.5} $$

Here and henceforward, Greek indices μ, ν, ρ, etc., pertain to $\mathrm{T}\mathscr{M}$, whereas Latin indices i, j, k, etc., pertain to $\mathrm{T}\mathscr{S}$. A vector v^i of $\mathrm{T}\mathscr{S}$ thus corresponds to a unique vector $v^\mu = \theta^\mu{}_i v^i$ in $\iota^*(\mathrm{T}\mathscr{M})$. In this sense, $\mathrm{T}\mathscr{S}$ can be regarded as a sub-bundle of $\iota^*(\mathrm{T}\mathscr{M})$:

$$\mathrm{T}\mathscr{S} \simeq \{(p, v^\mu) \in \iota^*(\mathrm{T}\mathscr{M}) \mid v^\mu \in \mathrm{im}(\theta^\mu{}_i|_p)\} \,. \tag{2.6}$$

Complementary to the tangential vectors, $\iota^*(\mathrm{T}\mathscr{M})$ also contains normal vectors. Generally, one can define the normal bundle $\mathrm{N}\mathscr{S}$ as

$$\mathrm{N}\mathscr{S} = \iota^*(\mathrm{T}\mathscr{M})/\theta(\mathrm{T}\mathscr{S}) \,, \tag{2.7}$$

where the quotient is taken point-wise, i.e., for $p \in \mathscr{S}$ the fiber $\mathrm{N}_p\mathscr{S}$ is given by the quotient vector space $\iota_p^*(\mathrm{T}\mathscr{M})/\theta(\mathrm{T}_p\mathscr{S})$ [57, Sect. 15.6]. This gives rise to the short exact sequence

$$0 \to \mathrm{T}\mathscr{S} \xrightarrow{\theta} \iota^*(\mathrm{T}\mathscr{M}) \xrightarrow{q} \mathrm{N}\mathscr{S} \to 0 \,, \tag{2.8}$$

where $q : \iota^*(\mathrm{T}\mathscr{M}) \to \mathrm{N}\mathscr{S}$ is the canonical projection, mapping vectors to their equivalence classes. If the immersion of $\mathscr{S}$ in $\mathscr{M}$ is non-degenerate with respect to the Lorentzian metric ${}^{(4)}g_{\mu\nu}$, one can construct a Gauss map using which this short exact sequence can be split.

Gauss Map For spacelike hypersurfaces, which will be considered throughout the remainder of this chapter, the sequence (2.8) splits in a canonical way (a similar statement applies to timelike hypersurfaces). This is readily seen using the notion of a Gauss map: As immersions are local embeddings [54, Theorem 4.12], there exists a local co-normal field Γ_μ, i.e., a section of the pull-back of $\mathscr{M}$'s cotangent bundle, $\iota^*(\mathrm{T}^*\mathscr{M})$, such that for all $p \in \mathscr{S}$ it holds that

$$\ker(\Gamma_\mu|_p) = \mathrm{im}(\theta^\mu{}_i|_p) \,. \tag{2.9}$$

The assumption that $\mathscr{S}$ is spacelike within $\mathscr{M}$ is equivalent to the condition that Γ_μ is timelike, so that Γ_μ can be normalized to

$${}^{(4)}g^{\mu\nu}\Gamma_\mu\Gamma_\nu = -1 \,. \tag{2.10}$$

Such a (local) unit co-normal, which is henceforward referred to as a Gauss map, is unique up to an overall sign. The metrically equivalent vector field is the unit normal

$$\Gamma^\mu = {}^{(4)}g^{\mu\nu}\Gamma_\nu \,, \tag{2.11}$$

which has the same sign ambiguity as the unit co-normal. The Gauss map Γ_μ gives rise to the orthogonal projections

$$P^\mu{}_\nu = \delta^\mu_\nu + \Gamma^\mu \Gamma_\nu \,, \qquad\qquad Q^\mu{}_\nu = -\Gamma^\mu \Gamma_\nu \,, \tag{2.12}$$

which project vectors in $\iota^*(\mathrm{T}\mathscr{M})$ onto their tangential and orthogonal parts, respectively.

Structure of the Normal Bundle Generally, the normal bundle $\mathrm{N}\mathscr{S}$ is defined as the quotient given in Eq. (2.7), so its elements are equivalence classes of vectors of $\iota^*(\mathrm{T}\mathscr{M})$ up to tangent vectors. The projection $Q^\mu{}_\nu$ singles out representatives of these equivalence classes: $[v^\mu]$ has the representative $Q^\mu{}_\nu v^\mu = -\Gamma^\mu \Gamma_\nu v^\nu$. In this way, the normal bundle $\mathrm{N}\mathscr{S}$ can be regarded as a sub-bundle of $\iota^*(\mathrm{T}\mathscr{M})$ whose fiber at $p \in \mathscr{S}$ is given by the span of $\Gamma^\mu|_p$:

$$\mathrm{N}\mathscr{S} \simeq \{(p, v^\mu) \in \iota^*(\mathrm{T}\mathscr{M}) \mid v^\mu \propto \Gamma^\mu|_p\} \,. \tag{2.13}$$

Structure of the Tangent Bundle The soldering $\theta^\mu{}_i$ constitutes a map from $\mathrm{T}\mathscr{S}$ into $\iota^*(\mathrm{T}\mathscr{M})$. Using the operator $P^\mu{}_\nu$, however, one can also construct a map in the opposite direction: The image of $P^\mu{}_\nu$ at a point $p \in \mathscr{S}$ equals the kernel of $\Gamma_\mu|_p$, which further equals the image of $\theta^\mu{}_i|_p$. Since $\theta^\mu{}_i$ is everywhere injective, it admits a left-inverse, which, via composition with $P^\mu{}_\nu$, gives rise to an "inverse soldering" map

$$\theta^i{}_\mu : \iota^*(\mathrm{T}\mathscr{M}) \to \mathrm{T}\mathscr{S} \tag{2.14}$$

with the properties

$$\theta^i{}_\mu \theta^\mu{}_j = \delta^i_j \,, \qquad\qquad \theta^\mu{}_i \theta^i{}_\nu = P^\mu{}_\nu \,. \tag{2.15}$$

Decomposition of $\iota^*(\mathrm{T}\mathscr{M})$ Using the notions described above, one finds that the short exact sequence (2.8) splits as

$$0 \to \mathrm{T}\mathscr{S} \to \mathrm{T}\mathscr{S} \oplus \mathrm{N}\mathscr{S} \to \mathrm{N}\mathscr{S} \to 0 \,, \tag{2.16}$$

where $\oplus$ denotes the Whitney sum (in fact, this splitting is orthogonal). This is accomplished by the bundle isomorphisms

$$f : \iota^*(\mathrm{T}\mathscr{M}) \to \mathrm{T}\mathscr{S} \oplus \mathrm{N}\mathscr{S} \qquad f(p, v^\mu) = (\theta^i{}_\mu v^\mu, [Q^\mu{}_\nu v^\nu]) \,, \tag{2.17}$$

$$f^{-1} : \mathrm{T}\mathscr{S} \oplus \mathrm{N}\mathscr{S} \to \iota^*(\mathrm{T}\mathscr{M}) \qquad f_p^{-1}(v^i, [w^\mu]) = (p, \theta^\mu{}_i v^i + Q^\mu{}_\nu w^\nu) \,. \tag{2.18}$$

At this stage, it is useful to define some notation: Given a tangent vector $v^i \in \mathrm{T}\mathscr{S}$, let $v^\mu = \theta^\mu{}_i v^i$ denote the corresponding vector in $\iota^*(\mathrm{T}\mathscr{M})$. Conversely, for a vector $w^\mu \in \iota^*(\mathrm{T}\mathscr{M})$, let $w^i = \theta^i{}_\mu w^\mu$ denote the $\mathrm{T}\mathscr{S}$-vector corresponding to the tangential projection of w^μ to $\mathscr{S}$. An analogous notation will be used for co-vectors and also for

tensors of arbitrary valence. In this way, one can identify tensors on $\mathscr{S}$ with those tensors along ι all of whose contractions with Γ_μ and Γ^μ vanish.

Induced Metric The space-time metric ${}^{(4)}g_{\mu\nu}$ on $\mathscr{M}$ induces a metric on $\mathscr{S}$ via the pull-back: ${}^{(3)}g_{ij}v^i w^j = {}^{(4)}g_{\mu\nu}v^\mu w^\nu$. In the notation introduced above, one thus has the equivalent descriptions

$$ {}^{(3)}g_{ij} = {}^{(4)}g_{\mu\nu}\theta^\mu{}_i\theta^\nu{}_j\,, \qquad {}^{(3)}g_{\mu\nu} = {}^{(4)}g_{\rho\sigma}P^\rho{}_\mu P^\sigma{}_\nu = {}^{(4)}g_{\mu\nu} + \Gamma_\mu\Gamma_\nu\,, \tag{2.19} $$

where, in the first equation, ${}^{(3)}g_{ij}$ is regarded as a tensor on $\mathscr{S}$ and, in the second equation, ${}^{(3)}g_{\mu\nu}$ is regarded as a tensor along ι.

Induced Volume Form Similarly to the metric, the space-time volume form ${}^{(4)}\epsilon_{\mu\nu\rho\sigma}$ induces a volume form ${}^{(3)}\epsilon_{ijk}$ on $\mathscr{S}$ via contraction with the unit normal:

$$ {}^{(3)}\epsilon_{ijk} = \Gamma^\sigma\,{}^{(4)}\epsilon_{\sigma\mu\nu\rho}\theta^\mu{}_i\theta^\nu{}_j\theta^\rho{}_k\,, \qquad {}^{(3)}\epsilon_{\mu\nu\rho} = \Gamma^\sigma\,{}^{(4)}\epsilon_{\sigma\mu\nu\rho}\,. \tag{2.20} $$

Induced Connection Further, a Koszul connection, also referred to as a covariant derivative, ${}^{(4)}\nabla_\mu$ on $\mathscr{M}$ induces a covariant derivative ${}^{(3)}\nabla_i$ on $\mathscr{S}$ via the following equation (with the soldering made explicit):

$$ {}^{(3)}\nabla_i w^j = \theta^\mu{}_i\theta^j{}_\nu\,{}^{(4)}\nabla_\mu(\theta^\nu{}_k w^k)\,. \tag{2.21} $$

Specifically, one can show that if ${}^{(4)}\nabla_\mu$ is the Levi-Civita derivative of ${}^{(4)}g_{\mu\nu}$, then ${}^{(3)}\nabla_i$ is the Levi-Civita derivative of ${}^{(3)}g_{ij}$ [58, Sect. 2.1; 59, p. 25 f.].

Extrinsic Curvature If tangent vectors v^i and w^i of $\mathscr{S}$ are regarded as vectors in $\iota^*(\mathrm{T}\mathscr{S})$, one can compare the expressions $v^\nu\,{}^{(3)}\nabla_\nu w^\mu$ and $v^\nu\,{}^{(4)}\nabla_\nu w^\mu$ with the result

$$ v^\nu\,{}^{(3)}\nabla_\nu w^\mu = v^\nu\,{}^{(4)}\nabla_\nu w^\mu + \Gamma^\mu\,{}^{(3)}K_{\nu\rho}v^\nu w^\rho\,, \tag{2.22} $$

where ${}^{(3)}K_{\mu\nu}$ is the extrinsic curvature

$$ {}^{(3)}K_{\mu\nu} = -{}^{(4)}\nabla_\mu\Gamma_\nu\,. \tag{2.23} $$

The extrinsic curvature ${}^{(3)}K_{\mu\nu}$ is a symmetric tangential tensor [59, p. 24] that relates the intrinsic derivative ${}^{(3)}\nabla$ to the extrinsic derivative ${}^{(4)}\nabla$ and thus quantities to what extent geodesic in $\mathscr{S}$ fail to be geodesics in $\mathscr{M}$.[1]

The extrinsic curvature ${}^{(3)}K_{ij}$ also relates the "intrinsic" curvature tensor ${}^{(3)}R_{ijkl}$ (derived from the induced metric ${}^{(3)}g_{ij}$) to certain projections of the "ambient" curvature tensor

[1] As Γ_μ is hitherto defined up to an overall sign, so is ${}^{(3)}K_{\mu\nu}$. However, the product $\Gamma^\mu\,{}^{(3)}K_{\nu\rho}$ is free of this sign-ambiguity. This concept of a vector-valued extrinsic curvature is useful in the case of higher co-dimensions.

${}^{(4)}R_{\mu\nu\rho\sigma}$ (derived from the metric ${}^{(4)}g_{\mu\nu}$) via the Gauss equation [60, Theorem 8.5]

$$ {}^{(3)}R_{ijkl} + {}^{(3)}K_{ik}\,{}^{(3)}K_{jl} - {}^{(3)}K_{il}\,{}^{(3)}K_{jk} = {}^{(4)}R_{ijkl}\,, \tag{2.24} $$

and the Codazzi–Mainardi equation [60, Theorem 8.9]

$$ {}^{(3)}\nabla_i\,{}^{(3)}K_{kj} - {}^{(3)}\nabla_j\,{}^{(3)}K_{ki} = \Gamma_\rho\,{}^{(4)}R^{\rho}{}_{kij}\,. \tag{2.25} $$

2.3 Geometry of Space-Time

Generally, space-times do not admit any distinguished splitting into space and time. In fact, some space-times do not even admit so-called time functions, as exemplified by the Gödel metric [61]. The existence of such splittings is closely related to the causal properties of the space-time under consideration, see, e.g., Ref. [62] and references therein. The discussions in this document are restricted to *globally hyperbolic* space-times, see, e.g., Refs. [63; 64; 65, Sect. 6.6] for definitions and discussions of basic properties, for which such splittings do exist (although they are not unique).

Any globally hyperbolic space-time $\mathscr{M}$ is diffeomorphic (but generally not isomeric) to a product of the form

$$ \mathscr{M} \simeq \mathbf{R} \times \mathscr{S}\,, \tag{2.26} $$

where $\mathscr{S}$ is a three-dimensional manifold, such that (the images of) all surfaces $\{t\} \times \mathscr{S}$, where $t \in \mathbf{R}$, are Cauchy surfaces in $\mathscr{M}$ [64–66].

Such a diffeomorphism determines a time function t acting on $\mathbf{R} \times \mathscr{S}$ as $t(t', p) = t'$ (the level sets of which are Cauchy surfaces) as well as a timelike vector field X^μ that is tangent to the curves $t' \mapsto (t', p)$. One then has $(\mathrm{d}t)_\mu X^\mu = 1$.

Lapse and Shift For each $t \in \mathbf{R}$, the diffeomorphism (2.26) defines an embedding $\iota_t : \mathscr{S} \to \mathscr{M}$, so the spatial geometry at each instance of "time" t can be described via the methods of Section 2.2. Whereas the Gauss map Γ_μ for a generic embedding is unique up to sign, a time orientation on $\mathscr{M}$ singles out the future-pointing unit co-normal

$$ \Gamma_\mu = -\zeta (\mathrm{d}t)_\mu\,, \tag{2.27} $$

and corresponding unit normal

$$ \Gamma^\mu = -\zeta\,{}^{(4)}g^{\mu\nu}(\mathrm{d}t)_\nu\,, \tag{2.28} $$

where ζ is the lapse function [67, Sect. 4.3.1]

$$ \zeta = 1/\sqrt{-{}^{(4)}g^{\mu\nu}(\mathrm{d}t)_\mu(\mathrm{d}t)_\nu}\,. \tag{2.29} $$

The vector field X^μ can then be decomposed into its parts parallel and orthogonal to Γ^μ as

$$X^\mu = \zeta \Gamma^\mu + \xi^\mu \,, \tag{2.30}$$

where ξ^μ is the shift vector field [67, Sect. 5.2.2]

$$\xi^\mu = [\delta^\mu_\nu + \Gamma^\mu \Gamma_\nu] X^\nu \,. \tag{2.31}$$

The first summand in Eq. (2.30), $\zeta \Gamma^\mu$, is sometimes referred to as the normal evolution vector [67, Sect. 4.3.2].

ADM-Form of the Metric If x^1, x^2, x^3 are (local) coordinates on $\mathscr{S}$, the diffeomorphism (2.26) gives rise to local coordinates on $\mathscr{M}$ with $x^0 = t$ being the time function whose level sets are the Cauchy surfaces $\{t\} \times \mathscr{S}$. The foliation vector field X^μ then reduces to ∂_0, and a direct calculation yields the following results for the components of the space-time metric ${}^{(4)}g_{\mu\nu}$:

$$ {}^{(4)}g_{00} = -\zeta^2 + {}^{(3)}g_{ij} \xi^i \xi^j \,, \tag{2.32}$$

$$ {}^{(4)}g_{0i} = \xi_i \,, \tag{2.33}$$

$$ {}^{(4)}g_{ij} = {}^{(3)}g_{ij} \,, \tag{2.34}$$

hence

$$\begin{aligned} {}^{(4)}g &= -(\zeta^2 - {}^{(3)}g_{ij} \xi^i \xi^j) \mathrm{d}x^0 \mathrm{d}x^0 + 2 \xi_i \mathrm{d}x^0 \mathrm{d}x^i + {}^{(3)}g_{ij} \mathrm{d}x^i \mathrm{d}x^j \\ &= -\zeta^2 \mathrm{d}x^0 \mathrm{d}x^0 + {}^{(3)}g_{ij} (\mathrm{d}x^i + \xi^i \mathrm{d}x^0)(\mathrm{d}x^j + \xi^j \mathrm{d}x^0) \,. \end{aligned} \tag{2.35}$$

The matrix representations of ${}^{(4)}g_{\mu\nu}$ and ${}^{(4)}g^{\mu\nu}$ are thus

$$ ({}^{(4)}g_{\mu\nu}) = \begin{pmatrix} -\zeta^2 + \|\xi\|^2 & \xi_j \\ \xi_i & {}^{(3)}g_{ij} \end{pmatrix} , \qquad ({}^{(4)}g^{\mu\nu}) = \begin{pmatrix} -1/\zeta^2 & \xi^j/\zeta^2 \\ \xi^i/\zeta^2 & {}^{(3)}g^{ij} - \xi^i \xi^j/\zeta^2 \end{pmatrix} . \tag{2.36}$$

This method of decomposing ${}^{(4)}g_{\mu\nu}$ is known as the ADM-decomposition, named after Arnowitt, Deser, and Misner [68].

Landau–Lifshitz Metric The tensor field ${}^{(3)}g_{ij}$ is the metric induced by ${}^{(4)}g_{\mu\nu}$ on the spatial slices of constant t, which are orthogonal to the vector field Γ^μ. In general, this metric does not coincide with the projection of ${}^{(4)}g_{\mu\nu}$ onto the subspaces orthogonal to the vector field X^μ, which is given by

$$\ell_{\mu\nu} = {}^{(4)}g_{\mu\nu} - X_\mu X_\nu / (X_\rho X^\rho) \,. \tag{2.37}$$

This tensor describes the spatial geometry as seen by an observer at rest in the considered coordinate system [69, § 84] and is commonly referred to as the Landau–Lifshitz metric or radar metric [70; 71]. However, $\ell_{\mu\nu}$ cannot, in general, be regarded as a metric induced by ${}^{(4)}g_{\mu\nu}$ on appropriately chosen spacelike hypersurfaces, as the vector field X^μ need not be hypersurface-orthogonal.

Since $\ell_{\mu\nu}$ has a kernel (spanned by X^μ), it does not admit a proper inverse. However, one can define a "spatial inverse" $\ell^{\mu\nu}$ via the conditions

$$\ell^{\mu\nu} X_\nu = 0\,, \qquad\qquad \ell^{\mu\rho}\ell_{\rho\nu} = \delta^\mu_\nu - X^\mu X_\nu/(X_\rho X^\rho)\,, \tag{2.38}$$

which yields

$$\ell^{\mu\nu} = {}^{(4)}g^{\mu\nu} - X^\mu X^\nu/(X_\rho X^\rho)\,. \tag{2.39}$$

When expressed in local coordinates as described above, one obtains

$$\ell = \ell_{ij}\,\mathrm{d}x^i \mathrm{d}x^j\,, \tag{2.40}$$

with

$$\begin{aligned}\ell_{ij} &= {}^{(4)}g_{ij} - {}^{(4)}g_{0i}\,{}^{(4)}g_{0j}/{}^{(4)}g_{00} \\ &= {}^{(3)}g_{ij} + \xi_i\xi_j/(\zeta^2 - \xi_k\xi^k)\,,\end{aligned} \tag{2.41}$$

and the spatial inverse takes the form

$$\ell^{ij} = {}^{(3)}g^{ij} - \xi^i\xi^j/\zeta^2\,. \tag{2.42}$$

For later reference, note that the components of both $\ell_{\mu\nu} = {}^{(4)}g_{\mu\nu} - X_\mu X_\nu/(X_\rho X^\rho)$ and $\ell^{\mu\nu} = {}^{(4)}g^{\mu\nu} - X^\mu X^\nu/(X_\rho X^\rho)$ in matrix notation take the form

$$(\ell_{\mu\nu}) = \begin{pmatrix} 0 & 0 \\ 0 & \ell_{ij} \end{pmatrix}\,, \qquad\qquad (\ell^{\mu\nu}) = \begin{pmatrix} \frac{\xi_k\xi^k}{\zeta^2(\zeta^2 - \xi_l\xi^l)} & \xi^j/\zeta \\ \xi^j/\zeta & \ell^{ij} \end{pmatrix}\,. \tag{2.43}$$

2.4 Linearized Gravity

So far, the space-time metric ${}^{(4)}g_{\mu\nu}$ was left unspecified. Starting from the nonlinear Einstein field equations (described in Section 2.4.1) and their linearization (Section 2.4.2), this section describes specific models for ${}^{(4)}g_{\mu\nu}$ that describe Earth's gravitational field (Sections 2.4.3 and 2.4.4).

2.4.1 Einstein's Field Equations

As described in Section 2.1, the field equations for the metric ${}^{(4)}g_{\mu\nu}$ in Einstein's theory of general relativity are given by

$$ {}^{(4)}R_{\mu\nu} - \tfrac{1}{2}{}^{(4)}R\,{}^{(4)}g_{\mu\nu} + \Lambda\,{}^{(4)}g_{\mu\nu} = 8\pi T_{\mu\nu}\,. \tag{2.44} $$

As the Ricci curvature tensor ${}^{(4)}R_{\mu\nu}$ depends non-linearly on ${}^{(4)}g_{\mu\nu}$, the Einstein field equations constitute a nonlinear system of partial differential equations for ${}^{(4)}g_{\mu\nu}$ with a gauge symmetry arising from diffeomorphism invariance.

If gauge degrees of freedom are fixed appropriately, Eq. (2.44) implies evolution and constraint equations for the geometry of spatial slices (which can be described using the methods introduced in the preceding section). These equations are well known in mathematical and numerical relativity [67; 72–74], but their explicit form is not relevant to the present considerations. Instead, the next sections describe concrete space-time metrics (modeling weak gravitational fields), as well as adapted coordinate systems, the choice of which determines the induced metric ${}^{(3)}g_{ij}$, lapse ζ, and shift ξ_i.

2.4.2 Linearized Einstein Equations

The present work is mostly concerned with weak gravitational fields with $\Lambda = 0$. One method of describing such configurations is to consider a metric tensor ${}^{(4)}g_{\mu\nu}$ that, in appropriate coordinates, is close to the Minkowski metric $\eta_{\mu\nu}$. Formally, this is described by a perturbative scheme based on the ansatz

$$ {}^{(4)}g_{\mu\nu} = \eta_{\mu\nu} + h_{\mu\nu}\,, \tag{2.45} $$

where $h_{\mu\nu}$ is regarded as a small perturbation on the order of a perturbation parameter $\epsilon \ll 1$. The form of the metric perturbation $h_{\mu\nu}$ can be constrained by an appropriate choice of coordinates (gauge condition). Requiring the coordinates x^μ to satisfy the massless scalar wave equation $\Box x^\mu = 0$ (harmonic gauge) leads (at first order in ϵ) to the gauge condition

$$ \partial^\mu(h_{\mu\nu} - \tfrac{1}{2}h\eta_{\mu\nu}) = 0\,, \tag{2.46} $$

where $\partial^\mu = \eta^{\mu\nu}\partial_\nu$, and $h = \eta^{\mu\nu}h_{\mu\nu}$ is the trace of the metric perturbation with respect to the unperturbed metric. In such a coordinate system, the Ricci tensor of space-time takes the form

$$ {}^{(4)}R_{\mu\nu} = -\tfrac{1}{2}\Box h_{\mu\nu} + O(\epsilon^2)\,, \tag{2.47} $$

where $\Box = \eta^{\rho\sigma}\partial_\rho\partial_\sigma$ is the d'Alembertian of the unperturbed metric. Defining the trace-reverse of a tensor $X_{\mu\nu}$ as $\bar{X}_{\mu\nu} = X_{\mu\nu} - \frac{1}{2}\eta_{\mu\nu}\eta^{\rho\sigma}X_{\rho\sigma}$, the linearized Einstein field equations

with $\Lambda = 0$ can be written as

$$\Box \bar{h}_{\mu\nu} = -16\pi T_{\mu\nu} \,, \tag{2.48}$$

or equivalently

$$\Box h_{\mu\nu} = -16\pi \bar{T}_{\mu\nu} \,. \tag{2.49}$$

These equations serve as the basis of the description of post-Newtonian gravitational fields.

2.4.3 Post-Newtonian Gravitation

The stress-energy-momentum tensor $T_{\mu\nu}$ can generally be decomposed according to

$$T^{00} = \mu \,, \qquad T^{0i} = p^i \,, \qquad T^{ij} = \sigma^{ij} \,, \tag{2.50}$$

where indices of $T_{\mu\nu}$ were raised using the contravariant Minkowski metric $\eta^{\mu\nu}$. Here, μ is the mass density (or energy density), p^i is the momentum density, and σ^{ij} is the stress tensor. The relative orders of magnitude involved in this problem can be read from the conversion between SI units and the geometric units used throughout this document (to two significant digits):

$$\begin{aligned} 1\,\mathrm{g/cm^3} &\doteq 7.4 \times 10^{-25}\,\mathrm{m^{-2}} \,, \\ 1\,(\mathrm{g/cm^3})(\mathrm{km/s}) &\doteq 2.5 \times 10^{-30}\,\mathrm{m^{-2}} \,, \\ 1\,\mathrm{GPa} &\doteq 8.3 \times 10^{-36}\,\mathrm{m^{-2}} \,. \end{aligned}$$

In practical applications,[(2)] stresses yield negligibly small contributions to $T_{\mu\nu}$ and the mass density μ exceeds the pressure density p_i by multiple orders of magnitude. Neglecting the gravitational field produced by p^i and σ^{ij} leads to the *Newtonian* approximation, whereas the *post-Newtonian* approximation considered here takes contributions from the momentum density p^i into account, but neglects contributions from the stress tensor σ^{ij} [75, §39.7].

The stress-energy-momentum tensor in the post-Newtonian (PN) approximation is thus given by

$$T^{\mathrm{PN}}_{00} = \mu \,, \qquad T^{\mathrm{PN}}_{0i} = -p_i \,, \qquad T^{\mathrm{PN}}_{ij} = 0 \,, \tag{2.51}$$

with μ and p_i denoting the mass and momentum density, respectively. The components of

[(2)] Earth's average density is about $5\,\mathrm{g\,cm^{-3}}$, its equatorial speed due to rotation is about $0.5\,\mathrm{km\,s^{-1}}$, and the pressure at Earth's core is on the order of 360 GPa. One thus has the order-of-magnitude estimates $\mu \approx 4 \times 10^{-24}\,\mathrm{m^{-2}}$, $p \approx 3 \times 10^{-30}\,\mathrm{m^{-2}}$, and $\sigma \approx 3 \times 10^{-33}\,\mathrm{m^{-2}}$.

the trace-reversed tensor then reduce to

$$\bar{T}^{\text{PN}}_{00} = \tfrac{1}{2}\mu\,, \qquad \bar{T}^{\text{PN}}_{0i} = -p_i\,, \qquad \bar{T}^{\text{PN}}_{ij} = \tfrac{1}{2}\mu\,\delta_{ij}\,. \tag{2.52}$$

For time-independent gravitational fields, the d'Alembertian $\Box$ in Eq. (2.49) reduces to the Laplacian Δ. Using the corresponding Green's function, one then finds

$$h^{\text{PN}}_{00}(x) = 2\int \frac{\mu(y)}{\|x-y\|}\mathrm{d}^3y\,, \tag{2.53a}$$

$$h^{\text{PN}}_{ij}(x) = 2\delta_{ij}\int \frac{\mu(y)}{\|x-y\|}\mathrm{d}^3y\,, \tag{2.53b}$$

$$h^{\text{PN}}_{0i}(x) = -4\int \frac{p_i(y)}{\|x-y\|}\mathrm{d}^3y\,, \tag{2.53c}$$

which, in the notation of Section 2.3, corresponds to the following results for the lapse ζ, shift ξ_i, and spatial metric ${}^{(3)}g_{ij}$:

$$\zeta^{\text{PN}}(x) = 1 - \int \frac{\mu(y)}{\|x-y\|}\mathrm{d}^3y\,, \tag{2.54a}$$

$$\xi^{\text{PN}}_i(x) = -4\int \frac{p_i(y)}{\|x-y\|}\mathrm{d}^3y\,, \tag{2.54b}$$

$${}^{(3)}g^{\text{PN}}_{ij}(x) = \left[1 + 2\int \frac{\mu(y)}{\|x-y\|}\mathrm{d}^3y\right]\delta_{ij}\,. \tag{2.54c}$$

Multipole Expansion In the far-field region of an isolated mass distribution, the gravitational field can be approximated using a multipole expansion. In the center-of-mass coordinate system, the leading-order terms are given by

$$\int \frac{\mu(y)}{\|x-y\|}\mathrm{d}^3y = \frac{1}{r}M + O(r^{-2})\,, \tag{2.55}$$

$$\int \frac{p_i(y)}{\|x-y\|}\mathrm{d}^3y = \frac{1}{2r^3}\varepsilon_{ijk}J^j x^k + O(r^{-3})\,, \tag{2.56}$$

where r is the distance from the center of mass, M is the system's total mass, and J^i its total angular momentum [75, §19.1; 76, Sect. 4.7]. The effect of the mass M is thus to curve the spatial metric ${}^{(3)}g_{ij}$, and to alter the flow of time via the lapse function ζ, whereas the angular momentum J_i causes a non-zero shift vector field ξ_i (a phenomenon known as frame-dragging).

The formulas presented in this section serve as the basic description of Earth's gravitational field, but the metric given here is expressed in asymptotically flat coordinates that do not necessarily coincide with those adapted to a laboratory on Earth. The transition to such coordinates is described in Section 2.5 below, after the more general family of parameterized post-Newtonian metrics is introduced in Section 2.4.4.

2.4.4 Parameterized Post-Newtonian Formalism

In the weak-field limit, general relativity leads to the post-Newtonian (PN) metrics described above. The parameterized post-Newtonian (PPN) formalism [53] provides a deformation of the PN metrics via a set of PPN parameters. Experimental tests of gravity can then constrain these PPN parameters to a range consistent with experimental observations. A bound on the deviation of the PPN parameters from the values predicted by general relativity (GR) can then be regarded as an assessment of the goodness-of-fit of general relativity, whereas a statistically significant deviation from the GR values would correspond to a deviation from Einstein's theory of gravity.

Expansion Parameter The PPN formalism is a perturbative scheme for weak gravity and thus describes perturbations of the Minkowski metric. This scheme is based on one perturbation parameter, here denoted by ε_{PPN}, for which the following estimates are assumed [53, Sect. 4.1.2]:

- the Newtonian gravitational potential φ is of order $O(\varepsilon_{\text{PPN}})$,
- typical velocities of gravitating masses are of order $O(\varepsilon_{\text{PPN}}^{1/2})$,
- the internal pressure per unit mass of gravitating bodies is of order $O(\varepsilon_{\text{PPN}})$,
- the internal energy per unit mass of gravitating bodies is of order $O(\varepsilon_{\text{PPN}})$.

PPN Metric In the "standard PPN gauge," the PPN metric [53, Sect. 4.2.2] is given by

$$\begin{aligned} {}^{(4)}g = &- \left\{1 + 2\varphi + O(\varepsilon_{\text{PPN}}^2)\right\} \mathrm{d}t^2 \\ &- \left\{[4(1+\gamma_{\text{PPN}}) + \alpha_{\text{PPN}}]V_i \; + O(\varepsilon_{\text{PPN}}^{3/2})\right\} \mathrm{d}x^i \mathrm{d}t \\ &+ \left\{(1 - 2\gamma_{\text{PPN}}\varphi)\delta_{ij} + O(\varepsilon_{\text{PPN}}^2)\right\} \mathrm{d}x^i \mathrm{d}x^j \,, \end{aligned} \tag{2.57}$$

where φ is the gravitational potential

$$\varphi(x) = -\int \frac{\mu(y)}{\|x-y\|} \, \mathrm{d}^3 y \,, \tag{2.58}$$

with μ denoting the mass density, and V_i is the vector field

$$V_i\,(x) = \int \frac{p_i(y)}{\|x-y\|} \, \mathrm{d}^3 y \,, \tag{2.59}$$

where p_i is the momentum density of matter. Up to a constant (which depends on conventions) V_i coincides with the "gravito-magnetic potential," see, e.g., Ref. [77]. Hence,

the lapse ζ, shift ξ_i, and spatial metric ${}^{(3)}g_{ij}$ in the standard PPN gauge are

$$\zeta^{\mathrm{PPN}} = 1 + \varphi + \tfrac{1}{2}[2(1+\gamma_{\mathrm{PPN}}) + \tfrac{1}{2}\alpha_{\mathrm{PPN}}]^2 \|V\|^2 + O(\varepsilon_{\mathrm{PPN}}^2)\,, \tag{2.60a}$$

$$\xi_i^{\mathrm{PPN}} = -[2(1+\gamma_{\mathrm{PPN}}) + \tfrac{1}{2}\alpha_{\mathrm{PPN}}]V_i + O(\varepsilon_{\mathrm{PPN}}^{3/2})\,, \tag{2.60b}$$

$${}^{(3)}g_{ij}^{\mathrm{PPN}} = (1 + 2\gamma_{\mathrm{PPN}}\varphi)\delta_{ij} + O(\varepsilon_{\mathrm{PPN}}^2)\,. \tag{2.60c}$$

The PPN parameter γ_{PPN} thus describes the strength of spatial curvature induced by the mass density μ, and the strength of frame-dragging caused by the momentum density p_i. The parameter α_{PPN} describes potential further contributions to frame-dragging that are uncorrelated with the spatial curvature.

In general relativity, one has

$$\gamma_{\mathrm{PPN}}^{\mathrm{GR}} = 1\,, \qquad\qquad \alpha_{\mathrm{PPN}}^{\mathrm{GR}} = 0\,, \tag{2.61}$$

so deviations of the PPN parameters from these reference values describe deviations from Einstein's theory of gravity. The current experimental bound on γ_{PPN} is derived from the Cassini–Huygens space mission: $\gamma_{\mathrm{PPN}} - 1 = (2.1 \pm 2.3) \times 10^{-5}$, and observations of the white-dwarf binary system PSR J1738+0333 constrain α_{PPN} to $|\alpha_{\mathrm{PPN}}| \leq 4 \times 10^{-5}$ [78; 79].

The PPN formalism can be extended beyond the regime of linearized gravity [79], but for the present considerations, the level of accuracy of Eq. (2.57) suffices.

2.5 Fermi Coordinates

This section introduces the notions of Fermi–Walker transport and Fermi coordinates. These concepts will serve as a tool for constructing coordinate systems adapted to a laboratory in curved space-time, such as a laboratory on Earth's surface. Such coordinates were first introduced by Fermi in Ref. [80], where the space-time metric components near an arbitrary timelike curve were computed to leading order in the distance away from the curve, at which order no curvature terms arise. Higher-order corrections, which include such curvature terms, were computed by Manasse and Misner for non-rotating spatial coordinates [81], and by Ni and Zimmermann in the general case [82].

Let γ be a timelike curve with proper-time t, four-velocity u^μ, and four-acceleration a^μ. The (space-time) Fermi–Walker derivative ${}^{(4)}\mathrm{D}_t$ is a differential operator, acting on tensor fields along γ, defined by its action on vectors as [65, Sect. 4.1]

$${}^{(4)}\mathrm{D}_t v^\mu = {}^{(4)}\nabla_u v^\mu + a^\mu u_\nu v^\nu - u^\mu a_\nu v^\nu\,. \tag{2.62}$$

For a geodesic, the Fermi–Walker derivative reduces to the covariant derivative along the curve.

Similarly to the covariant derivative ${}^{(4)}\nabla_u = u^\mu {}^{(4)}\nabla_\mu$, the Fermi–Walker derivative is metric-compatible in the sense that ${}^{(4)}\mathrm{D}_t {}^{(4)}g_{\mu\nu} = 0$. Additionally, since ${}^{(4)}\mathrm{D}_t u^\mu = 0$

for arbitrary timelike curves, the inner product of u^μ with a Fermi–Walker transported vector v^μ, i.e., a vector field satisfying ${}^{(4)}\mathrm{D}_t v^\mu = 0$, remains constant along the curve γ: ${}^{(4)}\mathrm{D}_t({}^{(4)}g_{\mu\nu}u^\mu v^\nu) = 0$. An analogous statement holds for the covariant derivative only under the restriction that γ is a geodesic.

The Fermi–Walker derivative is useful for analyzing the dynamics of frames along a curve. Let $(\mathfrak{e}^\mu_{\hat\alpha})_{\hat\alpha=0}^3$ be a pseudo-orthonormal frame along γ such that $\mathfrak{e}^\mu_0 = u^\mu$. Setting ${}^{(3)}\epsilon_{\mu\nu\rho} = u^\sigma {}^{(4)}\epsilon_{\sigma\mu\nu\rho}$ to be the "spatial volume form" and defining the vector field Ω^μ by

$$\Omega_\mu = \tfrac{1}{2}\eta^{\hat\alpha\hat\beta}{}^{(3)}\epsilon_{\mu\nu\rho}\mathfrak{e}^\nu_{\hat\alpha}({}^{(4)}\mathrm{D}_t\mathfrak{e}^\rho_{\hat\beta})\,, \tag{2.63}$$

where $\eta^{\hat\alpha\hat\beta}$ is the Minkowski metric, one obtains

$${}^{(4)}\mathrm{D}_t\mathfrak{e}^\mu_{\hat\alpha} = {}^{(3)}\epsilon^\mu{}_{\nu\rho}\Omega^\nu\mathfrak{e}^\rho_{\hat\alpha}\,. \tag{2.64}$$

Hence, Ω^ν is the vector about which the spatial triad $\mathfrak{e}^\mu_{\hat i}$ rotates.

Equation (2.64) can be used in two ways: One may either prescribe a frame $\mathfrak{e}^\mu_{\hat\alpha}$ and compute Ω_μ such that Eq. (2.64) holds, or one may prescribe Ω_μ and solve Eq. (2.64) for the frame $\mathfrak{e}^\mu_{\hat\alpha}$ along the entire curve, given a frame at one point along the curve.

In either case, one may construct an adapted coordinate system by the map

$$\psi(t,x) = \exp_{\gamma(t)}[x^i\mathfrak{e}_{\hat i}(t)]\,, \tag{2.65}$$

describing spacelike geodesics that emanate from $\gamma(t)$ along the spatial triad $\mathfrak{e}^\mu_{\hat i}$. The implicit function theorem asserts that (t,x^i) constitutes a chart in the vicinity of γ. The coordinates (t,x^i) are generally referred to as Fermi coordinates. The cases $\Omega_\mu = 0$ and $\Omega_\mu \neq 0$ are sometimes referred to as Fermi normal coordinates, and generalized Fermi coordinates, respectively.

Since the coordinate frame ∂_0, ∂_i is aligned with the pseudo-orthonormal frame $\mathfrak{e}_0, \mathfrak{e}_{\hat i}$, the metric tensor along γ reduces to the Minkowski metric: ${}^{(4)}g_{\mu\nu} = \eta_{\mu\nu}$. Additionally, the connection coefficients in Fermi coordinates are fully determined by the acceleration a_i and the rotation Ω_i: up to symmetry, the only non-zero Christoffel symbols along γ are

$${}^{(4)}\Gamma_{i00} = +a_i\,, \qquad {}^{(4)}\Gamma_{00i} = -a_i\,, \qquad {}^{(4)}\Gamma_{ij0} = \varepsilon_{ikj}\Omega^k\,. \tag{2.66}$$

Moreover, expanding the metric tensor as a Taylor series around $x^i = 0$, one obtains

$$\begin{aligned} {}^{(4)}g = &-\left[(1+a_ix^i)^2 - \varepsilon_{ijk}\Omega^j x^k\varepsilon^i{}_{lm}\Omega^l x^m + {}^{(4)}R_{titj}x^ix^j\right]\mathrm{d}t^2 \\ &+ 2\left[\varepsilon_{ijk}\Omega^j x^k + \tfrac{2}{3}{}^{(4)}R_{tjki}x^jx^k\right]\mathrm{d}t\,\mathrm{d}x^i \\ &+ \left[\delta_{ij} + \tfrac{1}{3}{}^{(4)}R_{iklj}x^kx^l\right]\mathrm{d}x^i\mathrm{d}x^j + O(r^3)\,, \end{aligned} \tag{2.67}$$

with $r^2 = \delta_{ij}x^ix^j$, and where the curvature tensor ${}^{(4)}R_{\mu\nu\rho\sigma}$ is to be evaluated at $x^i = 0$ (so the components depend on t only) [83]. Accordingly, the metric tensor ${}^{(4)}g_{\mu\nu}$ reduces to

the Minkowski metric $\eta_{\mu\nu}$ along the entire curve γ, the leading-order corrections are fully determined by the acceleration a^μ and the rotation Ω^μ, and the curvature enters only at order $O(r^2)$.

Whereas the terms depending on acceleration, rotation, and curvature are additive to the considered order, the terms of order r^3 include products of these quantities [83].

Space-Time Decomposition In the notation of Section 2.3, the lapse ζ, shift ξ_i, and spatial metric ${}^{(3)}g_{ij}$ in the Fermi coordinate system thus take the form

$$\zeta = 1 + a_i x^i + \tfrac{1}{2}{}^{(4)}R_{tklj}x^k x^l + O(r^3)\,, \tag{2.68a}$$

$$\xi_i = \varepsilon_{ijk}\Omega^j x^k + \tfrac{2}{3}{}^{(4)}R_{tkli}x^k x^l + O(r^3)\,, \tag{2.68b}$$

$${}^{(3)}g_{ij} = \delta_{ij} + \tfrac{1}{3}{}^{(4)}R_{iklj}x^k x^l + O(r^3)\,. \tag{2.68c}$$

Since Fermi coordinates are orthonormal along γ, they provide an accurate representation of distances and angles, provided the regions under consideration are sufficiently small so that corrections arising from a_μ, Ω_μ, and ${}^{(4)}R_{\mu\nu\rho\sigma}$ are negligible. This motivates the terminology of "proper coordinates" sometimes used in the literature [84].

The spatial metric in Eq. (2.68c) has the standard form of Riemannian normal coordinates. This implies that the spatial curvature tensor ${}^{(3)}R_{ijkl}$ is given by

$${}^{(3)}R_{ijkl} = {}^{(4)}R_{ijkl} + O(r)\,. \tag{2.69}$$

Whereas the lapse and the shift depend on both the kinematic quantities a_i and Ω_i, as well as on the space-time curvature ${}^{(4)}R_{\mu\nu\rho\sigma}$, the spatial geometry is insensitive to the frame kinematics, and its curvature is a direct consequence of the curvature of space-time.

2.6 Earthbound Fermi Coordinates

In Section 2.4.4, the PPN metric was expressed in asymptotically flat coordinates. To describe experiments taking place on Earth's surface (where the laboratory rotates with the planet), it is advantageous to use Fermi coordinates as introduced in Section 2.5.

Consider the PPN metric as in Eq. (2.57), with error terms suppressed:

$${}^{(4)}g = -(1+2\varphi)\mathrm{d}T^2 - [4(1+\gamma_{\mathrm{PPN}}) + \alpha_{\mathrm{PPN}}]V_i\,\mathrm{d}x^i\mathrm{d}T + (1 - 2\gamma_{\mathrm{PPN}}\varphi)\delta_{ij}\mathrm{d}x^i\mathrm{d}x^j\,. \tag{2.70}$$

For simplicity, the calculations here are restricted to a gravitational potential with axial symmetry,

$$\varphi = \varphi(r,\theta)\,, \tag{2.71}$$

where r is the distance from the center of mass, and the vector field V_i is truncated at

leading-order in the multipole expansion, cf. Eq. (2.56). One then has

$$V_i = \frac{1}{2r^3}\varepsilon_{ikl}J^k x^l\,, \tag{2.72}$$

where J_i is the vector of total angular momentum, which is assumed to be aligned with the symmetry axis of the potential φ. Using spherical coordinates (r,θ,ϕ) whose north pole is aligned with the unit vector directed along J_i, the metric tensor takes the form

$$\begin{aligned}{}^{(4)}g = &-(1+2\varphi)\mathrm{d}T^2 - \tfrac{1}{2}[4(1+\gamma_{\mathrm{PPN}})+\alpha_{\mathrm{PPN}}]Jr^{-1}\sin^2\theta\,\mathrm{d}T\,\mathrm{d}\phi \\ &+[1-2\gamma_{\mathrm{PPN}}\varphi][\mathrm{d}r^2+r^2\mathrm{d}\theta^2+r^2\sin^2\theta\,\mathrm{d}\phi^2]\,.\end{aligned} \tag{2.73}$$

The transition to rotating coordinates is then accomplished by the substitution $\phi \to \phi + \Omega_\infty T$, where Ω_∞ is the coordinate angular frequency, i.e., the angular frequency as seen from far away. This leads to the metric

$$\begin{aligned}{}^{(4)}g = &-\left[1+2\varphi+\tfrac{1}{2}[4(1+\gamma_{\mathrm{PPN}})+\alpha_{\mathrm{PPN}}]J\Omega_\infty r^{-1}\sin^2\theta-(1-2\gamma_{\mathrm{PPN}}\varphi)\Omega_\infty^2 r^2\sin^2\theta\right]\mathrm{d}T^2 \\ &+2\left[(1-2\gamma_{\mathrm{PPN}}\varphi)\Omega_\infty r^2-(1+\gamma_{\mathrm{PPN}}+\tfrac{1}{4}\alpha_{\mathrm{PPN}})Jr^{-1}\right]\sin^2\theta\,\mathrm{d}T\,\mathrm{d}\phi \\ &+[1-2\gamma_{\mathrm{PPN}}\varphi][\mathrm{d}r^2+r^2\mathrm{d}\theta^2+r^2\sin^2\theta\,\mathrm{d}\phi^2]\,.\end{aligned} \tag{2.74}$$

World-lines of material points on Earth's surface can then be modeled as curves of constant spatial coordinates (r,θ,ϕ). An adapted orthonormal frame is given by

$$\mathfrak{e}_0 = \frac{1}{\sqrt{-{}^{(4)}g_{TT}}}\partial_T\,, \qquad \mathfrak{e}_r = \frac{1}{\sqrt{{}^{(4)}g_{rr}}}\partial_r\,, \tag{2.75}$$

$$\mathfrak{e}_\theta = \frac{1}{\sqrt{{}^{(4)}g_{\theta\theta}}}\partial_\theta\,, \qquad \mathfrak{e}_\phi = \frac{1}{\sqrt{{}^{(4)}g_{\phi\phi}-\frac{({}^{(4)}g_{T\phi})^2}{{}^{(4)}g_{TT}}}}\left(\partial_\phi - \frac{{}^{(4)}g_{T\phi}}{{}^{(4)}g_{TT}}\partial_T\right)\,. \tag{2.76}$$

The vector $\mathfrak{e}_0$ is the normalized four-velocity of world-lines that have constant spatial coordinates, $\mathfrak{e}_r$ and $\mathfrak{e}_\theta$ are unit vectors in the radial and polar directions, respectively, and $\mathfrak{e}_\phi$ is a unit vector in the azimuthal direction, which contains a ∂_T-contribution due to the rotation of the coordinate grid and the frame-dragging effect.

This frame can be related to a quasi-Cartesian frame by

$$\begin{pmatrix}\mathfrak{e}_x\\ \mathfrak{e}_y\\ \mathfrak{e}_z\end{pmatrix} = \begin{pmatrix}\sin\theta\cos\phi & \cos\theta\cos\phi & -\sin\phi\\ \sin\theta\sin\phi & \cos\theta\sin\phi & \cos\phi\\ \cos\theta & -\sin\theta & 0\end{pmatrix}\begin{pmatrix}\mathfrak{e}_r\\ \mathfrak{e}_\theta\\ \mathfrak{e}_\phi\end{pmatrix}\,, \tag{2.77}$$

in which the acceleration vector takes the form

$$\boldsymbol{a} = \boldsymbol{\nabla}\varphi + \boldsymbol{\Omega}_\infty \times \boldsymbol{v} + O(\varepsilon_{\mathrm{PPN}}^{3/2})\,, \tag{2.78}$$

where gradients and cross products are as in flat space, $\boldsymbol{\Omega}_\infty = \Omega_\infty \mathfrak{e}_z$, and $\boldsymbol{v} = \boldsymbol{\Omega}_\infty \times \boldsymbol{R}$.

The first term in Eq. (2.78) is the acceleration that compensates for the gravitational attraction towards the central mass, and the second term is the centripetal acceleration caused by rotation. Furthermore, the rotation vector takes the form

$$\boldsymbol{\Omega} = \boldsymbol{\Omega}_0 + \boldsymbol{\Omega}_{\mathrm{Th}} + \boldsymbol{\Omega}_{\mathrm{dS}} + \boldsymbol{\Omega}_{\mathrm{LT}} + O(\varepsilon_{\mathrm{PPN}}^{3/2}) \,, \tag{2.79}$$

where

$$\boldsymbol{\Omega}_0 = (1 - \varphi + \tfrac{1}{2}\boldsymbol{v}^2)\boldsymbol{\Omega}_\infty \,, \tag{2.80a}$$

$$\boldsymbol{\Omega}_{\mathrm{Th}} = \tfrac{1}{2}\boldsymbol{v} \times \boldsymbol{a} \,, \tag{2.80b}$$

$$\boldsymbol{\Omega}_{\mathrm{dS}} = (\tfrac{1}{2} + \gamma_{\mathrm{PPN}})\boldsymbol{v} \times \boldsymbol{\nabla}\varphi \,, \tag{2.80c}$$

$$\boldsymbol{\Omega}_{\mathrm{LT}} = -(1 + \gamma_{\mathrm{PPN}} + \tfrac{1}{4}\alpha_{\mathrm{PPN}})\boldsymbol{\nabla} \times \boldsymbol{V} \,. \tag{2.80d}$$

The term $\boldsymbol{\Omega}_0$ can be interpreted as the angular velocity, corrected by gravitational and kinematic time dilation, $\boldsymbol{\Omega}_{\mathrm{TS}}$ and $\boldsymbol{\Omega}_{\mathrm{dS}}$ encode the Thomas precession and the de Sitter effect, respectively, and $\boldsymbol{\Omega}_{\mathrm{LT}}$ accounts for the Lense–Thirring effect caused by frame-dragging [5; 85]. Note that the decomposition of the sum $\boldsymbol{\Omega}_{\mathrm{Th}} + \boldsymbol{\Omega}_{\mathrm{dS}}$ can be ambiguous since the de Sitter precession itself is sometimes interpreted as a "Thomas precession caused by gravitation" [86, p. 237] or decomposed into a Thomas precession term and a curvature term [87, p. 136; 88, p. 235]. For the present purposes, however, the decomposition of $\boldsymbol{\Omega}$ is not essential.

With these results for the kinematic quantities $\boldsymbol{a}$ and $\boldsymbol{\Omega}$, one can compute the metric tensor in Fermi coordinates according to either Eq. (2.67) or Eq. (2.68). If curvature terms are neglected, one obtains

$${}^{(4)}g \approx -(1 - 2a_i x^i)\mathrm{d}t^2 + 2\varepsilon_{ijk}\Omega^j x^k \mathrm{d}t\,\mathrm{d}x^i + \delta_{ij}\mathrm{d}x^i\mathrm{d}x^j \,. \tag{2.81}$$

This simple expression already captures the main non-inertial effects relevant to photon interferometry on Earth: a_i describes the gravitational acceleration and the centrifugal acceleration due to Earth's spin, and Ω_i accounts for both the rotation of the coordinate system and the Lense–Thirring effect.

It is worth noting that the expression for the metric tensor in Eq. (2.81) depends (apart from the neglected curvature terms) solely on the local acceleration $\boldsymbol{a}$ and the rotation vector $\boldsymbol{\Omega}$. This is a manifestation of the equivalence principle, as it shows that all curves with the same values of $\boldsymbol{a}$ and $\boldsymbol{\Omega}$ are locally indistinguishable, regardless of whether they even lie in the same space-time manifold.

As discussed more extensively in Chapter 5, the acceleration term gives rise to the gravitational redshift, and the rotation term gives rise to the Sagnac effect in optical interferometers.

Chapter 3

Classical Optics

Having formulated a model of the gravitational field, the next step towards a description of the interaction of gravity and light is the formulation of a model for optics. The main model applied in this document is based on Maxwell's equations. Here, this term refers not to the equations as Maxwell originally formulated them, but to their generalization to curved space-times that can be expressed either as first-order equations for the electromagnetic field strength or as second-order equations for the electromagnetic potential. Section 3.1 describes the field-strength formulation of these equations in vacuo and in linear isotropic dielectrics (as will be considered in later chapters). The constitutive equations in this setting are commonly formulated using Gordon's optical metric (defined in Eq. (3.10) below), but can also be described using an alternative optical metric that is conformally related to Gordon's metric (see Eq. (3.12) below). At the level of field strengths, the choice of optical metric makes little difference, but at the level of the electromagnetic potential they lead to different generalizations of the Lorenz gauge condition to linear isotropic dielectrics. Section 3.2 presents gauge-fixed field equations based on such a generalized Lorenz gauge that makes use of the newly introduced optical metric. These equations serve as the basis of the Gupta–Bleuler quantization scheme described in Chapter 4.

In addition to the wave-optics considerations in Sections 3.1 and 3.2, Section 3.3 provides a description of geometrical optics in curved space-times that applies both to light propagation in vacuo and in linear isotropic media. The eikonal equation arising there provides useful insights into light propagation in scenarios where diffraction is negligible. In particular, as shown in Chapter 5, this equation provides a good estimate for the evolution of the electromagnetic phase in single-mode optical fibers.

3.1 Maxwell's Equations – Field-Strength Formulation

At the level of field strengths, electrodynamics in curved space-times can be regarded as a theory of (i) a two-form $F_{\mu\nu}$, called the electromagnetic field strength, (ii) an antisymmetric two-contravariant tensor field $G^{\mu\nu}$, called the electromagnetic excitation, and (iii) a divergence-free vector field j^{μ}, the electric four-current. These fields are assumed

to satisfy Maxwell's equations in curved space-time

$$(\mathrm{d}F)_{\mu\nu\rho} = 0\,, \tag{3.1}$$
$$^{(4)}\nabla_\mu G^{\mu\nu} + j^\nu = 0\,, \tag{3.2}$$

which must be supplemented by constitutive equations that determine $G^{\mu\nu}$ in terms of $F_{\mu\nu}$ (or vice-versa). In vacuo, the constitutive equations are given by

$$G^{\mu\nu} = {}^{(4)}g^{\mu\rho}\,{}^{(4)}g^{\nu\sigma}F_{\rho\sigma}\,, \tag{3.3}$$

so that $G^{\mu\nu}$ and $F_{\mu\nu}$ are metrically equivalent.

The metric tensor ${}^{(4)}g_{\mu\nu}$, which encodes the gravitational field, thus enters Maxwell's equations in two ways: once via the constitutive equation (3.3), and once via the Levi-Civita connection in the inhomogeneous Maxwell equation (3.2). Whereas Eq. (3.3) only applies in vacuo, more general constitutive equations typically also depend on the space-time metric.

Experimental setups at the interface of optics and gravitation typically involve light propagation in vacuo or optical fibers. For example, the light rays in gravitational wave detectors such as LIGO, Virgo, and KAGRA propagate in vacuo, and many proposals for gravitational quantum interferometry rely on light propagation in optical fibers to obtain sufficiently long interaction times of the photons with Earth's gravitational field.

3.1.1 Linear Isotropic Media

Optical fibers are typically modeled as linear isotropic dielectrics. For such materials, the formulation of Maxwell's equations is particularly simple. However, such equations are not always accurate: the model assumptions of isotropy and linearity are often violated as fiber bending induces optical anisotropies through photoelasticity and optical fibers are not perfectly linear, leading, i.a., to the Kerr effect [89; 90]. However, these effects are not essential to the understanding of the interaction of light with gravitation and are thus neglected in this document.

An electromagnetic medium is said to be linear if the excitation $G^{\mu\nu}$ depends linearly on the field strength $F_{\mu\nu}$, i.e., there is a tensor field $\chi^{\mu\nu\rho\sigma}$, called the constitutive tensor field, such that

$$G^{\mu\nu} = \chi^{\mu\nu\rho\sigma}F_{\rho\sigma}\,, \tag{3.4}$$

where $\chi^{\mu\nu\rho\sigma}$ has the symmetries of an "algebraic curvature tensor":

$$\chi^{\mu\nu\rho\sigma} = -\chi^{\nu\mu\rho\sigma}\,, \qquad \chi^{\mu\nu\rho\sigma} = -\chi^{\mu\nu\sigma\rho}\,, \qquad \chi^{\mu\nu\rho\sigma} = +\chi^{\rho\sigma\mu\nu}\,. \tag{3.5}$$

Anti-symmetry in the first and last pair of indices accounts for the anti-symmetry of $G^{\mu\nu}$ and $F_{\mu\nu}$, respectively, and the pair-exchange symmetry arises naturally in variational

formulations, see Section 3.2 below and also Ref. [91] for further discussion of these symmetry properties. In this sense, vacuum can be regarded as a linear medium with constitutive tensor $\chi^{\mu\nu\rho\sigma}_{\text{vac.}} = \frac{1}{2}({}^{(4)}g^{\mu\rho}{}^{(4)}g^{\nu\sigma} - {}^{(4)}g^{\mu\sigma}{}^{(4)}g^{\nu\rho})$.

In linear isotropic media with permittivity ε, permeability μ, and four-velocity u^μ, the constitutive tensor is given by

$$\begin{aligned}\chi^{\mu\nu\rho\sigma} &= \tfrac{1}{2}\mu^{-1}[\ell^{\mu\rho}\ell^{\nu\sigma} - \ell^{\mu\sigma}\ell^{\nu\rho}] \\ &\quad + \tfrac{1}{2}\varepsilon^{+1}[u^\mu\ell^{\nu\rho}u^\sigma - u^\mu\ell^{\nu\sigma}u^\rho + u^\nu\ell^{\mu\sigma}u^\rho - u^\nu\ell^{\mu\rho}u^\sigma]\,,\end{aligned} \tag{3.6}$$

where $\ell^{\mu\nu}$ is the (contravariant) Landau–Lifshitz metric $\ell^{\mu\nu} = {}^{(4)}g^{\mu\nu} + u^\mu u^\nu$.

The physical interpretation of the above constitutive relation can be understood as follows: The field strength $F_{\mu\nu}$ and excitation $G^{\mu\nu}$ can be decomposed into the electric and magnetic fields E_μ, D^μ, $B_{\mu\nu}$, $H^{\mu\nu}$, relative to the four-velocity u^μ, via the equations

$$F_{\mu\nu} = u_\mu E_\nu - E_\mu u_\nu + B_{\mu\nu}\,, \tag{3.7}$$

$$G^{\mu\nu} = u^\mu D^\nu - D^\mu u^\nu + H^{\mu\nu}\,. \tag{3.8}$$

Here, the fields E_μ, D^μ, $B_{\mu\nu}$, $H^{\mu\nu}$ are all orthogonal to u^μ. The constitutive relation (3.4) with the constitutive tensor given in Eq. (3.6) then takes the form

$$D^\mu = \varepsilon\,{}^{(4)}g^{\mu\nu}E_\nu\,, \qquad\qquad B_{\mu\nu} = \mu\,{}^{(4)}g_{\mu\rho}{}^{(4)}g_{\nu\sigma}H^{\rho\sigma}\,, \tag{3.9}$$

which coincides with the standard constitutive relations for linear isotropic media, expressed in the rest frame [92, Sect. 6.1].

In Ref. [52], Gordon defined a contravariant optical metric

$$\bar{g}^{\mu\nu} = {}^{(4)}g^{\mu\nu} + (1 - n^2)u^\mu u^\nu\,, \tag{3.10}$$

where $n = \sqrt{\varepsilon\mu}$ is the refractive index. With this definition, the constitutive tensor for linear isotropic media can be written as

$$\chi^{\mu\nu\rho\sigma} = \frac{1}{2\mu}[\bar{g}^{\mu\rho}\bar{g}^{\nu\sigma} - \bar{g}^{\mu\sigma}\bar{g}^{\nu\rho}]\,. \tag{3.11}$$

For the present purposes, it proves advantageous not to define the optical metric by Gordon's expression (3.10), but to use the conformally related contravariant metric

$$\tilde{g}^{\mu\nu} = \frac{1}{\sqrt{\mu}}\bar{g}^{\mu\nu} = \frac{1}{\sqrt{\mu}}({}^{(4)}g^{\mu\nu} + u^\mu u^\nu) - \sqrt{\mu}\varepsilon\,u^\mu u^\nu\,. \tag{3.12}$$

Using this optical metric, the constitutive tensor can be written as

$$\chi^{\mu\nu\rho\sigma} = \tfrac{1}{2}[\tilde{g}^{\mu\rho}\tilde{g}^{\nu\sigma} - \tilde{g}^{\mu\sigma}\tilde{g}^{\nu\rho}]\,. \tag{3.13}$$

Optical Formulation Denoting by $\tilde{\nabla}_\mu$ the optical derivative, i.e., the Levi-Civita connection of the covariant optical metric

$$\tilde{g}_{\mu\nu} = \sqrt{\mu}({}^{(4)}g_{\mu\nu} + u_\mu u_\nu) - \frac{1}{\varepsilon\sqrt{\mu}} u_\mu u_\nu \,, \tag{3.14}$$

and using the fact that $\sqrt{-{}^{(4)}g}/\sqrt{-\tilde{g}} = \sqrt{\varepsilon/\mu}$, Eq. (3.2) is seen to be equivalent to

$$\tilde{\nabla}_\mu G^{\mu\nu} - G^{\mu\nu}\tilde{\nabla}_\mu \ln\eta + j^\nu = 0 \,, \tag{3.15}$$

where η is the wave impedance

$$\eta = \sqrt{\mu/\varepsilon} \,. \tag{3.16}$$

As a consequence, the electromagnetic field strength $F_{\mu\nu}$ satisfies the wave equation

$$\tilde{\Box} F_{\mu\nu} + 2\tilde{R}_{[\mu}{}^{\alpha} F_{\nu]\alpha} + 2\tilde{R}_{[\mu}{}^{\alpha}{}_{\nu]}{}^{\beta} F_{\alpha\beta} = 2\tilde{g}_{\alpha[\mu}\tilde{\nabla}_{\nu]}(j^\alpha + G^{\alpha\beta}\tilde{\nabla}_\beta \ln\eta) \,, \tag{3.17}$$

where $\tilde{\Box} = \tilde{g}^{\mu\nu}\tilde{\nabla}_\mu\tilde{\nabla}_\nu$ is the optical d'Alembertian, $\tilde{R}_{\mu\nu\rho\sigma}$ and $\tilde{R}_{\mu\nu}$ are the optical Riemann and Ricci tensors, respectively, i.e., the curvature tensors derived from the optical metric defined in Eq. (3.14), and square brackets indicate the anti-symmetrization of indices.

The optical metric $\tilde{g}^{\mu\nu}$ thus determines the principal symbol of the wave equation satisfied by the electromagnetic field in isotropic media. Additionally, if the impedance η is constant, the electromagnetic field $F_{\mu\nu}$ in the medium satisfies a wave equation that is identical to the corresponding wave equation in vacuo where the space-time metric ${}^{(4)}g_{\mu\nu}$ is replaced by the optical metric $\tilde{g}_{\mu\nu}$.

If, instead of using the optical metric as defined in Eq. (3.12), one uses Gordon's optical metric $\bar{g}^{\mu\nu}$ as defined in Eq. (3.10), together with its associated derivative $\bar{\nabla}_\nu$ and curvature tensors $\bar{R}_{\mu\nu\rho\sigma}$ and $\bar{R}_{\mu\nu}$, the wave equation takes the form

$$\bar{\Box} F_{\mu\nu} + 2\bar{R}_{[\mu}{}^{\alpha} F_{\nu]\alpha} + 2\bar{R}_{[\mu}{}^{\alpha}{}_{\nu]}{}^{\beta} F_{\alpha\beta} = 2\bar{g}_{\alpha[\mu}\bar{\nabla}_{\nu]}(\mu j^\alpha + \mu G^{\alpha\beta}\bar{\nabla}_\beta \ln\eta) \,. \tag{3.18}$$

The comparison of Eq. (3.17) with Eq. (3.18) illustrates the advantage of defining the optical metric according to Eq. (3.12) over Gordon's expression given in Eq. (3.10): whereas Eq. (3.17) reduces to the "standard form" of the wave equation (as described above) whenever the wave impedance η is constant, Eq. (3.18) does so only under the further requirement that $\mu = 1$. This is related to the fact that, in regions of constant wave impedance η, the continuity equation ${}^{(4)}\nabla_\mu j^\mu = 0$ implies that j^μ is also divergence-free in the optical metric $\tilde{g}^{\mu\nu}$ ($\tilde{\nabla}_\mu j^\mu = 0$) but not in the Gordon metric $\bar{g}^{\mu\nu}$ as $\bar{\nabla}_\mu j^\mu = -j^\nu(\mathrm{d}\ln\mu)_\nu$.

Interface Conditions The above method of expressing the field equations using optical derivatives fails at material interfaces where the permeability μ and permittivity ε are discontinuous. For such interfaces, Maxwell's equations imply matching conditions for

the electromagnetic field. To study these interface conditions, consider a hypersurface with spacelike unit co-normal ν_μ, across which $\tilde{g}^{\mu\nu}$ is discontinuous. Denoting by $[\![F]\!]_{\mu\nu}$ and $[\![G]\!]^{\mu\nu}$ the jumps of the electromagnetic field tensors in the direction of ν^μ, Maxwell's equations in the form of Eqs. (3.1) and (3.2) imply the interface conditions

$$[\![F]\!]_{[\mu\nu}\nu_{\rho]} = 0\,, \tag{3.19a}$$

$$[\![G]\!]^{\mu\rho}\nu_\rho = \jmath^\mu\,, \tag{3.19b}$$

where $\jmath^\mu$ is the density of surface charges and surface currents,[(1)] see Ref. [49, Sect. D] for an explicit derivation. This provides a generally covariant formulation of the standard junction conditions for the electromagnetic field that are commonly stated only in terms of the electric and magnetic fields and excitations [92, Sect. 6.1; 93, Sect. I.5].

Together, these interface conditions provide six independent equations. Hence, if the electromagnetic field $F_{\mu\nu}$ (with its six independent degrees of freedom) is known at one side of a material interface, the value of $F_{\mu\nu}$ on the other side of the interface is fully determined by the surface charges and currents encoded in $\jmath^\mu$.

Applications The equations described in this section form the basis of the analysis of the influence of Earth's rotation on light in Ref. [94] and of the effect of gravitational waves on light, propagating either in free space or in optical fibers, as described in Refs. [95; 96].

3.2 Maxwell's Equations – Gauge Formulation

As an alternative to the field-strength formulation, one may express Maxwell's equations as a U(1)-gauge theory based on a gauge potential A_μ, such that the field strength $F_{\mu\nu}$ is identified with the curvature of the U(1)-connection one-form A_μ:

$$F_{\mu\nu} = (\mathrm{d}A)_{\mu\nu} = {}^{(4)}\nabla_\mu A_\nu - {}^{(4)}\nabla_\nu A_\mu\,. \tag{3.20}$$

In this formulation, the homogeneous Maxwell equation (3.1) is identically satisfied as the repeated application of the exterior derivative, d, to any differential form vanishes. The field A_μ may be either regarded as a "fundamental field" [92], or one may consider A_μ as being derived from $F_{\mu\nu}$ under the assumption that (3.1) holds. The latter is made possible by Poincaré's lemma, which states that on any smoothly contractible region (in particular, in star-shaped coordinate patches), every closed differential form is exact. Independent of the point of view taken here, the field A_μ has a "gauge freedom," meaning that one may redefine

$$A_\mu \to A_\mu + (\mathrm{d}\lambda)_\mu\,, \tag{3.21}$$

[(1)] These equations are independent of the surface's orientation, as a reversal of the orientation implies both $\nu_\mu \to -\nu_\mu$ and $[\![\,\cdot\,]\!] \to -[\![\,\cdot\,]\!]$.

where λ is any smooth function, and fields related by such a gauge transformation are regarded as physically equivalent.

A consequence of the gauge ambiguity is that Maxwell's equations per se do not provide a well-posed initial value problem for the potential A_μ. This can be dealt with in multiple ways that are here referred to as the *reduction method* and the *extension method.*

Reduction Method The starting point of the reduction method is a system of gauge conditions (written abstractly as $\chi = 0$) that are restrictive enough to fix the gauge uniquely. Further, one requires that the *reduced Maxwell equations*, defined as the restriction of Maxwell's equations to those gauge-fixed potentials A_μ, give rise to a well-posed Cauchy problem for the gauge-fixed fields with initial data uniquely determined from the initial values of $F_{\mu\nu}$ and j^μ. In this case, one obtains a bijection between (i) initial values of the electromagnetic field strength and current and (ii) solutions to Maxwell's equations up to gauge transformations.

Extension Method The extension method, on the other hand, does not require such restrictive gauge conditions χ. Instead, the starting point of the extension method is the formulation of a set of *extended field equations* that agree with Maxwell's equations under the condition of $\chi = 0$ but constitute a well-posed Cauchy problem for the potential A_μ without any restriction on the initial data. If the gauge condition $\chi = 0$ is preserved under the evolution of the extended equations, one obtains a bijection between (i) the subset of initial data for the extended equations that is compatible with the gauge condition $\chi = 0$, and (ii) solutions to Maxwell's equations up to gauge transformations.

Comparison The main differences between Maxwell's equations and the extended and reduced systems are summarized in Table 3.1. One key distinction between the reduction method and the extension method lies in the fact that the respective evolution equations are defined on different spaces of fields. In the reduction method, time evolution takes place in the space of fields satisfying a "strong" gauge condition, so that initial data is *a priori* constrained. The extension method, however, formulates field equations that are defined for all possible initial data, and the restriction to Cauchy data satisfying a gauge condition is done only *a posteriori.*

To illustrate the distinction between the reduction method and the extension method, consider Maxwell's equations in Minkowski space-time and compare the Coulomb gauge ($\chi = {}^{(3)}g^{ij}\,{}^{(3)}\nabla_i A_j$) with the Lorenz gauge ($\chi = {}^{(4)}g^{\mu\nu}\,{}^{(4)}\nabla_\mu A_\nu$). The Coulomb condition determines the potential A_μ uniquely,[(2)] and the reduced equations comprise the Poisson equation for the scalar potential and an inhomogeneous wave equation for the vector

[(2)] More precisely, initial data for A_μ is uniquely determined by the initial values of $F_{\mu\nu}$ and j^μ. Using global pseudo-orthonormal coordinates as well as the notation $(A_\mu) = (-\varphi, \boldsymbol{A})$ and $(j^\mu) = (\varrho, \boldsymbol{j})$, such Cauchy data is of the form $(\varphi, \dot\varphi, \boldsymbol{A}, \dot{\boldsymbol{A}})$ satisfying $\Delta\varphi = -\varrho$, $\Delta\dot\varphi = \boldsymbol{\nabla}\cdot\boldsymbol{j}$, $\Delta\boldsymbol{A} = -\boldsymbol{\nabla}\times\boldsymbol{B}$, and $\Delta\dot{\boldsymbol{A}} = \boldsymbol{\nabla}\varrho - \Delta\boldsymbol{E}$ at a given time t_0. As these equations are elliptic, their solutions are unique if suitable spatial decay properties are imposed.

	Extended equations	Maxwell's equations	Reduced equations
Cauchy problem	Well-posed	Ill-posed	Well-posed
Cauchy data	Unconstrained		Constrained
Ghost solutions	Yes	No	No
Gauge solutions	Yes	Yes	No

Table 3.1: Comparison of Maxwell's equations with the extended and reduced field equations. Whereas Maxwell's equations per se do not provide a well-posed Cauchy problem for A_μ, the extended equations yield a deterministic evolution for arbitrary initial data, and the reduced system does so for constrained initial data. The extended system has more solutions than Maxwell's equations, which are referred to as ghost solutions. The reduced system, on the other hand, has fewer solutions than Maxwell's equations: the difference lies in pure-gauge solutions that are considered physically trivial.

potential subject to the Coulomb gauge constraint. As this gauge condition is preserved by the wave equation, solutions to Maxwell's equations can be constructed from initial data satisfying the Coulomb gauge by evolving this data in time according to the reduced equations. The Lorenz gauge condition, on the other hand, does not fix the gauge uniquely,[3] so the reduction method cannot be applied. However, the extension method works if one takes as extended equations the wave equation of one-forms: ${}^{(4)}g^{\rho\sigma}\,{}^{(4)}\nabla_\rho\,{}^{(4)}\nabla_\sigma A_\mu = 0$. This equation is equivalent to Maxwell's equations for those potentials that satisfy the Lorenz gauge but provides a well-posed Cauchy problem independent of this gauge condition.

At face value, the extended field equations allow for more degrees of freedom than the reduced Maxwell equations. In particular, the former generally admit *gauge modes*, i.e., solutions of the extended equations that are exact one-forms (they are thus gauge-equivalent to zero and hence physically trivial) as well as *ghost modes*, i.e., solutions to the extended equations that violate the gauge condition. If the extended equations imply a well-posed evolution equation for the gauge function, the distinction between physical modes and ghost modes can be made at the level of initial data.

The reduction method is commonly used in Hamiltonian analyses of Maxwell's equations, see, e.g., Ref. [97, Sect. E.2], and in textbooks on quantum optics [98, Chap. 4; 99, Chap. 2; 100, Chap. 10]. The extension method, on the other hand, is more commonly used in particle physics [101, Chap. 7; 102, Sect. 3-2] and has, so far, not been used in the study of gravitational effects on light. In quantum theory, the reduction method leads to the reduced-phase-space quantization, whereas the extension method leads to the Gupta–Bleuler quantization (described in Chapter 4 below).

[3] Indeed, if $(\varphi, \dot\varphi, \boldsymbol{A}, \dot{\boldsymbol{A}})$ is any Cauchy data corresponding to given initial values of $F_{\mu\nu}$ and j^μ that satisfies $\chi = 0$ initially, then another such set of Cauchy data is given by $(\varphi - \kappa, \dot\varphi - \Delta\lambda, \boldsymbol{A} + \boldsymbol{\nabla}\lambda, \dot{\boldsymbol{A}} + \boldsymbol{\nabla}\kappa)$, where κ and λ are arbitrary functions (with suitable decay properties). As a consequence, initial values of $F_{\mu\nu}$ and j^μ do not determine unique Cauchy data for A_μ.

3.2.1 Gauge-Fixed Field Equations

In the following, Maxwell's equations for the gauge potential A_μ are studied using the extension method. The motivation for this is three-fold.

- The extension method allows working with the fully covariant Lorenz gauge (or generalizations thereof), whereas the reduction method typically necessitates further structure (for example, the Coulomb gauge requires a preferred foliation).
- For the extended field equations, a consistent quantization scheme (based on the Gupta–Bleuler method) is known for generally curved space-times (under the assumption of global hyperbolicity).
- The use of the potential A_μ facilitates the comparison with models for massive electrodynamics, which are commonly formulated using Proca's equation for a massive vector field.

The presence of gauge and ghost modes may be considered a downside of the extension method. It has been shown, however, that such artifacts are unavoidable in manifestly covariant quantization schemes [103–106].

Lagrangian One method for obtaining gauge-fixed field equations in the extension method is to consider the Euler–Lagrange equations of a gauge-fixed Lagrangian.

In vacuo, extended field equations based on the Lorenz gauge are commonly derived from the R_ξ-gauge-fixed Lagrangian

$$\mathrm{L}_{\text{vac.}} = -\tfrac{1}{4}\,{}^{(4)}g^{\mu\nu}\,{}^{(4)}g^{\rho\sigma}F_{\mu\rho}F_{\nu\sigma} - \tfrac{1}{2\xi}\chi_{\text{vac.}}^2 + A_\mu j^\mu\,, \tag{3.22}$$

where

$$\chi_{\text{vac.}} = {}^{(4)}g^{\mu\nu}\,{}^{(4)}\nabla_\mu A_\nu\,, \tag{3.23}$$

and ξ is a constant, see, e.g., Ref. [107, Sect. 2.6]. The corresponding field equations then take the form

$$\Box A_\mu - {}^{(4)}R_\mu{}^\nu A_\nu - \left(1 - \tfrac{1}{\xi}\right){}^{(4)}\nabla_\mu({}^{(4)}g^{\rho\sigma}\,{}^{(4)}\nabla_\rho A_\sigma) + {}^{(4)}g_{\mu\nu}j^\nu = 0\,, \tag{3.24}$$

where $\Box = {}^{(4)}g^{\mu\nu}\,{}^{(4)}\nabla_\mu\,{}^{(4)}\nabla_\nu$ is the d'Alembertian and ${}^{(4)}R_{\mu\nu}$ is the Ricci tensor of ${}^{(4)}g_{\mu\nu}$. In particular, in the Feynman–'t Hooft gauge

$$\xi = 1\,, \tag{3.25}$$

one obtains

$$\Box A_\mu - {}^{(4)}R_\mu{}^\nu A_\nu + {}^{(4)}g_{\mu\nu}j^\nu = 0\,. \tag{3.26}$$

An extension to linear isotropic dielectrics is provided by the Lagrangian

$$\mathrm{L} = -\tfrac{1}{4}\tilde{g}^{\mu\nu}\tilde{g}^{\rho\sigma}F_{\mu\rho}F_{\nu\sigma} - \tfrac{1}{2\xi}\chi^2 + A_\mu j^\mu\,, \tag{3.27}$$

where $\tilde{g}^{\mu\nu}$ is the optical metric defined in Eq. (3.12) and χ is the gauge function

$$\chi = \tfrac{1}{\sqrt{\mu}}{}^{(4)}\nabla_\mu(\sqrt{\mu}\,\tilde{g}^{\mu\nu}A_\nu)\,, \tag{3.28}$$

which generalized previous gauge functions considered for inertial media in flat space-time [108–110], general linear media in flat space-time [111–113], as well as linear media with $\mu = 1$ in curved space-time [49]. It differs, however, from the gauge function considered in Ref. [114] for static problems in curved space-times, where the factor $\sqrt{\mu}$ is replaced by $\varepsilon\sqrt{\mu}$. The reason for the specific choice of the factor $\sqrt{\mu}$ is explained below. The corresponding field equations take the form

$${}^{(4)}\nabla_\mu G^{\mu\nu} + \tfrac{\sqrt{\mu}}{\xi}\tilde{g}^{\mu\nu}{}^{(4)}\nabla_\mu(\chi/\sqrt{\mu}) + j^\nu = 0\,, \tag{3.29}$$

which are equivalent to Maxwell's equations (3.2) if $\chi = 0$. In local coordinates, the extended Maxwell equations (3.29) are of the form

$$\tilde{g}^{\rho\sigma}\partial_\rho\partial_\sigma A_\mu - \left(1 - \tfrac{1}{\xi}\right)\tilde{g}^{\rho\sigma}\partial_\mu\partial_\rho A_\sigma + (\text{lower-order terms}) = (\text{source terms})\,. \tag{3.30}$$

In the Feynman–'t Hooft gauge, one thus obtains the manifestly hyperbolic equation

$$\tilde{g}^{\rho\sigma}\partial_\rho\partial_\sigma A_\mu + (\text{lower-order terms}) = (\text{source terms})\,. \tag{3.31}$$

Under the assumption of sufficient regularity of $\tilde{g}^{\mu\nu}$, Eq. (3.29) with $\xi = 1$ thus provides a well-posed Cauchy problem. Furthermore, Eq. (3.29) implies the following evolution equation for the gauge function χ:

$${}^{(4)}\nabla_\mu[\sqrt{\mu}\tilde{g}^{\mu\nu}{}^{(4)}\nabla_\nu(\chi/\sqrt{\mu})] = 0\,, \tag{3.32}$$

which is the Euler–Lagrange equation of the Lagrangian

$$\mathrm{L}' = -\tfrac{1}{2}\sqrt{\mu}\tilde{g}^{\mu\nu}{}^{(4)}\nabla_\mu(\chi/\sqrt{\mu})\,{}^{(4)}\nabla_\nu(\chi/\sqrt{\mu})\,. \tag{3.33}$$

Under the same regularity assumptions as above, Eq. (3.32) implies that initial data for Eq. (3.29) that induce trivial initial data for Eq. (3.32) give rise to solutions that satisfy the gauge condition $\chi = 0$ throughout their entire time of existence. One may thus construct solutions to Maxwell's equations by constructing initial data $(A_\mu, \dot{A}_\mu)$ such that χ and $\dot{\chi}$ vanish initially and then evolve the Cauchy data in time according to Eq. (3.29). Initial data for Eq. (3.29) that violates $\chi = 0$, however, leads to "ghost solutions," i.e., solutions to the extended Maxwell equations that are not solutions to the original Maxwell equations.

Optical Formulation The above formulation of the extended Maxwell equations expresses all derivatives in terms of the space-time derivative ${}^{(4)}\nabla_\mu$, i.e., the Levi-Civita connection of the space-time metric ${}^{(4)}g_{\mu\nu}$. However, in regions where $\tilde{g}^{\mu\nu}$ is sufficiently regular, the field equations also admit an alternative formulation based on "optical derivatives." In particular, if $\tilde{g}_{\mu\nu}$ admits a Levi-Civita connection $\tilde{\nabla}_\mu$ (the optical derivative), the gauge function χ, defined in Eq. (3.28), can be expressed as

$$\chi \equiv \tfrac{1}{\sqrt{\mu}}{}^{(4)}\nabla_\mu(\sqrt{\mu}\,\tilde{g}^{\mu\nu}A_\nu) = \tfrac{1}{\sqrt{\varepsilon}}\tilde{\nabla}_\mu(\sqrt{\varepsilon}\,\tilde{g}^{\mu\nu}A_\nu)\,, \tag{3.34}$$

which follows from $\sqrt{-{}^{(4)}g}/\sqrt{-\tilde{g}} = \sqrt{\varepsilon/\mu}$. Moreover, in regions where $\tilde{g}^{\mu\nu}$ is sufficiently regular as to admit a well-defined curvature tensor $\tilde{R}^\mu{}_{\nu\rho\sigma}$, the field equations can be written in the form

$$\begin{aligned}\tilde{\Box}A_\mu - \tilde{R}_\mu{}^\nu A_\nu - [1-1/\xi][\tilde{\nabla}_\mu(\tilde{g}^{\rho\sigma}\tilde{\nabla}_\rho A_\sigma) + (\tilde{\nabla}^\nu \ln\eta)F_{\nu\mu}] + \tilde{g}_{\mu\nu}j^\nu \\ - \tfrac{1}{\xi}\tilde{g}^{\rho\sigma}[\tilde{\nabla}_\rho A_\mu \tilde{\nabla}_\sigma \ln\eta + A_\rho \tilde{\nabla}_\mu \tilde{\nabla}_\sigma \ln\eta] \\ + \tfrac{1}{\xi}[\tilde{\nabla}_\mu(\tilde{g}^{\rho\sigma}A_\rho\tilde{\nabla}_\sigma \ln\sqrt{\mu}) - \chi\tilde{\nabla}_\mu \ln\sqrt{\mu}] = 0\,,\end{aligned} \tag{3.35}$$

where $\tilde{\Box} = \tilde{g}^{\mu\nu}\tilde{\nabla}_\mu\tilde{\nabla}_\nu$ is the optical d'Alembertian and $\eta = \sqrt{\mu/\varepsilon}$ is the wave impedance. In particular, in the Feynman–'t Hooft gauge (3.25), the field equations in regions of constant ε and μ reduce to

$$\tilde{\Box}A_\mu - \tilde{R}_\mu{}^\nu A_\nu + \tilde{g}_{\mu\nu}j^\nu = 0\,, \tag{3.36}$$

which has the same structure as Eq. (3.26) for vacuo, but with ${}^{(4)}g_{\mu\nu}$ being replaced by $\tilde{g}_{\mu\nu}$.

This equation will be used in Chapter 5 to describe step-index optical fibers in which the permittivity ε and the permeability μ are locally constant. To obtain a global solution, however, the local solutions for the core and cladding must be matched across the core-cladding interface where $\tilde{g}^{\mu\nu}$ is discontinuous.

Interface Conditions As in the field-strength formulation of Maxwell's equations (Section 3.1), a common strategy for solving the field equations in media with discontinuous refractive indices is to solve, first, in the regions of continuous $\tilde{g}^{\mu\nu}$, and then to match them across the surface of discontinuity. The corresponding matching conditions for Eq. (3.29), expressed in the same notation as was used in Eq. (3.19), are

$$[\![A]\!]_\mu = 0\,, \tag{3.37a}$$

$$[\![\chi/\sqrt{\mu}]\!] = 0\,, \tag{3.37b}$$

$$[\![G]\!]^{\mu\rho}\nu_\rho = \jmath^\mu\,. \tag{3.37c}$$

This provides eight independent equations, stating that the potential A_μ is continuous and that discontinuities of derivatives of A_μ are related to discontinuities of $\tilde{g}^{\mu\nu}$ as well as to surface charges and surface currents encoded in $\jmath^\mu$.

As was mentioned above, one might consider variations of the gauge function defined in Eq. (3.28) with different factors inside and outside the derivative. However, the above definition is optimal in the following sense: only with this choice, the field equations in the Feynman-'t Hooft gauge (3.25) reduce, in regions of constant ε and μ, to Eq. (3.36), which is directly analogous to the corresponding equation in vacuo, Eq. (3.26), and, additionally, all the components of A_μ are continuous across material interfaces. The form of the equations (3.36) necessitates that the factors outside and inside the derivative in Eq. (3.28) are inverse to each other and the requirement of $\nu^\mu A_\mu$ being continuous across a material interface with unit normal ν^μ is compatible only with the factors of $\sqrt{\mu}$ given in Eq. (3.28). In Ref. [49], the same situation was considered for the special case where $\mu = 1$, in which case one has $\chi = {}^{(4)}\nabla_\mu(\tilde{g}^{\mu\nu}A_\nu) = {}^{(4)}\nabla_\mu(\bar{g}^{\mu\nu}A_\nu)$, where $\bar{g}^{\mu\nu}$ is Gordon's optical metric defined in Eq. (3.10). The gauge condition $\chi = 0$ with χ defined as in Eq. (3.28) extends this result to arbitrary μ.

Applications The gauge-fixed equations derived here are used in Chapter 5 to describe the propagation of light in optical fibers in a gravitational field. In this case, Eq. (3.36) holds exactly in the core and cladding of a step-index optical fiber and the respective solutions are matched across the core-cladding interface using the junction conditions given in Eq. (3.37). The extended Maxwell equations presented here also serve as the basis of the Gupta–Bleuler quantization of the electromagnetic described in Chapter 4.

3.3 Geometrical Optics

Maxwell's equations provide an established basis for classical electromagnetism. However, being a system of partial differential equations, exact solutions for physically realistic setups are scarce. Approximations are thus needed to make explicit predictions. A widespread approximation scheme geared towards the description of light is geometrical optics.

Formally, geometrical optics can be regarded as a high-frequency limit of Maxwell's equations, which means that the wavelength of light is assumed to be negligibly small compared to all other length scales under consideration [69, Chap. 7; 115, Chap. 3]. One way of expressing this mathematically is to consider the following formal power series ansatz

$$F_{\mu\nu} = \sum_{j=0}^{\infty} \varepsilon^j F_{(j)\mu\nu}\, e^{i\tilde{\Psi}/\varepsilon}\,, \tag{3.38}$$

where ε is considered as a small parameter. The geometrical optics approximation then constitutes the leading-order approximation

$$F^{\mathrm{GO}}_{\mu\nu} = F_{(0)\mu\nu} e^{i\Psi}\,, \tag{3.39}$$

where $\Psi = \tilde{\Psi}/\varepsilon$. The quality of this approximation will be discussed below.

As the precise form of Maxwell's equations depends on the details of the constitutive relations, so do the equations of geometrical optics. However, some general statements can be made on the interpretation of the function Ψ, known as the eikonal, irrespective of such details. The level sets of the eikonal Ψ define three-dimensional surfaces that are referred to as wavefronts. Further, the derivative $k_\mu = (\mathrm{d}\Psi)_\mu$ is referred to as the wave covector, with the interpretation that the integral of k_μ along a curve corresponds to $2\pi \times$ (the number of wavelengths along the curve), which equals the difference in eikonal at the endpoints of the curve. Since k_μ is exact, it is also closed, $(\mathrm{d}k)_{\mu\nu} = 0$, a fact that is known as the Runge–Sommerfeld law [116].

Light rays are then modeled as integral curves of a vector field K^μ along which the eikonal is constant, so $K^\mu k_\mu = 0$. The precise form of K^μ depends on the details of the constitutive equation. Similarly, the equations for $F^{\mathrm{GO}}_{\mu\nu}$ depend on such details. The general pattern of the cases discussed below is that $F^{\mathrm{GO}}_{\mu\nu}$ satisfies algebraic equations involving k_μ and K^μ, as well as transport equations along the field K^μ.

3.3.1 Ray Optics in Vacuo

Inserting the formal power series (3.38) into Maxwell's equations in vacuo, one obtains the eikonal equation

$$ {}^{(4)}g^{\mu\nu}(\mathrm{d}\Psi)_\mu(\mathrm{d}\Psi)_\nu \equiv {}^{(4)}g^{\mu\nu}k_\mu k_\nu = 0\,, \tag{3.40} $$

together with the following equations for $F^{\mathrm{GO}}_{\mu\nu}$:

$$ k_{[\mu}F^{\mathrm{GO}}_{\nu\rho]} = 0\,, \tag{3.41} $$

$$ K^\mu F^{\mathrm{GO}}_{\mu\nu} = 0\,, \tag{3.42} $$

$$ {}^{(4)}\nabla_K F^{\mathrm{GO}}_{\mu\nu} = -\tfrac{1}{2}({}^{(4)}\nabla_\rho K^\rho)F^{\mathrm{GO}}_{\mu\nu}\,, \tag{3.43} $$

where $K^\mu = {}^{(4)}g^{\mu\nu}k_\nu$, see Ref. [117, App. A] for an explicit derivation. In vacuo, light rays thus follow integral curves of K^μ. Using the fact that k_μ is the gradient of Ψ, which satisfies the eikonal equation (3.40), one finds that K^μ satisfies the geodesic equation:

$$ K^{\nu\,(4)}\nabla_\nu K^\mu = {}^{(4)}g^{\mu\rho}K^{\nu\,(4)}\nabla_\rho k_\nu = \tfrac{1}{2}\,{}^{(4)}g^{\mu\rho\,(4)}\nabla_\rho(K^\nu k_\nu) = 0\,. \tag{3.44} $$

In this model, light rays are thus null geodesics along which Ψ is constant.

The algebraic conditions stated in Eqs. (3.41) and (3.42) restrict the degrees of freedom in $F^{\mathrm{GO}}_{\mu\nu}$ to two, which correspond to the two possible polarization states of light. This can be seen as follows. Equation (3.41) implies that $F^{\mathrm{GO}}_{\mu\nu}$ can be written as $F^{\mathrm{GO}}_{\mu\nu} = f_\mu k_\nu - f_\nu k_\mu$, with f_μ encoding only three degrees of freedom as the resulting expression is invariant under the substitution $f_\mu \mapsto f_\mu + \lambda k_\mu$. In combination with the eikonal equation, Eq. (3.42) implies $K^\mu f_\mu = 0$, which reduces the degrees of freedom to two.

The transport equation (3.43) can be analyzed by splitting $F^{\mathrm{GO}}_{\mu\nu}$ into a scalar amplitude

$\mathcal{A}$ and a polarization tensor $\mathcal{F}_{\mu\nu}$ as $F^{\mathrm{GO}}_{\mu\nu} = \mathcal{A}\mathcal{F}_{\mu\nu}$, with $\mathcal{A}$ and $\mathcal{F}_{\mu\nu}$ satisfying the equations

$$
\begin{aligned}
{}^{(4)}\nabla_K \mathcal{A} &= -\tfrac{1}{2}({}^{(4)}\nabla_\mu K^\mu)\mathcal{A}\,, && (3.45)\\
{}^{(4)}\nabla_K \mathcal{F}_{\mu\nu} &= 0\,. && (3.46)
\end{aligned}
$$

This factorization highlights that focussing of light rays (${}^{(4)}\nabla_\mu K^\mu > 0$) leads to the dilution of the amplitude $\mathcal{A}$ and focussing (${}^{(4)}\nabla_\mu K^\mu > 0$) entails an increase in amplitude, whereas the polarization two-form $\mathcal{F}_{\mu\nu}$ is parallel-propagated along the rays under all circumstances. Equation (3.45) can also be written as a conservation law

$$
{}^{(4)}\nabla_\mu(\mathcal{I} K^\mu) = 0\,, \tag{3.47}
$$

where $\mathcal{I} = \mathcal{A}^2$ is the light intensity. As a consequence, one can define an effective stress-energy-momentum tensor $T^{\mu\nu}_{\mathrm{GO}} = \mathcal{I} K^\mu K^\nu$ that is symmetric and divergence-free:

$$
{}^{(4)}\nabla_\mu(\mathcal{I} K^\mu K^\nu) = 0\,. \tag{3.48}
$$

To summarize: geometrical optics models light rays in vacuo as null geodesics along which the eikonal Ψ is constant. The amplitude $\mathcal{A}$ satisfies the transport law (3.45), and the polarization $\mathcal{F}_{\mu\nu}$ satisfies the transport law (3.46) together with the two algebraic constraints (3.41) and (3.42).

3.3.2 Ray Optics in Dielectrics

As shown in Chapter 3, the equations of electrodynamics in linear isotropic dielectrics with constant permeability μ and permittivity ε take the same form as those in vacuo, but with the space-time metric ${}^{(4)}g_{\mu\nu}$ replaced by the optical metric $\tilde{g}_{\mu\nu}$, or equivalently, by Gordon's optical metric $\bar{g}_{\mu\nu}$, which will be used there for notational simplicity. As a consequence, the equations of geometrical optics also take the same form as in the previous section, with the same substitution applied:

$$
\begin{aligned}
\bar{g}^{\mu\nu} k_\mu k_\nu &= 0\,, && (3.49)\\
K^\mu &= \bar{g}^{\mu\nu} k_\nu\,, && (3.50)\\
\bar{\nabla}_K \mathcal{A} &= -\tfrac{1}{2}(\bar{\nabla}_\mu K^\mu)\mathcal{A}\,, && (3.51)\\
\bar{\nabla}_K \mathcal{F}_{\mu\nu} &= 0\,, && (3.52)\\
K^\mu \mathcal{F}_{\mu\nu} &= 0\,, && (3.53)\\
k_{[\mu}\mathcal{F}_{\nu\rho]} &= 0\,. && (3.54)
\end{aligned}
$$

Here, $\bar{\nabla}_\mu$ is the Levi-Civita derivative of Gordon's optical metric $\bar{g}_{\mu\nu}$.

Extensions of these equations to the case of non-constant permittivity ε and permeability μ can be found, e.g., in Refs. [118; 119, Chap. 2]. Whereas non-constant ε and μ lead to correction terms in the transport equations, the eikonal equation remains unchanged.

The fact that geometrical optics in linear dielectrics takes the same form as in vacuo, but with the space-time metric ${}^{(4)}g_{\mu\nu}$ replaced by Gordon's optical metric $\bar{g}_{\mu\nu}$ can be regarded as an instance of analog gravity [120]. By suitable choice of the dielectric's four-velocity u^μ and refractive index n, one may thus probe light propagation in geometries that do not necessarily satisfy Einstein's field equations.

The condition of K^μ being null with respect to $\bar{g}_{\mu\nu} = {}^{(4)}g_{\mu\nu} + (1-n^{-2})u_\mu u_\nu$ is equivalent to the condition that the light rays have a constant velocity $v = 1/n$ relative to the four-velocity u^μ of the dielectric medium:

$$v^2 = \frac{\ell_{\mu\nu}K^\mu K^\nu}{(u_\rho K^\rho)^2} = \frac{({}^{(4)}g_{\mu\nu} + u_\mu u_\nu)K^\mu K^\nu}{(u_\rho K^\rho)^2} = \frac{(\bar{g}_{\mu\nu} + n^{-2}u_\mu u_\nu)K^\mu K^\nu}{(u_\rho K^\rho)^2} = \frac{1}{n^2}\,. \tag{3.55}$$

Anomalous Doppler Effect A notable feature of geometrical optics in dielectrics is that light rays propagate along the vector field $K^\mu = \bar{g}^{\mu\nu}k_\nu$ and not along ${}^{(4)}g^{\mu\nu}k_\nu$. Whereas the former field is timelike (in the space-time metric ${}^{(4)}g_{\mu\nu}$), the latter is spacelike:

$${}^{(4)}g_{\mu\nu}K^\mu K^\nu = (n^{-2}-1)(u^\mu k_\mu)^2 < 0\,, \tag{3.56}$$

$${}^{(4)}g^{\mu\nu}k_\mu k_\nu = (n^{+2}-1)(u^\mu k_\mu)^2 > 0\,. \tag{3.57}$$

This leads to the anomalous Doppler effect: In vacuo, the sign of the wave frequency relative to a four-velocity U^μ, defined as

$$\omega(U) = -U^\mu k_\mu\,, \tag{3.58}$$

is Lorentz invariant, i.e., if U' is any other four-velocity that is consistently oriented with U, then $\omega(U)$ and $\omega(U')$ have the same sign. In the present setup, however, this is not the case. If $\omega(u)$ denotes the frequency of k_μ in the rest-frame of the medium (assumed positive), one can write $k_\mu = \omega(u)u_\mu + k^\perp_\mu$ with $u^\mu k^\perp_\mu = 0$. Similarly, any other (future-pointing) four-velocity U^μ can be decomposed as $U^\mu = \gamma(u^\mu + v^\mu)$, where γ is the Lorentz factor and v^μ is the relative velocity satisfying $u^\mu v_\mu = 0$. Denoting by θ the angle between $k^\perp_\mu$ and v_μ, one finds

$$\omega(U) = \gamma\omega(u)(1 - nv\cos\theta)\,, \tag{3.59}$$

so that $\omega(U)$ assumes negative values inside the Cherenkov cone

$$nv\cos\theta > 1\,. \tag{3.60}$$

The consequences of this non-invariance of the sign of ω are discussed in Section 4.7 below.

3.3.3 Limits of Ray Optics

Being a simplified model of light propagation, geometrical optics necessarily has its limitations. For example, geometrical optics does not describe diffraction [121]. Additionally,

caustics are formed wherever light rays intersect, which leads to divergent expressions for the field amplitudes even though such divergences are not necessarily present in the corresponding solutions to the exact Maxwell equations [122, Chap. 9]. This has led to the development of refined models, see, e.g., Ref. [123], which are, however, beyond the scope of this document. A related issue is that the series (3.38) is generally only asymptotic to certain exact solutions [124–126], but does not necessarily converge. Moreover, as the ray transport equations are well posed even for initial data prescribed on timelike hypersurfaces [127, Sect. 2.1.4], in which case the initial-value problem for wave equations is generally ill-posed [128], the validity of the geometrical optics approximation must generally be determined on a case-by-case basis.

Experimental applications of ray optics in curved space-time include laser-interferometric gravitational wave detection and measurements of the influence of Earth's gravitational field on single photons. For laser-interferometric gravitational wave detection, a detailed analysis of Maxwell's equations in Ref. [95] demonstrated the accuracy of the geometrical optics prediction of Ref. [117], which generalized previous results by solving not only the eikonal equation [129–133], but also solving the transport equations for the scalar amplitude $\mathscr{A}$ and the polarization $\mathscr{F}_{\mu\nu}$. Experimental proposals for gravitational photon interferometry, on the other hand, commonly include fiber optics to expose single photons for a long time to Earth's gravitational field. As single-mode optical fibers have core radii on the same order of magnitude as the wavelength of light propagating therein, the short wavelength assumption is not met there. Nonetheless, the eikonal equation is commonly used in experimental proposals for gravitational fiber optics [2; 21; 36; 38; 39; 134]. The accuracy of the ray-optics model for such applications is established in Chapter 5.

3.4 Summary

The fact that the constitutive equations for linear isotropic media (either in flat or curved space-times) can be written in terms of an optical metric tensor is well known since the first introduction of such an optical metric by Gordon in Ref. [52]. Generalizations of the Lorenz gauge condition to account for dielectric properties of materials, based on such optical metrics, have been used in various contexts [49; 108–114]. However, the gauge-fixed equations arising from such Gordon–Lorenz gauges have, so far, not been analyzed for the junction conditions they imply at material interfaces where the permittivity and permeability are discontinuous. The present analysis considered the Euler–Lagrange equations of the gauge-fixed Lagrangian

$$\mathrm{L} = -\tfrac{1}{4}\tilde{g}^{\mu\nu}\tilde{g}^{\rho\sigma}F_{\mu\rho}F_{\nu\sigma} - \tfrac{1}{2}\chi^2 + A_\mu j^\mu \,,$$

where χ is the gauge function

$$\chi = \tfrac{1}{\sqrt{\mu}}{}^{(4)}\nabla_\mu(\sqrt{\mu}\,\tilde{g}^{\mu\nu}A_\nu) \,,$$

with $\tilde{g}^{\mu\nu}$ being the optical metric

$$\tilde{g}^{\mu\nu} = \frac{1}{\sqrt{\mu}}({}^{(4)}g^{\mu\nu} + u^\mu u^\nu) - \sqrt{\mu}\varepsilon\, u^\mu u^\nu \,,$$

where u^μ is the medium's four-velocity, ε its permittivity, and μ its permeability. The associated Euler–Lagrange equations reduce to the wave equation

$$\tilde{\Box}A_\mu - \tilde{R}_\mu{}^\nu A_\nu + \tilde{g}_{\mu\nu}j^\nu = 0 \,,$$

whenever ε and μ are constant, and simultaneously ensure that all components of the electromagnetic potential A_μ are continuous at material interfaces, where ε and μ may be discontinuous.

Chapter 4

Quantum Optics

The description of the electromagnetic field given in the previous chapter does not take any quantum properties of light into account. An appropriate framework to model such quantum properties, in particular: to describe single photons, is given by quantum field theory. Previous quantization schemes for the electromagnetic field have covered either fiber optics in flat space-time [135; 136] or light propagation in vacuous curved space-time [137–142], and Ref. [114] developed a quantization scheme that simultaneously allows for dielectric media and curved space-time backgrounds. However, as the latter model is restricted to the case of smooth permeability and permittivity functions, it cannot be applied to step-index optical fibers. Hence, a quantization scheme for the electromagnetic field that allows both for dielectric media with discontinuous dielectric properties and for curved space-times needs to be developed to describe planned experiments on gravitational fiber optics. This chapter develops such a theory by quantizing the gauge-fixed field equations put forward in Section 3.2.

As described in Sections 3.1 and 3.2, there are multiple ways of formulating classical electrodynamics. Similarly, there are multiple ways of formulating quantized theories. On the one hand, one may quantize the field strengths $F_{\mu\nu}$ and $G^{\mu\nu}$ without using the gauge potential A_μ, see, e.g., Ref. [143, Chap. 4]. On the other hand, if one works with the potential A_μ, there are multiple options on how to deal with the gauge redundancy. These schemes can be classified as outlined in Section 3.2, see in particular Table 3.1. Quantization schemes based on the reduced equations are commonly referred to as "reduced-phase-space methods," and are commonly used in quantum optics [98; 99; 144]. This approach has the advantage of eliminating all gauge redundancy from the onset but has the disadvantages of making the gauge invariance of the theory non-manifest, requiring a preferred notion of time (to formulate a Coulomb gauge condition), and making the field commutation relations non-trivial due to the presence of constraints [145, Sect. 8.3]. The Gupta–Bleuler quantization scheme, on the other hand, is based on the extended field equations [146; 147; 102, Sect. 3.3; 101, Sect. 7.4]. This scheme does not rely on any preferred notion of time and thus exhibits manifest general covariance but requires working, at intermediate stages, with an indefinite Krein space $\mathfrak{K}$ before one can construct a Hilbert space $\mathfrak{H}$ accounting

for all physical states of the theory. Due to its manifest general covariance, the facilitated comparison with models for massive photons (based on Proca's equation) and the already existing literature on quantization methods in curved space-times, this work uses the Gupta–Bleuler scheme.

4.1 Formal Aspects of the Classical Theory

To describe the quantum theory of electrodynamics in linear dielectrics, it is useful to consider complex fields. The source-free Lagrangian is

$$\mathrm{L}[A^*, A'] = -\tfrac{1}{2}\chi^{\mu\nu\rho\sigma} F^*_{\mu\nu} F'_{\rho\sigma} - \tfrac{1}{\xi}\chi^* \chi' \,, \tag{4.1}$$

where $\chi^{\mu\nu\rho\sigma}$ is the constitutive tensor as defined in Eq. (3.6), $F_{\mu\nu} = (\mathrm{d}A)_{\mu\nu}$ is the field strength, χ is the gauge function defined in Eq. (3.28), and ξ is a constant.

The Euler–Lagrange equations are

$$\mathrm{E}^\nu[A] \equiv {}^{(4)}\nabla_\mu G^{\mu\nu} + \tfrac{1}{\xi}\sqrt{\mu}\tilde{g}^{\mu\nu\,(4)}\nabla_\mu(\chi/\sqrt{\mu}) = 0 \,, \tag{4.2}$$

where $\tilde{g}^{\mu\nu}$ is the optical metric as defined in Eq. (3.12). The induced Klein–Gordon product, as defined according to the general methods described in Appendix A.2, takes the form

$$(A \mid A') = \frac{i}{\hbar}\int_\Sigma (A^*_\mu \Pi'^\mu - A'_\mu \Pi^{*\mu})\,{}^{(3)}\boldsymbol{\epsilon} \,, \tag{4.3}$$

with

$$\Pi^\mu[A] = -(G^{\mu\nu} - \tfrac{1}{\xi}\tilde{g}^{\mu\nu}\chi)\Gamma_\nu \,, \tag{4.4}$$

where Σ is any Cauchy surface, Γ_μ is the unit-conormal (oriented such that ${}^{(4)}g^{\mu\nu}\Gamma_\nu$ is future-pointing), and ${}^{(3)}\boldsymbol{\epsilon}$ is the volume form induced by the space-time volume form ${}^{(4)}\boldsymbol{\epsilon}$.

The evolution equation for the gauge function is

$$\mathrm{E}'[\chi] \equiv {}^{(4)}\nabla_\mu[\sqrt{\mu}\,\tilde{g}^{\mu\nu\,(4)}\nabla_\nu(\chi/\sqrt{\mu})] = 0 \,, \tag{4.5}$$

which can be derived from the Lagrangian

$$\mathrm{L}'[\chi^*, \chi'] = -\sqrt{\mu}\tilde{g}^{\mu\nu\,(4)}\nabla_\mu(\chi^*/\sqrt{\mu})\,{}^{(4)}\nabla_\nu(\chi'/\sqrt{\mu}) \,. \tag{4.6}$$

The induced Klein–Gordon product of solutions to this equation is

$$(\chi \mid \chi')' = \frac{i}{\hbar}\int_\Sigma [\chi^{*\,(4)}\nabla_\mu(\chi'/\sqrt{\mu}) - \chi'^{\,(4)}\nabla_\mu(\chi^*/\sqrt{\mu})]\tilde{g}^{\mu\nu}\Gamma_\nu\,{}^{(3)}\boldsymbol{\epsilon} \,. \tag{4.7}$$

The products defined in Eqs. (4.3) and (4.7) are related through the following identity: if A_μ is any solution to the extended Maxwell equations $\mathrm{E}^\mu[A] = 0$ and ϕ is any solution

to the gauge evolution equation $\mathrm{E}'[\phi] = 0$ (both with suitable spatial decay), then $\mathrm{d}(\phi/\sqrt{\mu})$ is another solution to extended Maxwell equations and one has

$$(A \mid \mathrm{d}(\phi/\sqrt{\mu})) = -\tfrac{1}{\xi}(\chi[A] \mid \phi)' \,. \tag{4.8}$$

Apart from defining conserved quantities for pairs of solutions to the field equations, the Klein–Gordon products also arise naturally when the fields A_μ and χ are regarded not as classical functions but as distributions. Indeed, as explained in detail in Appendix A.3, if the equations of motion are Green-hyperbolic, i.e., if they admit unique advanced and retarded Green's functions [148], then, for any compactly supported smooth vector field j^μ and any compactly supported smooth function ψ, one has

$$\frac{i}{\hbar}\int_{\mathscr{M}} A^*_\mu \, j^\mu \, {}^{(4)}\boldsymbol{\epsilon} = (A \mid \Delta[j]) \,, \qquad\qquad \frac{i}{\hbar}\int_{\mathscr{M}} \chi^* \psi \, {}^{(4)}\boldsymbol{\epsilon} = (\chi \mid \Delta'[\psi])' \,, \tag{4.9}$$

in which Δ is the Pauli–Jordan distribution for the field equation E^μ, and Δ' is the corresponding distribution for E'. These equations show that A_μ and χ are fully determined by the linear forms $(A \mid \cdot)$ and $(\chi \mid \cdot)'$, cf. Ref. [149, Lemma 3.2.1].

At this stage, it is worth noting that the notion of a Pauli–Jordan distribution Δ for discontinuous optical metrics $\tilde{g}_{\mu\nu}$ may well be problematic. For this reason, this thesis will not make explicit use of Eq. (4.9) and will work with the spatial integrals $(\cdot \mid \cdot)$ and $(\cdot \mid \cdot)'$ involving only solutions to the field equation instead of considering space-time integrals involving arbitrary test functions.

4.2 Energy in Stationary Space-Times

In stationary space-times, a commonly used method for obtaining an expression for the energy (a conserved quantity associated with time-translation invariance) is to start from a stress-energy-momentum tensor $T_{\mu\nu}[A^*, A']$ that is bilinear in the fields (similar to the Lagrangian $\mathrm{L}[A^*, A']$ considered above), symmetric, and divergence-free. Contraction with a Killing vector field $\mathscr{K}^\mu$ yields a divergence-free vector field that can be integrated over any Cauchy surface Σ to yield the Ashtekar–Magnon bracket

$$\{A \mid A'\} = \int_\Sigma T^\mu{}_\nu[A^*, A'] \mathscr{K}^\nu \Gamma_\mu \, {}^{(3)}\boldsymbol{\epsilon} \,, \tag{4.10}$$

which is independent of the Cauchy surface Σ. The classical Hamiltonian $\mathscr{H}$ (associated to the field $\mathscr{K}^\mu$) can then be defined via the equation

$$\{A \mid A'\} = (A \mid \mathscr{H} A') \,, \tag{4.11}$$

see Refs. [150, Sect. 4; 149, Sect. 4.3].

However, in linear dielectric media, there are competing definitions of the stress-energy-momentum tensor $T_{\mu\nu}$. Whereas Minkowski's tensor, introduced in Ref. [151], is not

symmetric, Abraham's tensor, first defined in Ref. [152], is symmetric but generally not divergence-free. Despite numerous theoretical and experimental attempts to resolve the Abraham–Minkowski controversy, a generally accepted stress-energy-momentum tensor for the electromagnetic field has not been found, see Ref. [153] for a review. As a consequence, Eq. (4.10) cannot be used in the present context.

Despite the Abraham–Minkowski controversy remaining unresolved, it is nonetheless possible to introduce a notion of energy for the considered problem. This is made possible by Noether's theorem in the form described in Appendix A.1: If $\mathcal{K}^\mu$ is a Killing vector field both for the space-time metric ${}^{(4)}g_{\mu\nu}$ and the optical metric $\tilde{g}_{\mu\nu}$, Noether's theorem asserts that if A_μ and A'_μ satisfy the source-free field equations and have suitable spatial decay, then the expression

$$\{A \mid A'\} = \int_\Sigma ([\pounds_\mathcal{K} A^*_\mu]\Pi'^\mu + [\pounds_\mathcal{K} A'_\mu]\Pi^{*\mu} + \mathcal{K}^\mu \mathit{\Gamma}_\mu \mathrm{L}[A^*, A'])^{(3)}\boldsymbol{\epsilon} \tag{4.12}$$

is independent of the Cauchy surface Σ, hence defines a conserved quantity.

Even though the condition that $\mathcal{K}^\mu$ is a Killing field for ${}^{(4)}g_{\mu\nu}$ and $\tilde{g}_{\mu\nu}$ simultaneously is a strong restriction, it is nonetheless satisfied in the scenarios considered here, in which $\mathcal{K}^\mu$ is a Killing field of ${}^{(4)}g_{\mu\nu}$, the four-velocity of the medium u^μ is proportional to $\mathcal{K}^\mu$, and ε and μ are time-independent in the sense that $\pounds_u \varepsilon = \pounds_u \mu = 0$. One then has

$$\pounds_\mathcal{K} {}^{(4)}g_{\mu\nu} = 0\,, \qquad \pounds_\mathcal{K} \varepsilon = 0\,, \qquad \pounds_\mathcal{K} \mu = 0\,, \qquad u^\mu \propto \mathcal{K}^\mu\,, \tag{4.13}$$

under which circumstances $\mathcal{K}^\mu$ is also a Killing field for $\tilde{g}_{\mu\nu}$, and the above conservation law applies.

In this setup, the definition of the Ashtekar–Magnon bracket $\{\cdot \mid \cdot\}$ according to Eq. (4.12) provides a replacement for the here ill-defined expression in Eq. (4.10), and the classical Hamiltonian $\mathcal{H}$ can be defined using Eq. (4.11). One can then show that the field equations on stationary space-times imply the "symplectically smeared" Schrödinger equation

$$(A \mid i\hbar \pounds_\mathcal{K} A') = (A \mid \mathcal{H} A')\,, \tag{4.14}$$

see Appendix A.4 for a derivation.

In general, the spectrum of the Hamiltonian $\mathcal{H}$, as defined through Eq. (4.11), is not bounded from below. This is because relativistic field equations generally admit solutions with both positive and negative frequencies. In the Feynman–Stückelberg interpretation, these two kinds of solutions are regarded as describing particles and anti-particles, respectively [154; 155]. Henceforward, it will be assumed that there exist projectors $P_\pm$ that map solutions onto their positive-energy or negative-energy parts, respectively, and satisfy

$$P_\pm A^* = (P_\mp A)^*\,, \tag{4.15}$$

as well as

$$(A \mid A') = (P_+ A \mid P_+ A') + (P_- A \mid P_- A')\,. \tag{4.16}$$

This last requirement expresses the condition that positive-frequency and negative-frequency solutions are mutually orthogonal.

4.3 Quantization in Stationary Space-Times

In standard quantum optics textbooks, the quantum field operator $\hat{A}$ is commonly described as an operator-valued field [98, Sect. 4.4; 156, Sect. 8.3; 144, Chap. 2]. However, taken literally, this method leads to mathematical difficulties [149, Sect. 3.1] that can be overcome using a distributional approach. In view of Eq. (4.9), one is led to consider expressions of the form $(\hat{A} \mid A')$, where A' is any classical solution to the field equations, and to characterize such expressions abstractly instead of attempting to define $\hat{A}$ directly [149, Sect. 3.2; 157, Sect. 2.2; 158, Sect. 2]. Although being a well-established approach to field quantization in curved space-times, this method appears not to have been used previously to describe the gravitational redshift at the quantum level.

The algebraic approach to quantum field theory is thus concerned with an (abstract) unital algebra $\mathfrak{A}$, called the algebra of "basic observables," that is generated by expressions of the form $\hat{\Phi}(A)$ and $\hat{\Phi}^\dagger(A)$, where A is any classical solution to the field equations (4.2) (with suitable decay properties). Informally, $\hat{\Phi}(A)$ and $\hat{\Phi}^\dagger(A)$ may be thought of as representing "symplectically smeared quantum fields"

$$\hat{\Phi}(A') = (A' \mid \hat{A})\,, \qquad\qquad \hat{\Phi}^\dagger(A') = (\hat{A} \mid A')\,, \tag{4.17}$$

but, in general, such expressions are not to be taken literally.

Since the Klein–Gordon product $(\cdot \mid \cdot)$ is anti-linear in its first argument and linear in the second, it is natural to require

$$\hat{\Phi}(A_1 + \lambda A_2) = \hat{\Phi}(A_1) + \lambda^* \hat{\Phi}(A_2)\,, \tag{4.18a}$$

$$\hat{\Phi}^\dagger(A_1 + \lambda A_2) = \hat{\Phi}^\dagger(A_1) + \lambda \hat{\Phi}^\dagger(A_2)\,, \tag{4.18b}$$

where A_1 and A_2 are classical solutions and $\lambda \in \mathbf{C}$.

To formulate a generalization of the classical relation $(A_1 \mid A_2) = (A_2 \mid A_1)^*$, one requires $\mathfrak{A}$ to be endowed with an involution, here denoted by $\dagger$, that makes $\mathfrak{A}$ into a $*$-algebra and acts on the generators of $\mathfrak{A}$ as

$$\hat{\Phi}(A)^\dagger = \hat{\Phi}^\dagger(A)\,, \qquad\qquad \hat{\Phi}^\dagger(A)^\dagger = \hat{\Phi}(A)\,, \tag{4.19}$$

which is consistent with the informal interpretation (4.17). Further, taking the classical identity $(A_1 \mid A_2) = -(A_2^* \mid A_1^*)$ as guidance, one may formulate what it means for the

quantized electromagnetic potential to be "real" or "Hermitian," namely

$$\hat{\Phi}(A^*) = -\hat{\Phi}^\dagger(A)\,. \tag{4.20}$$

Additionally, one requires a commutation relation for the smeared field operators. In the description used here, the Heisenberg equal-time commutation relations take the form

$$[\hat{\Phi}(A_1), \hat{\Phi}^\dagger(A_2)] = (A_1 \mid A_2)\,. \tag{4.21}$$

This can be motivated through the heuristic notation (4.17): if one formally expands $[\hat{\Phi}(A_1), \hat{\Phi}^\dagger(A_2)]$ in terms of Klein–Gordon products of the classical solutions A_1 and A_2 with the "quantum field" $\hat{A}$ and its associated momentum $\hat{\Pi}$, then Eq. (4.21) is obtained by imposing the relations

$$[\hat{A}_\mu(t,\boldsymbol{x}), \hat{\Pi}^\nu(t,\boldsymbol{y})] = i\hbar\delta_\mu^\nu\delta(\boldsymbol{x},\boldsymbol{y})\,, \tag{4.22a}$$
$$[\hat{A}_\mu(t,\boldsymbol{x}), \hat{A}_\nu(t,\boldsymbol{y})] = 0\,, \tag{4.22b}$$
$$[\hat{\Pi}^\mu(t,\boldsymbol{x}), \hat{\Pi}^\nu(t,\boldsymbol{y})] = 0\,, \tag{4.22c}$$

where t is a time coordinate whose level sets define a family of Cauchy surfaces, and $\delta(\boldsymbol{x},\boldsymbol{y})$ is the Dirac delta on such a Cauchy surface Σ. Whereas Eq. (4.22) is to be interpreted formally (strictly speaking, such equations make sense only when smeared with suitable test functions), Eq. (4.21) is free of such issues.

The above considerations thus motivate describing basic observables in the theory of a quantized electromagnetic field as a unital $*$-algebra $\mathfrak{A}$ (whose involution is here denoted by $\dagger$), generated by expressions of the form $\hat{\Phi}(A)$, where A ranges over all classical solutions with suitable decay, such that

$$\hat{\Phi}(A_1 + \lambda A_2) = \hat{\Phi}(A_1) + \lambda^*\hat{\Phi}(A_2)\,, \tag{4.23a}$$
$$\hat{\Phi}(A)^\dagger + \hat{\Phi}(A^*) = 0\,, \tag{4.23b}$$
$$[\hat{\Phi}(A_1), \hat{\Phi}^\dagger(A_2)] = (A_1 \mid A_2)\,. \tag{4.23c}$$

One may ask whether such a mathematical structure exists. The answer is affirmative: one can explicitly construct $\mathfrak{A}$ as a quotient of the free $*$-algebra over the set of classical solutions A by a suitably chosen ideal [159, Sect. 5.2; 160, Sect. 5.5].

Hamiltonian The next step in the description of quantum optics in curved space-time is the characterization of the quantum Hamiltonian $\hat{\mathscr{H}}$. Again, the interpretation (4.17) can provide some guiding intuition. Starting, heuristically, from the Heisenberg equation

$$i\hbar\mathfrak{L}_{\mathscr{K}}\hat{A} + [\hat{\mathscr{H}}, \hat{A}] = 0\,, \tag{4.24}$$

formally applying $(A' \mid \cdot)$ and using $(A_1 \mid i\hbar\pounds_K A_2) = (i\hbar\pounds_K A_1 \mid A_2)$ (which, strictly speaking, only holds for classical solutions) as well as the classical Schrödinger equation (4.14), one is led to

$$[\hat{\mathscr{H}}, \hat{\Phi}(A)] = -\hat{\Phi}(\mathscr{H}A)\,. \tag{4.25}$$

Using Eq. (4.20) and $(\mathscr{H}A)^* = -\mathscr{H}A^*$, one obtains

$$[\hat{\mathscr{H}}, \hat{\Phi}^\dagger(A)] = +\hat{\Phi}^\dagger(\mathscr{H}A)\,, \qquad [\hat{\mathscr{H}}, \hat{\Phi}(A)] = -\hat{\Phi}(\mathscr{H}A)\,. \tag{4.26}$$

Despite the arguments leading to these equations being heuristic, Eq. (4.26) can be regarded as an abstract definition of $\hat{\mathscr{H}}$ by prescribing its commutators with all generators of $\mathfrak{A}$, which determines $\hat{\mathscr{H}}$ up to a multiple of the identity, cf. Ref. [149, Sect. 2.3].

Ground State For stationary space-times, the postulate of the existence of a "ground state" $|0\rangle$, i.e., a normalized state of minimal energy (which is here assumed to be zero), is commonly formulated by the following two conditions:

$$\hat{\mathscr{H}}|0\rangle = 0\,, \tag{4.27}$$

$$\hat{\Phi}(A)|0\rangle = 0 \qquad \text{for all positive-frequency } A. \tag{4.28}$$

A partial justification for Eq. (4.28) is the following: If A is a classical solution that has non-zero norm, $(A \mid A) \neq 0$, and positive but not necessarily definite frequency in the sense of $(A \mid \mathscr{H}A)/(A \mid A) > 0$, then if $|\psi\rangle = \hat{\Phi}(A)|0\rangle$ is non-zero, its expectation value of $\hat{\mathscr{H}}$ is negative:

$$\frac{\langle\psi|\hat{\mathscr{H}}|\psi\rangle}{\langle\psi|\psi\rangle} = -\frac{(A \mid \mathscr{H}A)}{(A \mid A)} < 0\,. \tag{4.29}$$

Hence, the requirement of $|0\rangle$ being the state of the least energy leads to Eq. (4.28) for A with non-zero Klein–Gordon norm. The validity of Eq. (4.28) for fields of vanishing Klein–Gordon norm, however, cannot be motivated in this manner. The present method of working with the gauge degeneracy of the problem thus requires considering Eq. (4.28) as an independent postulate rather than a direct consequence of the assumption that $|0\rangle$ has minimal energy.

Whereas $\hat{\Phi}(A)|0\rangle$ is required to vanish for positive-frequency A, the states $\hat{\Phi}^\dagger(A)|0\rangle$ are generally non-zero, for they have non-trivial inner products with other states:

$$\langle 0|\hat{\Phi}(A')\hat{\Phi}^\dagger(A)|0\rangle = \langle 0|[\hat{\Phi}(A'), \hat{\Phi}^\dagger(A)]|0\rangle = (A' \mid A)\,. \tag{4.30}$$

The postulate (4.28) thus requires a separate treatment of modes with positive or negative frequency. Since $\hat{\Phi}(A^*) = -\hat{\Phi}^\dagger(A)$, it suffices to study the operators $\hat{\Phi}$ and $\hat{\Phi}^\dagger$ for positive-frequency solutions. If A_1 and A_2 are both positive-frequency solutions, then

Eq. (4.21) in combination with Eq. (4.16) implies

$$[\hat{\Phi}\ (A_1), \hat{\Phi}^\dagger(A_2)] = (A_1 \mid A_2)\,, \tag{4.31a}$$
$$[\hat{\Phi}\ (A_1), \hat{\Phi}\ (A_2)] = 0\,, \tag{4.31b}$$
$$[\hat{\Phi}^\dagger(A_1), \hat{\Phi}^\dagger(A_2)] = 0\,, \tag{4.31c}$$

and one requires

$$\hat{\Phi}(A)|0\rangle = 0\,, \qquad \hat{\Phi}^\dagger(A)|0\rangle \neq 0\,, \tag{4.32}$$

where A is any positive-frequency solution to Eq. (4.2).

Fock Construction So far, the description of the space of states was abstract and the commutation relation of the "smeared field operators" $\hat{\Phi}$ and $\hat{\Phi}^\dagger$ was postulated, not proven. One may thus ask whether such a space of states, together with operators satisfying the above commutation relations, can be constructed to put the above model on a solid foundation. The answer is affirmative: an appropriate space of states together with a set of ladder operators can be obtained by the Fock construction, outlined, e.g., in Refs. [149, p. 192 ff.; 161, p. 59; 162, Sect. 2].

The Fock construction yields a space of states $\mathfrak{K}$, together with ladder operators $\hat{a}(A)$ and $\hat{a}^\dagger(A)$, where A is restricted to positive-frequency solutions, satisfying

$$[\hat{a}\ (A_1), \hat{a}^\dagger(A_2)] = (A_1 \mid A_2)\,, \tag{4.33a}$$
$$[\hat{a}\ (A_1), \hat{a}\ (A_2)] = 0\,, \tag{4.33b}$$
$$[\hat{a}^\dagger(A_1), \hat{a}^\dagger(A_2)] = 0\,. \tag{4.33c}$$

Furthermore, the Fock construction provides a distinguished vector $|0\rangle \in \mathfrak{K}$ that is normalized to $\langle 0|0\rangle = 1$ and satisfies

$$\hat{a}(A)|0\rangle = 0 \qquad \text{for all positive-frequency solutions } A. \tag{4.34}$$

Denoting by P_+ the map that projects a classical solution onto its positive-frequency part, as in Eq. (4.16), the smeared quantum-field operators $\hat{\Phi}$ and $\hat{\Phi}^\dagger$ can be defined as

$$\hat{\Phi}\ (A) = \hat{a}\ (P_+A) - \hat{a}^\dagger(P_+A^*)\,, \tag{4.35a}$$
$$\hat{\Phi}^\dagger(A) = \hat{a}^\dagger(P_+A) - \hat{a}\ (P_+A^*)\,, \tag{4.35b}$$

cf. Ref. [149, Eq. (3.2.10)]. This provides a solid mathematical foundation for the description of free quantum fields in stationary space-times.

Indefinite Norm The space obtained from the Fock construction mentioned above contains states that are considered as "pure gauge" or "unphysical." This is because

the Klein–Gordon product of classical solutions to the extended field equations (4.2) is generally indefinite (see Section 4.7 for explicit examples in flat space-time). The reason for this lies in the presence of gauge and ghost solutions to the classical field equations, cf. Section 3.2.1. Gauge solutions generally have vanishing Klein–Gordon norm and are orthogonal to physical solutions (this is a consequence of Eq. (4.8)), so the non-degeneracy of $(\cdot \mid \cdot)$ implies that the Klein–Gordon product of gauge solutions with ghost solutions is generically non-zero. This implies that ghost modes can generally have norms of arbitrary sign. It follows that the space of states obtained from the Fock construction in the present setup does not form a Hilbert space $\mathfrak{H}$, but rather a Krein space $\mathfrak{K}$. The main method for the construction of a "physical" Hilbert space $\mathfrak{H}$ from $\mathfrak{K}$ is the Gupta–Bleuler condition, the formulation of which requires the notion of a quantized gauge operator.

Quantized Gauge Operator The description of the gauge function χ at the quantum level proceeds in a manner analogous to the description of the quantized electromagnetic potential A in terms of the operators $\hat{\Phi}$ and $\hat{\Phi}^\dagger$ given above. The intuitive interpretation of $\hat{\Phi}$ and $\hat{\Phi}^\dagger$ stated in Eq. (4.17), together with the classical formula

$$(\chi' \mid \chi[A])' = -\xi(\mathrm{d}(\chi'/\sqrt{\mu}) \mid A)\,, \tag{4.36}$$

cf. Eq. (4.8), suggests the definition

$$\hat{\mathfrak{X}}(\chi) = -\xi\,\hat{\Phi}(\mathrm{d}[\chi/\sqrt{\mu}])\,, \qquad \hat{\mathfrak{X}}^\dagger(\chi) = -\xi\,\hat{\Phi}^\dagger(\mathrm{d}[\chi/\sqrt{\mu}])\,, \tag{4.37}$$

where χ is any solution to Eq. (3.32) (with suitable decay properties).

Using Eq. (4.21) and the fact that pure-gauge modes have vanishing momentum Π^μ, one finds that the smeared gauge operators commute:

$$[\hat{\mathfrak{X}}(\chi_1), \hat{\mathfrak{X}}^\dagger(\chi_2)] = 0\,. \tag{4.38}$$

Moreover, their commutation relation with smeared potential operators is given by

$$[\hat{\mathfrak{X}}(\chi), \hat{\Phi}^\dagger(A')] = (\chi \mid \chi')'\,, \tag{4.39}$$

where χ' is the gauge function of the solution A'.

4.4 Gauge Invariance

The above scheme provides a quantization of the gauge-fixed field equations (4.2) by constructing quantum field operators $\hat{\Phi}$ and $\hat{\mathfrak{X}}$ as operators on a Krein space $\mathfrak{K}$. However, as $\mathfrak{K}$ has an indefinite inner product, it cannot be interpreted as a space of physical states with positive norms. Such a space, however, can be constructed by eliminating gauge and ghost states using the Gupta–Bleuler condition.

Gupta–Bleuler Condition Having defined a quantum field operator corresponding to the gauge function of the quantized electromagnetic field, one can use the Gupta–Bleuler condition to identify physical states within the Krein space $\mathfrak{K}$. Specifically, a state $|\psi\rangle \in \mathfrak{K}$ is said to satisfy the Gupta–Bleuler condition if, for all positive-frequency solutions χ of the gauge-evolution equation (3.32), one has

$$\hat{\mathfrak{X}}(\chi)|\psi\rangle = 0\,. \tag{4.40}$$

Evidently, the ground state $|0\rangle$ satisfies this condition. Moreover, by Eq. (4.39), any state of the form $\hat{a}^\dagger(A')|0\rangle$ satisfies the Gupta–Bleuler condition if A' satisfies the gauge condition $\chi' \equiv \chi[A'] = 0$ since one then has

$$\hat{\mathfrak{X}}(\chi)\hat{a}^\dagger(A')|0\rangle = \hat{\mathfrak{X}}(\chi)\hat{\Phi}^\dagger(A')|0\rangle = [\hat{\mathfrak{X}}(\chi), \hat{\Phi}^\dagger(A')]|0\rangle = (\chi \mid \chi')'|0\rangle = 0\,. \tag{4.41}$$

More generally, if $(A_j)_{j=1}^n$ are classical positive-frequency solutions satisfying the gauge condition, then $\hat{a}^\dagger(A_1)\cdots\hat{a}^\dagger(A_n)|0\rangle$ satisfies the Gupta–Bleuler condition. In this way, states satisfying the Gupta–Bleuler condition can be generated from $|0\rangle$ by repeated action of the creation operator corresponding to positive-frequency solutions satisfying the gauge condition.

Gauge States The space of all states satisfying the Gupta–Bleuler condition can be written as

$$\mathfrak{Z} = \bigcap_\chi \ker \hat{\mathfrak{X}}(\chi)\,, \tag{4.42}$$

where χ ranges over all positive-frequency solutions of the gauge evolution equation (4.5). The reduction from $\mathfrak{K}$ to $\mathfrak{Z}$ eliminates all ghost modes. In the applications considered below, this removes all states of negative norm. However, the inner product on $\mathfrak{Z}$ (induced from $\mathfrak{K}$) is still indefinite due to the presence of gauge modes. Indeed, if $|\psi\rangle \in \mathfrak{Z}$, then $\hat{\mathfrak{X}}^\dagger(\chi)|\psi\rangle$ also lies in $\mathfrak{Z}$, as can be seen from Eq. (4.38). Moreover, $\hat{\mathfrak{X}}^\dagger(\chi)|\psi\rangle$ is orthogonal to all of $\mathfrak{Z}$ since for any $|\phi\rangle \in \mathfrak{Z}$ one has

$$\langle\phi|\hat{\mathfrak{X}}^\dagger(\chi)|\psi\rangle = \langle\psi|\hat{\mathfrak{X}}(\chi)|\phi\rangle^* = 0\,. \tag{4.43}$$

This identifies the images of $\hat{\mathfrak{X}}^\dagger(\cdot)$ as spaces of pure-gauge states. Hence, the space of all gauge states in $\mathfrak{Z}$ can be defined as

$$\mathfrak{B} = \mathfrak{Z} \cap \left(\bigcup_\chi \operatorname{im} \hat{\mathfrak{X}}^\dagger(\chi)\right)\,, \tag{4.44}$$

where, as above, χ ranges over all positive-frequency solutions of Eq. (4.5).

Space of States Given the above descriptions, one has the interpretation

$$\mathfrak{Z} = (\text{states satisfying the Gupta–Bleuler condition}),$$
$$\mathfrak{B} = (\text{pure-gauge states}).$$

The physically relevant space of states $\mathfrak{H}$ can then be defined as the quotient

$$\mathfrak{H} = \mathfrak{Z}/\mathfrak{B}, \tag{4.45}$$

or informally:

$$\mathfrak{H} = (\text{states satisfying the Gupta–Bleuler condition})/(\text{pure-gauge states}).$$

One may thus regard all $\mathfrak{K}$-states of the form

$$\hat{a}^\dagger(A_1)\cdots\hat{a}^\dagger(A_n)|0\rangle,$$

with all $\chi[A_k] = 0$, as defining physical states, since their equivalence classes lie in $\mathfrak{H}$.

Gauge Invariance To work with states in $\mathfrak{H}$, which are equivalence classes in $\mathfrak{K}$, it is useful to write

$$|\psi\rangle\!\rangle = |\psi\rangle + \mathfrak{B}, \tag{4.46}$$

where $|\psi\rangle + \mathfrak{B}$ denotes the equivalence class of $|\psi\rangle \in \mathfrak{Z}$ modulo $\mathfrak{B}$. The space $\mathfrak{H}$ inherits an inner product from $\mathfrak{K}$ by

$$\langle\!\langle\phi|\psi\rangle\!\rangle = \langle\phi|\psi\rangle, \tag{4.47}$$

which is well-defined due to the Gupta–Bleuler condition (4.40).

However, the operators $\hat{\Phi}(A)$ on $\mathfrak{K}$ do not directly induce operators on $\mathfrak{H}$. This is because $\mathfrak{B}$ is not closed under the action of $\hat{\Phi}(A)$ as can be seen as follows: Let $|\phi\rangle \in \mathfrak{Z}\setminus\mathfrak{B}$ and χ' be any positive-frequency solution to the gauge-evolution equation. Then $\hat{\mathfrak{X}}^\dagger(\chi')|\phi\rangle$ lies in $\mathfrak{B}$ by definition (4.44). If A is any positive-frequency solution to the gauge-fixed field equations, Eq. (4.39) implies

$$\hat{\Phi}(A)\hat{\mathfrak{X}}^\dagger(\chi')|\phi\rangle = [\hat{\Phi}(A), \hat{\mathfrak{X}}^\dagger(\chi')]|\phi\rangle + \mathfrak{B} = (\chi \mid \chi')'|\phi\rangle + \mathfrak{B}, \tag{4.48}$$

where $\chi = \chi[A]$. But as $|\phi\rangle$ lies in the complement of $\mathfrak{B}$, $\hat{\Phi}(A)\hat{\mathfrak{X}}^\dagger(\chi')|\phi\rangle$ is contained in $\mathfrak{B}$ only if $(\chi \mid \chi')' = 0$, so $\mathfrak{B}$ is not preserved under the action of $\hat{\Phi}(A)$ unless $\chi = 0$.

The above reasoning shows that $\hat{\Phi}(A)$ can only define an operator in $\mathfrak{H}$ if A satisfies the gauge condition $\chi[A] = 0$. Hence, for such A, one may define

$$|\hat{\Phi}(A)\psi\rangle\!\rangle = \hat{\Phi}(A)|\psi\rangle + \mathfrak{B}. \tag{4.49}$$

However, some gauge redundancy persists: if A satisfies the gauge condition, then so does $A' = A + \mathrm{d}(\chi/\sqrt{\mu})$ if χ satisfies the gauge evolution equation (4.5). One then has

$$\hat{\Phi}(A') = \hat{\Phi}(A) - \xi^{-1}\hat{\mathfrak{X}}(\chi^+) + \xi^{-1}\hat{\mathfrak{X}}^\dagger(\chi^+)\,, \tag{4.50}$$

where χ^+ denotes the positive-frequency part of χ. When acting on a vector in $\mathfrak{B}$, the second term gives zero and the third term produces an element of $\mathfrak{B}$. Hence, one finds

$$|\hat{\Phi}(A')\psi\rangle\!\rangle = |\hat{\Phi}(A)\psi\rangle\!\rangle\,, \tag{4.51}$$

which demonstrates a restricted gauge invariance of the quantized theory. Finally, one may define a manifestly gauge-invariant operator $\hat{\Psi}(F)$, where F is any solution to Maxwell's equations, by

$$|\hat{\Psi}(F)\psi\rangle\!\rangle = |\hat{\Phi}(A)\psi\rangle\!\rangle\,, \tag{4.52}$$

where A is any potential for F, i.e., $F = \mathrm{d}A$, that satisfies the gauge condition $\chi[A] = 0$. By the above considerations, this operator is well-defined and independent of the particular choice of potential A. The operator $\hat{\Psi}(F)$ can be interpreted as the quantized electromagnetic field, symplectically smeared by the classical field F. Operators $\hat{\Psi}^\dagger(F)$ can be constructed analogously, and their commutation relation is found to be given by

$$[\hat{\Psi}(F), \hat{\Psi}^\dagger(F')] = (F \mid F')\,, \tag{4.53}$$

with

$$(F \mid F') = -\frac{i}{\hbar}\int_\Sigma (A^*_\mu G'^{\mu\nu} - A'_\mu G^{\mu\nu}) \Gamma_\nu \, {}^{(3)}\boldsymbol{\epsilon}\,, \tag{4.54}$$

where A and A' are potentials for F and F', respectively, which need not satisfy the gauge conditions $\chi = 0$ or $\chi' = 0$, Σ is any Cauchy surface, Γ_ν denotes its future-pointing unit co-normal and ${}^{(3)}\boldsymbol{\epsilon}$ its volume form. Although $(F \mid F')$ is defined through concrete potentials A and A', Stokes' theorem shows that the resulting integral is invariant under gauge transformations so that $(F \mid F')$ is well-defined. Note that in vacuo, $(F \mid F')$ reduces to the standard Klein–Gordon product of electrodynamics as defined, e.g., in Refs. [149, Sect. 4.8; 157, Sect. 2.1].

Equation (4.53), together with the gauge-invariance of $(F \mid F')$ demonstrates the full gauge-invariance of the quantization scheme described here. This completes the Gupta–Bleuler quantization of electrodynamics in curved space-times for linear isotropic media.

4.5 Formal Mode Expansion

The quantization scheme describe in Section 4.3 is based on an abstract $*$-algebra generated by expressions of the form $\hat{\Phi}(A')$ where A' is any classical solution to the field equations with finite Klein–Gordon norm. Whereas such expressions can be interpreted using the heuristic expressions given in Eq. (4.17), the above does not require the notion of a quantized field operator $\hat{A}$. However, quantization schemes based on the notion of field operators continue to be used in the literature despite the fact that some expressions arising in such formalisms are mathematically ill-defined [149, Sect. 3.1]. This section describes the relation of the abstract quantization scheme of Section 4.3 to such heuristic methods, as well as the differences in these approaches.

Whereas mode expansions for systems with positive-definite Klein–Gordon products are commonly based on "complete orthonormal sets" [107, Sect. 3.2; 97, Sect. 14.2; 161, Chap. 3], the indefinite Klein–Gordon product arising in the current setup requires a different approach. Let (X, μ) be a measure space and, for each $k \in X$, let A_k and $\underline{A}_k$ be positive-frequency solutions such that the Klein–Gordon product of any pair of solutions A' and A'' with suitable spatial decay can be written as

$$(A' \mid A'') = \int_X \{(A' \mid A_k)(\underline{A}_k \mid A'') - (A' \mid A_k^*)(\underline{A}_k^* \mid A'')\} \, \mathrm{d}\mu(k) \,, \tag{4.55}$$

which can be loosely interpreted as "completeness relations" stating that any finite-norm solution A' can be expanded using the "mode set" A_k as

$$A' = \int_X \{(\underline{A}_k \mid A') A_k - (\underline{A}_k^* \mid A') A_k^*\} \, \mathrm{d}\mu(k) \,, \tag{4.56}$$

and also in the "reciprocal mode set" $\underline{A}_k$ as

$$A' = \int_X \{(A_k \mid A') \underline{A}_k - (A_k^* \mid A') \underline{A}_k^*\} \, \mathrm{d}\mu(k) \,. \tag{4.57}$$

However, the formal meaning of such equations lies mainly in Eq. (4.55). If one uses Eq. (4.56) repeatedly and disregards convergence issues, one formally obtains

$$A' = \int_{X^2} \{(\underline{A}_k \mid A_{k'})(A_{k'} \mid A') A_k + (\underline{A}_k^* \mid A_{k'}^*)(A_{k'}^* \mid A') A_k^*\} \, \mathrm{d}\mu(k) \, \mathrm{d}\mu(k') \,. \tag{4.58}$$

Comparison with Eq. (4.56) then suggests the formal result

$$(\underline{A}_k \mid A_{k'}) = +\delta(k, k') \,, \qquad (\underline{A}_k^* \mid A_{k'}^*) = -\delta(k, k') \,, \tag{4.59}$$

where δ denotes a Dirac delta.

The formal expansion of the field operator $\hat{A}$ in terms of the mode set A_k then reads

$$\hat{A} = \int_X \{A_k\, \hat{a}(\underline{A}_k) + A_k^*\, \hat{a}^\dagger(\underline{A}_k)\}\, \mathrm{d}\mu(k)\,, \tag{4.60}$$

and the expansion in terms of the reciprocal mode set $\underline{A}_k$ takes the form

$$\hat{A} = \int_X \{\underline{A}_k\, \hat{a}(A_k) + \underline{A}_k^*\, \hat{a}^\dagger(A_k)\}\, \mathrm{d}\mu(k)\,, \tag{4.61}$$

where the formal ladder operators $\hat{a}(A_k)$ and $\hat{a}^\dagger(A_k)$ are required to satisfy the commutation relations

$$[\hat{a}(A_k), \hat{a}(\underline{A}_{k'})] = 0\,, \qquad [\hat{a}(A_k), \hat{a}^\dagger(\underline{A}_{k'})] = 0\,, \qquad [\hat{a}(A_k), \hat{a}^\dagger(\underline{A}_{k'})] = \delta(k,k')\,. \tag{4.62}$$

In this picture, the ladder operators thus play the role of "generalized Fourier coefficients" arising in the mode expansion of classical solutions.

The practical justification for such mode expansions is that if one "computes" $(A' \mid A)$ using Eqs. (4.3), (4.60) and (4.61), one obtains ladder operators satisfying the Heisenberg commutation relations (4.21). Moreover, if the gauge function $\hat{\chi}$ of $\hat{A}$ is computed term-by-term in the above expansion and then smeared by a classical solution ϕ to Eq. (4.5) using Eq. (4.7), one obtains an operator with the same algebraic properties as $\hat{\mathfrak{X}}(\phi)$ defined in Eq. (4.37). Finally, this notation motivates the nomenclature of $\hat{a}(A')$ and $\hat{a}^\dagger(A')$ as annihilation and creation operators, as for any positive-frequency solution A one has

$$[\hat{A}, \hat{a}^\dagger(A)] = +A\,, \qquad\qquad [\hat{A}, \hat{a}(A)] = -A^*\,. \tag{4.63}$$

Taking Klein–Gordon products of these equations with another classical solution A' reproduces Eq. (4.31).

Mode expansions as in Eqs. (4.60) and (4.61) are commonly used in textbooks on particle physics [102; 145; 163; 164], quantum optics [98; 144; 156], and also in recent work on quantum optics in curved space-times [5; 41–44; 46; 165]. However, the general quantization scheme described in Section 4.3 does not rely on such mode solutions, which shows that certain quantum properties of the electromagnetic field can be described without detailed knowledge of the full spectrum of solutions to the classical equations. This is particularly relevant to the applications considered in this document: describing the propagation of quantum states of light in optical fibers in a curved space-time does not require any knowledge of light propagation far away from the fiber. This approach is used in Chapter 6 to describe photon interferometry in stationary space-times using only a finite number of classical wave packets instead of an infinite set of modes.

4.6 Single Modes

Whereas the mode expansion described above requires a complete set of modes, the general methods described in Section 4.3 show that the ladder operators $\hat{a}(A)$ and $\hat{a}^\dagger(A)$ of a single classical solution A can be described consistently without the need to compute further modes to obtain a complete mode expansion. This section describes standard concepts used in the description of such single modes.

If $\hat{a}$ and $\hat{a}^\dagger$ are the ladder operators corresponding to a normalized classical solution A, one has

$$[\hat{a}, \hat{a}] = 0\,, \qquad [\hat{a}^\dagger, \hat{a}^\dagger] = 0\,, \qquad [\hat{a}, \hat{a}^\dagger] = 1\,. \tag{4.64}$$

As $\hat{a}$ cannot be Hermitian, it is not an observable. However, one can define the quadrature operators

$$\hat{q} = \tfrac{1}{\sqrt{2}}(\hat{a}^\dagger + \hat{a})\,, \qquad \hat{p} = \tfrac{i}{\sqrt{2}}(\hat{a}^\dagger - \hat{a})\,, \tag{4.65}$$

which are Hermitian. The commutation relation of $\hat{a}$ with $\hat{a}^\dagger$ implies

$$[\hat{q}, \hat{p}] = i\,, \tag{4.66}$$

so that $\hat{q}$ and $\hat{p}$ behave similarly to position and momentum in non-relativistic quantum mechanics.

Displacement Operator To study coherent states of light, it is customary to define the unitary displacement operator [166]

$$\hat{D}(\alpha, A) = \exp\left[\alpha\, \hat{a}^\dagger(A) - \alpha^* \hat{a}(A)\right]\,, \tag{4.67}$$

where A is a normalized positive-frequency solution and $\alpha \in \mathbf{C}$ is a complex "displacement parameter." Since, in the current formalism, $\hat{a}$ and $\hat{a}^\dagger$ are also well-defined for solutions that are not normalized, and since $\hat{a}^\dagger$ is linear whereas $\hat{a}$ is linear, it suffices to consider expressions of the form

$$\hat{D}(A) = \exp\left[\hat{a}^\dagger(A) - \hat{a}(A)\right]\,, \tag{4.68}$$

where A is any positive-frequency solution (not necessarily normalized). A key property of this operator is that if A and A' are any positive-frequency solutions, one has

$$\hat{D}^\dagger(A')\ \hat{a}(A)\hat{D}(A') = \hat{a}(A)\ \ + (A \mid A')\,, \tag{4.69}$$

$$\hat{D}^\dagger(A')\hat{a}^\dagger(A)\hat{D}(A') = \hat{a}^\dagger(A) + (A' \mid A)\,, \tag{4.70}$$

as one can readily show using a special case of the Lie–Hadamard formula stating that if X and Y commute with $[X,Y]$, then $e^X Y e^{-X} = Y + [X,Y]$. Using Eq. (4.35), one further obtains

$$\hat{D}^\dagger(A')\ \hat{\Phi}(A)\hat{D}(A') = \hat{\Phi}(A) + (A \mid 2\,\mathrm{Re}\,A')\,, \tag{4.71a}$$
$$\hat{D}^\dagger(A')\hat{\Phi}^\dagger(A)\hat{D}(A') = \hat{\Phi}^\dagger(A) + (2\,\mathrm{Re}\,A' \mid A)\,. \tag{4.71b}$$

In the heuristic notation Eq. (4.17), the displacement operator thus acts on $\hat{A}$ as

$$\hat{D}^\dagger(A')\hat{A}\hat{D}(A') = \hat{A} + 2\,\mathrm{Re}\,A'\,. \tag{4.72}$$

This shifting property motivates naming $\hat{D}(A)$ a displacement operator.

Coherent States Using the above definition of the displacement operator, one can define coherent states as

$$|\mathrm{coh}(A')\rangle = \hat{D}(A')|0\rangle\,. \tag{4.73}$$

Whereas the ground-state has a vanishing one-point function, $\langle 0|\hat{\Phi}^\dagger(A)|0\rangle = 0$, Eq. (4.71) shows that $|\mathrm{coh}(A')\rangle$ has a non-trivial one-point function:

$$\langle \mathrm{coh}(A')|\hat{\Phi}^\dagger(A)|\mathrm{coh}(A')\rangle = (2\,\mathrm{Re}\,A' \mid A)\,. \tag{4.74}$$

In the heuristic notation of Eq. (4.17), this is commonly written as

$$\langle \mathrm{coh}(A')|\hat{A}|\mathrm{coh}(A')\rangle = 2\,\mathrm{Re}\,A' = A' + \mathrm{c.c.}\,, \tag{4.75}$$

where c.c. stands for the complex conjugate of the preceding term. Coherent states thus closely resemble classical states of light.

An explicit expansion of coherent states in terms of Fock states can be obtained using the formula

$$\hat{D}(A) = e^{-\frac{1}{2}(A|A)} \exp[+\hat{a}^\dagger(A)] \exp[-\hat{a}(A)]\,, \tag{4.76}$$

which follows from the Kermack–McCrea identity [167]. With this expression, one finds

$$|\mathrm{coh}(A')\rangle = e^{-\frac{1}{2}(A'|A')} \exp[\hat{a}^\dagger(A')]|0\rangle\,. \tag{4.77}$$

In particular, if $A' = \alpha A$ with $(A \mid A) = 1$, one obtains

$$|\mathrm{coh}(A')\rangle = e^{-\frac{1}{2}|\alpha|^2} \sum_{n=0}^{\infty} \frac{\alpha^n}{n!} (\hat{a}^\dagger(A))^n |0\rangle = e^{-\frac{1}{2}|\alpha|^2} \sum_{n=0}^{\infty} \frac{\alpha^n}{\sqrt{n!}} |(A,n)\rangle\,, \tag{4.78}$$

where $|(A,n)\rangle$ is the Fock state describing n excitations in the mode A. This shows that the

photon numbers in a coherent state $|\mathrm{coh}(A')\rangle$ follow a Poisson distribution with parameter $|\alpha|^2 = (A' \mid A')$.

4.7 Illustration: Jauch–Watson Problem

To demonstrate the methods developed so far, this section briefly discusses the simple case of light propagating in a linear dielectric in flat space-time, where the medium's four-velocity u^μ is covariantly constant and both the permittivity ε and the permeability μ are constant. Such a setup was first considered using alternative methods by Jauch and Watson in Refs. [108–110]. Here, the problem is first approached using the method of formal mode expansions, as described in Section 4.5, and the algebraic approach is presented at the end of this section.

In flat space-time, ${}^{(4)}g_{\mu\nu}$ reduces to the Minkowski metric

$$ {}^{(4)}g_{\mu\nu}\mathrm{d}x^\mu \mathrm{d}x^\nu = -\mathrm{d}t^2 + \mathrm{d}x^2 + \mathrm{d}y^2 + \mathrm{d}z^2 \,, \tag{4.79} $$

and the optical metric for a medium at rest in the considered inertial coordinate system is given by

$$ \tilde{g}_{\mu\nu}\mathrm{d}x^\mu \mathrm{d}x^\nu = -\frac{\mathrm{d}t^2}{\varepsilon\sqrt{\mu}} + \sqrt{\mu}(\mathrm{d}x^2 + \mathrm{d}y^2 + \mathrm{d}z^2) \,. \tag{4.80} $$

The evolution equation for the gauge function χ, generally given by Eq. (4.5), takes the form

$$ \tilde{g}^{\rho\sigma}\partial_\rho\partial_\sigma\chi = 0 \,, \tag{4.81} $$

which has plane-wave solutions of the form $e^{ik.x}$, where $k.x = k_\mu x^\mu$, and k_μ is lightlike with respect to the optical metric $\tilde{g}^{\mu\nu}$. In the following, such wave covectors will be referred to as future-pointing (or past-pointing) if $K^\mu = \tilde{g}^{\mu\nu}k_\nu$ is future-pointing (or past-pointing). For future-pointing k_μ and k'_μ, the Klein–Gordon product defined in Eq. (4.7) yields

$$ (e^{\pm ik.x} \mid e^{\pm ik'.x}) = \pm\delta(k, k') \,, \tag{4.82} $$

$$ (e^{\pm ik.x} \mid e^{\mp ik'.x}) = 0 \,, \tag{4.83} $$

with

$$ \delta(k, k') = -\tfrac{2}{\hbar}\tilde{g}^{\mu\nu}k_\mu\Gamma_\nu\,(2\pi)^3\delta(\boldsymbol{k} - \boldsymbol{k}') \,, \tag{4.84} $$

where $\boldsymbol{k}$ denotes the spatial part of k_μ. Similarly, the field equation for A_μ reduces to

$$ \tilde{g}^{\rho\sigma}\partial_\rho\partial_\sigma A_\mu = 0 \,, \tag{4.85} $$

which also has plane-wave solutions:

$$A_\mu = a_\mu e^{ik.x}\,, \tag{4.86}$$

whose gauge functions take the form

$$\chi = i\tilde{g}^{\mu\nu}k_\mu a_\nu e^{ik.x}\,. \tag{4.87}$$

For future-pointing wave covectors k_μ and k'_μ, Eq. (4.3) yields

$$(ae^{\pm ik.x} \mid a'e^{\pm ik'.x}) = \pm\tilde{g}^{\mu\nu}a^*_\mu a'_\nu\,\delta(k,k')\,, \tag{4.88}$$
$$(ae^{\pm ik.x} \mid a'e^{\mp ik'.x}) = 0\,. \tag{4.89}$$

Further, Eq. (4.12) for the Ashtekar–Magnon bracket yields

$$\{ae^{\pm ik.x} \mid a'e^{\pm ik'.x}\} = (\mp\hbar\mathcal{K}^\mu k_\mu)(ae^{\pm ik.x} \mid a'e^{\pm ik'.x})\,, \tag{4.90}$$
$$\{ae^{\pm ik.x} \mid a'e^{\mp ik'.x}\} = 0\,, \tag{4.91}$$

so that the Hamiltonian $\mathcal{H}$ is found to act on plane waves as

$$\mathcal{H}(ae^{ik.x}) = (-\hbar\mathcal{K}^\mu k_\mu)(ae^{ik.x})\,. \tag{4.92}$$

Equivalently, the energy of plane wave modes relative to the Killing vector field $\mathcal{K}^\mu$ is given by

$$E = -\hbar\mathcal{K}^\mu k_\mu\,, \tag{4.93}$$

which is in agreement with the general Schrödinger equation (4.14).

As described in Section 3.3.2, the anomalous Doppler effect implies that the sign of E is not invariant under Lorentz transformations of the Killing field $\mathcal{K}^\mu$, which shows that different choices of $\mathcal{K}^\mu$ lead to different notions of photons. This observation has applications in the theoretical description of the Cherenkov effect [168–170], which, however, lies beyond the scope of this work. Hence, the remainder of this section uses $\mathcal{K}^\mu = u^\mu$, as stated in Eq. (4.13), in which case the notion of k_μ being future-pointing and having positive frequency coincide.

Gupta–Bleuler Condition It follows from the general considerations in Section 4.3 that $\hat{a}^\dagger(A)|0\rangle$ defines a physical state in the sense of the Gupta–Bleuler scheme if and only if A satisfies the gauge condition. For wave packets built out of the Fourier modes described here, this requires that each Fourier component $a_\mu e^{+ik.x}$ satisfies $\tilde{g}^{\mu\nu}a_\mu k_\nu = 0$. For completeness, and to make contact with notation commonly used in quantum optics, this section describes the Gupta–Bleuler condition using the formal method of mode expansions described in Section 4.5.

Every future-pointing k_μ can be extended to an optical null frame $(k_\mu, l_\mu, e_{(1)\mu}, e_{(2)\mu})$, with k_μ and l_μ being real, and $e_{(i)\mu}$ complex, satisfying

$$\tilde{g}^{\mu\nu} k_\mu k_\nu = 0\,, \qquad \tilde{g}^{\mu\nu} l_\mu l_\nu = 0\,, \qquad \tilde{g}^{\mu\nu} k_\mu l_\nu = 1\,, \tag{4.94a}$$

$$\tilde{g}^{\mu\nu} k_\mu e_{(i)\nu} = 0\,, \qquad \tilde{g}^{\mu\nu} l_\mu e_{(i)\nu} = 0\,, \qquad \tilde{g}^{\mu\nu} e^*_{(i)\mu} e_{(j)\nu} = \delta_{ij}\,. \tag{4.94b}$$

The mode expansion (4.60) then takes the form

$$\hat{A} = \int \Big\{ e_{(1)} \hat{a}_1(k) + e_{(2)\mu} \hat{a}_2(k) + k \hat{c}(k) + l \hat{b}(k) \Big\} e^{+ik.x} \, \mathrm{d}\mu(k) + \text{H.c.} \tag{4.95}$$

Here, the integral extends over the set of all future-pointing k_μ, satisfying $\tilde{g}^{\mu\nu} k_\mu k_\nu = 0$, with the measure

$$\mathrm{d}\mu(k) = \frac{\hbar}{-2 \tilde{g}^{\mu\nu} k_\mu \Gamma_\nu} \frac{\mathrm{d}^3 \boldsymbol{k}}{(2\pi)^3}\,, \tag{4.96}$$

H.c. denotes the formal adjoint of the preceding term, and $\hat{a}_i(k)$, $\hat{b}_i(k)$, and $\hat{c}_i(k)$ are the ladder operators associated to physical modes, gauge modes, and ghost modes, respectively:

$$\hat{a}_i(k) = \hat{a}(e_{(i)} e^{ik.x})\,, \qquad \hat{b}(k) = \hat{a}(k e^{ik.x})\,, \qquad \hat{c}(k) = \hat{a}(l e^{ik.x})\,, \tag{4.97}$$

and the k-dependence of the null frame was suppressed for notational simplicity. Computing the gauge function term by term, one obtains

$$\hat{\chi} = i \int \Big\{ \hat{b}(k) e^{+ik.x} - \hat{b}^\dagger(k) e^{-ik.x} \Big\} \, \mathrm{d}\mu(k)\,. \tag{4.98}$$

The positive-frequency component is then given by

$$\hat{\chi}^{(+)} = i \int \hat{b}(k) e^{+ik.x} \mathrm{d}\mu(k)\,, \tag{4.99}$$

and the Gupta–Bleuler condition for a state $|\psi\rangle$ then requires that

$$\hat{b}(k) |\psi\rangle = 0 \qquad\qquad \text{for all future-pointing } k_\mu. \tag{4.100}$$

Note that this does not remove gauge excitations since

$$\hat{b}(k) \hat{b}^\dagger(k') |0\rangle = [\hat{b}(k), \hat{b}^\dagger(k')] |0\rangle = (k e^{ik.x} \mid k e^{ik'.x}) |0\rangle = 0\,, \tag{4.101}$$

as gauge solutions have vanishing norms. Instead, this condition correctly removes ghost excitations as

$$\hat{b}(k) \hat{c}^\dagger(k') |0\rangle = [\hat{b}(k), \hat{c}^\dagger(k')] |0\rangle = (k e^{ik.x} \mid l e^{ik.x}) |0\rangle = \delta(k, k') |0\rangle \neq 0\,. \tag{4.102}$$

Hence, the space $\mathfrak{Z}$ consists of all states generated from $|0\rangle$ by repeated application of

$\hat{a}_i^\dagger$ and $\hat{b}^\dagger$, whereas $\mathfrak{B}$ consists of all states generated from $|0\rangle$ by a sequence of raising operators containing at least one gauge-creation operator $\hat{b}^\dagger$. The quotient $\mathfrak{H}$ defined in Eq. (4.45) can thus be identified with the space of states generated from $|0\rangle$ by repeated application of $\hat{a}_i^\dagger$. This confirms the expectation that every photon wave vector allows for two states of polarization.

Algebraic Description Even though the above discussion of the problem was based on the non-rigorous mode expansion (4.95), it is not difficult to extend the description to the algebraic framework described in Section 4.3. Indeed, positive-frequency wave packet solutions to Eq. (4.85) are given by Fourier integrals of the form

$$A = \int \left\{ \sum_{i=1}^{2} \psi_i(k) e_{(i)} + \psi_0(k) k + \psi_-(k) l \right\} e^{+ik.x} \, \mathrm{d}\mu(k) \,. \tag{4.103}$$

According to Section 4.4, the corresponding state $\hat{\Phi}^\dagger(A)|0\rangle = \hat{a}^\dagger(A)|0\rangle$ satisfies the Gupta–Bleuler condition (4.40) if and only if the classical solution satisfies the gauge condition $\chi = 0$, which is equivalent to $\psi_- = 0$. Since ψ_0 describes pure-gauge contributions and is thus physically irrelevant for defining quantum states, there is no loss of generality in setting $\psi_0 = 0$. Using Plancherel's theorem, the Klein–Gordon norm of such wave packets can be written as

$$(A \mid A) = \sum_{i=1}^{2} \int \psi_i^*(k) \psi_i(k) \, \mathrm{d}\mu(k) \,, \tag{4.104}$$

so that finite-norm solutions are obtained whenever this integral converges. Each normalized wave packet A of this form then gives rise to a positive-norm state $\hat{a}^\dagger(A)|0\rangle$ in the Krein space $\mathfrak{K}$, whose equivalence class defines a quantum state in the Hilbert space $\mathfrak{H}$. Inner products of such states can then be computed using Eq. (4.33a). For example, one has

$$\langle 0 | \hat{a}(A) \hat{a}^\dagger(A') | 0 \rangle = \sum_{i=1}^{2} \int \psi_i^*(k) \psi_i'(k) \, \mathrm{d}\mu(k) \,, \tag{4.105}$$

which is the same result as one would obtain from the mode-expansion approach using Eqs. (4.17) and (4.95). In this way, results from the mode-expansion quantization approach can be translated to the algebraic approach by forming normalizable wave packets.

4.8 Summary

The model developed here describes the quantum electromagnetic field in arbitrarily linear isotropic media in general globally hyperbolic space-times, provided the configuration is static in the sense that there is a vector field $\mathcal{K}^\mu$ satisfying both $\mathfrak{L}_\mathcal{K}\, {}^{(4)}g^{\mu\nu} = 0$ and $\mathfrak{L}_\mathcal{K}\tilde{g}^{\mu\nu} = 0$, where ${}^{(4)}g^{\mu\nu}$ is the (contravariant) space-time metric and $\tilde{g}^{\mu\nu}$ is the optical metric

$$\tilde{g}^{\mu\nu} = \frac{1}{\sqrt{\mu}}({}^{(4)}g^{\mu\nu} + u^\mu u^\nu) - \sqrt{\mu\varepsilon}\, u^\mu u^\nu \,,$$

with u^μ, ε, and μ denoting the dielectric's four-velocity, permittivity, and permeability, respectively.

In the present model, the physical states are generated from the ground state $|0\rangle$ by repeated action of creation operators of the form $\hat{a}^\dagger(A)$, where A is any classical positive-frequency solution of suitable spatial decay that satisfies the gauge condition $\chi[A] = 0$, where χ is the gauge function

$$\chi = \tfrac{1}{\sqrt{\mu}}\, {}^{(4)}\nabla_\mu(\sqrt{\mu}\, \tilde{g}^{\mu\nu} A_\nu) \,.$$

The inner product of such states is expressible in terms of the Klein–Gordon product

$$(A \mid A') = \frac{i}{\hbar}\int_\Sigma (A^*_\mu \Pi'^\mu - A'_\mu \Pi^{*\mu})\, {}^{(3)}\boldsymbol{\epsilon} \,,$$

where Σ is any Cauchy surface, ${}^{(3)}\boldsymbol{\epsilon}$ is the volume form on Σ induced by the space-time volume form ${}^{(4)}\boldsymbol{\epsilon}$, and Π^μ is the momentum

$$\Pi^\mu[A] = -(G^{\mu\nu} - \tfrac{1}{\xi}\tilde{g}^{\mu\nu}\chi) \Gamma_\nu \,,$$

where Γ_μ is the Gauss map (unit co-normal) of the Cauchy surface Σ, and the excitation $G^{\mu\nu}$ is related to the field strength $F_{\mu\nu} = (\mathrm{d}A)_{\mu\nu}$ via the constitutive relation

$$G^{\mu\nu} = \tilde{g}^{\mu\rho}\tilde{g}^{\nu\sigma} F_{\rho\sigma} \,.$$

In particular, the inner product of two one-photon states is given by

$$\langle 0|\hat{a}(A_1)\hat{a}^\dagger(A_2)|0\rangle = (A_1 \mid A_2) \,.$$

The general methods used to construct the presented quantum theory are well known in various fields of theoretical physics: the usage of algebraic formulations is standard in the field of quantum field theory in curved space-times, as is the Gupta–Bleuler method, which was developed in the field of particle physics. Also, generalizations of the Lorenz gauge to account for the permeability and permittivity of dielectric materials have been used previously in classical and quantum optics (mostly without particular emphasis on

either special or general relativity). The present chapter shows that these methods can be combined to develop a quantum theory of the electromagnetic field that simultaneously accounts for stationary gravitational fields and linear isotropic dielectrics with potentially discontinuous permeability and permittivity functions.

The algebraic structure of the quantum theory described here is seen to be independent of the concrete details of the space-time under consideration and the dielectric media located therein. However, to make concrete predictions for a specific setup, one needs to solve the field equations to obtain classical solutions A that serve as the basis of the quantum description of the electromagnetic field in a curved space-time. Such explicit calculations are presented in the next chapter.

Chapter 5

Gravitational Fiber Optics

Having laid out a quantization scheme for the electromagnetic field that accounts both for linear dielectric media and stationary gravitational fields, the next step towards making concrete experimental predictions is to find explicit solutions to the field equations formulated in Section 3.2.1. As explained in the introduction, current experimental proposals suggest using optical fibers to guide light through Earth's gravitational field along prescribed trajectories. Hence, one is facing the task of modeling optical fibers in curved space-time and solving the field equations in this setting.

Whereas the resolution of Maxwell's equations for straight step-index optical fibers in flat space-time is textbook material [171, Chap. 3; 172, Chap. 16], their solution in more general scenarios is not as simple. The first explicit (perturbative) solution to Maxwell's equations in straight optical fibers at a constant gravitational potential was provided in Ref. [48], see also Ref. [4]. This calculation was carried out before the development of the gauge-fixed field equations described in Section 3.2.1 and was thus performed at the level of the field strength $F_{\mu\nu}$ and excitation $G^{\mu\nu}$. Later work extended these results by including the shift vector arising from Earth's rotation in Ref. [94] and demonstrating the viability of obtaining a consistent quantum theory of gravitational fiber optics from the gauge-fixed field equations by solving them exactly for the case of a locally constant lapse function and vanishing shift vector [49]. A method of solving these equations for more general fiber geometries (but assuming space-time to be flat) was developed in Ref. [173]. Generalizing these previous results, this section provides a general perturbative solution to the gauge-fixed field equations for step-index optical fibers of arbitrary geometry in arbitrary stationary gravitational fields.

5.1 Methodology

To obtain concrete equations for fiber optics in the presence of gravity, one must model optical fibers in curved space-time. Whereas general relativity is most efficiently described in the language of space-time geometry, in practice, experimental setups are described in a language that distinguishes between space and time. This suggests using the methods

described in Section 2.3, where the geometry of space-time is expressed in terms of the spatial metric ${}^{(3)}g_{ij}$, the lapse ζ, and the shift ξ_i. The geometry of optical fibers can then be described in the language of three-dimensional spatial geometry, i.e., the fibers are modeled as extended objects in a Riemannian manifold $(\mathscr{S}, {}^{(3)}g_{ij})$. Concrete predictions for $({}^{(3)}g_{ij}, \zeta, \xi_i)$ were already discussed in Section 2.6. However, one can solve (in a perturbative manner) the field equations of electrodynamics for optical fibers in a general setting that relies only on few assumptions (specified below) on $({}^{(3)}g_{ij}, \zeta, \xi_i)$ but does not require explicit expressions for these quantities. This can be done using the following method, which first constructs coordinates adapted to the problem, models the problem in these adapted coordinates, and sets up a perturbative calculation scheme.

The first step is to erect spatial Fermi coordinates (analogous to the space-time Fermi coordinate system described in Section 2.5) around the baseline γ of the optical fiber. This coordinate system then provides an optimized Taylor-series expansion of the spatial metric ${}^{(3)}g_{ij}$ around γ, which is valid for all times as the space-time is assumed to be stationary, and the optical fiber is assumed to follow timelike Killing trajectories. Similarly, one can approximate the lapse ζ and shift ξ_i in the vicinity of γ using the Taylor series in the adapted Fermi coordinates. Effectively, this constitutes an expansion of the space-time metric around γ in powers of the distance from the fiber's baseline. This scheme thus reduces the required information on the space-time geometry to a limited set of functions along the baseline γ which characterize, for example, the bending of the curve and the space-time curvature along it.

The second step is to model the geometry of the fiber cross-section in this framework. Since the aforementioned Fermi coordinates are orthonormal along the baseline and deviations from orthonormality in the cross-sectional plane are typically negligible (they are on the order of the squared fiber radius multiplied by certain components of the Riemann curvature tensor), these coordinates can be considered as quasi-Cartesian over the fiber cross-section without significant error. Hence, the problem is reduced to describing the fiber cross-section and refractive index profile in such quasi-Cartesian coordinates. Even though the explicit calculations in this document rely on the simplifying assumption of a translation-invariant refractive index profile of a step-index fiber, the general formalism described below allows for arbitrary transverse fiber geometries.

Irrespective of the precise details of the fiber cross-section model, one further assumption is required to obtain explicitly solvable equations for light propagation in this setup. The main assumption underlying the calculations presented in this chapter is that all functions describing either the space-time geometry in the vicinity of the fiber or the cross-sectional geometry of the fiber are slowly varying in the following sense: To an electromagnetic wave in an optical fiber, one may associate a characteristic length scale ℓ_0, such as the optical wavelength or the core radius (in single-mode fibers, these two quantities are typically on the same order of magnitude). Similarly, any other external parameter ϕ (such as any component of the fiber normal or the Riemann curvature tensor, expressed in Fermi coordinates) is associated with a length scale ℓ_1. If, in geometric units, ϕ has the dimension

$(\text{length})^k$ and if s denotes the arc length along the fiber's baseline γ, the following equations assume that ϕ can be written as

$$\phi = \ell_1^k \psi(s/\ell_1)\,, \tag{5.1}$$

where ψ is a dimensionless function at most on the order of unity, whose derivatives are at the same order of magnitude. If $\varepsilon = \ell_0/\ell_1 \ll 1$, one can write

$$\phi = \ell_1^k \psi(\varepsilon s/\ell_0)\,, \tag{5.2}$$

and use the method of multiple scales [174, Chap. 11; 175, Chap. 6] to set up an explicitly solvable perturbative scheme, see also Refs. [176; 177] for applications of the multiple-scales method in related problems.

This assumption on the separation of scales, which requires all external parameters to vary on length scales much longer than the optical wavelength, is met in most applications. For example: typical single-mode fibers have core radii on the order of micrometers. If such a fiber is bent over the length scale of centimeters, the Fermi components of the baseline's normal can be written in the above form with $\varepsilon = \mu\text{m/cm} = 10^{-4}$ and $\psi \lesssim 1$ [173]. Similarly, for a fiber placed vertically in a $1/r$ potential $\varphi = -M/r$ with $r = R + s$, $s \ll R$ and $R > 2M$, second derivatives of φ (which determine the Riemann curvature tensor) can be written in the above form with $\ell_1 = R$ and $\psi(s/R) = (2M/R)(1 - 3s/R)$. For illustration: setting M equal to Earth's mass and R equal to Earth's radius, one obtains $\varepsilon \sim 10^{-13}$ and $\psi \lesssim 10^{-9}$.

The scheme outlined above is implemented in the following calculations, which are structured as follows: Section 5.2 describes the spatial Fermi coordinate system adapted to the fiber baseline and provides explicit formulæ for the Taylor-series expansion of the lapse ζ, shift ξ_i, and spatial metric ${}^{(3)}g_{ij}$. Section 5.3 then provides a classification of the various terms arising in such an expansion and identifies the terms of main interest for the applications considered in this document. To gain first insights into the problem, simplified models based on the eikonal equation and the proper-time of light rays are discussed in Sections 5.4 and 5.5. Section 5.6 then provides a perturbative solution of the gauge-fixed Maxwell equations for optical fibers in stationary gravitational fields that incorporates effects arising both from the lapse, ζ, and the tangential component of the shift vector, $\xi_\parallel$. The results for single-frequency modes and wave packets are described in Section 5.7 and Section 5.8, respectively. Finally, extensions of this perturbative scheme are discussed in Section 5.9.

5.2 Geometry of Curves

To describe the geometry of optical fibers in curved space, this section reviews the basic notions of the geometry of curves in three-dimensional Riemannian manifolds and describes an adapted coordinate system that serves as the basis of the explicit calculations below.

Frenet–Serret Frame Consider a curve γ forming the baseline of an optical fiber. If s denotes its arc length, the unit tangent vector is given by

$$T^i = \mathrm{d}\gamma^i(s)/\mathrm{d}s\,, \tag{5.3}$$

and the normal vector is

$$\nu^i = {}^{(3)}\nabla_T T^i\,. \tag{5.4}$$

Defining the curvature κ as the norm of ν^i ($\kappa^2 = \nu_i \nu^i$) and setting $N^i = \nu^i/\kappa$ to be the unit normal (in regions of non-zero curvature), one has

$$\nu^i = \kappa N^i\,. \tag{5.5}$$

Furthermore, the binormal B^i is defined as the cross-product

$$B_i = {}^{(3)}\epsilon_{ijk} T^j N^k\,. \tag{5.6}$$

In regions of non-zero curvature κ, one thus obtains the orthonormal Serret–Frenet frame (T, N, B). The evolution of this frame along the curve is described by the Serret–Frenet equations [178, p. 34]

$${}^{(3)}\nabla_T T^i = \kappa N^i\,, \qquad {}^{(3)}\nabla_T N^i = -\kappa T^i + \tau B^i\,, \qquad {}^{(3)}\nabla_T B^i = -\tau N^i\,, \tag{5.7}$$

where τ is the torsion

$$\tau = B_i\, {}^{(3)}\nabla_T N^i = -N_i\, {}^{(3)}\nabla_T B^i\,. \tag{5.8}$$

Fermi–Walker Transport The Fermi–Walker derivative ${}^{(3)}\mathrm{D}_s$ along a curve γ is a differentiation operator of tensor fields along γ, defined by its action on vector fields v^i as

$${}^{(3)}\mathrm{D}_s v^i = {}^{(3)}\nabla_T v^i + T^i \nu_j v^j - \nu^i T_j\, v^j\,, \tag{5.9}$$

see, e.g., Ref. [179]. This expression differs from the Fermi–Walker derivative along timelike curves in Lorentzian manifolds by the sign of the last two terms, cf. Eq. (2.62). One readily verifies that this derivative is metric-compatible, ${}^{(3)}\mathrm{D}_s\, {}^{(3)}g_{ij} = 0$. Whereas ${}^{(3)}\nabla_T T^i$ vanishes only if γ is a geodesic, the Fermi–Walker derivative satisfies ${}^{(3)}\mathrm{D}_s T^i = 0$ for all curves. It follows that if v^i is Fermi–Walker transported along γ, that is to say ${}^{(3)}\mathrm{D}_s v^i = 0$, then the inner product $T_i\, v^i$ remains constant along the curve.

In terms of the Fermi–Walker derivative, the Frenet–Serret equations (5.7) take the form

$${}^{(3)}\mathrm{D}_s T^i = 0\,, \qquad {}^{(3)}\mathrm{D}_s N^i = +\tau B^i\,, \qquad {}^{(3)}\mathrm{D}_s B^i = -\tau N^i\,. \tag{5.10}$$

If p is any point on γ (without loss of generality, let $p = \gamma(0)$), one may choose an orthonormal frame $(T^i, {e_1}^i, {e_2}^i)$ on p. This frame can then be extended along the entire curve γ by Fermi–Walker transport:

$$ {}^{(3)}\mathrm{D}_s {e_1}^i = {}^{(3)}\mathrm{D}_s {e_2}^i = 0 \,. \tag{5.11} $$

Explicitly, these vectors can be constructed from the unit normal N^i and the binormal B^i using

$$ \begin{pmatrix} {e_1}^i(s) \\ {e_2}^i(s) \end{pmatrix} = \begin{pmatrix} \cos\vartheta(s) & -\sin\vartheta(s) \\ \sin\vartheta(s) & \cos\vartheta(s) \end{pmatrix} \begin{pmatrix} N^i(s) \\ B^i(s) \end{pmatrix} , \tag{5.12} $$

where the rotation angle ϑ is given by integrated torsion along the curve:

$$ \vartheta(s) = \int_0^s \tau(s') \, \mathrm{d}s' + \text{const.} \tag{5.13} $$

The integration constant is fixed by the initial angle between the frame $({e_1}^i, {e_2}^i)$ and the transverse Serret–Frenet frame (N^i, B^i) at the reference point $p = \gamma(0)$. Whereas s was previously defined only on γ, this constriction extends s to a coordinate function in the neighborhood of the curve that reduces to the arc length when restricted to γ. An illustration of the Serret–Frenet frame and the Fermi–Walker frame is given in Fig. 5.1a: whereas $({e_1}^i, {e_2}^i)$ coincides with (N^i, B^i) at the lower end of the curve, the Fermi–Walker frame is visibility rotated against the Frenet–Serret frame at the upper end of the curve. The rotation angle at that point is equal to the integral of the torsion between the two endpoints.

Fermi Normal Coordinates The Fermi normal coordinate system $(s, x^\alpha) \equiv (s, x, y)$ with $\alpha = 1, 2$ is then defined through the chart

$$ \phi(s, x, y) = \exp_{\gamma(s)}[x^\alpha e_\alpha(s)] \,, \tag{5.14} $$

where $\exp : \mathrm{T}\mathscr{S} \to \mathscr{S}$ is the exponential map on the spatial manifold $\mathscr{S}$ (which maps tangent vectors to the point reached by the corresponding geodesic at unit affine parameter). Figure 5.1b illustrates such a coordinate system for the curve considered in Fig. 5.1a: the transverse coordinate grid is aligned with the Fermi–Walker frame $({e_1}^i, {e_2}^i)$ and hence rotated against the Frenet–Serret frame by an angle that increases along the curve by a rate equal to the torsion.

Expansion of the Metric Tensor Since the frame $(T^i, {e_1}^i, {e_2}^i)$ is orthonormal, the metric tensor ${}^{(3)}g_{ij}$ in Fermi normal coordinates reduces to its standard form δ_{ij} when evaluated on the curve γ. Additionally, the only non-zero spatial Christoffel symbols along

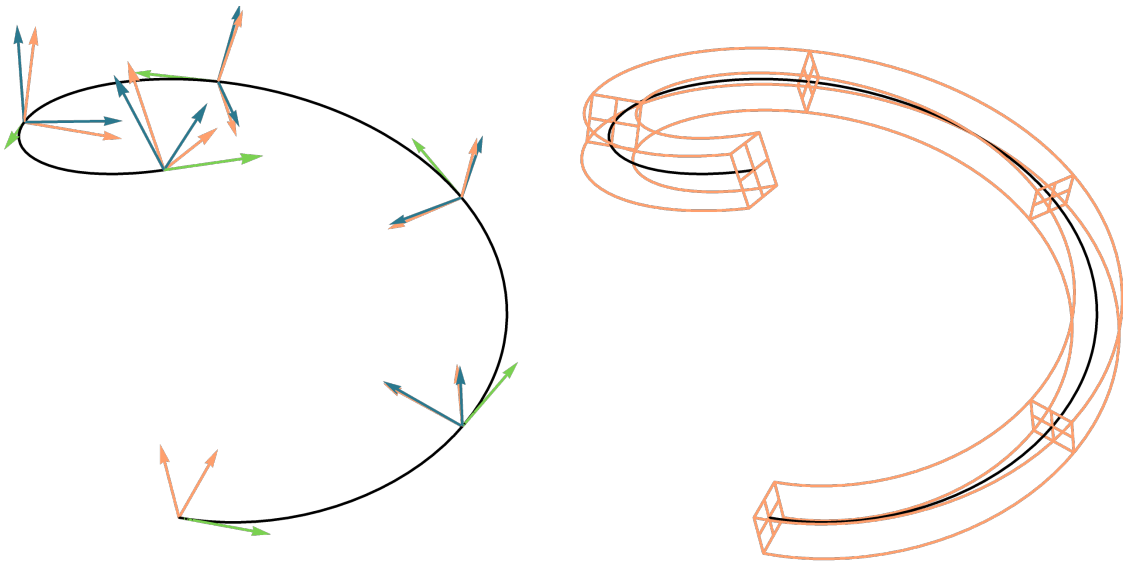

(a) Comparison of the Frenet–Serret frame (blue) with the Fermi–Walker frame (orange). At each point along the curve, the Frenet–Serret frame is obtained by rotating the Fermi–Walker frame around the tangent (green) by an angle equal to the integrated torsion.

(b) Illustration of Fermi normal coordinates in a tubular neighborhood of a curve. The coordinate axes are aligned with the Fermi–Walker frame (shown in orange in the left figure).

Figure 5.1: Illustration of the Frenet–Serret frame and the Fermi–Walker frame along a spatial curve (a) as well as of Fermi normal coordinates along the same curve (b).

the curve are determined by the normal ν_α:

$$ {}^{(3)}\Gamma_{\alpha ss} = -{}^{(3)}\Gamma_{s\alpha s} = -{}^{(3)}\Gamma_{ss\alpha} = \nu_\alpha \,. \tag{5.15} $$

Expanding the spatial metric ${}^{(3)}g_{ij}$ as a Taylor series around the curve γ, one obtains

$$ \begin{aligned} {}^{(3)}g = &\left[(1-\nu_\alpha x^\alpha)^2 - {}^{(3)}R_{s\alpha s\beta} x^\alpha x^\beta\right] \mathrm{d}s^2 \\ &+ \tfrac{4}{3}\,{}^{(3)}R_{s\alpha\beta\gamma} x^\alpha x^\beta \mathrm{d}s\,\mathrm{d}x^\gamma \\ &+ \left[\delta_{\alpha\beta} - \tfrac{1}{3}\,{}^{(3)}R_{\alpha\gamma\beta\delta} x^\gamma x^\delta\right] \mathrm{d}x^\alpha \mathrm{d}x^\beta + O(r^3)\,, \end{aligned} \tag{5.16} $$

where $r^2 = \delta_{\alpha\beta} x^\alpha x^\beta = x^2 + y^2$. In this expression, the components of the spatial curvature tensor are to be evaluated on the baseline, i.e., $x^\alpha = 0$, and are thus functions of the arc length s only. Note that, in three dimensions, the Riemann tensor ${}^{(3)}R_{ijkl}$ is fully determined by the Ricci tensor ${}^{(3)}R_{ij}$ [60, Corollary 7.26]. However, this does not yield a significant simplification of the local expansion of the metric tensor.

To study light propagation in bent fibers in flat space-time, Lai et al. introduced a slightly different coordinate system based on the Frenet–Serret frame instead of the Fermi–Walker frame [180; 181], see also Ref. [182]. In such a coordinate system, however, the normal ν_α enters in three metric components ${}^{(3)}g_{si}$, but in Fermi normal coordinates only ${}^{(3)}g_{ss}$ depends on ν_α. Moreover, as the Frenet–Serret frame is undefined in regions

where the curvature vanishes, such coordinates are undefined at straight fiber segments whereas the Fermi normal coordinates are also well-defined there.

Expansion of the Lapse and Shift Analogously to the components of the metric tensor, ${}^{(3)}g_{ij}$, one can expand the lapse function ζ as a Taylor series in powers of the transverse coordinates x^α:

$$\begin{aligned}\zeta(s,x,y) &= \zeta(s,0,0) + \nabla_\alpha\zeta(s,0,0)x^\alpha + \tfrac{1}{2}\nabla_\alpha\nabla_\beta\zeta(s,0,0)x^\alpha x^\beta + O(r^3) \\ &\equiv \zeta(s) + \nabla_\alpha\zeta(s)x^\alpha + \tfrac{1}{2}\nabla_\alpha\nabla_\beta\zeta(s)x^\alpha x^\beta + O(r^3)\,.\end{aligned} \tag{5.17}$$

Here, $\zeta(s)$ is the lapse along the baseline of the optical fiber, ∇ is the flat connection in the transverse plane, i.e., $\nabla_\alpha = \partial_\alpha$ in Fermi normal coordinates, and $\nabla_\alpha\zeta(s)$ and $\nabla_\alpha\nabla_\beta\zeta(s)$ are the first two transverse derivatives of the lapse, evaluated on the baseline. A similar expansion can be applied to the shift vector ξ_i with the following result:

$$\xi^i(s,x,y) = \xi^i(s) + \nabla_\alpha\xi^i(s)x^\alpha + \tfrac{1}{2}\nabla_\alpha\nabla_\beta\xi^i(s)x^\alpha x^\beta + O(r^3)\,. \tag{5.18}$$

Complex Triad For the subsequent calculations, it proves advantageous to introduce the vector fields

$$\mathfrak{e}_\parallel = \partial_s\,, \qquad \mathfrak{e}_\pm = \tfrac{1}{\sqrt{2}}(\partial_r \mp \tfrac{i}{r}\partial_\theta) = \tfrac{1}{\sqrt{2}}e^{\pm i\theta}(\partial_x \mp i\partial_y)\,, \tag{5.19}$$

where (s,r,θ) are cylindrical coordinates related to the Fermi normal coordinates (s,x,y) via

$$x = r\cos\theta\,, \qquad y = r\sin\theta\,. \tag{5.20}$$

The corresponding co-triad is given by

$$\mathfrak{e}^\parallel = \mathrm{d}s\,, \qquad \mathfrak{e}^\pm = \tfrac{1}{\sqrt{2}}(\mathrm{d}r \pm ir\mathrm{d}\theta) = \tfrac{1}{\sqrt{2}}e^{\mp i\theta}(\mathrm{d}x \pm i\mathrm{d}y)\,. \tag{5.21}$$

The reason for introducing this frame is the following: if one expands, for example, the term $x^\alpha\nabla_\alpha\zeta(s)$ arising in the Taylor expansion (5.17) as a Fourier series, one has

$$x^\alpha\nabla_\alpha\zeta(s) = \tfrac{1}{\sqrt{2}}r[\nabla_+\zeta(s) + \nabla_-\zeta(s)]\,, \tag{5.22}$$

where $\nabla_\pm\zeta(s)$ depends on the angle θ as $e^{\pm i\theta}$:

$$\nabla_\pm\zeta(s) \equiv \nabla_{\mathfrak{e}_\pm}\zeta(s) = \tfrac{1}{\sqrt{2}}[\nabla_x\zeta(s) \mp i\nabla_y\zeta(s)]e^{\pm i\theta}\,. \tag{5.23}$$

This structure also extends to higher derivatives. For example, $\nabla_\pm\nabla_\pm\zeta(s)$ depends on the angle θ as $e^{\pm 2i\theta}$, whereas $\nabla_\pm\nabla_\mp\zeta(s)$ is independent of θ. For vector fields, however, the

situation is different: the contravariant components of the lapse $\xi^{\pm}$ depend on θ as $e^{\mp i\theta}$:

$$\xi^{\pm}(s) = \tfrac{1}{\sqrt{2}}(\xi^x \pm i\xi^y)e^{\mp i\theta}\,. \tag{5.24}$$

However, since $\mathfrak{e}^{\pm}$ is metrically equivalent to $\mathfrak{e}_{\mp}$ (on the baseline), the covariant components have the expected angular dependence:

$$\xi_{\pm}(s) = \xi^{\mp}(s)\,, \qquad \text{and thus} \qquad \xi_{\pm}(s) = \tfrac{1}{\sqrt{2}}(\xi_x(s) \mp i\xi_y(s))e^{\pm i\theta}\,. \tag{5.25}$$

Hence, in cylindrical Fermi coordinates, the *covariant* frame indices separate the various Fourier components of any tensor along the baseline. This Fourier decomposition serves as the basis of the classification of the metric coefficients described in the next section.

5.3 Classification of Terms

Before doing explicit calculations, it is useful to discuss the interpretation of the various terms arising in the above expansion of the metric tensor and to categorize them in order to structure the subsequent analysis.

In view of the explicit expressions for the lapse ζ, shift ξ_i, and spatial metric ${}^{(3)}g_{ij}$ in space-time Fermi normal coordinates described in Section 2.5, one has the following interpretation:

- $\nu_\alpha(s)$ is the normal of the fiber's baseline,
- $\zeta(s)$ encodes the gravitational redshift along the baseline,
- $\nabla_\alpha\zeta(s)$ describes the gravitational acceleration transverse to the baseline,
- $\nabla_\alpha\nabla_\beta\zeta(s)$ describes second variations of the lapse in the fiber cross-section,
- $\xi_\parallel(s)$ is the shift (mostly arising from rotation) along the baseline,
- $\xi_\alpha(s)$ describes the shift in the fiber cross-section,
- ${}^{(3)}R_{\alpha\beta\gamma\delta}(s)$ is the spatial curvature evaluated on the baseline, thus describing the deviation from flatness in the fiber cross-section.

These quantities fully describe the space-time geometry along optical fibers in a stationary space-time. To model the propagation of light in such fibers, one must also characterize their kinematic and optical properties. Specifically, one has to specify

- the four-velocity of the fiber,
- the optical properties of the fiber core and fiber cladding
- the geometry of the core-cladding interface.

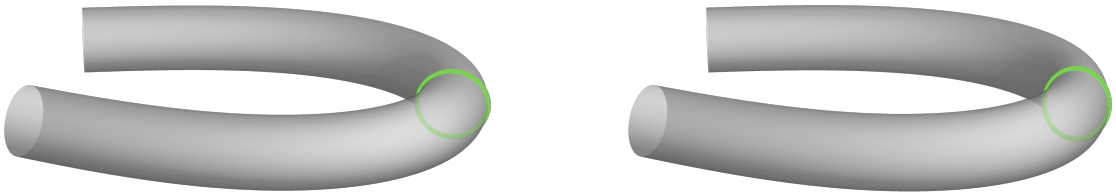

(a) The currently used model assumes the fiber cross-section to be circular throughout.

(b) More realistic models may include bending-induced deformations of the fiber cross-section.

Figure 5.2: A simplified model of the deformation of a fiber's cross-section due to bending is obtained by assuming the core-cladding interface to be compressed in the direction of the normal N_i and stretched in the direction of the binormal B_i by an amount depending on the curvature κ. The left panel shows the currently used model that neglects such effects, and the right panel shows such a fiber deformation with stretching and compression factors of equal magnitude. Additional deformations may arise from forces applied to support the fiber in a gravitational field (not shown).

In the following, the four-velocity u^μ of the fiber will be assumed to be proportional to the Killing vector field $(\mathcal{K}^\mu) = (1, \mathbf{0})$, so the components of u^μ are fully determined by the lapse ζ and the shift ξ_i via the equation

$$(u^\mu) = (1/\sqrt{\zeta^2 - \|\xi\|^2}, \mathbf{0})\,. \tag{5.26}$$

This fully determines the kinematic properties of the optical fiber so that it remains to model its dielectric properties. As the following calculations are based on Fourier series in the angular variable θ, and the decomposition of the aforementioned geometric quantities using the complex frame Eq. (5.19) separates such Fourier components, it is useful to describe the remaining optical properties in a similar manner. For example, the defining equation for the core-cladding interface $r = \rho(\theta, s)$ can be expanded in a Fourier series as

$$\rho(\theta, s) = \sum_{m \in \mathbf{Z}} \rho_m(s) e^{im\theta}\,. \tag{5.27}$$

Optical properties in the fiber core and cladding, such as the refractive index $n(r, \theta, s)$ can similarly be expanded as Fourier series in θ where the Fourier coefficients depend both on the radial variable r and the arc length s. Contrary to the various geometric functions described above, however, it is not appropriate to expand the refractive index n as a Taylor series in r around the baseline. For example, in step-index fibers, the refractive index is piecewise constant so that a Taylor expansion around the baseline would not capture the discontinuous transition to the refractive index in the cladding or that of ambient air.

The calculations in this chapter are based on the simplifying assumption that the core and the cladding are linear media with constant refractive indices n_1 and n_2, respectively, and that the core-cladding interface is circular at constant r (in the adapted Fermi normal

coordinate system). This model thus neglects nonlinear optical properties of the fiber materials, inhomogeneities and anisotropies in the optical properties (as induced from fiber bending via photoelastic effects, see, e.g., Refs. [183–185]), as well as deviations from a circular core-cladding interface (e.g., due to bending or arising from deformations of the fiber under its own weight, cf. Fig. 5.2). Wave-optics models of some of these effects are currently being investigated by F. Steininger.

As mentioned above, it is useful to supplement the interpretation of the various terms in the metric expansion around the fiber's baseline by a classification that allows for a structured approach in subsequent calculations.

In the unperturbed problem of a straight optical fiber in flat space-time, fiber modes can be computed using the ansatz

$$A_b = \tilde{A}_b(r) e^{i(\beta s + m\theta - \omega t)}\,, \tag{5.28}$$

where A_b refers to certain complex frame components of the electromagnetic field (see Eq. (5.50) below), β is the propagation constant, m is the azimuthal mode index, and ω is the optical frequency [171, Sect. 3; 172, Sect. 16.10]. Maxwell's equations then reduce to a radial Helmholtz equation

$$\underline{\mathrm{H}}_m \tilde{A}_b(r) = 0\,, \tag{5.29}$$

see Section 5.6 for an explicit expression for $\underline{\mathrm{H}}_m$. In single-mode fibers, the Helmholtz operator $\underline{\mathrm{H}}_m$ has a non-trivial kernel only if $m = \pm 1$ (corresponding to the handedness of circular polarization), and if β and ω satisfy a certain dispersion relation (described in detail below). In a perturbative scheme, a perturbation of the wave operator with a potentially non-trivial angular dependence induces perturbations of the form

$$\delta A_b = \delta\tilde{A}_b(r) e^{i(\beta s + m'\theta - \omega t)}\,, \tag{5.30}$$

with the value of m' determined by the angular dependence of the metric perturbation, e.g. $m' \in \{\pm 1\}$ for θ-independent perturbations, and $m' \in \{-2, \ldots, +2\}$ for metric perturbations with angular dependence $e^{\pm i\theta}$, etc. The field equations then yield inhomogeneous Helmholtz equations of the form

$$\underline{\mathrm{H}}_{m'} \delta\tilde{A}_b(r) = (\text{source terms})\,, \tag{5.31}$$

where one can distinguish two cases:

- For *off-resonant* perturbations, where $m' \neq \pm 1$, $\underline{\mathrm{H}}_{m'}$ is invertible and the field $\delta\tilde{A}_b(r)$ is on the same order of magnitude as the metric perturbation.

- For *resonant* perturbations, where $m' = \pm 1$, the operator $\underline{\mathrm{H}}_{m'}$ is not invertible and a solution exists only if the source term lies in the image of $\underline{\mathrm{H}}_{m'}$. This case requires

special analysis. In the cases considered below, such metric perturbations lead to corrections to the dispersion relation.

An intuitive interpretation is that resonant perturbations lead to phase shifts, whereas off-resonant perturbations correspond to amplitude perturbations. As phase shifts are experimentally more accessible than small perturbations of spatial mode profiles, the subsequent calculations are predominantly concerned with resonant perturbations.

Name		Term	Radial index	Fourier index
Lapse		ζ	0	0
	Gradient	$\nabla_\pm\zeta$	1	±1
	Laplacian	$\nabla_+\nabla_-\zeta$	2	0
	Hessian	$\nabla_\pm\nabla_\pm\zeta$	2	±2
Longitudinal Shift		$\xi_\parallel$	0	0
	Gradient	$\nabla_\pm\xi_\parallel$	1	±1
	Laplacian	$\nabla_+\nabla_-\xi_\parallel$	2	0
	Hessian	$\nabla_\pm\nabla_\pm\xi_\parallel$	2	±2
Transverse Shift		$\xi_\pm$	0	±1
		$\nabla_\pm\xi_\mp$	1	0
		$\nabla_\pm\xi_\pm$	1	±2
Bending		$\nu_\pm$	1	±1
		$\nu_+\nu_-$	2	0
		$\nu_\pm\nu_\pm$	2	±2
Spatial curvature		${}^{(3)}R_{\parallel+\parallel-}$	2	0
		${}^{(3)}R_{+-+-}$	2	0
		${}^{(3)}R_{\parallel\pm+-}$	2	±1
		${}^{(3)}R_{\parallel\pm\parallel\pm}$	2	±2

Table 5.1: Overview of metric coefficients up to and including those depending on the radial variable as r^2. The only "direct terms" with both the radial index and the Fourier index equal to zero are the lapse $\zeta(s)$ and the longitudinal shift $\xi_\parallel(s)$.

To describe how the various terms in the metric tensor can lead to resonant perturbations, it is useful to classify them according to the angular dependence of their contribution to the wave operator. Table 5.1 lists the Fourier index, i.e., the integer m in the angular dependence $e^{im\theta}$, for the various terms introduced in the previous section, as well as their radial index, i.e., the exponent of r characterizing the radial dependence of the term.

The relevance of the Fourier index in perturbation theory is illustrated in Fig. 5.3: terms with Fourier index ±1 yield a resonant coupling only at *second* order in perturbation theory (via the indirect couplings $\pm1 \leftrightarrow 0 \leftrightarrow \pm1$, $\pm1 \leftrightarrow 0 \leftrightarrow \mp1$ and $\pm1 \leftrightarrow \pm2 \leftrightarrow \pm1$), whereas a term with Fourier index ±2 produces such a resonant coupling already at first order in perturbation theory (via the direct coupling $\pm1 \leftrightarrow \mp1$). As is suggested by a simplified eikonal model considered in Section 5.4, and confirmed by the wave-optics analysis in Section 5.6, the terms of main relevance in the present setup are the "direct

terms" for which both the radial index and the Fourier index vanish. The effects of the remaining terms are described in Section 5.9.

The analysis shows that terms with vanishing Fourier index (such as $\nabla_+\nabla_-\zeta$, $\nabla_+\nabla_-\xi_\parallel$, $\nabla_\pm\xi_\mp$ and certain components of the Riemann tensor) give rise to perturbations of the optical phase, see Section 5.9.1. Terms with non-zero Fourier index, however, cause perturbations of the electromagnetic polarization, see Section 5.9.2. In line with the above considerations, one finds that terms with Fourier index ±2 (such as ${}^{(3)}R_{\parallel\pm\parallel\pm}$) produce such polarization effects at first order in perturbation theory, whereas terms with Fourier index ±1 (such as the baseline normal ν_i, which describes fiber bending) induce such effects only at second order in perturbation theory.

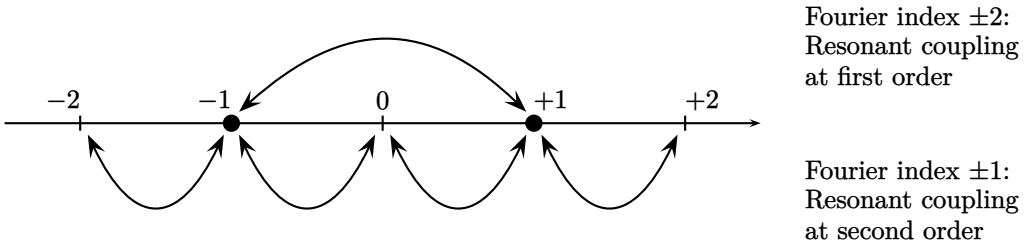

Figure 5.3: Schematic illustration of resonant perturbations arising from metric coefficients with different Fourier indices. For single-mode fibers, resonant perturbations occur at the Fourier indices $m = +1$ and $m = -1$. Starting from an unperturbed solution containing only $m = \pm1$ excitations, resonant coupling arises at first order in perturbation theory if the perturbation has Fourier index ±2 (i.e., angular dependence $e^{\pm2i\theta}$), whereas for field perturbations with Fourier index ±1 (i.e., angular dependence $e^{\pm i\theta}$) such a resonant coupling arises only at second order in perturbation theory.

5.4 Eikonal Model

Before considering the full wave-optics model, it is useful to consider a simplified model based on concepts of geometrical optics as described in Section 3.3.

For a dielectric at rest in a considered coordinate system (where the metric tensor can be decomposed in the form described in Section 2.3), Gordon's contravariant optical metric, defined in Eq. (3.10), takes the form

$$\bar{g}^{00} = -\frac{1}{\zeta^2}\frac{n^2 - \|\xi\|^2/\zeta^2}{1 - \|\xi\|^2/\zeta^2}\,, \tag{5.32}$$

$$\bar{g}^{0i} = \xi^i/\zeta^2\,, \tag{5.33}$$

$$\bar{g}^{ij} = {}^{(3)}g^{ij} - \xi^i\xi^j/\zeta^2\,, \tag{5.34}$$

where n is the medium's refractive index, ζ is the lapse function, ξ^i is the shift vector, and

${}^{(3)}g^{ij}$ is the contravariant spatial metric (all assumed to be time-independent). Seeking an eikonal of the form

$$\Psi(t,s) = -\omega t + \psi(s)\,, \tag{5.35}$$

the eikonal equation (3.49) leads to

$$\psi'(s) = \pm n\frac{\omega}{\zeta} + \frac{\omega}{\zeta^2}\xi_{\parallel} + O(\omega\|\xi\|^2)\,, \tag{5.36}$$

where the two signs correspond to different directions of propagation. Setting $\omega_{\mathrm{ph}} = \omega/\zeta$ to be the "physical frequency" (as measured in the dielectric's local rest frame), one obtains

$$\psi'(s) = \pm n\omega_{\mathrm{ph}} + \omega_{\mathrm{ph}}\xi_{\parallel}/\zeta + O(\omega\|\xi\|^2)\,. \tag{5.37}$$

In the absence of a shift vector ($\xi_i = 0$), this is the standard dispersion relation (in the dielectric's rest frame), with the sign determining the direction of light propagation, and the first-order shift correction accounts, i.a., for the Sagnac effect, see Section 6.4.

For light propagating along a given spatial curve γ, the spatial eikonal ψ thus evaluates to

$$\psi_\gamma = \pm\int_\gamma n\omega\zeta^{-1}\,\mathrm{d}s + \int_\gamma \omega\zeta^{-2}\xi + O(\omega\ell\|\xi\|^2)\,, \tag{5.38}$$

where, in the second term, ξ is regarded as a differential one-form (pulled back to the curve γ), and ℓ in the error term denotes the length of the curve γ.

Even though geometrical optics is generally assumed to be ill-suited for the description of light in single-mode fibers [186] because the fiber core radius is of the same order of magnitude as the optical wavelength, which makes high-frequency approximations difficult to justify, the calculations in Section 5.6 show that a similar formula also follows from Maxwell's equations for optical fibers (in the aforementioned approximation scheme).

5.5 Proper-Time Model

In the semi-classical approximation to quantum interferometry of massive particles, the quantum phase is determined by the proper-time elapsed along the particle's world-line [1]. As light propagates through media with a speed lower than in vacuo, one can define a notion of proper-time for such light rays (as for any other timelike curve) [31]. However, contrary to the theory of massive particles, this quantity turns out to be inadequate for describing gravitational photon interferometry.

To compute this proper-time $\tilde{\tau}$, consider a light ray with tangent vector K^μ that is null with respect to Gordon's optical metric

$$\bar{g}_{\mu\nu} = {}^{(4)}g_{\mu\nu} + (1-n^{-2})u_\mu u_\nu\,, \tag{5.39}$$

where u^μ is the four-velocity of the medium given in Eq. (5.26). By Eq. (3.55), this is equivalent to the condition that the light ray has a constant velocity equal to $1/n$ relative to the medium. Denoting by $\tilde{\lambda}$ the affine parameter of the light ray, one obtains

$$(u_\mu K^\mu)^2 = n^2 (\mathrm{d}\ell/\mathrm{d}\tilde{\lambda})^2 \,, \tag{5.40}$$

where $\mathrm{d}\ell^2 = ({}^{(4)}g_{\mu\nu} + u_\mu u_\nu)\mathrm{d}x^\mu \mathrm{d}x^\nu$ is the Landau–Lifshitz metric defined in Eq. (2.41), which encodes the spatial geometry in the rest-frame associated to the material's four-velocity. One then calculates

$$(\mathrm{d}\tilde{\tau}/\mathrm{d}\tilde{\lambda})^2 = -{}^{(4)}g_{\mu\nu} K^\mu K^\nu = (u_\mu K^\mu)^2 - (\mathrm{d}\ell/\mathrm{d}\tilde{\lambda})^2 = (n^2 - 1)(\mathrm{d}\ell/\mathrm{d}\tilde{\lambda})^2 \,, \tag{5.41}$$

hence

$$\mathrm{d}\tilde{\tau} = \sqrt{n^2 - 1}\, \mathrm{d}\ell \,. \tag{5.42}$$

The proper-time $\tilde{\tau}$ is thus directly proportional to the distance traveled by the light ray, as measured in the rest frame of the dielectric.

For an interferometer where two light rays propagate in different arms with the same refractive index n, the difference in proper-time $\tilde{\tau}$ is thus fully determined by the difference in proper length ℓ of the two interferometer arms:

$$\Delta\tilde{\tau} = \sqrt{n^2 - 1}\, \Delta\ell \,. \tag{5.43}$$

If both interferometer arms are equally long, the difference in proper-time $\tilde{\tau}$ along the corresponding light rays vanishes. Comparing with the eikonal result given in Eq. (5.38), it is clear that the effective proper-time of light rays in dielectrics does not determine the phase shift predicted by the eikonal model,[(1)] which is a good approximation to the phase computed from Maxwell's equations, as is shown in Section 5.6. For optical interferometry, the proper-time difference $\tilde{\tau}$ thus cannot serve as a basis of explanation for the gravitational phase shift, the Sagnac effect, or related effects. This is in contrast to interferometry of massive particles, where the proper-time difference $\Delta\tilde{\tau}$ determines the phase difference via $\Delta\Psi = m\Delta\tilde{\tau}/\hbar$ [1; 23].

5.6 Wave-Optics Model

This section describes the propagation of light in bent optical fibers in a wave optics model, i.e., using Maxwell's equations in the metric described in Section 5.2. This resolves the tension between the eikonal model (Section 5.4) and the proper-time model (Section 5.5) as

[(1)] A simple example is obtained by considering a static space-time in which the shift ξ_i vanishes, as in that case one has $\Delta\ell = \Delta s$, see Eq. (2.41). If γ_1 and γ_2 are curves of equal length, then $\Delta s = 0$ and hence $\Delta\tilde{\tau} = 0$, but according to Eq. (5.38), $\Delta\psi$ depends on the difference in integrals of ζ^{-1} along the curves. Hence, if $\int_{\gamma_1} \mathrm{d}s/\zeta \neq \int_{\gamma_2} \mathrm{d}s/\zeta$, one obtains $\Delta\psi \neq 0$ despite the fact that $\Delta\tilde{\tau} = 0$.

it is shown that the eikonal model provides an accurate prediction for the electromagnetic phase in optical fibers as derived from Maxwell's equations.

Throughout, the following calculations assume the dielectrics forming the waveguide to be non-magnetic, i.e., $\mu = 1$. In this case, the optical metric defined in Eq. (3.12) coincides with Gordon's metric given in Eq. (3.10). Moreover, as was the case in Section 5.4, all calculations will be performed up to order $O(\xi_\parallel^2)$, i.e., only terms that are at most linear in $\xi_\parallel$ are retained.

Setup This section focuses on the dominant effects in light propagation in bent optical fibers in a non-trivial space-time metric ${}^{(4)}g_{\mu\nu}$. Specifically, only the "direct terms" identified in the classification of Section 5.3 are considered: the lapse $\zeta(s)$ and the longitudinal shift $\xi_\parallel(s)$, evaluated on the fiber's baseline. These terms are the only ones listed in Table 5.1 which have both a vanishing radial index and a vanishing Fourier index. Compared to the dominant terms considered here, the neglected terms are suppressed by either a positive power of the ratio of the fiber radius to the characteristic length scale of the neglected term (such as the fiber's curvature radius or the curvature of ambient space), or produce resonant perturbations (according to the nomenclature of Section 5.3) only at higher order in perturbation theory. Such corrections are discussed in Section 5.9.

Within this approximation, the calculations are carried out in the effective metric

$$ {}^{(4)}g = -\zeta(s)^2 \mathrm{d}t^2 + 2\xi_\parallel(s)\mathrm{d}t\,\mathrm{d}s + \mathrm{d}r^2 + r^2\mathrm{d}\vartheta^2 + \mathrm{d}s^2\,. \tag{5.44} $$

In practice, the lapse $\zeta(s)$ and the longitudinal shift $\xi_\parallel(s)$ are not arbitrary functions along the fiber, but they are slowly varying. This means that these functions change significantly only over length scales much larger than the fiber core radius or the wavelength of light propagating therein. For example, in an optical fiber spool with a radius of curvature on the order of 10 cm, the functions $\zeta(s)$ and $\xi_\parallel(s)$ change on length scales of the same order of magnitude, which is much larger than the typical core radius of single-mode fibers (about 4 µm) or commonly used optical wavelengths (about 1500 nm).

If distances are measured in multiples of the fiber core radius so that the core-cladding interface lies at $r = 1$, and if ε is the ratio of the fiber core radius to the long-distance scale, e.g., $\varepsilon \sim 1\,\mu\mathrm{m}/10\,\mathrm{cm} = 10^{-5}$, the following calculations assume that ζ and $\xi_\parallel$ are of the form

$$ \zeta = \zeta(\varepsilon s)\,, \qquad\qquad \xi_\parallel = \xi_\parallel(\varepsilon s)\,. \tag{5.45} $$

One may thus think of s as measuring the arc length in units of micrometers (short distance scale), and $\varsigma = \varepsilon s$ as measuring the arc length in tens of centimeters (long distance scale). The small parameter ε will be referred to as the slowness parameter and will function as a perturbative expansion parameter in the following calculations.

The nomenclature is thus the following:

$s =$ short distance scale ,

$\varsigma =$ long distance scale ,

$\varepsilon = \varsigma/s =$ slowness parameter ,

and the metric under consideration takes the form

$$ {}^{(4)}g = -\zeta(\varsigma)^2 \mathrm{d}t^2 + 2\xi_{\parallel}(\varsigma)\mathrm{d}t\,\mathrm{d}s + \mathrm{d}r^2 + r^2\mathrm{d}\vartheta^2 + \mathrm{d}s^2 \,. \tag{5.46} $$

Complex Tetrad Section 5.2 introduced a complex triad $(\mathfrak{e}_{\parallel}, \mathfrak{e}_{+}, \mathfrak{e}_{-})$ to separate the Fourier components of various terms entering the metric tensor, expressed in cylindrical coordinates, see Section 5.3, and in particular Table 5.1. To analyze the field equations for the electromagnetic potential A, it is advantageous to extend the triad to a tetrad:

$$ \mathfrak{e}_0 = \partial_t \,, \qquad \mathfrak{e}_{\sharp} = \tfrac{1}{\sqrt{2}}(\partial_r + \tfrac{i}{r}\partial_\theta) \,, \tag{5.47a} $$

$$ \mathfrak{e}_{\parallel} = \partial_s \,, \qquad \mathfrak{e}_{\flat} = \tfrac{1}{\sqrt{2}}(\partial_r - \tfrac{i}{r}\partial_\theta) \,. \tag{5.47b} $$

The corresponding co-tetrad is given by

$$ \mathfrak{e}^0 = \mathrm{d}t \,, \qquad \mathfrak{e}^{\sharp} = \tfrac{1}{\sqrt{2}}(\mathrm{d}r - ir\mathrm{d}\vartheta) \,, \tag{5.48a} $$

$$ \mathfrak{e}^{\parallel} = \mathrm{d}s \,, \qquad \mathfrak{e}^{\flat} = \tfrac{1}{\sqrt{2}}(\mathrm{d}r + ir\mathrm{d}\vartheta) \,, \tag{5.48b} $$

using which the metric tensor can be written as

$$ \begin{aligned} {}^{(4)}g = &- \zeta(\varsigma)^2\, \mathfrak{e}^0 \otimes \mathfrak{e}^0 + 2\xi_{\parallel}(\varsigma)[\mathfrak{e}^0 \otimes \mathfrak{e}^{\parallel} + \mathfrak{e}^{\parallel} \otimes \mathfrak{e}^0] \\ &+ \mathfrak{e}^{\parallel} \otimes \mathfrak{e}^{\parallel} + \mathfrak{e}^{\sharp} \otimes \mathfrak{e}^{\flat} + \mathfrak{e}^{\flat} \otimes \mathfrak{e}^{\sharp} \,. \end{aligned} \tag{5.49} $$

Using this tetrad, the electromagnetic potential A_μ can be decomposed as

$$ A_\mu = A_b \mathfrak{e}^b{}_\mu \,, \tag{5.50} $$

where the subscript b is a frame index relative to the complex co-tetrad (5.48).

Interface Conditions In terms of the frame components A_b, the junction conditions of Eq. (3.37) can be expressed as follows. Denote, for any A_b, by $\boldsymbol{\Delta}[A]$ an eight-component

column vector defined as

$$\boldsymbol{\Delta}_1[A] = [\![A_0]\!]\,, \tag{5.51a}$$
$$\boldsymbol{\Delta}_2[A] = [\![A_\parallel]\!]\,, \tag{5.51b}$$
$$\boldsymbol{\Delta}_3[A] = [\![A_\sharp]\!]\,, \tag{5.51c}$$
$$\boldsymbol{\Delta}_4[A] = [\![A_\flat]\!]\,, \tag{5.51d}$$
$$\boldsymbol{\Delta}_5[A] = [\![\mathrm{C}^-_{+1} A_\sharp - \mathrm{C}^+_{-1} A_\flat]\!]\,, \tag{5.51e}$$
$$\boldsymbol{\Delta}_6[A] = [\![\partial_r A_\parallel + \xi_\parallel \zeta^{-2} \partial_r A_0]\!]\,, \tag{5.51f}$$
$$\boldsymbol{\Delta}_7[A] = [\![- n^2 \zeta^{-2} \partial_t A_0 + \tfrac{1}{\sqrt{2}} \mathrm{C}^-_{+1} A_\sharp + \tfrac{1}{\sqrt{2}} \mathrm{C}^+_{-1} A_\flat]\!]\,, \tag{5.51g}$$
$$\boldsymbol{\Delta}_8[A] = [\![n^2 \{\partial_r A_0 - \tfrac{1}{\sqrt{2}} \partial_t A_\sharp - \tfrac{1}{\sqrt{2}} \partial_t A_\flat\} - \xi_\parallel \partial_r A_\parallel]\!]\,, \tag{5.51h}$$

where $[\![\ ]\!]$ denotes the jump across the core-cladding interface at $r = 1$ and $\mathrm{C}^\pm_m$ is the differential operator

$$\mathrm{C}^\pm_m = \frac{\partial}{\partial r} \mp \frac{1}{r} \left(\frac{1}{i} \frac{\partial}{\partial \theta} + m \right) . \tag{5.52}$$

With this notation, the matching conditions of Eq. (3.37) without surface charges and surface currents can be expressed concisely as

$$\boldsymbol{\Delta}[A] = 0\,, \tag{5.53}$$

where, as mentioned above, μ was set to unity and terms of order $O(\xi_\parallel^2)$ were neglected.

Perturbative Expansion Mode solutions to the field equations described in Section 3.2 can be obtained using the ansatz

$$A_b(t, r, \theta, s) = a_b(r, \varsigma) e^{i(\psi + m\theta - \omega t)}\,, \tag{5.54}$$

where the frame-components of the amplitude a_b are expanded in a power series in the slowness parameter ε as

$$a_b = a_b^{(0)} + \varepsilon a_b^{(1)} + O(\varepsilon^2)\,. \tag{5.55}$$

Here, the integer m denotes the azimuthal mode index, ω is the optical frequency, and ψ is the optical phase

$$\psi(s) = \int_0^s \beta(\varepsilon s')\, \mathrm{d}s'\,. \tag{5.56}$$

For straight fibers in flat space-time, β is a constant, commonly referred to as the *propagation constant*. In the present context, however, β varies with the long-distance scale $\varsigma = \varepsilon s$ in a way that is determined by the field equations.

Field Equations at Order ε^0 To express the field equations of Section 3.2, applied to the present context, in a concise notation, define the Helmholtz operator

$$\mathrm{H}_m = \frac{\partial^2}{\partial r^2} + \frac{1}{r}\frac{\partial}{\partial r} - \frac{m^2}{r^2} + \frac{n^2\omega^2}{\zeta^2} + \frac{2\beta\omega\xi_\parallel}{\zeta^2} - \beta^2\,, \tag{5.57}$$

and extend it to a sequence of frame components

$$a_\flat = \begin{pmatrix} a_0 & a_\parallel & a_\sharp & a_\flat \end{pmatrix} \tag{5.58}$$

by

$$\underline{\mathrm{H}}_m a_\flat = \begin{pmatrix} \mathrm{H}_m a_0 & \mathrm{H}_m a_\parallel & \mathrm{H}_{m+1} a_\sharp & \mathrm{H}_{m-1} a_\flat \end{pmatrix}. \tag{5.59}$$

The gauge-fixed field equations at order ε^0 then take the form

$$\underline{\mathrm{H}}_m a_\flat^{(0)} = 0\,. \tag{5.60}$$

The homogeneous solution to $\mathrm{H}_m f = 0$ that is regular on the axis $r = 0$ and decays for large r is given by

$$f_m(q_1, q_2, r) = \begin{cases} q_1 J_m(Ur) & r < 1\,, \\ q_2 K_m(Wr) & r > 1\,, \end{cases} \tag{5.61}$$

where J_m are Bessel functions of the first kind, K_m are modified Bessel functions of the second kind, q_1 and q_2 are arbitrary functions of the long distance scale ς, and U and W are the normalized transverse wave numbers

$$U = \sqrt{+n_1^2\omega^2/\zeta^2 - \beta^2 + 2\beta\omega\xi_\parallel/\zeta^2}\,, \tag{5.62a}$$

$$W = \sqrt{-n_2^2\omega^2/\zeta^2 + \beta^2 - 2\beta\omega\xi_\parallel/\zeta^2}\,. \tag{5.62b}$$

Even though the designations for U and W used here follow the standard nomenclature of step-index fibers in flat space-time [187] where U and W are constants, in the present case these quantities may vary along the fiber due to the explicit dependence on ζ and $\xi_\parallel$, and also because β varies along the fiber (as is shown below). In the following, it will be assumed that $U > 0$ and $W > 0$, for otherwise the modes would not be guided [171, Sect. 3.1].

The solution to Eq. (5.60) can then be written as

$$a_0^{(0)}(\varsigma, r) = f_m(q_1^0(\varsigma), q_5^0(\varsigma), r)\,, \qquad a_\sharp^{(0)}(\varsigma, r) = f_{m+1}(q_3^0(\varsigma), q_7^0(\varsigma), r)\,, \tag{5.63a}$$

$$a_\parallel^{(0)}(\varsigma, r) = f_m(q_2^0(\varsigma), q_6^0(\varsigma), r)\,, \qquad a_\flat^{(0)}(\varsigma, r) = f_{m-1}(q_4^0(\varsigma), q_8^0(\varsigma), r)\,, \tag{5.63b}$$

where the values of the amplitude coefficient q_i^0 are still to be determined. Since such

expressions will arise again in the calculations below, it is useful to abbreviate such a system of equations as

$$a^{(0)} = f_m[\boldsymbol{q}^{(0)}]\,, \tag{5.64}$$

where $\boldsymbol{q}^{(0)}$ is the column vector $\boldsymbol{q}^0 = (q_1^0, \dots, q_8^0)^{\mathrm{T}}$, whose entries may depend on ς.

So far, Eq. (5.64) solves the field equations in the core and cladding separately. To obtain a globally valid solution, however, the field must satisfy the matching conditions (5.53). This constraint determines both the dispersion relation and the coefficients $\boldsymbol{q}^{(0)}$ up to an amplitude factor.

Interface Conditions at Order $\boldsymbol{\varepsilon^0}$ As the fields $a_b^{(0)}$ depend linearly on the parameters $\boldsymbol{q}^0 = (q_1^0, \dots, q_8^0)^{\mathrm{T}}$, so do the jumps at the core-cladding interface $r = 1$, which can thus be expressed in matrix notation as

$$\boldsymbol{\Delta}[A^{(0)}] = \mathbf{M}\mathbf{N}\,\boldsymbol{q}^{(0)} e^{i(\psi + m\theta - \omega t)} + O(\xi_\parallel^2)\,, \tag{5.65}$$

where $\mathbf{M}$ and $\mathbf{N}$ are the following complex 8×8 matrices:

$$\mathbf{M} = \begin{bmatrix} +1 & 0 & 0 & 0 & -1 & 0 & 0 & 0 \\ 0 & +1 & 0 & 0 & 0 & -1 & 0 & 0 \\ 0 & 0 & -U\mathscr{J}^+ & 0 & 0 & 0 & +W\mathscr{K}^+ & 0 \\ 0 & 0 & 0 & +U\mathscr{J}^- & 0 & 0 & 0 & +W\mathscr{K}^- \\ 0 & 0 & +U & +U & 0 & 0 & +W & -W \\ +\xi_\parallel \frac{U^2}{\varsigma^2}\mathscr{J} & +U^2\mathscr{J} & 0 & 0 & -\xi_\parallel \frac{W^2}{\varsigma^2}\mathscr{K} & -W^2\mathscr{K} & 0 & 0 \\ +in_1^2\frac{\omega}{\varsigma^2} & 0 & +\frac{U}{\sqrt{2}} & -\frac{U}{\sqrt{2}} & -in_2^2\frac{\omega}{\varsigma^2} & 0 & +\frac{W}{\sqrt{2}} & +\frac{W}{\sqrt{2}} \\ +n_1^2U^2\mathscr{J} & -\xi_\parallel U^2\mathscr{J} & -in_1^2\frac{\omega U}{\sqrt{2}}\mathscr{J}^+ & +in_1^2\frac{\omega U}{\sqrt{2}}\mathscr{J}^- & -n_2^2W^2\mathscr{K} & +\xi_\parallel W^2\mathscr{K} & +in_2^2\frac{\omega W}{\sqrt{2}}\mathscr{K}^+ & +in_2^2\frac{\omega W}{\sqrt{2}}\mathscr{K}^- \end{bmatrix}, \tag{5.66}$$

$$\mathbf{N} = \operatorname{diag}(\underbrace{J_m(U), \dots, J_m(U)}_{\text{four times}}, \underbrace{K_m(W), \dots, K_m(W)}_{\text{four times}})\,. \tag{5.67}$$

Here, the following abbreviations were used:

$$\mathscr{J}_m(U) = \frac{J_m'(U)}{U J_m(U)}\,, \qquad \mathscr{K}_m(W) = \frac{K_m'(W)}{W K_m(W)}\,, \tag{5.68}$$

$$\mathscr{J}_m^\pm(U) = \mathscr{J}_m(U) \mp m/U^2\,, \qquad \mathscr{K}_m^\pm(W) = \mathscr{K}_m(W) \mp m/W^2\,, \tag{5.69}$$

and indices and function arguments were suppressed for typographic reasons. The interface conditions $\boldsymbol{\Delta}[A^{(0)}] = 0$ are thus equivalent to the equation $\mathbf{M}\mathbf{N}\boldsymbol{q}^{(0)} = 0$, which admits a non-trivial solution only if the matrix $\mathbf{M}\mathbf{N}$ is singular.

The requirement $\det(\mathbf{M}\mathbf{N}) = 0$ yields a transcendental equation for the wave vector β in terms of the frequency ω (depending also on the azimuthal mode index m as well as the refractive indices n_1 and n_2). In this context, it is useful to define the normalized

frequency as

$$V = \frac{\omega}{\zeta}\sqrt{n_1^2 - n_2^2}\,. \tag{5.70}$$

Since $U^2 + W^2 = V^2$, there exists a number b in the range $[0, 1]$ such that

$$U = \sqrt{1-b}V\,, \qquad\qquad W = \sqrt{b}V\,. \tag{5.71}$$

The parameter b is commonly referred to as the normalized guide index [171, Sect. 3.5], using which one defines the effective refractive index $\bar{n}$ via

$$\bar{n}^2 = b\,n_1^2 + (1-b)\,n_2^2\,. \tag{5.72}$$

With this notation, the determinant of $\mathbf{MN}$ can be written as

$$\det(\mathbf{MN}) = -\sqrt{2}\mathscr{D}_{\mathrm{ph}}\mathscr{D}_{\mathrm{g}}^2 + O(\xi_\parallel^2)\,, \tag{5.73}$$

where

$$\begin{aligned}\mathscr{D}_{\mathrm{ph}} &= J_m(U)^2 K_m(W)^2 \\ &\quad\times \left\{[\mathscr{J}_m(U) + \mathscr{K}_m(W)][n_1^2\mathscr{J}_m(U) + n_2^2\mathscr{K}_m(W)] - \bar{m}^2\right\}\,,\end{aligned} \tag{5.74}$$

with

$$\bar{m} = \frac{m\bar{n}V^2}{U^2W^2}\,. \tag{5.75}$$

and

$$\begin{aligned}\mathscr{D}_{\mathrm{g}} &= UWJ_m(U)K_m(W)\left\{U^2\,\mathscr{J}_m(U) - W^2\mathscr{K}_m(W)\right\} \\ &= UW\left\{UJ'_m(U)K_m(W) - WK'_m(W)J_m(U)\right\}\,.\end{aligned} \tag{5.76}$$

The requirement $\det(\mathbf{MN}) = 0$ thus reduces to the condition that either $\mathscr{D}_{\mathrm{g}}$ or $\mathscr{D}_{\mathrm{ph}}$ vanishes. This determinant condition has the same form as for straight fibers in flat space-time [171, Eq. (3.27)], but note that in the present case, U, V, and W explicitly depend on the lapse ζ and the tangential shift $\xi_\parallel$, as can be seen from the definitions in Eqs. (5.62a), (5.62b) and (5.70). This generalizes previous results obtained for simplified problems where it was assumed that $\xi_i = 0$ and $\zeta = \text{const.}$ [4; 48].

As shown in Ref. [49], roots of $\mathscr{D}_{\mathrm{g}}$ correspond to gauge and ghost modes, i.e., solutions that are either pure gradients or violate the gauge condition and thus satisfy the gauge-fixed field equations, but not Maxwell's equations proper. The main objects of interest are the physical modes, which correspond to roots of $\mathscr{D}_{\mathrm{ph}}$.

For prescribed values of the refractive indices n_1 and n_2, the normalized frequency V and the azimuthal mode index m, the equation $\mathscr{D}_{\mathrm{ph}} = 0$ admits multiple roots for the normalized guide index b, which can be labeled by a radial mode index $\varkappa$. Such mode spectra are shown in Figs. 5.4 and 5.5: the different curves correspond to various solutions for b as a function of V, labeled by m and $\varkappa$. As the resulting plots are independent of the sign of m, only non-negative values of m are shown here. Whereas the fundamental

mode ($m = 1$, $\varkappa = 1$) extends to $V = 0$, all other modes have a finite cutoff value for the normalized frequency V.

The parameters $n_1 = 1.4712$ and $n_2 = 1.4659$ considered in Fig. 5.4 correspond to commercially available telecommunication fibers, and the parameters $n_1 = 1.4712$ and $n_2 = 1$ correspond to fibers made of fused silica glass (forming the core, as in the first parameter set) without any cladding, so that the ambient refractive index is that of a vacuum. In the first case, the refractive index contrast $\Delta = \sqrt{n_1^2 - n_2^2}$ is small compared to the effective refractive index $\bar{n}$, a condition commonly referred to as weak guidance [188]. In this limit, the determinant function $\mathscr{D}_{\text{ph}}$ can be approximated by

$$\mathscr{D}_{\text{ph}} \approx \bar{n}^2 J_m(U)^2 K_m(W^2) \left\{ [\mathscr{J}_m(U) + \mathscr{K}_m(W)]^2 - m^2 V^2 / (U^2 W^2) \right\} , \tag{5.77}$$

which shows that the relation between b and V in weakly guiding fibers is independent of the precise values of the refractive indices n_1 and n_2. Hence, the mode diagram shown in Fig. 5.4 is the same for all such weakly guiding fibers. Alternatively, if the index contrast Δ is non-negligible compared to $\bar{n}$, the functional form of $b(V)$ depends explicitly on the refractive indices, as can be seen by comparing Figs. 5.4 and 5.5. Whereas in Fig. 5.4, pairs of curves with $m = 0$ closely follow curves with $m = 2$, this is no longer the case in Fig. 5.5 where pairs of curves with $m = 0$ are visibility separated and distinct from those with $m = 2$.

Optical Phase The effects of the lapse ζ and the shift $\xi_{\parallel}$ can now be analyzed as follows. Along the fiber, the variation of the lapse ζ causes a variation in the normalized frequency $V = V(\varsigma)$ according to Eq. (5.70). This can be interpreted as a redshift, as the Killing frequency ω is related to the physical frequency ω_{ph}, i.e., the frequency as measured in

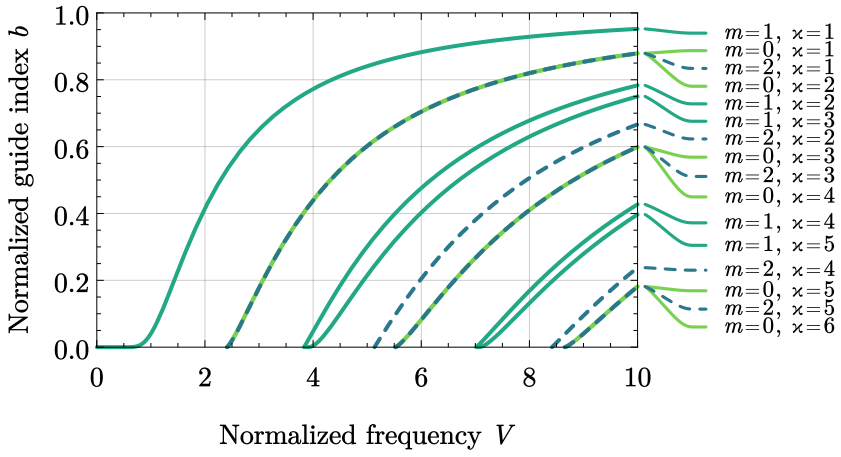

Figure 5.4: Mode diagram for a step-index optical fiber with $n_1 = 1.4712$ and $n_2 = 1.4659$. The low index contrast $\Delta^2 = n_1^2 - n_2^2 \approx 1.56 \times 10^{-2}$ causes adjacent modes with azimuthal mode index $m = 0$ to be almost degenerate (e.g. $\varkappa = 1$ with $\varkappa = 2$, or $\varkappa = 3$ with $\varkappa = 4$). Additionally, $m = 0$ modes have a normalized guide index b that is close to but not identical with $m = 2$ modes.

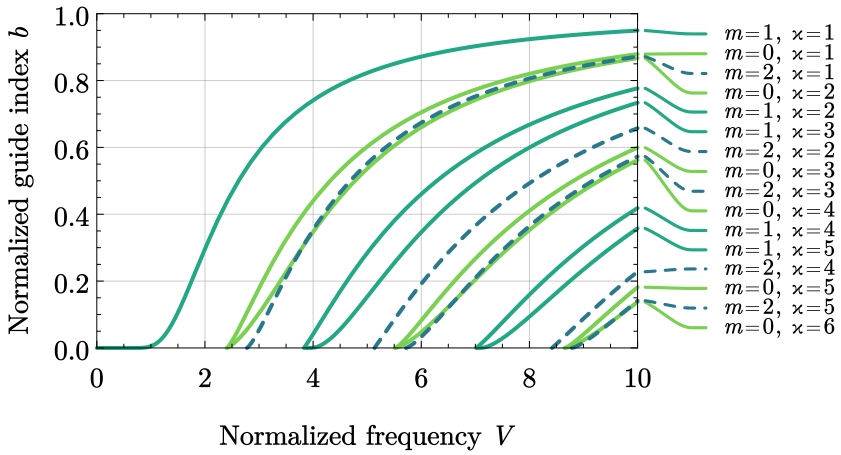

Figure 5.5: Mode diagram for a step-index optical fiber with $n_1 = 1.4712$ and $n_2 = 1$. The high index contrast $\Delta^2 = n_1^2 - n_2^2 \approx 1.16$ breaks the degeneracy of adjacent $m = 0$ modes and causes a visible separation between the modes with $m = 0$ and those with $m = 2$.

the rest frame of the medium, by $\omega_{\mathrm{ph}} = \omega/\zeta$. In turn, such a redshift causes a variation of the normalized guide index $b = b(V(\varsigma))$. In the local rest frame of the medium, one thus has the same relation between b and ω_{ph} as in flat space-time. This also extends to the effective refractive index $\bar{n}$ as defined in Eq. (5.72). Given b and V, the transverse wave numbers U and W can be computed from Eq. (5.71), and using Eqs. (5.62a) and (5.62b) one obtains β in terms of $\bar{n}$, ω, ζ and $\xi_\parallel$:

$$\beta(\varsigma) = \pm\bar{n}\omega/\zeta + \omega\xi_\parallel/\zeta^2 + O(\omega\|\xi\|^2)\,. \tag{5.78}$$

The phase ψ along the fiber can then be computed using Eq. (5.56):

$$\psi_\gamma = \pm\int_\gamma \bar{n}\omega\zeta^{-1}\,\mathrm{d}s + \int_\gamma \omega\zeta^{-2}\xi + O(\omega\ell\|\xi\|^2)\,, \tag{5.79}$$

where ℓ denotes the length of the curve γ formed by the fiber's baseline. This result closely resembles the eikonal formula given in Eq. (5.38), but differs slightly from it, as $\bar{n}$ was assumed to be constant in Eq. (5.38), whereas $\bar{n}$ here depends on ς via Eq. (5.72) and $b = b(V(\varsigma))$.

Material and Waveguide Dispersion At this stage, it is worth mentioning that there are generally two contributions to dispersion in optical fibers, commonly referred to as *material dispersion* and *waveguide dispersion*, respectively. Material dispersion arises from the intrinsic dependence of the refractive indices on the optical wavelength. This effect was neglected in the models considered so far, as the refractive indices n_1 and n_2 were assumed to be constant. One may model this effect by assuming that n_1 and n_2 depend on the physical optical frequency (as measured in the material's rest frame) through Sellmeier's equations [48, Sect. 4.7; 4, Sect. 4.2.6]. As the physical frequency varies along the fiber due to the gravitational redshift ($\omega_{\mathrm{ph}} = \omega/\zeta$, with the Killing frequency ω remaining constant

along the fiber), this results in an explicit dependence of n_1 and n_2 on the lapse ζ. However, this correction is negligible in practical applications: compared to the explicit dependence of β on ζ in Eq. (5.78), the material dispersion correction is suppressed by two orders of magnitude [4; 48]. Additionally, the dependence of the normalized frequency V on the lapse ζ according to Eq. (5.70) gives rise to waveguide dispersion: the effective refractive index $\bar{n}$ depends on the normalized guide index b, which further depends on $V(\zeta(\varsigma))$. However, this effect is also negligible in typical step-index optical fibers since

$$\frac{\partial \bar{n}^2}{\partial \zeta} = (n_1^2 - n_2^2)\frac{\partial b}{\partial \zeta} \equiv \Delta^2 \frac{\partial b}{\partial \zeta}\,, \tag{5.80}$$

with the difference in squared refractive indices being on the order $\Delta^2 = n_1^2 - n_2^2 \approx 10^{-2}$ for typical telecommunication single-mode fibers. The effect of waveguide dispersion is thus of similar order as the negligible material dispersion correction. In practice, this means that one can treat $\bar{n}$ in Eqs. (5.78) and (5.79) as a constant (computed, e.g., at the starting point of the curve γ) without introducing significant errors.

Mode Profiles Having determined the evolution of the electromagnetic phase along the fiber, one can proceed to determine the amplitude. If the dispersion relation of physical modes is satisfied, $\mathscr{D}_{\mathrm{ph}} = 0$, the matrix $\mathbf{M}$, defined in Eq. (5.66), has a one-dimensional kernel spanned by the vector

$$\hat{\boldsymbol{q}} = \begin{pmatrix} \zeta \\ -\frac{\xi_\parallel}{\zeta} \\ \frac{-i\sqrt{\Delta}V}{\sqrt{2}U}\,\frac{\bar{m}-\bar{n}\mathscr{K}U^2/V^2}{\bar{m}-\bar{n}(\mathscr{J}+\mathscr{K})} \\ \frac{+i\sqrt{\Delta}V}{\sqrt{2}U}\,\frac{\bar{m}+\bar{n}\mathscr{K}U^2/V^2}{\bar{m}+\bar{n}(\mathscr{J}+\mathscr{K})} \\ \zeta \\ -\frac{\xi_\parallel}{\zeta} \\ \frac{-i\sqrt{\Delta}V}{\sqrt{2}W}\,\frac{\bar{m}-\bar{n}\mathscr{J}V^2/W^2}{\bar{m}-\bar{n}(\mathscr{J}+\mathscr{K})} \\ \frac{-i\sqrt{\Delta}V}{\sqrt{2}W}\,\frac{\bar{m}+\bar{n}\mathscr{J}V^2/W^2}{\bar{m}+\bar{n}(\mathscr{J}+\mathscr{K})} \end{pmatrix}. \tag{5.81}$$

The coefficients $\boldsymbol{q}^{(0)}$ are thus of the form

$$\boldsymbol{q}^{(0)} = \mathscr{E}^{(0)}(\varsigma)\mathbf{N}^{-1}\hat{\boldsymbol{q}}\,. \tag{5.82}$$

The evolution of the amplitude $\mathscr{E}^{(0)}$ can be determined from the field equations at the next order in the perturbative expansion. Before doing so, however, it is advantageous to discuss the spatial field profile to gain some insight into the problem.

Weak Guidance In telecommunication single-mode fibers, the dimensionless index contrast is typically small, so that $\Delta^2 = n_1^2 - n_2^2 \ll 1$. In this weak-guidance limit, the limiting behavior of $\hat{\boldsymbol{q}}^{(0)}$ depends on the sign of $m = \pm 1$: if one normalizes the reference

vectors $\hat{\boldsymbol{q}}_\pm$ to $\hat{\boldsymbol{q}}_\pm^\dagger \hat{\boldsymbol{q}}_\pm = 1$, one obtains

$$\hat{\boldsymbol{q}}_+ = \begin{pmatrix} 0 & 0 & 0 & -i\sqrt{b} & 0 & 0 & 0 & -i\sqrt{1-b} \end{pmatrix}^{\mathrm{T}} + O(\Delta)\,, \tag{5.83a}$$

$$\hat{\boldsymbol{q}}_- = \begin{pmatrix} 0 & 0 & +i\sqrt{b} & 0 & 0 & 0 & -i\sqrt{1-b} & 0 \end{pmatrix}^{\mathrm{T}} + O(\Delta)\,, \tag{5.83b}$$

regardless of ζ and $\xi_\parallel$. The signs and factors of i were chosen for later convenience. Hence, in the weak-guidance limit, the only non-zero field component for right-hand circular polarization ($m = +1$) is $A_\flat$, whereas for left-hand circular polarization ($m = -1$) only $A_\sharp$ is non-zero (to leading order in perturbation theory).

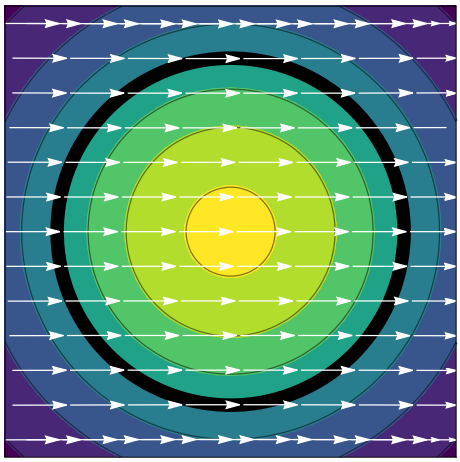

(a) $\mathcal{J}_\pm = 1/\sqrt{2}$ in a fiber with $n_1 = 1.4712$ and $n_2 = 1.4659$

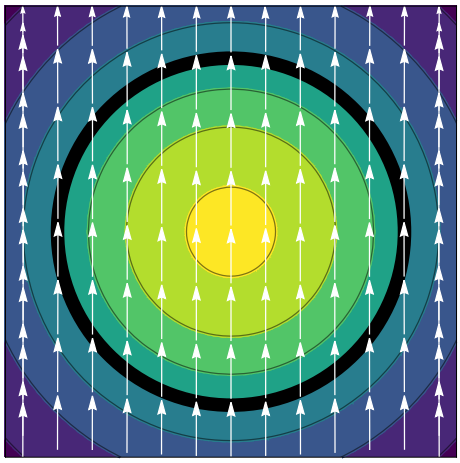

(b) $\mathcal{J}_\pm = \mp i/\sqrt{2}$ in a fiber with $n_1 = 1.4712$ and $n_2 = 1.4659$

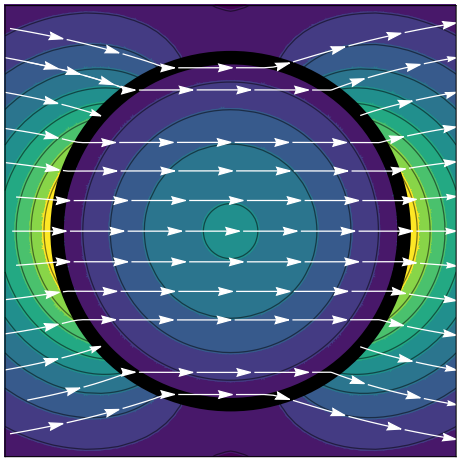

(c) $\mathcal{J}_\pm = 1/\sqrt{2}$ in a fiber with $n_1 = 1.4712$ and $n_2 = 1$

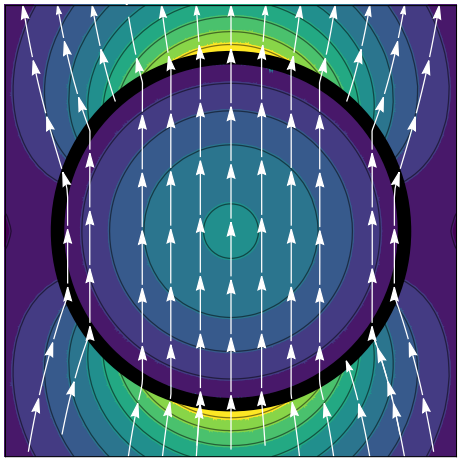

(d) $\mathcal{J}_\pm = \mp i/\sqrt{2}$ in a fiber with $n_1 = 1.4712$ and $n_2 = 1$

Figure 5.6: Transverse field profiles for horizontal polarization (left) and vertical polarization (right) in two optical fibers with $n_1 = 1.4712$ and $n_2 = 1.4659$ (upper figures) and $n_1 = 1.4712$ and $n_2 = 1$ (lower figures). In all figures, the normalized frequency was set to $V = 1.25$. The white arrows indicate the direction of the electric field E_i, and the colored contours indicate the relative norm of E_i. No axis labels are shown as the field configurations are scale-invariant.

So far, the analysis was restricted to single Fourier components with angular dependence $e^{im\theta}$. As the dispersion relation is independent of the sign of m, solutions with either sign of the azimuthal mode index can be excited simultaneously: in single-mode fibers, this leads to superpositions of solutions with $m = +1$ and $m = -1$. Using the notation introduced in Eq. (5.64), such superpositions can be written as

$$A^{(0)} = \left(\mathcal{E}_+ f_+ [\mathbf{N}_+^{-1}\hat{\boldsymbol{q}}_+] e^{+i\theta} + \mathcal{E}_- f_- [\mathbf{N}_-^{-1}\hat{\boldsymbol{q}}_-] e^{-i\theta}\right) e^{i(\psi-\omega t)}\,, \tag{5.84}$$

where $\mathcal{E}_\pm$ denotes the amplitude of the (suitably normalized) solution with $m = \pm 1$, which generally depends on ς. The coefficients $\mathcal{E}_\pm$ can be regarded as components of a complex vector with Cartesian components $\mathcal{E}_x$ and $\mathcal{E}_y$ defined via

$$\begin{pmatrix}\mathcal{E}_x\\ \mathcal{E}_y\end{pmatrix} = \frac{1}{\sqrt{2}}\begin{pmatrix}1 & 1\\ +i & -i\end{pmatrix}\begin{pmatrix}\mathcal{E}_+\\ \mathcal{E}_-\end{pmatrix}, \qquad \begin{pmatrix}\mathcal{E}_+\\ \mathcal{E}_-\end{pmatrix} = \frac{1}{\sqrt{2}}\begin{pmatrix}1 & -i\\ 1 & +i\end{pmatrix}\begin{pmatrix}\mathcal{E}_x\\ \mathcal{E}_y\end{pmatrix}. \tag{5.85}$$

Defining the amplitude $\mathcal{A}$ as

$$\mathcal{A} = \sqrt{|\mathcal{E}_x|^2 + |\mathcal{E}_y|^2} = \sqrt{|\mathcal{E}_+|^2 + |\mathcal{E}_-|^2}\,, \tag{5.86}$$

one can define the Jones vector $\mathcal{J}_i$ as the unit vector along $\mathcal{E}_i$, such that

$$\mathcal{E}_i = \mathcal{A}\mathcal{J}_i\,. \tag{5.87}$$

The Jones vector $\mathcal{J}_i$ can be interpreted as a transverse unit vector specifying the polarization of the electromagnetic field. As shown in Fig. 5.6, $(\mathcal{J}_x, \mathcal{J}_y) = (1, 0)$ corresponds to horizontal polarization, whereas $(\mathcal{J}_x, \mathcal{J}_y) = (0, 1)$ describes vertical polarization (in the Fermi coordinate system). The overall factor $\mathcal{A}$ describes the amplitude of the electromagnetic wave. Whereas the electric field lines are exactly parallel only in the weakly-guiding limit [171, Sect. 3.2; 172, Sect. 16.13], Fig. 5.6 shows that the field lines are predominantly bent in the fiber cladding, but are well approximated by parallel lines in the fiber core. This justifies the interpretation of $\mathcal{J}_i$ as a Jones vector also for strongly guiding fibers.

The values of $\mathcal{A}$ and $\mathcal{J}_i$ can be freely specified at any given point along the fiber (this corresponds to the freedom of injecting radiation with arbitrary amplitude and polarization into the fiber). Their evolution along the fiber, however, is determined by the field equations.

Field Equations at Order $\boldsymbol{\varepsilon^1}$ Having established the interpretation of the coefficients $\mathcal{E}_\pm$ in Eq. (5.84) in terms of the amplitude $\mathcal{A}$ and the Jones vector $\mathcal{J}_i$, one can study their evolution along the fiber using the field equations at order ε^1. Using the Helmholtz operator defined in Eqs. (5.57) and (5.59), these evolution equations can be written as

$$\underline{\mathrm{H}}_m a_b^{(1)} = -2i\Sigma_b\,, \tag{5.88}$$

where the source terms Σ_b are given by

$$\Sigma_0 = \left(\beta - \frac{\omega\xi_\parallel}{\zeta^2}\right) a_0^{(0)\prime} + \frac{1}{2}\left[\beta' - \frac{\omega\xi_\parallel'}{\zeta^2} - \left(\beta - \frac{\omega\xi_\parallel}{\zeta^2}\right)\frac{\zeta'}{\zeta}\right] a_0^{(0)} - \frac{\omega\zeta'}{\zeta} a_\parallel^{(0)}\,, \tag{5.89a}$$

$$\begin{aligned}\Sigma_\parallel = \left(\beta - \frac{\omega\xi_\parallel}{\zeta^2}\right) a_\parallel^{(0)\prime} + \frac{1}{2}\left[\beta' - \frac{\omega\xi_\parallel'}{\zeta^2} + \left(\beta + 3\frac{\omega\xi_\parallel}{\zeta^2}\right)\frac{\zeta'}{\zeta}\right] a_\parallel^{(0)} \\ - \left[\left(\frac{n^2\omega}{\zeta^2} + \frac{\beta\xi_\parallel}{\zeta^2}\right)\frac{\zeta'}{\zeta} - \frac{\beta\xi_\parallel'}{\zeta^2}\right] a_0^{(0)}\,,\end{aligned} \tag{5.89b}$$

$$\Sigma_\sharp = \left(\beta - \frac{\omega\xi_\parallel}{\zeta^2}\right) a_\sharp^{(0)\prime} + \frac{1}{2}\left[\beta' - \frac{\omega\xi_\parallel'}{\zeta^2} + \left(\beta + \frac{\omega\xi_\parallel}{\zeta^2}\right)\frac{\zeta'}{\zeta}\right] a_\sharp^{(0)}\,, \tag{5.89c}$$

$$\Sigma_\flat = \left(\beta - \frac{\omega\xi_\parallel}{\zeta^2}\right) a_\flat^{(0)\prime} + \frac{1}{2}\left[\beta' - \frac{\omega\xi_\parallel'}{\zeta^2} + \left(\beta + \frac{\omega\xi_\parallel}{\zeta^2}\right)\frac{\zeta'}{\zeta}\right] a_\flat^{(0)}\,, \tag{5.89d}$$

where primes indicate derivatives with respect to ς. Such inhomogeneous Helmholtz equations can be solved using Green's functions. Indeed, for any set of functions a_b depending on r, define the Green operator

$$\underline{\mathrm{G}}_m[a] = \begin{pmatrix}\mathrm{G}_m[a_0] & \mathrm{G}_m[a_\parallel] & \mathrm{G}_{m+1}[a_\sharp] & \mathrm{G}_{m-1}[a_\flat]\end{pmatrix}\,, \tag{5.90}$$

where

$$\mathrm{G}_m[f] = \begin{cases}\mathrm{G}_m^<[f](r) & r < 1\,,\\ \mathrm{G}_m^>[f](r) & r > 1\,,\end{cases} \tag{5.91}$$

with $\mathrm{G}_m^<$ and $\mathrm{G}_m^>$ denoting the Green's functions in the core and cladding, respectively:

$$\begin{aligned}\mathrm{G}_m^<[f](r) = &+ \frac{\pi}{2} Y_m(Ur)\int_0^r J_m(Ur')f(r')r'\,\mathrm{d}r' \\ &+ \frac{\pi}{2} J_m(Ur)\int_r^1 Y_m(Ur')f(r')r'\,\mathrm{d}r'\,,\end{aligned} \tag{5.92a}$$

$$\begin{aligned}\mathrm{G}_m^>[f](r) = &- I_m(Wr)\int_r^\infty K_m(Wr')f'(r)r'\,\mathrm{d}r' \\ &- K_m(Wr)\int_1^r I_m(Wr')f'(r)r'\,\mathrm{d}r'\,,\end{aligned} \tag{5.92b}$$

where Y_m are Bessel functions of the second kind and I_m are modified Bessel functions of the first kind. The general solution to Eq. (5.88) can then be written as

$$a^{(1)} = f_m[\boldsymbol{q}^{(1)}] - 2i\underline{\mathrm{G}}_m[\Sigma]\,, \tag{5.93}$$

where the first part is a homogeneous solution expressed in the notation introduced in Eq. (5.64). This solves the field equations in the core and cladding separately so that it remains to impose the matching conditions at the core-cladding interface.

Interface Conditions at Order $\boldsymbol{\varepsilon^1}$ At order ε^1, the interface conditions at the core-cladding interface take the form

$$\mathbf{M}\mathbf{N}\boldsymbol{q}^{(1)} = 2i\boldsymbol{\Delta}[\underline{\mathrm{G}}_m[\Sigma]]\,, \tag{5.94}$$

where $\mathbf{M}$ and $\mathbf{N}$ are the matrices given explicitly in Eqs. (5.66) and (5.67), respectively, and the right-hand side encodes the jumps of the particular solution in Eq. (5.93) (with the phase factor $e^{i(m\theta+\psi-\omega t)}$ removed).

The matrix $\mathbf{M}$ is singular due to the dispersion relation, which constitutes an obstruction to the solvability of this set of linear equations for $\boldsymbol{q}^{(1)}$. The condition of solvability (which requires that the right-hand side of Eq. (5.94) lies in the image of the matrix $\mathbf{M}$) can be expressed as follows: if $\boldsymbol{\zeta}$ denotes any eight-component row-vector spanning the co-kernel of $\mathbf{M}$, i.e., $\boldsymbol{\zeta}\mathbf{M} = 0$, the above inhomogeneous equation is solvable if and only if

$$\boldsymbol{\zeta}\boldsymbol{\Delta}[\underline{\mathrm{G}}_m[\Sigma]] = 0\,. \tag{5.95}$$

This is equivalent to an evolution equation for the amplitude $\mathcal{E}^{(0)}$ of the general form

$$\frac{\mathrm{d}}{\mathrm{d}\varsigma}\ln\mathcal{E}^{(0)} = c_1(\varsigma)\frac{\mathrm{d}\zeta}{\mathrm{d}\varsigma} + c_1(\varsigma)\frac{\mathrm{d}\xi_\parallel}{\mathrm{d}\varsigma}\,, \tag{5.96}$$

where the coefficient functions c_1 and c_2 are expressible in terms of integrals of products of Bessel functions.

The explicit forms of the functions $c_1(\varsigma)$ and $c_2(\varsigma)$ are involved as they depend on the jumps of the particular solutions arising from the source terms given in Eq. (5.89), which further depend on the explicit solutions for $a_b^{(0)}$ given in Eq. (5.64) with the coefficients $\boldsymbol{q}$ given in Eq. (5.81) in which U and W are regarded as functions of V (according to the dispersion relation) and thus depend on $\zeta(\varsigma)$ and $\xi_\parallel(\varsigma)$.

To gain insight into the problem, it is advantageous to restrict the analysis to weakly guiding fibers, where $\Delta^2 \equiv n_1^2 - n_2^2 \ll 1$. In this limit, the coefficients $\boldsymbol{q}$ are given by Eq. (5.83). Using the fact that $\mathrm{d}V/\mathrm{d}\varsigma = O(\Delta)$, which implies that the ς-derivatives of b, U, W, and $\bar{n}$ are also of order $O(\Delta)$, one obtains

$$\frac{\mathrm{d}}{\mathrm{d}\varsigma}a_b^{(0)} = \frac{1}{\mathcal{E}^{(0)}}\frac{\mathrm{d}\mathcal{E}^{(0)}}{\mathrm{d}\varsigma}a_b^{(0)} + O(\Delta)\,. \tag{5.97}$$

Since only $a_\sharp^{(0)}$ and $a_\flat^{(0)}$ are non-zero for weakly guiding fibers, the only non-zero components of Σ_b are $\Sigma_\sharp$ and $\Sigma_\flat$, which factorize as

$$\Sigma_{\sharp/\flat} = (\text{radial function}) \times \tilde{\Sigma}\,, \tag{5.98}$$

where

$$\tilde{\Sigma} = \left(\beta - \frac{\omega\xi_\parallel}{\zeta^2}\right)\frac{\mathrm{d}\mathcal{E}^{(0)}}{\mathrm{d}\varsigma} + \frac{1}{2}\left[\beta' - \frac{\omega\xi_\parallel'}{\zeta^2} + \left(\beta + \frac{\omega\xi_\parallel}{\zeta^2}\right)\frac{\zeta'}{\zeta}\right]\mathcal{E}^{(0)}\,. \tag{5.99}$$

The consistency condition given in Eq. (5.95) then reduces to a multiple of $\tilde{\Sigma} = 0$. Whenever this factor is non-zero (which is generically the case), one obtains $\tilde{\Sigma} = 0$. Using the explicit form of β given in Eq. (5.78), the assumption of weak guidance leads to

$$\beta = \pm\frac{\bar{n}\omega}{\zeta} + \frac{\omega\xi_\parallel}{\zeta^2} + O(\omega\|\xi\|^2)\,, \tag{5.100}$$

$$\beta' = \mp\frac{\bar{n}\omega}{\zeta}\frac{\zeta'}{\zeta} - 2\frac{\omega\xi_\parallel}{\zeta^2}\frac{\zeta'}{\zeta} + \frac{\omega\xi'_\parallel}{\zeta^2} + O(\omega\|\xi\|^2) + O(\Delta)\,, \tag{5.101}$$

As a consequence, the entire second bracket in Eq. (5.99) is on the order $O(\|\xi\|^2) + O(\Delta)$, so the amplitude transport equation reduces to

$$\frac{\mathrm{d}}{\mathrm{d}\varsigma}\ln\mathcal{E}^{(0)} = O(\|\xi\|^2) + O(\Delta)\,. \tag{5.102}$$

In weakly guiding fibers, the amplitude $\mathcal{E}^{(0)}$ thus remains constant.

5.7 Evolution of Single-Frequency Modes

The calculation in the previous section provides explicit perturbative expressions for single-frequency modes in (arbitrarily bent) step-index optical fibers in generic stationary space-times. The results can now be compared with the predictions of the simplified models analyzed in Sections 5.4 and 5.5.

Phase Evolution The evolution of the spatial phase function ψ was found to be given by

$$\frac{\mathrm{d}}{\mathrm{d}s}\psi = \pm\bar{n}\omega/\zeta + \omega\xi_\parallel/\zeta^2\,, \tag{5.103}$$

where $\bar{n}$ is the effective refractive index, which depends on the details of the fiber and the frequency of light sent through it, see Eqs. (5.70) and (5.72), as well as Figs. 5.4 and 5.5. This result is well approximated by Eq. (5.36) derived from the eikonal model, provided one sets the refractive index n appearing therein equal to the effective refractive index $\bar{n}$ computed from the wave-optics model. In previously considered simplified problems, such agreement was assumed, e.g., in Ref. [31], and proven for particular cases in Refs. [48; 94, Sect. 7.1 and App. B]. Comparing with the proper-time model described in Section 5.5, however, one finds the optical phase of light is not correlated with the effective proper-time of light rays in optical fibers (which arises from light propagation at a velocity slower than in vacuo), as was considered in Ref. [31, App. A].

Polarization Evolution For weakly guiding single-mode fibers, the above analysis shows that the coefficients $\mathcal{E}_\pm$ are constant along the fiber. This, together with the absence of a coupling of the $m = \pm 1$ modes (at the considered order in perturbation theory), implies

that the Jones vector $\mathcal{J}_i$, as defined in Eq. (5.87), has constant components in the Fermi coordinate system, and is thus Fermi–Walker transported along the fiber:

$$ {}^{(3)}\mathrm{D}_s \mathcal{J}_i = 0 \,. \tag{5.104} $$

Figure 5.7 illustrates the consequences of this transport law: if light is sent through a bent fiber, the Jones vector is rotated relative to the Frenet–Serret frame by an angle equal to the integrated torsion, see Eqs. (5.12) and (5.13).

Transport laws of this kind are well known in flat space-time. Specifically, an equation of the form as Eq. (5.104) was first derived by Rytov in the context of geometrical optics in inhomogeneous media [189], and is thus known as Rytov's law [190; 191]. Experimentally, the Fermi–Walker transport of light polarization in optical fibers was first demonstrated experimentally by Ross [192] and Tomita–Chiao [193], and a derivation of Eq. (5.104) from Maxwell's equations in flat space-time was provided in Ref. [173]. Whereas these previous results were all limited to flat space-time, the analysis in Section 5.6 shows that Rytov's law extends to curved space as well, with the sole modification being that the Fermi–Walker derivative ${}^{(3)}\mathrm{D}_s$ is derived from the spatial connection ${}^{(3)}\nabla$ that need not be flat.

Whereas the single-frequency modes derived here exhibit simple transport behavior, such solutions are generally regarded as not physically realizable as they have infinite Klein–Gordon norm (due to their infinite spatial extent). However, they can be combined to form wave packets of finite norm, which are physically plausible models for experimentally produced light pulses in optical fibers.

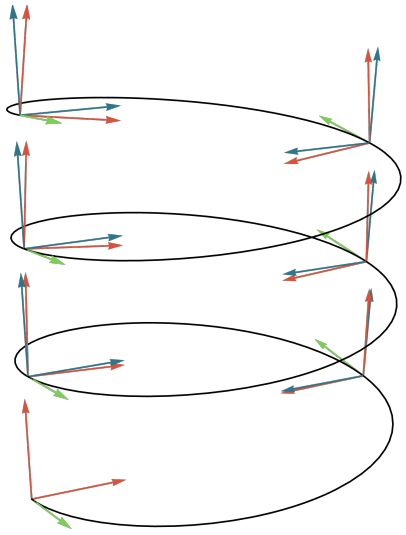

Figure 5.7: Illustration of Fermi–Walker transport of the electromagnetic polarization along a helix, following the curve from the bottom to the top (along the green arrows). For an electromagnetic wave that is initially linearly polarized, the polarization vector undergoes a rotation according to Rytov's law, which results in a total rotation angle equal to the integral of the torsion of the curve, as can be seen by comparing the Fermi–Walker frame (red) with the Frenet–Serret frame (blue).

5.8 Evolution of Wave Packets

Let $A_{\omega m \varkappa \pm}$ denote a mode solution with Killing frequency $\omega \in \mathbf{R}_+$, azimuthal mode index $m \in \mathbf{Z}$, radial mode index $\varkappa \in \mathbf{N}$, propagating either along $(+)$ or against $(-)$ an optical fiber with oriented baseline γ. Since such mode solutions have infinite spatial extent, they are generally not normalizable and are thus considered as not physically realizable. Instead, physically plausible field configurations are given by wave packets of the form

$$A = \sum_{m \in \mathbf{Z}} \sum_{\varkappa \in \mathbf{N}} \int_{\mathbf{R}} \psi_{m,\varkappa}(\omega) A_{\omega m \varkappa} \, \mathrm{d}\omega \,, \tag{5.105}$$

where the sign of $\omega = \pm|\omega|$ is used to encode the direction of wave-propagation:

$$A_{(\pm|\omega|)m\varkappa} = A_{|\omega| m \varkappa \pm} \,. \tag{5.106}$$

Generally, the Klein–Gordon product of two such field configurations can be written as

$$(A \mid A') = \sum_{m,m' \in \mathbf{Z}} \sum_{\varkappa,\varkappa' \in \mathbf{N}} \int_{\mathbf{R}^2} \underline{K}(m,m',\varkappa,\varkappa',\omega,\omega') \psi^*_{m,\varkappa}(\omega) \psi'_{m',\varkappa'}(\omega') \, \mathrm{d}\omega \, \mathrm{d}\omega' \,, \tag{5.107}$$

where $\underline{K}(m,m',\varkappa,\varkappa',\omega,\omega')$ is a (typically singular) integral kernel. Heuristically, this integral kernel may be interpreted as the formal Klein–Gordon product

$$\underline{K}(m,m',\varkappa,\varkappa',\omega,\omega') = (A_{\omega m \varkappa} \mid A_{\omega' m' \varkappa'}) \,, \tag{5.108}$$

but, strictly speaking, the right-hand side is not well-defined because the Klein–Gordon product $(\cdot \mid \cdot)$ is only defined for field configurations of suitable spatial decay. The mode functions $A_{\omega m \varkappa \pm}$ are said to be formally orthonormal if the integral kernel $\underline{K}$ takes the form

$$\underline{K}(m,m',\varkappa,\varkappa',\omega,\omega') = \delta_{m,m'} \delta_{\varkappa,\varkappa'} \delta(\omega - \omega') \,, \tag{5.109}$$

where the first two δ symbols are Kronecker deltas and the last one is a Dirac delta. For the special case of straight fibers with constant lapse ζ and vanishing shift ξ_i, formal mode orthogonality was shown explicitly in Ref. [49, App. B]. For more general setups, however, it is not a priori clear whether the (suitably normalized) mode functions $A_{\omega m \varkappa \pm}$, as computed in Section 5.6, are formally orthonormal as well. Since the following applications are limited to single-mode fibers where the azimuthal mode index is restricted to ± 1 and the radial mode index equals 1, it suffices to consider

$$\underline{K}(m,m',\omega,\omega') = \underline{K}(m,m',1,1,\omega,\omega') \,, \tag{5.110}$$

with m and m' equal to ± 1. Since the angular dependence of $A_{\omega m \varkappa \pm}$ is given by $e^{im\theta}$, it follows from Parseval's theorem that $\underline{K}(m,m',\omega,\omega')$ vanishes if $m \neq m'$, so that

$\underline{K}(m,m',\omega,\omega') = \underline{K}(m,m,\omega,\omega')\delta_{m,m'}$. To show formal mode orthogonality, it thus remains to show that $\underline{K}(m,m,\omega,\omega') = \delta(\omega-\omega')$. Even though this last condition is made plausible by the heuristic formula Eq. (5.108) and the general fact that the Klein–Gordon product of solutions to the field equation is time-independent (but, so far, this was only shown for fields of suitable spatial decay), a mathematical proof would require explicit computations of radial and longitudinal integrals involving squares of wave packets given in Eq. (5.105). For straight fibers at a constant lapse and vanishing shift, the radial integrals can be solved explicitly and the integrals along the fiber length s can be resolved using Plancherel's theorem [49, App. A and B]. In the more general case considered here, such an analysis would have to be extended to allow for slow variations of the longitudinal wave vector β and the transverse field profile along the arc length s. Mathematical methods for integrating such functions depending on multiple scales have been developed, i.a., in Refs. [194; 195]. However, in view of the physical plausibility, the present document *assumes* the formal orthogonality of the modes $A_{\omega m1\pm}$ in single-mode fibers. In particular, it will be assumed that the Klein–Gordon norm of wave packets of the form

$$A = \sum_{m=\pm1} \int_{\mathbf{R}} \psi_m(\omega) A_{\omega,m,1} \,\mathrm{d}\omega\,, \tag{5.111}$$

where the radial mode index is restricted to 1 for single-mode fibers, is given by

$$(A \mid A') = \sum_{m=\pm1} \int_{\mathbf{R}} \psi^*_m(\omega)\psi'_m(\omega) \,\mathrm{d}\omega\,. \tag{5.112}$$

The evolution properties of wave packets of the form Eq. (5.111) can be understood as follows. The mode solutions $A_{\omega,m,\varkappa}$ computed above have the general form $a_{\omega,m,\varkappa}(r,\varsigma)e^{im\theta}e^{i\Psi(t,s)}$, where Ψ is the eikonal

$$\Psi = -\omega t + \omega \int \left(\frac{\bar{n}}{\zeta}\mathrm{d}s + \frac{\xi}{\zeta^2}\right)\,, \tag{5.113}$$

see Eq. (5.38) for explicit error terms. When evaluated at the end of the curve γ, one has

$$\Psi(t,\ell) = \Psi(t-t^*,0)\,, \tag{5.114}$$

where ℓ is the length of γ and t^* is the delay time

$$t^* = \int_\gamma \left(\frac{\bar{n}}{\zeta}\mathrm{d}s + \frac{\xi}{\zeta^2}\right)\,. \tag{5.115}$$

In single-mode fibers, the variation of $a_{\omega,m,\varkappa}(r,\varsigma)$ with respect ς was found to be negligible in practical applications so that one can write $A_{\omega,m,\varkappa}(t,\ell,r,\theta) = A_{\omega,m,\varkappa}(t-t^*,0,r,\theta)$ with negligible error. If the spectral distribution ψ in Eq. (5.111) is sufficiently narrow, the frequency dependence of $\bar{n}$ is also negligible, and one finds that, in the Fermi coordinate system introduced in Section 5.2, the electromagnetic field at the end of a fiber γ coincides

with the field at the input at an earlier time:

$$A_\mu(t, \ell, r, \theta) = A_\mu(t - t^*, 0, r, \theta)\,. \tag{5.116}$$

This equation, together with the explicit result for the delay time t^* given in Eq. (5.115) allows describing classical fiber interferometry in stationary gravitational fields. Moreover, the analysis can be extended to interference experiments involving quantum states of light using Eq. (5.112) as well as the fact that the classical Klein–Gordon product determines the Hilbert-space inner product in the quantized theory. Before considering such interferometry experiments, however, the following sections describe higher-order corrections to the solutions obtained so far.

5.9 Higher-Order Corrections

The calculations in Section 5.6 have considered only effects arising from the lapse ζ and the longitudinal shift $\xi_\parallel$. The remaining terms identified in Section 5.3 differ from these "direct terms" by having either a non-zero Fourier index or a non-zero radial index, see Table 5.1. This section describes, in an abstract form, how such corrections can be incorporated into the calculations. As indicated above, terms with a vanishing Fourier index generally lead to phase perturbations (described in Section 5.9.1), whereas non-zero Fourier indices lead to polarization perturbations (Section 5.9.2).

5.9.1 Phase Perturbations

For any external parameter of order ϵ that has zero Fourier index, the field equations (5.60) at leading order in the adiabatic expansion are replaced by equations of the form

$$(\underline{\mathrm{H}}_m + \epsilon\delta\underline{\mathrm{H}}_m)a_b^{(0)} = 0\,, \tag{5.117}$$

where the superscript (0) refers to the leading order in the adiabatic expansion, as above, and where the operator $\delta\underline{\mathrm{H}}_m$ depends only on the radial coordinate r and the long-distance scale $\varsigma = \varepsilon s$, where ε is the slowness parameter. These equations can be solved perturbatively using the Green functions defined in Eqs. (5.90) to (5.92). Specifically, if $f_m[\boldsymbol{q}^{(0)}]$ denotes a solution to the homogeneous Helmholtz equation, as in Eq. (5.64), the general solution that is accurate to first order in ϵ is given by

$$a^{(0)} = f_m\,[\boldsymbol{q}^{(0)}] - \epsilon\,\underline{\mathrm{G}}_m[\delta\underline{\mathrm{H}}_m f_m\,[\boldsymbol{q}^{(0)}]] + O(\epsilon^2)\,. \tag{5.118}$$

The interface conditions (3.37) then reduce to a matrix equation differing from Eq. (5.65) by terms of order ϵ. Generally, the resulting equations are of the form

$$(\mathbf{M} + \epsilon\,\delta\mathbf{M})\mathbf{N}\boldsymbol{q}^{(0)} = 0\,, \tag{5.119}$$

where $\mathbf{M}$ and $\mathbf{N}$ are the matrices defined in Eqs. (5.66) and (5.67), and $\delta\mathbf{M}$ accounts both for perturbations in the radial mode profile (5.118) and for perturbations in the explicit form of the interface conditions (if any). This equation admits non-trivial solutions only if

$$\det(\mathbf{M} + \epsilon\,\delta\mathbf{M}) = 0\,. \tag{5.120}$$

Here, $\mathbf{M}$ can be regarded as a function of the normalized guide index b and the normalized frequency V, defined in Eqs. (5.70) and (5.72), respectively. If V is prescribed, b will generally deviate from its unperturbed value $b_0(V)$, i.e., one has $b = b_0 + \epsilon\delta b + O(\epsilon^2)$. Expanding the above equation to first order in ϵ using Jacobi's equation for the derivative of the determinant, one obtains

$$\det M(b_=) + \epsilon\,\mathrm{tr}\left(\mathrm{adj}(\mathbf{M}(b_0))\left[\frac{\partial\mathbf{M}}{\partial b}\delta b + \delta\mathbf{M}\right]\right) = O(\epsilon^2)\,, \tag{5.121}$$

where adj denotes the matrix adjugate, i.e., the transpose of the cofactor matrix. This leads to the result

$$\delta b = -\frac{\mathrm{tr}[\mathrm{adj}(\mathbf{M}(b_0))\delta\mathbf{M}]}{\mathrm{tr}[\mathrm{adj}(\mathbf{M}(b_0))\partial\mathbf{M}/\partial b]}\,. \tag{5.122}$$

This is the general formula for the perturbation of the normalized guide index b for arbitrary corrections to the Helmholtz operator with vanishing Fourier index. The specific form of $\delta\mathbf{M}$ depends on the details of the perturbation under consideration: in Ref. [94], this method was used to compute the Sagnac effect in straight optical fibers (before the more general approach described in Section 6.4 was found), and this technique also underlies the calculations on the influence of gravitational waves in optical fibers described in Ref. [96]. The explicit details of these results are, however, not relevant to the considerations in this document.

5.9.2 Polarization Perturbations

Whereas correction terms to the wave operator that are independent of the azimuthal coordinate θ give rise to phase perturbations, other terms with non-zero Fourier indices yield perturbations of the electromagnetic polarization. To study such effects, consider, first, a correction term to the d'Alembertian with Fourier-index $m = \pm 2$ that is slowly varying along the fiber baseline (according to the criterion given in Section 5.1) and thus corresponds to a dimensionless term of the form $\phi_\pm = \varepsilon\psi_\pm(\varsigma)e^{\pm 2i\theta}$ with $\varepsilon \ll 1$. An explicit dependence of the wave operator on θ means that various Fourier components of A_b cannot be considered independently of each other. For single-mode fibers, one thus has to consider multiple Fourier components in combination. Seeking solutions that, at order ε^0, only have $m = \pm 1$ contributions (in agreement with the fact that, in the unperturbed problem, single-mode fibers only admit $m = \pm 1$ solutions), a correction term to the wave equation with Fourier index ± 2 implies non-zero field perturbations with $m = \pm 1$ and $m = \pm 3$.

According to Section 5.3, the parts with $m = \pm 3$ are off-resonant and can thus be neglected in a first approximation. It thus remains to analyze the $m = \pm 1$ components $a^{(\pm)}$ that satisfy a coupled system of the general form

$$\underline{\mathrm{H}}_+ a^{(+)} + \varepsilon \delta \underline{\mathrm{H}}_+ a^{(-)} = 0\,, \tag{5.123a}$$

$$\underline{\mathrm{H}}_- a^{(-)} + \varepsilon \delta \underline{\mathrm{H}}_- a^{(+)} = 0\,. \tag{5.123b}$$

At order ε^0, the solutions are of the form given in Eq. (5.84). At next order, one obtains inhomogeneous equations analogous to Eq. (5.88) but with corrections to the right-hand side arising from $\delta \underline{\mathrm{H}}_+$:

$$\underline{\mathrm{H}}_\pm a^{(\pm,1)} = -2i\Sigma_\pm - \delta \underline{\mathrm{H}}_\pm a^{(\mp,0)}\,. \tag{5.124}$$

Such equations can be solved in the core and cladding separately using the Green functions defined in Eqs. (5.90) to (5.92). However, when formulating the matching conditions in a form analogous to Eq. (5.94), the solvability condition (5.95) acquires correction terms arising from the operators $\delta \underline{\mathrm{H}}_\pm$. This implies a correction to the right-hand side of the evolution equation (5.96). Whereas the right-hand side of Eq. (5.96) vanishes in the case of weak guidance, the new correction term does not necessarily vanish as well, leading to evolution equations for the amplitudes $\mathcal{E}_\pm$ of the general form

$$\frac{\mathrm{d}}{\mathrm{d}\varsigma} \begin{pmatrix} \mathcal{E}_+ \\ \mathcal{E}_- \end{pmatrix} = \varepsilon \begin{pmatrix} 0 & h_+(\varsigma) \\ h_-(\varsigma) & 0 \end{pmatrix} \begin{pmatrix} \mathcal{E}_+ \\ \mathcal{E}_- \end{pmatrix}\,, \tag{5.125}$$

where $h_\pm(\varsigma)$ are functions that depend on the details of the perturbation term $\psi_\pm$ and on the optical fiber mode under consideration.

Such a scheme can be used to obtain correction terms to Rytov's law (5.104) that arise, e.g., from second derivatives in the lapse function ($\nabla_\pm \nabla_\pm \zeta$), second derivatives in the longitudinal shift ($\nabla_\pm \nabla_\pm \xi_\parallel$), first derivatives of the transverse shift ($\nabla_\pm \xi_\pm$), as well as certain components of the Riemann curvature tensor (${}^{(3)}R_{\parallel\pm\parallel\pm}$), see Table 5.1. In all cases, $h_\pm$ will be proportional to the given perturbation term, with the coefficient of proportionality depending on the details of the optical fiber and the characteristics of the mode propagating therein. Effects arising from deformations of the core-cladding interface or inhomogeneities of the refractive indices can be treated similarly. Some of these corrections arising from curvature and fiber deformations are currently worked out by M. Hudelist and F. Steininger, respectively.

Such a perturbation scheme can also be extended to higher order in ε. This is needed, for example, to obtain corrections to Rytov's law which arise from coefficients with a Fourier index of ± 1, as such terms produce resonant coupling at second order in perturbation theory, cf. Fig. 5.3. Such an analysis was carried out in Ref. [173] to obtain corrections to Rytov's law which arise from fiber bending, as described by the baseline normal ν_i defined in Eq. (5.5). This analysis was carried out in flat space-time in which case it was found

that the Jones vector $\mathcal{J}_k$ satisfies an evolution equation of the form

$$ {}^{(3)}\mathrm{D}_s \mathcal{J}^k = i\xi(\nu^k \nu_l - \tfrac{1}{2}\kappa^2 \delta^k_l)\mathcal{J}^l + i\eta\kappa^2 \mathcal{J}^k \,, \tag{5.126} $$

up to terms of order $(\varrho\kappa)^3$, where ϱ is the core radius and κ the curvature of the fiber's baseline. Here, ξ and η are coupling constants (the polarization and phase curvature moments) that depend on the details of the optical fiber and the wavelength of light propagating therein. Similar equations were put forward in Refs. [180; 186] using different methods in slightly altered setups. The successful application of this scheme to second order in ε indicates that the general methods described here allow, in principle, to compute corrections to the solutions given in Section 5.6 that arise from the various terms listed in Table 5.1 to arbitrary order in perturbation theory.

5.10 Summary

The problem of describing light propagation in step-index optical fibers in the presence of gravity has been considered previously in Refs. [4; 47–49]. Whereas the calculations presented there were limited to weak static gravitational fields and a very restrictive class of fiber geometries (namely straight fibers or fiber-optic spools placed horizontally in a uniform gravitational field), the calculations presented here allow for arbitrarily bent optical fibers located in arbitrary stationary space-times: the assumption that the fiber's radius of curvature and the characteristic length scales of the space-time geometry far exceed the optical wavelength constitutes no significant restriction on the practical range of applicability of the model.

The analysis in this chapter shows that the electromagnetic modes in step-index optical fibers in curved space-times are characterized by their eikonal ψ and the Jones vector $\mathcal{J}_i$, describing the spatial dependence of the optical phase and the direction of electric polarization, respectively. The eikonal ψ was found to satisfy the evolution equation

$$\frac{\mathrm{d}\psi}{\mathrm{d}s} = \pm\bar{n}\frac{\omega}{\zeta} + \frac{\omega}{\zeta^2}\xi_{\parallel}\,,$$

where s is the arc length of the fiber's baseline (measured in the spatial metric ${}^{(3)}g_{ij}$), $\bar{n}$ is the effective refractive index (a quantity that depends on the fiber's refractive indices, its core radius, and the electromagnetic wavelength), ω is the Killing frequency, ζ is the lapse function, and $\xi_{\parallel}$ is the tangential component of the shift vector ξ_i. The Jones vector $\mathcal{J}_i$, on the other hand, was found to be Fermi–Walker transported along the fiber:

$${}^{(3)}\mathrm{D}_s\mathcal{J}_i = 0\,.$$

The evolution equation for the eikonal ψ accounts for two effects simultaneously: the first term describes the gravitational redshift and the second term corresponds to the Sagnac effect. Whereas previous results on fiber optics in curved space-times have described these effects separately from each other [4; 47; 48; 94], the present analysis accounts for both effects at once and extends these results to arbitrary fiber geometries and beyond the weak-field regime. The transport law for the Jones vector $\mathcal{J}_i$ is reminiscent of Rytov's law for geometrical optics in flat space-times [189]. A derivation of such an equation for optical fiber modes in flat space-time was recently given by the present author in collaboration with M. Oancea [173], and the present analysis extends this result to curved space-times.

Experimental signatures of the gravitational redshift and the Sagnac effect in optical fiber interferometers are described in the next chapter.

Chapter 6

Gravitational Photon Interferometry

In standard quantum optics, linear optical elements (such as beam splitters and phase-shifters) are modeled as unitary state transformations [196; 144, Sect. 6.5; 122, Sect. 14]. Previous descriptions of gravitationally induced quantum interference commonly modeled the gravitational redshift of single photons using similar methods, in which the effect on finite-norm wave packets was derived from a model of the corresponding effect on infinite-norm states of definite frequency, see, e.g., Refs. [39–43; 49]. However, the analogy between the gravitational redshift and other linear optics transformations is imperfect: in Refs. [44; 45] it was argued that gravitational redshifts on finite-norm wave packets can be modeled by unitary state transformations even though the corresponding transformation of infinite-norm states of definite frequency is not of the standard form. From a mathematical perspective, however, such models are not fully satisfactory as the notion of unitary transformations of states with infinite norms is generally ill-defined.

Based on the quantization scheme developed in Chapter 4, Sections 6.1 and 6.2 describe an alternative approach to this matter. As the quantization scheme used here is formulated in the Heisenberg picture, where quantum states do not evolve in time, no state transformations arise here. Instead, a decomposition of classical solutions in terms of their input and output wave profiles allows setting up a description of arbitrary linear optics circuits where each optical element is not described by a *transformation* of ladder operators, but by *equalities* that describe the decomposition of in-operators in terms of out-operators. Contrary to the aforementioned formalism, where the description of finite-norm wave packets is based on models for the behavior of infinite-norm states of definite frequency, the method described here considers finite-norm wave packets from the onset.

The general formalism developed here is then applied to Mach–Zehnder interferometers in general non-inertial frames (Section 6.3). The general formulas obtained there are then used to describe interferometers in rotating reference systems (Section 6.4) as well as interferometers in stationary gravitational fields (Section 6.5). Here, the aim is not to provide an exhaustive list of all potential experimental signatures of quantum interference

in non-inertial frames, but merely to demonstrate that the methods developed in this chapter (which are based on the quantization scheme described in Chapter 4 and the explicit calculations in Chapter 5) are sufficient to describe such interference experiments.

6.1 Classical Linear Optics Transformations

To describe optical interferometers, this section formulates a model of classical light propagation in general linear optical circuits. The transition to a quantum description is made in the next section.

A general linear optics circuit may consist of an arbitrary number of beam splitters and phase shifters, located at different positions in a gravitational field, between which light propagates through free space or optical fibers. This section is concerned with circuits connecting N input regions with N output regions, henceforward referred to as input and output ports.

General field configurations in such optical circuits correspond to light being sent into one or multiple input ports. If the optical circuit is linear, however, the output produced by sending light into multiple input ports simultaneously can be understood by studying the circuit's response to radiation sent into single input ports. The general case is then obtained by considering linear combinations of such fields.

The field A considered so far in this thesis describes single optical fibers in isolation. Such fields can be "stitched together" to obtain global solutions, denoted by $\underline{A}$, describing light propagation in optical circuits consisting of multiple optical fibers (if radiation leakage and potential crosstalk between the fibers is negligible). This requires introducing some notation, illustrated in Figs. 6.1a and 6.1b: If A_i^{in} is a wave-packet solution in the input region i (valid at "early times" $t < t_{\mathrm{in}}$, before the wave packet enters the optical circuit), denote by $\underline{A}_i^{\mathrm{in}}$ the corresponding electromagnetic field (defined in the entire interferometer for all times) that, at early times, is supported only in input region i and agrees with A_i^{in} there. Hence, $\underline{A}_i^{\mathrm{in}}$ and A_i^{in} differ in their domains of definition:

> $\underline{A}_i^{\mathrm{in}}$ is defined globally, i.e., on the entire interferometer,
>
> A_i^{in} is defined only in the input region i and at early times $t < t_{\mathrm{in}}$.

Accordingly, A_i^{in} describes the electromagnetic field in a single input port only, whereas $\underline{A}_i^{\mathrm{in}}$ describes how such radiation propagates through the interferometer, and the fields resulting in the various output ports. The field $\underline{A}_i^{\mathrm{in}}$ thus depends on the internals of the optical circuit under consideration, whereas A_i^{in} can be prescribed independently of such details.

Denoting by $\underline{A}|_i^{\mathrm{in}}$ the restriction of $\underline{A}$ to the input port i, one then has

$$\underline{A}_i^{\mathrm{in}}|_j^{\mathrm{in}} = 0 \text{ for } i \neq j\,, \qquad \underline{A}_i^{\mathrm{in}}|_i^{\mathrm{in}} = A_i^{\mathrm{in}} \text{ (no summation implied)}\,. \tag{6.1}$$

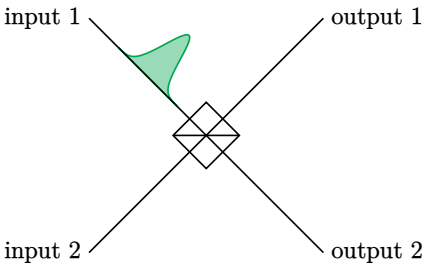

(a) $\underline{A}_1^{\text{in}}$ at $t < t_{\text{in}}$ describes a configuration where the electromagnetic field equals A_1^{in} in the input region 1 and zero in all other input regions.

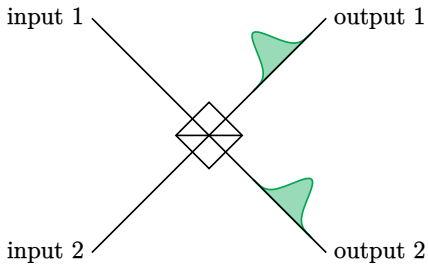

(b) $\underline{A}_1^{\text{in}}$ at $t > t_{\text{out}}$ describes the fields in the output regions that arise from the field A_1^{in} in input region 1. Note that A_1^{in} is not defined in the output regions.

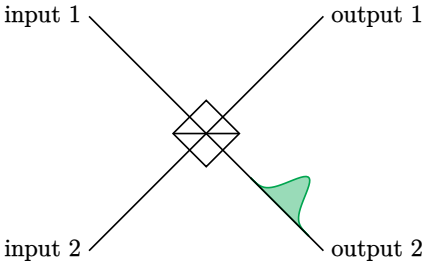

(c) $\underline{A}_{21}^{\text{out}}$ at $t > t_{\text{out}}$ describes the field that has the same field configuration as $\underline{A}_1^{\text{in}}$ in the output port 2 but is zero in all other output ports.

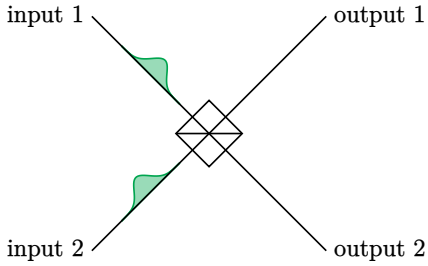

(d) $\underline{A}_{21}^{\text{out}}$ at $t < t_{\text{in}}$ describes the input that results in vanishing fields in all output ports except output number 2, where the resulting field is identical to that produced by $\underline{A}_1^{\text{in}}$. In general, $\underline{A}_{21}^{\text{out}}$ differs from $\underline{A}_1^{\text{in}}$.

Figure 6.1: Illustration of the nomenclature used to describe field configurations at a linear optical circuit: A_i^{in} corresponds to a field configuration defined in a single input region, and $\underline{A}_i^{\text{in}}$ describes its extension to the entire optical circuit (a). In particular, $\underline{A}_i^{\text{in}}$ can be evaluated at "late times" $t > t_{\text{out}}$, after the wave packets have left the optical circuit (b). The field $\underline{A}_{ki}^{\text{out}}$ encodes the excitation in output region k that arises from the input A_i^{in} (c). This field can be evolved backwards in time to obtain the input that would have produced $\underline{A}_i^{\text{in}}|_k^{\text{out}}$ in the output port k and zero in all other output ports.

The use of such a notational distinction between $\underline{A}_i^{\text{in}}$ and A_i^{in} is as follows: in spite of $\underline{A}_i^{\text{in}} \neq \underline{A}_j^{\text{in}}$ for $i \neq j$, it is possible that the input wave profiles of $\underline{A}_i^{\text{in}}$ and $\underline{A}_j^{\text{in}}$ coincide,[(1)] which will be expressed as $A_i^{\text{in}} = A_j^{\text{in}}$ (where an identification of the various input regions is not written explicitly).

As the various fields $\underline{A}_i^{\text{in}}$ have disjoint spatial support at early times, they are mutually orthogonal. If one further chooses the fields to be normalized, one has

$$(\underline{A}_i^{\text{in}} \mid \underline{A}_j^{\text{in}}) = \delta_{ij} \,, \tag{6.2}$$

[(1)] Strictly speaking, this is only meaningful if the input regions i and j are isometric. In practice, this is at best approximately true: for example, two optical fibers may have straight segments that are locally indistinguishable to a certain level of accuracy. A more rigorous statement than the equality $A_i^{\text{in}} = A_j^{\text{in}}$ would be the following: if ϕ is an isometry mapping region i to region j, then $A_i^{\text{in}} = \phi^* A_j^{\text{in}}$ (up to potential error terms). In the following, such isometries (or approximate isometries) will be left implicit.

where $(\cdot \mid \cdot)$ denotes the Klein–Gordon product defined in Eq. (4.3). Let $\underline{A}_i^{\text{in}}|_k^{\text{out}}$ denote the restriction of $\underline{A}_i^{\text{in}}$ to the output region k. For each such $\underline{A}_i^{\text{in}}|_k^{\text{out}}$, there exists a field $\underline{A}_{ki}^{\text{out}}$ (satisfying the field equations in the entire interferometer) which, at late times, is supported only in the output region k and coincides with $\underline{A}_i^{\text{in}}$ there, hence

$$\underline{A}_{ki}^{\text{out}}|_l^{\text{out}} = \delta_{kl} \underline{A}_i^{\text{in}}|_l^{\text{out}} \qquad \text{(no summation implied)}\,, \tag{6.3}$$

see Figs. 6.1c and 6.1d for a graphical illustration. Note that the fields $\underline{A}_{ki}^{\text{out}}$ are not necessarily normalized. Summing $\underline{A}_{ki}^{\text{out}}$ over k reproduces $\underline{A}_i^{\text{in}}$:

$$\underline{A}_i^{\text{in}} = \sum_{k=1}^{N} \underline{A}_{ki}^{\text{out}}\,, \tag{6.4}$$

which can be seen by noting that the field is fully determined by its restrictions to the output regions. Restricting $\underline{A}_i^{\text{in}}$ to the output l yields $\underline{A}_i^{\text{in}}|_l^{\text{out}}$, which agrees with the restriction of the right-hand side to output l on account of Eq. (6.3).

The Klein–Gordon products of the input fields are generally given by Eq. (6.2). The products of the output fields, here denoted by

$$U_{kilj} = (\underline{A}_{ki}^{\text{out}} \mid \underline{A}_{lj}^{\text{out}})\,, \tag{6.5}$$

depend on the details of the optical circuit. Since, at late times, $\underline{A}_{ki}^{\text{out}}$ is supported in output k whereas $\underline{A}_{lj}^{\text{out}}$ is supported in output l, their inner product vanishes if $k \neq l$. Hence, U_{kilj} is of the form

$$U_{kilj} = \delta_{kl} u_{kij} \qquad \text{(no summation implied)}\,. \tag{6.6}$$

The transfer coefficients u_{kij} can thus be regarded as a measure of indistinguishability of the fields $\underline{A}_i^{\text{in}}$ and $\underline{A}_j^{\text{in}}$, based solely on information available in the output region k. Since the Klein–Gordon product is Hermitian, u_{kij} satisfies

$$u_{kij}^* = u_{kji}\,, \tag{6.7}$$

i.e., for each k, u_{kij}, regarded as a matrix with row index i and column index j, is a Hermitian matrix. Inserting Eq. (6.4) into Eq. (6.2) and using Eqs. (6.5) and (6.6), one obtains

$$\sum_{k=1}^{N} u_{kij} = \delta_{ij}\,, \tag{6.8}$$

which expresses the fact that the inputs $\underline{A}_i^{\text{in}}$ and $\underline{A}_j^{\text{in}}$ can be perfectly distinguished by combining the information available in all output regions k.

Illustration: Symmetric Beam Splitters To illustrate this formalism, consider a symmetric beam splitter (which is commonly modeled as being point-like) with its two inputs and two outputs labeled as in Fig. 6.2. If $\mathscr{T}$ and $\mathscr{R}$ denote the transmission and reflection coefficients, respectively, one has

$$A_{11}^{\text{out}} = \mathscr{T} A_1^{\text{in}}\,, \qquad A_{12}^{\text{out}} = \mathscr{R} A_2^{\text{in}}\,, \qquad A_{21}^{\text{out}} = \mathscr{R} A_1^{\text{in}}\,, \qquad A_{22}^{\text{out}} = \mathscr{T} A_2^{\text{in}}\,. \tag{6.9}$$

A direct computation yields the following expressions for the transfer coefficients

$$(u_{1ij}) = \begin{pmatrix} |\mathscr{T}|^2 & \mathscr{T}^* \mathscr{R} w \\ \mathscr{R}^* \mathscr{T} w^* & |\mathscr{R}|^2 \end{pmatrix} \qquad (u_{2ij}) = \begin{pmatrix} |\mathscr{R}|^2 & \mathscr{R}^* \mathscr{T} w \\ \mathscr{T}^* \mathscr{R} w^* & |\mathscr{T}|^2 \end{pmatrix}, \tag{6.10}$$

where w describes the indistinguishability of the incoming wave profiles:

$$w = (A_1^{\text{in}} \mid A_2^{\text{in}})\,. \tag{6.11}$$

Equation (6.8) then implies the conditions

$$|\mathscr{T}|^2 + |\mathscr{R}|^2 = 1\,, \qquad \mathscr{T}^* \mathscr{R} + \mathscr{R}^* \mathscr{T} = 0\,, \tag{6.12}$$

which are known as the reciprocity relations for symmetric beam splitters [197]. Whereas the standard formalism for linear beam splitters, described, e.g, in Refs. [198; 199], starts from "unitary transformations" among non-normalizable plane waves, from which finite-norm wave packets are constructed afterward, the present formalism allows to circumvent the use of infinite-norm solutions and applies to finite-norm waves directly.

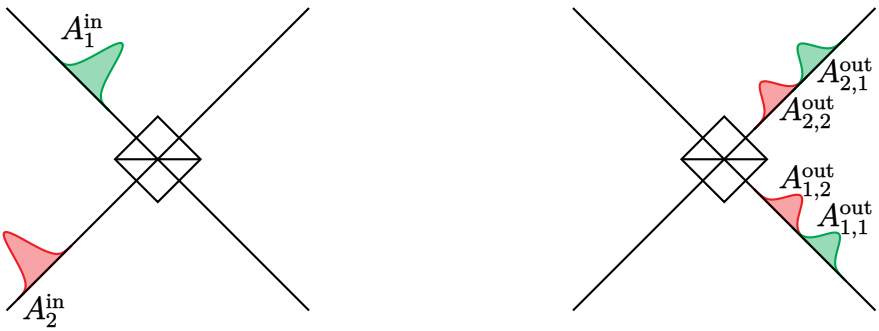

Figure 6.2: Schematic representation of the splitting of wave packets at a beam splitter. For light pulses reaching at the beam splitter at different times (left panel), the wave packets at the outputs are not linearly dependent as would be the case for indistinguishable inputs.

Composition of Optical Circuits In the standard optics formalism of transformations of monochromatic waves, linear optical components are represented by unitary matrices that can be multiplied to describe the composition of the transformations induced by applying various optical elements in succession. In the present formalism, a similar statement holds. To formulate such a relation, consider an optical circuit with N inputs and outputs, coupled via N intermediate regions. The coupling between input and intermediate regions can be described as above: if $\underline{A}_i^{\mathrm{in}}$ denotes a (normalized) field supported, at early times, in the input region i, and if $\underline{A}_{ki}^{\mathrm{int}}$ denotes the excitation in the intermediate region k, caused by input $\underline{A}_i^{\mathrm{in}}$, one has $\underline{A}_i^{\mathrm{in}} = \sum_{k=1}^N \underline{A}_{ki}^{\mathrm{int}}$, see Eq. (6.4). The transfer coefficients u_{kij}, describing the transition amplitudes of this first coupling region, can be computed using $u_{kij} = (\underline{A}_{ki}^{\mathrm{int}} \mid \underline{A}_{kj}^{\mathrm{int}})$ (no summation implied). Next, consider the coupling of the intermediate region to the output region. The "intermediate" fields $\underline{A}_{ki}^{\mathrm{int}}$ are indexed by two numbers: k labels the intermediate region and i labels the input region. Each such field gives rise to various excitations in the output regions, here indexed by m, that are denoted by $\underline{A}_{mki}^{\mathrm{out}}$. Such a field can be interpreted as describing the excitation in output m that arises from the input i only via the intermediate region k. The field in output m arising from input i is thus obtained by summing over all k: $\underline{A}_{mi}^{\mathrm{out}} = \sum_{k=1}^N \underline{A}_{mki}^{\mathrm{out}}$. Now, the coupling of the intermediate region to the output regions determines the transfer coefficients $v_{mkilj} = (\underline{A}_{mki}^{\mathrm{out}} \mid \underline{A}_{mlj}^{\mathrm{out}})$ (no summation implied) from which one can compute the overall transfer coefficients according to

$$w_{mij} = \sum_{k=1}^{N} \sum_{l=1}^{N} v_{mkilj} \,. \tag{6.13}$$

Using this formula, models of arbitrarily complex optical circuits can be constructed from simpler circuits (such as beam splitters and phase shifters).

6.2 Quantum Linear Optics Transformations

The above considerations on linear optics transformations were purely classical. The corresponding equations for the quantized theory are obtained by applying the linear raising operator $\hat{a}^\dagger(\cdot)$, which maps a classical solution to the corresponding Fock operator, to both sides of Eq. (6.4). One obtains

$$\hat{a}_i^{\dagger \mathrm{in}} = \sum_{k=1}^{N} \hat{a}_{ki}^{\dagger \mathrm{out}} \,, \tag{6.14}$$

and, on account of Eq. (4.33a) together with Eqs. (6.2), (6.5) and (6.6), these operators satisfy the commutation relations

$$[\hat{a}_i^{\mathrm{in}}, \hat{a}_j^{\dagger \mathrm{in}}] = \delta_{ij} \,, \qquad\qquad [\hat{a}_{ki}^{\mathrm{out}}, \hat{a}_{lj}^{\dagger \mathrm{out}}] = \delta_{kl} u_{kij} \,, \tag{6.15}$$

with no summation implied in the last expression.

With these equations, one can compute single-photon transition probabilities in arbitrary linear optics circuits. For example, in an interferometer with two inputs and two outputs ($N = 2$), the state corresponding to a single photon in input 1 is denoted by $\hat{a}_1^{\text{in}}|0\rangle$ and the decomposition into the output-basis is

$$\hat{a}_1^{\dagger\text{in}}|0\rangle = \hat{a}_{11}^{\dagger\text{out}}|0\rangle + \hat{a}_{21}^{\dagger\text{out}}|0\rangle\,. \tag{6.16}$$

Projecting onto the space spanned by $\hat{a}_{1i}^{\text{out}}|0\rangle$ yields $\hat{a}_{11}^{\dagger\text{out}}|0\rangle$, whose squared norm gives the probability of the photon reaching the output 1:

$$p_{1,1} = \langle 0|\hat{a}_{11}^{\text{out}}\hat{a}_{11}^{\dagger\text{out}}|0\rangle = \langle 0|[\hat{a}_{11}^{\text{out}}, \hat{a}_{11}^{\dagger\text{out}}]|0\rangle = u_{111}\,. \tag{6.17}$$

Likewise, the probability for the photon (injected into input 1) to reach the output 2 is

$$p_{2,1} = \langle 0|\hat{a}_{21}^{\text{out}}\hat{a}_{21}^{\dagger\text{out}}|0\rangle = \langle 0|[\hat{a}_{21}^{\text{out}}, \hat{a}_{21}^{\dagger\text{out}}]|0\rangle = u_{211}\,. \tag{6.18}$$

Analogously, if the photon is injected into input 2 instead of 1, one obtains the probabilities

$$p_{1,2} = u_{122}\,, \qquad\qquad p_{2,2} = u_{222}\,. \tag{6.19}$$

That the probabilities add to unity, i.e., $p_{1,1} + p_{2,1} = p_{1,2} + p_{2,2} = 1$, is ensured by Eq. (6.8).

The transfer coefficients u_{kij} with $i \neq j$ arise only if multiple inputs are combined. For example, given the two-photon input $\hat{a}_1^{\dagger\text{in}}\hat{a}_2^{\dagger\text{in}}|0\rangle$, the coincidence probability p of one photon entering output 1 and output 2, each, is given by

$$p = u_{111}u_{222} + u_{211}u_{122} + u_{112}u_{221} + u_{212}u_{121}\,. \tag{6.20}$$

Comparison with the above results yields

$$p = p_{1,1}\,p_{2,2} + p_{1,2}\,p_{2,1} + u_{112}u_{221} + u_{212}u_{121}\,, \tag{6.21}$$

so that the last two terms can be attributed to two-photon interference.

Illustration: Symmetric Beam Splitters For symmetric beam splitters, whose transfer coefficients are given in Eq. (6.10), one obtains the single-photon transition probabilities

$$p_{1,1} = p_{2,2} = |\mathscr{T}|^2\,, \qquad\qquad p_{1,2} = p_{2,1} = |\mathscr{R}|^2\,, \tag{6.22}$$

which support the interpretation of $\mathscr{T}$ and $\mathscr{R}$ as transmission and reflection amplitudes, since their squared moduli coincide with transmission and reflection probabilities, respectively.

In particular, symmetric 50:50 beam splitters are characterized by $|\mathscr{T}| = |\mathscr{R}| = 1/\sqrt{2}$.

The reciprocity relations (6.12) then imply $\mathscr{R} = \pm i\mathscr{T}$. For simplicity, the following calculations assume

$$\mathscr{T} = 1/\sqrt{2}\,, \qquad\qquad \mathscr{R} = i/\sqrt{2}\,. \tag{6.23}$$

If one photon is injected into each of the two inputs of such a beam splitter, Eq. (6.20) yields the following coincidence detection probability:

$$p = \tfrac{1}{2}(1 - |w|^2)\,, \tag{6.24}$$

where $w = (A_1^{\text{in}} \mid A_2^{\text{in}})$ is the Klein–Gordon product of the two input profiles. For perfectly distinguishable inputs (as depicted in Fig. 6.2), w vanishes and one obtains $p = 1/2$, meaning that it is equally probable for the photons to enter separate or identical outputs. This is because the two-photon interference terms in Eq. (6.21) vanish for $w = 0$. However, for indistinguishable wave packets, where $w = 1$, one has $p = 0$, meaning that the photons never enter separate outputs but always enter the same output port (both outputs are reached with equal probability). This phenomenon of "photon bunching" is known as the Hong–Ou–Mandel effect [200].

The sensitivity of Hong–Ou–Mandel interference to the distinguishability of the interfering wave packets has resulted in multiple proposals of its use in photon interferometry in non-inertial systems, where initially indistinguishable wave packets are rendered distinguishable if they traverse different trajectories in a gravitational field or a rotating system, see, e.g., Refs. [3; 5; 43; 201].

6.3 Mach–Zehnder Interferometry in Non-Inertial Systems

In Chapter 5, it was shown that light, propagating in an optical fiber with baseline γ, located in a stationary space-time with lapse ζ, shift ξ_i and spatial metric ${}^{(3)}g_{ij}$, is retarded by a delay time equal to

$$t^* = \int_{\gamma_i} \left(\frac{\bar{n}}{\zeta} \mathrm{d}s + \frac{\xi}{\zeta^2} \right)\,, \tag{6.25}$$

see Eq. (5.115), and that the Jones vector $\mathcal{J}_i$ is Fermi-Walker transported along the fiber: ${}^{(3)}\mathrm{D}_s \mathcal{J}_i = 0$. Here, $\bar{n}$ is the effective refractive index of the optical fiber (which depends on the optical frequency) and s is the arc length of γ.

A Mach–Zehnder interferometer can be constructed using two such optical fibers, γ_1 and γ_2, connecting two beam splitters, see Fig. 6.3. For simplicity, the present analysis assumes that if both inputs have the same polarization, then so do the outputs (trivial holonomy). In this case, the transfer coefficients u_{kij} can be computed without detailed knowledge of the wave-packet polarization and its transport along the fibers. In a more general setting, differences in polarization transport can contribute to the distinguishability of wave packets that traverse different optical fibers.

A simple model of such a Mach–Zehnder interferometer can then be constructed as follows: The two beam splitters at the interferometer input and output can be modeled as in Eq. (6.9). The delay of the wave-packets along the two fibers can be modeled using delay operators $\mathscr{D}_i$, acting as $(\mathscr{D}_i\psi)(t,s) = \psi(t - t_i^*, s - \ell_i)$, where t_i^* is computed according to Eq. (6.25) and ℓ_i denotes the length of the fiber γ_i. Denoting by $\mathscr{T}_{\text{in/out}}$ and $\mathscr{R}_{\text{in/out}}$ the transmission and reflection amplitudes of the two beam splitters, one obtains

$$A_{11}^{\text{out}} = \mathscr{T}_{\text{out}}\mathscr{D}_1\mathscr{T}_{\text{in}}A_1^{\text{in}} + \mathscr{R}_{\text{out}}\mathscr{D}_2\mathscr{R}_{\text{in}}A_1^{\text{in}}\,, \tag{6.26a}$$
$$A_{12}^{\text{out}} = \mathscr{T}_{\text{out}}\mathscr{D}_1\mathscr{R}_{\text{in}}A_2^{\text{in}} + \mathscr{R}_{\text{out}}\mathscr{D}_2\mathscr{T}_{\text{in}}A_2^{\text{in}}\,, \tag{6.26b}$$
$$A_{21}^{\text{out}} = \mathscr{R}_{\text{out}}\mathscr{D}_1\mathscr{T}_{\text{in}}A_1^{\text{in}} + \mathscr{T}_{\text{out}}\mathscr{D}_2\mathscr{R}_{\text{in}}A_1^{\text{in}}\,, \tag{6.26c}$$
$$A_{22}^{\text{out}} = \mathscr{R}_{\text{out}}\mathscr{D}_1\mathscr{R}_{\text{in}}A_2^{\text{in}} + \mathscr{T}_{\text{out}}\mathscr{D}_2\mathscr{T}_{\text{in}}A_2^{\text{in}}\,. \tag{6.26d}$$

For simplicity of exposition, the following calculations assume

$$\mathscr{T}_{\text{in/out}} = 1/\sqrt{2}\,, \qquad\qquad \mathscr{R}_{\text{in/out}} = i/\sqrt{2}\,, \tag{6.27}$$

such that

$$A_{11}^{\text{out}} = +\tfrac{1}{2}\mathscr{D}_1A_1^{\text{in}} - \tfrac{1}{2}\mathscr{D}_2A_1^{\text{in}}\,, \tag{6.28a}$$
$$A_{12}^{\text{out}} = +\tfrac{i}{2}\mathscr{D}_1A_2^{\text{in}} + \tfrac{i}{2}\mathscr{D}_2A_2^{\text{in}}\,, \tag{6.28b}$$
$$A_{21}^{\text{out}} = +\tfrac{i}{2}\mathscr{D}_1A_1^{\text{in}} + \tfrac{i}{2}\mathscr{D}_2A_1^{\text{in}}\,, \tag{6.28c}$$
$$A_{22}^{\text{out}} = -\tfrac{1}{2}\mathscr{D}_1A_2^{\text{in}} + \tfrac{1}{2}\mathscr{D}_2A_2^{\text{in}}\,. \tag{6.28d}$$

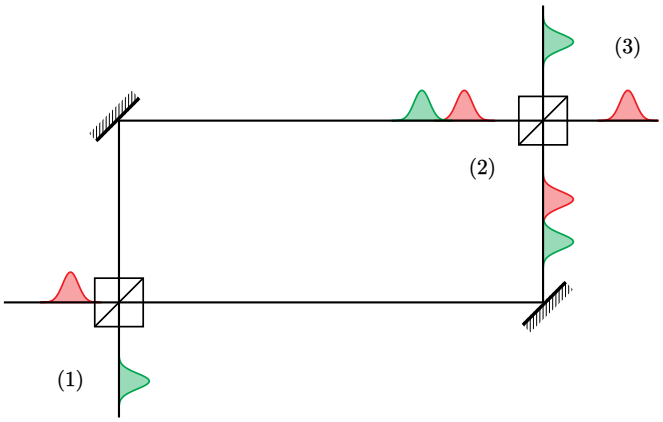

Figure 6.3: Schematic representation of two distinguishable wave packets traversing a Mach–Zehnder interferometer. A delay of incoming wave pulses (1) makes the inputs perfectly distinguishable. The wave packets are split at the first beam splitter, causing superpositions of wave packets to traverse the two interferometer arms (2). Interference at the second beam splitter causes the output probabilities to depend on the relative phase shifts arising from the two interferometer arms (3). For symmetric beam splitters and vanishing phase shifts, the wave packets produce definite outputs.

The transfer coefficients u_{kij} then take the form

$$(u_{1ij}) = \frac{1}{4}\begin{pmatrix} 2 - w_{11} - w_{11}^* & +i(w_{12} - w_{21}^*) \\ +i(w_{21} - w_{12}^*) & 2 + w_{22} + w_{22}^* \end{pmatrix}, \tag{6.29a}$$

$$(u_{2ij}) = \frac{1}{4}\begin{pmatrix} 2 + w_{11} + w_{11}^* & -i(w_{12} - w_{21}^*) \\ -i(w_{21} - w_{12}^*) & 2 - w_{22} - w_{22}^* \end{pmatrix}, \tag{6.29b}$$

where w_{ij} is the Klein–Gordon product

$$w_{ij} = (\mathscr{D}_1 A_i^{\mathrm{in}} \mid \mathscr{D}_2 A_j^{\mathrm{in}})\,. \tag{6.30}$$

In the particular case where both input profiles are equal, all w_{ij} coincide. For example, if both wave packets have the same spectral profile

$$\psi(\omega) = (2\pi\sigma^2)^{-1/4} \exp[-\tfrac{1}{4}(\omega - \omega_0)^2/\sigma^2]\,, \tag{6.31}$$

which describes a Gaussian frequency distribution of central frequency ω_0 and spectral width σ, one obtains

$$w_{ij} = e^{-i\omega_0 \Delta t} e^{-\sigma^2 \Delta t^2/2}\,, \tag{6.32}$$

where Δt is the difference in delays t_i^*:

$$\Delta t = t_1^* - t_2^*\,. \tag{6.33}$$

In this case, the transfer coefficients u_{kij} take the following form:

$$(u_{1ij}) = \frac{1}{2}\begin{pmatrix} 1 - e^{-\sigma^2\Delta t^2/2}\cos(\omega_0\Delta t) & -e^{-\sigma^2\Delta t^2/2}\sin(\omega_0\Delta t) \\ -e^{-\sigma^2\Delta t^2/2}\sin(\omega_0\Delta t) & 1 + e^{-\sigma^2\Delta t^2/2}\cos(\omega_0\Delta t) \end{pmatrix}, \tag{6.34}$$

$$(u_{2ij}) = \frac{1}{2}\begin{pmatrix} 1 + e^{-\sigma^2\Delta t^2/2}\cos(\omega_0\Delta t) & +e^{-\sigma^2\Delta t^2/2}\sin(\omega_0\Delta t) \\ +e^{-\sigma^2\Delta t^2/2}\sin(\omega_0\Delta t) & 1 - e^{-\sigma^2\Delta t^2/2}\cos(\omega_0\Delta t) \end{pmatrix}. \tag{6.35}$$

From Eqs. (6.17) to (6.19), one obtains the single-photon detection probabilities

$$p_{1,1} = p_{2,2} = \tfrac{1}{2}[1 - \mathscr{V}_1 \cos(\omega_0\Delta t)]\,, \tag{6.36a}$$

$$p_{1,2} = p_{2,1} = \tfrac{1}{2}[1 + \mathscr{V}_1 \cos(\omega_0\Delta t)]\,, \tag{6.36b}$$

where $\mathscr{V}_1$ is the visibility

$$\mathscr{V}_1 = \exp(-\tfrac{1}{2}\sigma^2\Delta t^2)\,. \tag{6.37}$$

In the limiting case of spectrally narrow wave packets, $\sigma^2\Delta t^2 \ll 1$, one obtains $\mathscr{V}_1 \approx 1$ and the resulting detection probabilities are fully determined by the phase shift associated with

the central frequency: $p_{1,1} \approx \sin^2(\omega_0 \Delta t/2)$. Alternatively, if $\sigma^2 \Delta t^2 \approx 1$, the interferometric visibility reduces to $\mathscr{V}_1 \approx 1/\sqrt{e} \approx 61\,\%$. Such a reduction in visibility can be understood intuitively as arising from a significant difference in arrival times at the second beam splitter, which renders the wave packets partially distinguishable. In the case where Δt arises from gravity, Ref. [2] argued the former case ($\sigma^2 \Delta t^2 \ll 1$) to be analogous to the Pound–Rebka experiment [10], whereas the latter case ($\sigma^2 \Delta t^2 \approx 1$) was interpreted as being analogous to the Shapiro delay experiment [202].

Additionally, Ref. [2] considered such single-photon experiments as clearly demonstrating signatures of general relativity and quantum theory simultaneously. However, as single-photon detection probabilities closely follow classical intensity distributions [203], one may consider multi-photon interferometry instead, as such experiments deviate from their classical counterparts more significantly.

For a two-photon input state, Eq. (6.20) yields the coincidence detection probability

$$p = \tfrac{1}{2}[1 + \mathscr{V}_2 \cos(2\omega_0 \Delta t)]\,, \tag{6.38}$$

with the visibility

$$\mathscr{V}_2 = \exp(-\sigma^2 \Delta t^2)\,. \tag{6.39}$$

Comparison with Eqs. (6.36) and (6.37) shows that such a two-photon interference experiment exhibits not only a doubled fringe frequency but also a squared visibility: $\mathscr{V}_2 = \mathscr{V}_1^2$. This non-classical behavior can be attributed to path-entangled two-photon NOON-states that are created at the first beam splitter and acquire a phase shift that is twice as large as for classical light or single-photon states [22], see also Fig. 1.1 on page 3.

Compared to the single-photon case, the two-photon experiment thus exhibits detection probabilities that differ strongly from the classical intensity distributions. Moreover, the doubled phase sensitivity makes it possible to detect delays Δt that would otherwise be too small to be measurable with single photons. Furthermore, such experiments are more sensitive to a reduction in visibility $\mathscr{V}$, as for $\sigma^2 \Delta t^2 \approx 1$ the one-photon visibility was found to be $\mathscr{V}_1 \approx 1/\sqrt{e} \approx 61\,\%$, whereas the two-photon visibility yields $\mathscr{V}_2 \approx 1/e \approx 37\,\%$.

Applications NOON-states are commonly used in quantum metrology since they allow for phase measurements at the Heisenberg limit [204]. For the present considerations, however, they can serve another purpose. If one wishes to design an experiment that shows, simultaneously, signatures of general relativity and quantum theory, one must demonstrate experimental outcomes that require both theories for their explanation and are thus not reproducible by either classical experiments in curved space-time or quantum experiments in flat space-time. In the present case, the gravitational redshift in optical fibers, described by the lapse ζ in the first term in Eq. (6.25) provides a characteristic signature of general relativity (or, more generally, of metric theories of gravitation) that is absent in Newtonian gravity due to the absence of a coupling between Maxwell's original

equations and the Newtonian potential φ. Likewise, the non-classical fringe frequency and visibility in Eqs. (6.38) and (6.39) are characteristic features of multi-photon quantum interference that cannot be reproduced using classical light sources.

Overall, by combining interferometric signatures of non-classical states of light with phase shifts that are absent in Newtonian gravity, one can construct experiments that demonstrate characteristic effects of quantum theory and general relativity simultaneously.

The next sections discuss such interferometer experiments where the phase shift arises from concrete non-inertial effects, namely the Sagnac effect and related phenomena (Section 6.4), as well as the gravitational redshift (Section 6.5).

6.4 Shift-Induced Delays: Rotation

The general formula for the optical delay given in Eq. (6.25) has two contributions: one describing the optical path length and one describing the Sagnac effect induced by the shift vector ξ_i. The latter contribution can be isolated by considering Sagnac interferometers, in which two light rays are brought to interference after traversing a given closed loop γ in opposite directions. Denoting by t_1^* and t_2^* the delays of these counter-propagating rays, one finds

$$t_1^* = \oint_\gamma n\zeta^{-1}\,\mathrm{d}s + \oint_\gamma \zeta^{-2}\xi\,, \qquad\qquad t_2^* = \oint_\gamma n\zeta^{-1}\,\mathrm{d}s - \oint_\gamma \zeta^{-2}\xi\,, \tag{6.40}$$

so that the time delay evaluates to

$$\Delta t = 2\oint_\gamma \zeta^{-2}\xi\,. \tag{6.41}$$

If γ is the boundary of a compact two-dimensional surface S (such that $\gamma = \partial S$), Stokes' theorem yields

$$\Delta t = 2\int_S \mathrm{d}(\zeta^{-2}\xi)\,. \tag{6.42}$$

Sagnac Phase Concrete expressions for the Sagnac delay Δt can be derived in Fermi coordinates (Section 2.5), for which one has

$$\zeta = 1 + a_i x^i + O(x^2)\,, \qquad\qquad \xi_i = \varepsilon_{ijk}\Omega^j x^k + O(x^2)\,, \tag{6.43}$$

where a_i and Ω^j denote the vectors of linear acceleration and rotation, respectively. Hence, one has $\zeta^{-2}\xi_i = \xi_i + O(x^2)$, and thus

$$\mathrm{d}(\zeta^{-2}\xi)_{ij} = 2\varepsilon_{ijk}\Omega^k + O(x)\,, \tag{6.44}$$

which implies the Sagnac formula

$$\Delta t \approx 4 \int_S \Omega^i \mathrm{d}S_i \,. \tag{6.45}$$

Previous derivations of this formula in curved space-time were restricted to ray optics [205; 206], and extensions to fiber optics were limited to fibers of special geometries in flat space-time [94; 207]. Equation (6.42) provides a general formula for arbitrarily shaped optical fibers in curved space-time (as derived from the fiber-optics calculation in Chapter 5, without using ray-optics methods) and Eq. (6.45) shows that the standard Sagnac formula is reproduced on sufficiently small scales.

Despite Eq. (6.45) being of the same form as the standard Sagnac delay known from ray-optics in special relativity [208; 209] the rotation vector Ω_i entering this formula does not coincide exactly with the angular velocity relative to stationary reference systems at large distances (if there are any). Indeed, by Eqs. (2.79) and (2.80), Ω_i contains relativistic corrections associated with time dilation, Thomas precession, the de Sitter effect, and the Lense–Thirring effect.

Experimental Tests Experimentally, the Sagnac effect in optical fibers is well tested both at the classical level, see, e.g., Refs. [210; 211] and references therein, and also at the single-photon level [212]. Experiments testing the Sagnac effect on pairs of entangled photons are currently ongoing at the University of Vienna [213]. Additionally, the GINGER project aims to build a Sagnac interferometer sensitive enough to resolve the sub-leading de Sitter and Lense–Thirring corrections to the Sagnac phase shift [214–216] that stem from the corresponding terms in the rotation vector Ω_i given by Eqs. (2.80c) and (2.80d).

Lense–Thirring Phase In Ref. [134] a thought experiment was considered, in which light is sent in a loop around a rotating massive object (see Ref. [217] for the assessment of an analogous setup involving massive particles instead of photons). Even though that paper considered light propagating in optical fibers, the derivation of the phase shift was carried out using a ray-optics model that did not take the optical properties of the fiber into account as the light ray was assumed to be null with respect to the space-time metric ${}^{(4)}g_{\mu\nu}$, and not with respect to Gordon's optical metric $\bar{g}_{\mu\nu}$. However, Eq. (6.42) shows that in Sagnac interferometers the time delay Δt is independent of the refractive index so that no corrections to the results of Ref. [134] arise. Indeed, to leading order in the multipole expansion of linearized gravity, the shift vector is given by $\xi_i = \frac{2}{r^3}\varepsilon_{ijk}x^j J^k$, where J_i is the total angular momentum, see Eqs. (2.54b) and (2.56). Comparing the phases of the light rays in the equatorial plane that are both emitted at the azimuthal angle $\phi = 0$ and reach $\phi = \pi$ via fibers that run clockwise or anti-clockwise around the central mass, respectively, one obtains the phase shift

$$\Delta\psi = 4\pi\omega J/r \,, \tag{6.46}$$

in agreement with Ref. [134, Eq. (4)]. Even though the calculations leading to the Lense–Thirring phase shift (6.46) are similar to those leading to the Sagnac phase shift (6.45), the physical effects underlying these phase shifts differ significantly: whereas the Sagnac effect arises from the rotation of the interferometer and can thus also occur in the absence of masses, the Lense–Thirring phase shift arises in a non-rotating interferometer and is caused by rotating mass distributions. As a consequence, the Sagnac phase shift increases with the radius of the fiber loop as r^2, whereas the Lense–Thirring phase decreases, for large distances, as $1/r$.

6.5 Lapse-Induced Delays: Redshift

Whereas the shift vector ξ_i in Eq. (6.25) gives rise to the Sagnac effect described above, the lapse ζ accounts for the redshift. To discuss the latter effect without the former, this section considers the case $\xi_i = 0$ (the overall result is the sum of these two contributions). In the absence of a shift vector, Eq. (6.25) yields the following result for the optical delay t_i^* along a curve γ_i:

$$t_i^* = \int_{\gamma_i} \frac{\bar{n}}{\zeta} \, \mathrm{d}s \,, \tag{6.47}$$

where $\bar{n}$ is the effective refractive index (which, in general, depends on the lapse ζ according to the calculations in Section 5.6, but can be regarded as a constant to a good level of approximation). As a consequence, the difference in delays arising from the two fibers γ_1 and γ_2, Δt, can be written as an integral along the closed loop $\gamma = \gamma_1 - \gamma_2$ obtained by joining γ_1 with the reversed curve $(-\gamma_2)$:

$$\Delta t = \oint_{\gamma} \frac{\bar{n}}{\zeta} \, \mathrm{d}s \,. \tag{6.48}$$

Such a relative delay can be measured, for example, in a Mach–Zehnder interferometer consisting of two fiber spools of equal length ℓ, separated vertically by a height difference h. If one approximates the integrals of $\bar{n}/\zeta$ along the fiber spools by $\bar{n}\ell/\zeta$ (thus neglecting inhomogeneities of the lapse across the fiber spools), and if the difference in delays arising from the vertical fiber segments is negligible compared to that arising from the fiber spools, one obtains

$$\Delta t \approx \bar{n}\ell \left[\frac{1}{\zeta(z_0)} - \frac{1}{\zeta(z_0 + h)} \right] = \frac{\bar{n}\ell}{\zeta(z_0)} \left[1 - \frac{\zeta(z_0)}{\zeta(z_0 + h)} \right] , \tag{6.49}$$

where z_0 denotes the altitude of the lower fiber spool.

For small-scale experiments, in which the Fermi coordinate system described in Sec-

tion 2.5 is a good model for the laboratory coordinate system, one has

$$\begin{aligned}\zeta &\approx 1 + \mathrm{g}_i x^i + \tfrac{1}{2}{}^{(4)}R_{titj}x^i x^j \\ &\approx 1 + \mathrm{g}z + \tfrac{1}{2}{}^{(4)}R_{tztz}z^2\,,\end{aligned} \tag{6.50}$$

provided that the gravitational field does not vary significantly across the horizontal extension of the experiment. The delay thus reduces to

$$\Delta t \approx \bar{n}\ell\left[\mathrm{g}h - (\mathrm{g}^2 - \tfrac{1}{2}{}^{(4)}R_{tztz})h^2\right]\,. \tag{6.51}$$

For an experiment taking place on Earth's surface, one has the following order-of-magnitude estimates (in geometric units):

$$\mathrm{g} \approx 10^{-16}\,\mathrm{m}^{-1}\,, \qquad \mathrm{g}^2 \approx 10^{-32}\,\mathrm{m}^{-2}\,, \qquad {}^{(4)}R_{tztz} \approx 10^{-23}\,\mathrm{m}^{-2}\,.$$

The dominant term is thus the one linear in gh, which describes the linearized gravitational redshift.

As a frequency shift, the gravitational redshift is well tested: it was first demonstrated by Pound and Rebka over a height difference of 22.5 m [10] and since then experiments have been developed that were able to measure the gravitational redshift at meter scales in 2010 [218] and at the millimeter scale in 2022 [219]. Additionally, larger-scale fiber-optic experiments over height differences of 450 m provide the current best Earth-based experimental test of the gravitational redshift, constraining the relative deviation from the theoretical prediction to $(1.4 \pm 9.1) \times 10^{-5}$ [220].

These frequency-shift experiments can be compared to experiments directly measuring the gravitationally induced phase shift given in Eq. (6.51). Such an experiment was first proposed by Tanaka in 1938 [47], but was hitherto not experimentally realizable. Extensions of such proposals to the single-photon level were made more recently in Refs. [2; 48] and are now considered experimentally viable in the currently planned GRAVITES experiment at the University of Vienna [4; 31].

As the setups described so far focused on the linear term in Eq. (6.51), they do not measure space-time curvature, which is encoded in the second-order term. Considering the term quadratic in h, the above estimates show that g^2 is negligible compared to the curvature term, leading to

$$\Delta t \approx n\ell\left[\mathrm{g}h + \tfrac{1}{2}{}^{(4)}R_{tztz}h^2\right]\,. \tag{6.52}$$

For a height difference of 450 m (as in Ref. [220]), the order-of-magnitude estimates given above show that the curvature correction is about four orders of magnitude below the linear term so that curvature corrections to the gravitational redshift in Earth-based interferometers might become experimentally accessible to frequency measurements in future experiments.

Satellite Experiments In addition to the small-scale experiments considered above, it is conceivable to test the gravitationally induced phase shift on light in space experiments by constructing a Mach–Zehnder interferometer with one fiber optic spool on Earth and another one on a satellite.

Compared to small-scale experiments, the main difference in the mathematical description of such large-scale experiments is that it is no longer possible to use the earthbound Fermi coordinate system described in Section 2.5. This is because for the gravitational potential $\varphi = -M/r$, the Taylor series around Earth's radius R converges only for altitudes in the range $h < R$.

If $\zeta_1 \approx 1/(1-\varphi_1)$ and $\zeta_2 \approx 1/(1-\varphi_2)$ denote the values of the lapse at ground level and at the satellite altitude, respectively, Eq. (6.49) yields

$$\Delta t \approx \bar{n}\ell(\varphi_2 - \varphi_1) = \frac{\bar{n}\ell M}{R}\left(1 - \frac{R}{R+h}\right) . \tag{6.53}$$

Whereas the altitude of low Earth orbit satellites (at 160 km to 2000 km) is below Earth's equatorial radius (about 6378 km), some medium Earth orbit satellites (between 2000 km and 35 786 km), geostationary orbits (at 35 786 km) and high Earth orbit satellites are at altitudes larger than Earth's radius. At such altitudes, a measurement of the gravitationally induced delay Δt would directly probe the $1/r$-dependence of the gravitational potential, as a linearization would not be mathematically meaningful. In this sense, measurements of Eq. (6.53) were argued as being sensitive to space-time curvature even though the Riemann tensor does not enter explicitly in the resulting phase shift [22]. However, in practice, the orbital motion of the satellite would also contribute to the phase shift, which requires adjustments to the experimental scheme to isolate the gravitational signal [35; 36; 221]. The details of such schemes, however, are beyond the scope of this document.

Chapter 7

Conclusion and Outlook

Even though quantum field theory in curved space-times is generally considered a well-established theory describing quantum fields in the presence of external classical gravitational fields, its direct application to setups as considered in experimental proposals for gravitational photon interferometry has been lacking. On the one hand, quantum-field theoretic descriptions of gravitationally induced phase shifts in single photons were restricted to light propagation in vacuo and hence do not apply to the proposed setups in which light is guided through optical fibers. On the other hand, previous assessments of the proposed experimental schemes that accounted for the guiding of light (either via ray-optics approximations or explicit fiber-optics calculations) relied on the assumption that, apart from the computed phase shifts, light propagation in a gravitational field can be described using the methods of quantum optics in flat space-time. It was the aim of the present thesis to close this gap by providing a comprehensive description of single-photon fiber interferometry in stationary gravitational fields that is based on the general framework of quantum field theory in curved space-times and takes into account the guiding of light by means of optical fibers.

7.1 Summary

The key points of the development of the theory of gravitational fiber optics described in this thesis can be summarized as follows:

- Chapter 3 introduced a new gauge condition for the electromagnetic potential A_μ in linear isotropic media (which may have arbitrary velocities and may be exposed to arbitrary gravitational fields) that generalizes the Lorenz gauge condition in such a way as to reduce the gauge-fixed field equations to a particularly simple form while simultaneously ensuring the field A_μ to be continuous even at material interfaces where the permittivity ε and the permeability μ are discontinuous.

- Chapter 4 provided a quantization of these newly developed gauge-fixed field equations for stationary configurations, in which the space-time metric ${}^{(4)}g_{\mu\nu}$ admits a timelike

Killing vector field $\mathcal{K}^\mu$, the four-velocity u^μ is proportional to $\mathcal{K}^\mu$, and both ε and μ are constant along the flow of $\mathcal{K}^\mu$. The quantization scheme used here, which is based on the Gupta–Bleuler method, relies on certain compatibility conditions of the field equations and the gauge choice: While it is trivial to construct solutions to the gauge-evolution equation from solutions to the gauge-fixed field equations, this formalism requires that solutions to the scalar gauge-evolution equation give rise to differential one-forms that satisfy the gauge-fixed equations. This is indeed the case for the gauge-choice introduced in Chapter 3, and Eq. (4.8) shows that this allows expressing the *scalar* Klein–Gordon product of the gauge function χ of a field configuration A in terms of the *full* Klein–Gordon product of A with another solution to the field equations. This non-trivial property makes possible the construction of the quantum gauge operator in Eq. (4.37), on which the Gupta–Bleuler quantization hinges. Additionally, it was found that a suitable quantum Hamiltonian can be derived from the Lagrangian via Noether's theorem even though there is no universally agreed-upon stress-energy-momentum tensor for electrodynamics in linear dielectrics (Abraham–Minkowski controversy).

- Chapter 5 developed a general perturbative solution to the gauge-fixed field equations for arbitrarily bent optical fibers in a stationary gravitational field. The underlying assumption of the perturbative scheme is that the optical wavelength of light propagating in the fiber is much shorter than the characteristic length scales of the functions describing variations in the fiber geometry or the space-time geometry along the fiber. Additionally, quadratic and higher-order corrections arising from the shift vector were assumed to be negligibly small. Both these assumptions are certainly satisfied in practical applications. Even though the solutions obtained here were derived using the gauge-fixed equations described above, the resulting fields satisfy Maxwell's equations (as they satisfy the gauge condition) and can thus be used in more general settings that do not rely on specific gauge choices.

- Finally, Chapter 6 provided a general formalism for describing gravitational fiber interferometry (in stationary space-times) at the single-photon level. The concrete predictions derived there demonstrate that the quantization scheme developed here, together with the explicit results on fiber optics in curved space-time, is indeed capable of describing general interferometry experiments testing quantum optics in non-inertial frames.

The description of gravitational photon interferometry developed here extends previous work on this subject in multiple aspects: the model is derived from the basic principles of quantum field theory in curved space-times, formulated within the algebraic approach to quantum field theory, provides a systematic perturbative scheme for describing fiber optics in a gravitational field, and has a wider range of applicability than previous models.

Basic Principles Previous descriptions of gravitational photon interferometry experiments at the quantum level generally fall within two classes: The first class comprises models that are based on the theory of quantum optics in *flat* space-time, with gravitational corrections added where found appropriate. The second class is formed by models that are based on the general framework of quantum field theory in *curved* space-times. However, these latter models did not describe the experimentally relevant setups of fiber optics in curved space-times but either described scalar or electromagnetic waves in vacuo. The present model does away with such simplifying assumptions as it describes gravitational fiber interferometry at the single photon level using the general principles of quantum field theory in curved space-times while simultaneously taking into account the full tensorial character of the electromagnetic field propagating in optical fibers.

Algebraic Approach Previous descriptions of gravitational photon interferometry within the framework of quantum field theory used mode-decomposition techniques in which the quantum field operator is expanded in a complete set of orthonormal modes. This entails that whenever single-mode excitations were considered, one had to ensure that complementary modes (which are typically not calculated explicitly) do not contribute to the observables under consideration [45]. The situation is significantly more transparent in the algebraic formulation of quantum field theory used here: the description of gravitational photon interferometry developed in Chapter 6 relies on a limited number of smeared field operators $\hat{\Phi}(A_i)$ and not on an infinite number of mode solutions.

Systematic Perturbative Scheme Hitherto-conducted calculations of gravitational effects in fiber optics relied on approximations in which the relevance or negligibility of various terms was determined "by inspection," i.e., by considering numerical estimates for representative scenarios. By contrast, the perturbative method developed here provides a more systematic approach as it is based on a Taylor expansion of the space-time metric in Fermi normal coordinates and a multiple-scales expansion of the electromagnetic field. When used in combination with the classification of the expansion coefficients given in Table 5.1, this allows for a structured computation of specific effects (such as phase or polarization perturbations) to arbitrary order in the perturbative expansion.

Range of Applicability Contrary to all previous models of gravitational photon interferometry, which were restricted to post-Newtonian gravitational fields, the model developed here is not restricted to the weak-field regime. Instead, the general methods developed here apply to arbitrary stationary gravitational fields. Moreover, the previously published calculations on fiber optics in curved space-times were limited to a small class of optical fiber geometries, namely straight fibers placed horizontally in a uniform gravitational field or infinitely-extended fiber spools whose symmetry axis lies horizontally in a uniform gravitational field [4; 48; 49]. The present model, instead, allows for arbitrary fiber geometries (provided that the fiber's radius of curvature far exceeds the optical wavelength, a condition

that is satisfied in all experimental setups proposed so far), regardless of the orientation of the fiber within the gravitational field.

7.2 Outlook

This thesis shows how the framework of quantum field theory in curved space-times can be used to describe experiments on single-photon interferometry in external gravitational fields. Even though the present model extends previous work in multiple aspects, several questions remain open. Some of them concern the technical details of theoretical models as considered here, while others concern the comparison with experiment and the general conclusions that can be drawn them.

- Whereas the fundamental modes of an optical fiber respond to the gravitational redshift by a mere phase shift, higher-order modes could be driven below their cutoff frequency. What is the behavior of the electromagnetic field in such circumstances and can such an effect be used to obtain more precise measurements of the redshift in optical fibers?

- In this document, optical fibers were modeled as lossless linear dielectrics. As optical attenuation is an important factor in concrete fiber-optics experiments, it would be interesting to extend the current model to include such effects. The issue here is that current models on attenuation and noise in optical fibers are non-relativistic and a coherent combination of such models with the present general-relativistic framework appears to be a non-trivial task.

- The explicit calculations in Chapter 5 are limited to step-index fibers. Is it possible to extend these results to other kinds of optical fibers, such as graded-index fibers or hollow-core fibers?

- How large are the corrections to fiber-optic modes arising from the various terms listed in Table 5.1 that have been neglected in the present calculations, and are they experimentally measurable?

- In Section 5.8 it was assumed that, in single-mode fibers, the modes of different frequency and angular mode index are formally orthogonal in the sense of Eq. (5.109). Can this be shown analytically, i.e., can one prove that the Klein–Gordon product of wave packets in single-mode fibers is given by Eq. (5.112)?

- How can the present analysis be extended to time-dependent settings? The calculations given in Chapter 5 can be adapted to slowly-varying space-time metrics using an adiabatic approximation. However, for time-dependent gravitational fields the quantization becomes more involved as there is no longer a preferred vacuum state. Although such ambiguities are not expected to produce drastically different

predictions in the considered setup, a mathematically sound analysis appears to be non-trivial.

- The present description of photon interferometry is based on a simplified model of photon detection. More realistic descriptions of such measurements can be obtained by modeling energy transfer from the electromagnetic field to absorbing materials such as superconducting nanowire single-photon detectors [222]. Such models thus require a quantum description of the stress-energy-momentum tensor. However, this tensor is known to have curvature-dependent renormalization ambiguities [158; 223]. How do these curvature ambiguities in the theoretical model affect the predictions for detection statistics, and can these ambiguities be resolved by an experiment?

- In the standard algebraic approach to quantum field theory, it is more common to smear quantum field operators via space-time integrals instead of using the symplectic smearing over Cauchy surfaces as was used here [160, Sect. 5.5]. For field equations with smooth coefficients, Eq. (4.9) provides an explicit translation between these two methods. However, in the considered case of discontinuous optical metrics, the existence of a Pauli–Jordan distribution Δ is not self-evident. Does a form of Eq. (4.9) hold in such setups? If not, this would suggest that there are two inequivalent quantization schemes for the considered setups that might produce different predictions in certain scenarios.

- In free quantum field theories, quantum states are typically required to satisfy the Hadamard criterion, which can be formulated as a restriction on the wave-front set of the two-point correlation function [224; 225]. In vacuo, this condition depends on the behavior of null geodesics in the space-time metric. Does this condition remain useful for the quantized electromagnetic field in media, or should it be generalized to take the optical metric into account? If so, what are the effects of discontinuities in the optical metric?

- The list of experimental setups considered in Chapter 6 is far from exhaustive. As the formalism developed here is structurally similar to that of quantum optics in flat space-time, descriptions of alternative experimental setups are expected to be simple to obtain. Indeed, the author hopes that the general considerations of this thesis will be found useful for planning and assessing future experiments on the interplay of quantum optics and general relativity.

The fact that some technical questions remain open does not impede the derivation of predictions for experiments. In particular, Chapter 6 derived concrete predictions for gravitationally induced interference of pairs of entangled photons – an effect that requires both quantum field theory and general relativity for its explanation. The GRAVITES project aims at measuring such effects in the coming years, thus providing the first direct experimental test of quantum field theory in curved space-times.

Appendix A

Properties of Lagrangian Field Theories

Let $\mathscr{M}$ be an oriented space-time manifold. Consider a Lagrangian $\mathbf{L}$, here regarded a differential form of top degree, that depends on a complex field ψ'_A (where A may refer to any index that need not be covariant), and a conjugate field ψ^*_A:

$$\mathbf{L} = \mathbf{L}[\psi^*, \psi'] \,. \tag{A.1}$$

In the following, $\delta\mathbf{L}[\psi^*, \psi'; \delta\psi^*, \delta\psi']$ will denote the variation of $\mathbf{L}$ at the configuration (ψ^*, ψ') along $(\delta\psi^*, \delta\psi')$. The general form of the variation $\delta\mathbf{L}$ is given by

$$\begin{aligned} \delta\mathbf{L}[\psi^*, \psi'; \delta\psi^*, \delta\psi'] = \delta\psi^*_A \mathbf{E}'^A + \delta\psi'_A \mathbf{E}^{*A} \\ + \mathrm{d}\{\delta\psi^*_A \boldsymbol{\Pi}'^A + \delta\psi'_A \boldsymbol{\Pi}^{*A}\} \,, \end{aligned} \tag{A.2}$$

where $\mathbf{E}^A$ and $\boldsymbol{\Pi}^A$ are the Eulerian and momentum forms, respectively [226].

A.1 Noether's Theorem

If ψ^* and ψ' satisfy the field equations, i.e., $\mathbf{E}^{*A} = \mathbf{E}'^A = 0$, and if, for some field variations $\delta\psi^*$ and $\delta\psi'$, the variation of the Lagrangian takes the form $\delta\mathbf{L} = \mathrm{d}\boldsymbol{\chi}[\psi^*, \psi']$, then the definition of the momenta implies that the form $\boldsymbol{\eta}$, defined as

$$\boldsymbol{\eta} = \delta\psi^*_A \boldsymbol{\Pi}'^A + \delta\psi'_A \boldsymbol{\Pi}^{*A} - \boldsymbol{\chi}[\psi^*, \psi'] \,, \tag{A.3}$$

is closed. If Ω is a space-time region bounded by Cauchy surfaces Σ_+ and Σ_- in the future and in the past, respectively, and if the fields decay sufficiently rapidly such that the integrals $\int_{\Sigma_\pm} \boldsymbol{\eta}$ are finite, Stokes' theorem implies

$$\int_{\Sigma_+} \boldsymbol{\eta} = \int_{\Sigma_-} \boldsymbol{\eta} \,. \tag{A.4}$$

Hence, the integral $\int_\Sigma \boldsymbol{\eta}$ is independent of the Cauchy surface used to evaluate it. In particular, if

$$\delta\psi^* = \mathfrak{L}_{\mathscr{K}}\psi^*\,, \qquad \delta\psi' = \mathfrak{L}_{\mathscr{K}}\psi'\,, \qquad \delta\mathbf{L} = \mathfrak{L}_{\mathscr{K}}\mathbf{L}\,, \tag{A.5}$$

for some vector field $\mathscr{K}$, then Cartan's formula implies $\delta\mathbf{L} = \mathrm{d}(\mathscr{K}\lrcorner\,\mathbf{L})$. In this case the above conservation law applies and the conserved quantity is known as the Noether charge

$$Q_{\mathscr{K}}[\psi^*,\psi'] = \int_\Sigma (\mathfrak{L}_{\mathscr{K}}\psi^*_A\boldsymbol{\Pi}'^A + \mathfrak{L}_{\mathscr{K}}\ \psi'_A\boldsymbol{\Pi}^{*A} - \mathscr{K}\lrcorner\,\mathbf{L}[\psi^*,\psi'])\,. \tag{A.6}$$

A.2 Symplectic Product

If the Lagrangian is bilinear (as is commonly the case for non-interacting theories), one has

$$\delta\mathbf{L}[0,\psi';\psi^*,0] = \delta\mathbf{L}[\psi^*,0;0,\psi']\,, \tag{A.7}$$

and thus

$$\psi^*_A\mathbf{E}'^A + \mathrm{d}(\psi^*_A\boldsymbol{\Pi}'^A) = \psi'_A\mathbf{E}^{*A} + \mathrm{d}(\psi'_A\boldsymbol{\Pi}^{*A})\,. \tag{A.8}$$

Now, if both ψ^* and ψ' satisfy the homogeneous field equations, $\mathbf{E}^* = \mathbf{E}' = 0$, one finds that $\psi^*_A\boldsymbol{\Pi}'^A - \psi'_A\boldsymbol{\Pi}^{*A}$ is closed. If, as before, Ω is a space-time region bounded by Cauchy surfaces Σ_+ and Σ_- in the future and in the past, respectively, and if the fields decay sufficiently rapidly such that the integrals $\int_{\Sigma_\pm}(\psi^*_A\boldsymbol{\Pi}'^A - \psi'_A\boldsymbol{\Pi}^{*A})$ are finite, Stokes' theorem implies

$$\int_{\Sigma_+}(\psi^*_A\boldsymbol{\Pi}'^A - \psi'_A\boldsymbol{\Pi}^{*A}) = \int_{\Sigma_-}(\psi^*_A\boldsymbol{\Pi}'^A - \psi'_A\boldsymbol{\Pi}^{*A})\,. \tag{A.9}$$

Hence, the symplectic product, defined as

$$\Omega(\psi^*,\psi') = \int_\Sigma (\psi^*_A\boldsymbol{\Pi}'^A - \psi'_A\boldsymbol{\Pi}^{*A})\,, \tag{A.10}$$

is independent of the Cauchy surface Σ used to evaluate the integral.

The conservation law for the symplectic product $\Omega(\psi^*,\psi')$ can also be derived from Noether's theorem if the Lagrangian is invariant under U(1)-transformations of the fields. Indeed, if $\mathbf{L}$ is invariant under the variations $\delta\psi^* = +i\psi^*$ and $\delta\psi' = -i\psi'$, then the associated Noether charge is $i\Omega(\psi^*,\psi')$.

If the manifold $\mathscr{M}$ is endowed with a volume form ${}^{(4)}\boldsymbol{\epsilon}$, which induces a volume form ${}^{(3)}\boldsymbol{\epsilon}$ on the Cauchy surface Σ, then the pull-back of $\boldsymbol{\Pi}^A[\psi]$ to Σ is necessarily proportional to ${}^{(3)}\boldsymbol{\epsilon}$ (as they are both forms of top degree on Σ) and can thus be expressed as $\Pi^A[\psi]\,{}^{(3)}\boldsymbol{\epsilon}$.

With this notation, the symplectic product can be written as

$$\Omega(\psi^*, \psi') = \int_\Sigma (\psi^*_A \Pi'^A - \psi'_A \Pi^{*A})^{(3)}\boldsymbol{\epsilon}\,. \tag{A.11}$$

The Klein–Gordon product is defined as

$$(\psi \mid \psi') = \frac{i}{\hbar}\Omega(\psi^*, \psi')\,, \tag{A.12}$$

which is dimensionless on account of the factor $1/\hbar$, sesquilinear (anti-linear in the first argument and linear in the second), and the factor i makes the Klein–Gordon product Hermitian in the sense that

$$(\varphi \mid \psi) = (\psi \mid \varphi)^*\,. \tag{A.13}$$

A.3 Pauli–Jordan Distribution

Another conclusion that can be drawn from Eq. (A.8) is the following: Let $\boldsymbol{j}^A$ be a differential form of top degree that is supported on a compact set K, and suppose that the inhomogeneous field equation

$$\mathbf{E}^A[\psi^\pm] + \boldsymbol{j}^A = 0 \tag{A.14}$$

admits a unique advanced solution ψ^-_A and a unique retarded solution ψ^+_A, such that ψ^-_A vanishes outside the causal past of K, whereas ψ^+_A vanishes outside the causal future of K. If ψ^* is a homogeneous solution, then Eq. (A.8) yields

$$\psi^*_A\, \boldsymbol{j}^A = \mathrm{d}(\psi^*_A \boldsymbol{\Pi}^{\pm A} - \psi^\pm_A \boldsymbol{\Pi}^{*A})\,. \tag{A.15}$$

If $\Sigma_\pm$ are Cauchy surfaces such that Σ_+ does not intersect the causal past of K and Σ_- does not intersect the causal future of K, one obtains

$$\int_{\mathscr{M}} \psi^*_A \boldsymbol{j}^A = +\int_{\Sigma_+} (\psi^*_A \boldsymbol{\Pi}^{+A} - \psi^+_A \boldsymbol{\Pi}^{*A}) = -\int_{\Sigma_-} (\psi^*_A \boldsymbol{\Pi}^{-A} - \psi^-_A \boldsymbol{\Pi}^{*A})\,. \tag{A.16}$$

The integrals are structurally similar to those arising in the symplectic product. However, the latter is defined for homogeneous solutions only, whereas $\psi^\pm$ are inhomogeneous solutions. Their difference, $\Delta = \psi^+ - \psi^-$, however, is a homogeneous solution, and is related to the inhomogeneity $\boldsymbol{j}^A$ via the Pauli–Jordan distribution (causal propagator) $\Delta = \Delta[j]$. The above formula then yields

$$\int_{\mathscr{M}} \psi^*_A\, \boldsymbol{j}^A = \Omega(\psi^*, \Delta[j])\,. \tag{A.17}$$

A.4 Schrödinger Equation

Let $\mathcal{K}$ be a symmetry vector field of a bilinear Lagrangian $\mathbf{L}[\psi^*, \psi']$ in the sense described in Appendix A.1, and define the Hamiltonian $\mathcal{H}$ by the formula

$$Q_{\mathcal{K}}[\psi^*, \psi'] = (\psi^* \mid \mathcal{H}\psi')\,, \tag{A.18}$$

where $Q_{\mathcal{K}}[\psi^*, \psi']$ is the conserved quantity defined in Eq. (A.6), and $(\cdot \mid \cdot)$ is the Klein–Gordon product defined in Eq. (A.12). If $(\cdot \mid \cdot)$ is non-degenerate, then the field equations imply that ψ satisfies the Schrödinger equation

$$i\hbar \pounds_{\mathcal{K}} \psi = \mathcal{H}\psi\,. \tag{A.19}$$

Indeed, by definition of the Klein–Gordon product, one has

$$\begin{aligned}(\psi \mid i\hbar \pounds_{\mathcal{K}} \psi') &= \int_\Sigma [(\pounds_{\mathcal{K}} \psi'_A)\mathbf{\Pi}^{*A} - \psi^*_A (\pounds_{\mathcal{K}} \mathbf{\Pi}'^A)] \\ &= \int_\Sigma [(\pounds_{\mathcal{K}} \psi'_A)\mathbf{\Pi}^{*A} + (\pounds_{\mathcal{K}} \psi^*_A)\mathbf{\Pi}'^A - \pounds_{\mathcal{K}}(\psi^*_A \mathbf{\Pi}'^A)]\,.\end{aligned} \tag{A.20}$$

Using Cartan's formula for the Lie derivative, one has

$$\int_\Sigma \pounds_{\mathcal{K}} (\psi^*_A \mathbf{\Pi}'^A) = \int_\Sigma \{\mathcal{K} \lrcorner\, \mathrm{d}(\psi^*_A \mathbf{\Pi}'^A) + \mathrm{d}[\mathcal{K} \lrcorner\, (\psi^*_A \mathbf{\Pi}'^A)]\}\,. \tag{A.21}$$

The last term vanishes under the assumption of suitable decay of the fields (or if the Cauchy surface is compact). Furthermore, for a bilinear Lagrangian $\mathbf{L}[\psi^*, \psi']$, one has

$$\mathrm{d}(\psi^*_A \mathbf{\Pi}'^A) = \mathbf{L}[\psi^*, \psi'] - \psi^* \mathbf{E}[\psi']\,, \tag{A.22}$$

so, by virtue of the Euler–Lagrange equations, one obtains

$$\begin{aligned}(\psi \mid i\hbar \pounds_{\mathcal{K}} \psi') &= \int_\Sigma \{(\pounds_{\mathcal{K}} \psi'_A)\mathbf{\Pi}^{*A} + (\pounds_{\mathcal{K}} \psi^*{}_A)\mathbf{\Pi}'^A - \mathcal{K} \lrcorner\, \mathbf{L}[\psi^*, \psi']\} \\ &= Q_{\mathcal{K}}[\psi^*, \psi'] = (\psi \mid \mathcal{H}\psi')\,,\end{aligned} \tag{A.23}$$

which is the "symplectically smeared" version of the Schrödinger equation. If $(\cdot \mid \cdot)$ is non-degenerate, this implies Eq. (A.19) for ψ'.

Bibliography

[1] L. Stodolsky. "Matter and light wave interferometry in gravitational fields". In: *General Relativity and Gravitation* 11.6 (Dec. 1979), pp. 391–405. DOI: 10.1007/BF00759302.

[2] M. Zych et al. "General relativistic effects in quantum interference of photons". In: *Classical and Quantum Gravity* 29.22, 224010 (Nov. 2012). DOI: 10.1088/0264-9381/29/22/224010. arXiv: 1206.0965 [quant-ph].

[3] S. Restuccia et al. "Photon Bunching in a Rotating Reference Frame". In: Phys. Rev. Lett. 123.11, 110401 (Sept. 2019). DOI: 10.1103/PhysRevLett.123.110401. arXiv: 1906.03400 [quant-ph].

[4] C. Hilweg. "Towards measuring gravitationally induced quantum interference with optical fiber interferometry". Doctoral thesis. University of Vienna, 2021. 245 pp. URN: urn:nbn:at:at-ubw:1-12944.02213.707923-6.

[5] A. J. Brady and S. Haldar. "Frame dragging and the Hong-Ou-Mandel dip: Gravitational effects in multiphoton interference". In: *Physical Review Research* 3.2, 023024 (Apr. 2021). DOI: 10.1103/PhysRevResearch.3.023024. arXiv: 2006.04221 [quant-ph].

[6] A. G. Klein. "Terrestrial gravity experiments with quantum objects". In: *Physica Scripta Volume T* 153, 014038 (Mar. 2013). DOI: 10.1088/0031-8949/2013/T153/014038.

[7] S. Pallister et al. "A blueprint for a simultaneous test of quantum mechanics and general relativity in a space-based quantum optics experiment". In: *EPJ Quantum Technology* 4.1 (2017), pp. 1–23.

[8] T. E. Cranshaw, J. P. Schiffer, and A. B. Whitehead. "Measurement of the Gravitational Red Shift Using the Mössbauer Effect in Fe^{57}". In: Phys. Rev. Lett. 4.4 (Feb. 1960), pp. 163–164. DOI: 10.1103/PhysRevLett.4.163.

[9] R. V. Pound and G. A. Rebka. "Gravitational Red-Shift in Nuclear Resonance". In: Phys. Rev. Lett. 3.9 (Nov. 1959), pp. 439–441. DOI: 10.1103/PhysRevLett.3.439.

[10] R. V. Pound and G. A. Rebka. "Apparent Weight of Photons". In: Phys. Rev. Lett. 4.7 (Apr. 1960), pp. 337–341. DOI: 10.1103/PhysRevLett.4.337.

[11] R. F. C. Vessot and M. W. Levine. “A test of the equivalence principle using a space-borne clock”. In: *General Relativity and Gravitation* 10.3 (Feb. 1979), pp. 181–204. DOI: 10.1007/BF00759854.

[12] R. F. C. Vessot et al. “Test of Relativistic Gravitation with a Space-Borne Hydrogen Maser”. In: Phys. Rev. Lett. 45.26 (Dec. 1980), pp. 2081–2084. DOI: 10.1103/PhysRevLett.45.2081.

[13] R. F. C. Vessot. “Clocks and spaceborne tests of relativistic gravitation”. In: *Advances in Space Research* 9.9 (Jan. 1989), pp. 21–28. DOI: 10.1016/0273-1177(89)90004-5.

[14] P. Delva et al. “Gravitational Redshift Test Using Eccentric Galileo Satellites”. In: Phys. Rev. Lett. 121.23, 231101 (Dec. 2018). DOI: 10.1103/PhysRevLett.121.231101. arXiv: 1812.03711 [gr-qc].

[15] R. Colella, A. W. Overhauser, and S. A. Werner. “Observation of Gravitationally Induced Quantum Interference”. In: Phys. Rev. Lett. 34.23 (June 1975), pp. 1472–1474. DOI: 10.1103/PhysRevLett.34.1472.

[16] G. M. Tino. “Testing gravity with cold atom interferometry: results and prospects”. In: *Quantum Science and Technology* 6.2, 024014 (Apr. 2021). DOI: 10.1088/2058-9565/abd83e. arXiv: 2009.01484 [gr-qc].

[17] M. A. Hohensee et al. “Force-Free Gravitational Redshift: Proposed Gravitational Aharonov-Bohm Experiment”. In: Phys. Rev. Lett. 108.23, 230404 (June 2012). DOI: 10.1103/PhysRevLett.108.230404. arXiv: 1109.4887 [quant-ph].

[18] A. Roura. “Gravitational Redshift in Quantum-Clock Interferometry”. In: *Physical Review X* 10.2, 021014 (Apr. 2020). DOI: 10.1103/PhysRevX.10.021014.

[19] D. Rideout et al. “Fundamental quantum optics experiments conceivable with satellites–reaching relativistic distances and velocities”. In: *Classical and Quantum Gravity* 29.22, 224011 (Nov. 2012). DOI: 10.1088/0264-9381/29/22/224011. arXiv: 1206.4949 [quant-ph].

[20] A. Brodutch et al. “Post-Newtonian gravitational effects in optical interferometry”. In: Phys. Rev. D 91.6, 064041 (Mar. 2015). DOI: 10.1103/PhysRevD.91.064041. arXiv: 1412.2440 [quant-ph].

[21] S. Y. Chen and T. C. Ralph. “Estimation of gravitational acceleration with quantum optical interferometers”. In: Phys. Rev. A 99.2, 023803 (Feb. 2019). DOI: 10.1103/PhysRevA.99.023803.

[22] T. B. Mieling, C. Hilweg, and P. Walther. “Measuring space-time curvature using maximally path-entangled quantum states”. In: Phys. Rev. A 106.3, L031701 (Sept. 2022). DOI: 10.1103/PhysRevA.106.L031701. arXiv: 2202.12562 [gr-qc].

[23] M. Zych et al. “Quantum interferometric visibility as a witness of general relativistic proper time”. In: *Nature Communications* 2, 505 (Oct. 2011). DOI: 10.1038/ncomms1498. arXiv: 1105.4531 [quant-ph].

[24] I. Pikovski et al. “Time dilation in quantum systems and decoherence”. In: *New Journal of Physics* 19.2, 025011 (Feb. 2017). DOI: 10.1088/1367-2630/aa5d92.

[25] S. Bose et al. “Spin Entanglement Witness for Quantum Gravity”. In: Phys. Rev. Lett. 119.24, 240401 (Dec. 2017). DOI: 10.1103/PhysRevLett.119.240401. arXiv: 1707.06050 [quant-ph].

[26] C. Marletto and V. Vedral. “Gravitationally Induced Entanglement between Two Massive Particles is Sufficient Evidence of Quantum Effects in Gravity”. In: Phys. Rev. Lett. 119.24, 240402 (Dec. 2017). DOI: 10.1103/PhysRevLett.119.240402. arXiv: 1707.06036 [quant-ph].

[27] M. Zych. *Quantum Systems Under Gravitational Time Dilation*. Springer Theses. Cham, CH: Springer International Publishing, 2017. 139 pp. ISBN: 978-3-319-53191-5. DOI: 10.1007/978-3-319-53192-2.

[28] A. Belenchia et al. “Quantum superposition of massive objects and the quantization of gravity”. In: Phys. Rev. D 98.12, 126009 (Dec. 2018). DOI: 10.1103/PhysRevD.98.126009. arXiv: 1807.07015 [quant-ph].

[29] A. Belenchia et al. “Information content of the gravitational field of a quantum superposition”. In: *International Journal of Modern Physics D* 28.14, 1943001-140 (Jan. 2019), pp. 1943001–140. DOI: 10.1142/S0218271819430016. arXiv: 1905.04496 [quant-ph].

[30] V. Fragkos, M. Kopp, and I. Pikovski. “On inference of quantization from gravitationally induced entanglement”. In: *AVS Quantum Science* 4.4, 045601 (Dec. 2022). DOI: 10.1116/5.0101334. arXiv: 2206.00558 [quant-ph].

[31] C. Hilweg et al. “Gravitationally induced phase shift on a single photon”. In: *New Journal of Physics* 19.3, 033028 (Mar. 2017). DOI: 10.1088/1367-2630/aa638f. arXiv: 1612.03612 [quant-ph].

[32] S. Manly and E. Page. “Experimental feasibility of measuring the gravitational redshift of light using dispersion in optical fibers”. In: Phys. Rev. D 63.6, 062003 (Mar. 2001). DOI: 10.1103/PhysRevD.63.062003. arXiv: gr-qc/0008004.

[33] J. Dressel et al. “Gravitational redshift and deflection of slow light”. In: Phys. Rev. A 79.1, 013834 (Jan. 2009). DOI: 10.1103/PhysRevA.79.013834. arXiv: 0810.4849 [physics.optics].

[34] F. Spengler et al. “Optical solitons in curved spacetime”. In: *Classical and Quantum Gravity* 40.14, 145008 (July 2023). DOI: 10.1088/1361-6382/acdd43. arXiv: 2301.04986 [gr-qc].

[35] D. R. Terno et al. “Proposal for an optical interferometric measurement of the gravitational redshift with satellite systems”. In: Phys. Rev. D 108.8, 084063 (Oct. 2023). DOI: 10.1103/PhysRevD.108.084063. arXiv: 1811.04835 [gr-qc].

[36] D. R. Terno et al. “Large-scale optical interferometry in general spacetimes”. In: Phys. Rev. D 101.10, 104052 (May 2020). DOI: 10.1103/PhysRevD.101.104052. arXiv: 1911.05156 [gr-qc].

[37] Q. Exirifard and E. Karimi. “Gravitational distortion on photon state at the vicinity of the Earth”. In: Phys. Rev. D 105.8, 084016 (Apr. 2022). DOI: 10.1103/PhysRevD.105.084016. arXiv: 2110.13990 [gr-qc].

[38] M. Rivera-Tapia, A. Delgado, and G. Rubilar. “Weak gravitational field effects on large-scale optical interferometric Bell tests”. In: *Classical and Quantum Gravity* 37.19, 195001 (Oct. 2020). DOI: 10.1088/1361-6382/ab8a60. arXiv: 1908.08179 [quant-ph].

[39] M. Rivera-Tapia et al. “Outperforming classical estimation of Post-Newtonian parameters of Earth’s gravitational field using quantum metrology”. Jan. 2021. arXiv: 2101.12126 [gr-qc].

[40] D. E. Bruschi et al. “Quantum estimation of the Schwarzschild spacetime parameters of the Earth”. In: Phys. Rev. D 90.12, 124001 (Dec. 2014). DOI: 10.1103/PhysRevD.90.124001. arXiv: 1409.0234 [quant-ph].

[41] D. E. Bruschi et al. “Spacetime effects on satellite-based quantum communications”. In: Phys. Rev. D 90.4, 045041 (Aug. 2014). DOI: 10.1103/PhysRevD.90.045041. arXiv: 1309.3088 [quant-ph].

[42] D. E. Bruschi et al. “Spacetime effects on wavepackets of coherent light”. In: Phys. Rev. D 104.8, 085015 (Oct. 2021). DOI: 10.1103/PhysRevD.104.085015. arXiv: 2106.12424 [quant-ph].

[43] R. Barzel et al. “Observer dependence of photon bunching: The influence of the relativistic redshift on Hong-Ou-Mandel interference”. In: Phys. Rev. D 105.10, 105016 (May 2022). DOI: 10.1103/PhysRevD.105.105016. arXiv: 2202.07950 [gr-qc].

[44] L. A. Alanís Rodríguez, A. W. Schell, and D. E. Bruschi. “Introduction to gravitational redshift of quantum photons propagating in curved spacetime”. In: *Journal of Physics Conference Series*. Vol. 2531. Journal of Physics Conference Series. June 2023, 012016. DOI: 10.1088/1742-6596/2531/1/012016. arXiv: 2303.17412 [quant-ph].

[45] D. E. Bruschi and A. W. Schell. “Gravitational Redshift Induces Quantum Interference”. In: *Annalen der Physik* 535.1 (Jan. 2023), p. 2200468. DOI: 10.1002/andp.202200468. arXiv: 2109.00728 [quant-ph].

[46] C. Anastopoulos and B.-L. Hu. “Relativistic Particle Motion and Quantum Optics in a Weak Gravitational Field”. June 2021. arXiv: 2106.12514 [quant-ph].

[47] K. Tanaka. “How to Detect the Gravitationally Induced Phase Shift of Electromagnetic Waves by Optical-Fiber Interferometry”. In: Phys. Rev. Lett. 51.5 (Aug. 1983), pp. 378–380. DOI: 10.1103/PhysRevLett.51.378.

[48] R. Beig et al. “Weakly gravitating isotropic waveguides”. In: *Classical and Quantum Gravity* 35.24, 244001 (Dec. 2018). DOI: 10.1088/1361-6382/aae873. arXiv: 1807.04156 [gr-qc].

[49] T. B. Mieling. “Gupta-Bleuler quantization of optical fibers in weak gravitational fields”. In: Phys. Rev. A 106.6, 063511 (Dec. 2022). DOI: 10.1103/PhysRevA.106.063511. arXiv: 2207.13537 [quant-ph].

[50] P. K. Schwartz and D. Giulini. “Post-Newtonian Hamiltonian description of an atom in a weak gravitational field”. In: Phys. Rev. A 100.5, 052116 (Nov. 2019). DOI: 10.1103/PhysRevA.100.052116. arXiv: 1908.06929 [quant-ph].

[51] L. B. Okun, K. G. Selivanov, and V. L. Telegdi. “On the interpretation of the redshift in a static gravitational field”. In: *American Journal of Physics* 68.2 (Feb. 2000), pp. 115–119. DOI: 10.1119/1.19382. arXiv: physics/9907017 [physics.ed-ph].

[52] W. Gordon. “Zur Lichtfortpflanzung nach der Relativitätstheorie”. In: *Annalen der Physik* 377.22 (Jan. 1923), pp. 421–456. DOI: 10.1002/andp.19233772202.

[53] C. M. Will. *Theory and Experiment in Gravitational Physics*. Second edition. Cambridge, UK: Cambridge University Press, 2018. 350 pp. ISBN: 978-1-107-11744-0. DOI: 10.1017/9781316338612.

[54] J. M. Lee. *Introduction to Smooth Manifolds*. Second Edition. Graduate Texts in Mathematics 218. New York, US-NY: Springer, 2013. 708 pp. ISBN: 978-1-4419-9981-8. DOI: 10.1007/978-1-4419-9982-5.

[55] D. Husemoller. *Fibre Bundles*. Third Edition. Graduate Texts in Mathematics 20. New York, US-NY: Springer, 1966. 353 pp. ISBN: 0-387-94087-1.

[56] C. J. Isham. *Modern Differential Geometry For Physicists*. Second Edition. World Scientific Lecture Notes in Physics 61. Singapore, SG: World Scientific Publishing, 2003. 290 pp. ISBN: 9810235550.

[57] T. t. Dieck. *Algebraic Topology*. EMS Textbooks in Mathematics. Zurich, CH: European Mathematical Society, 2008. 567 pp. ISBN: 978-3-03719-048-7.

[58] H. Friedrich and A. Rendall. “The Cauchy Problem for the Einstein Equations”. In: *Einstein’s Field Equations and Their Physical Implications*. Ed. by B. G. Schmidt. Vol. 540. 2000, p. 127. arXiv: gr-qc/0002074.

[59] P. T. Chruściel. “Cauchy problems for the Einstein equations: an Introduction”. 2018. URL: https://homepage.univie.ac.at/piotr.chrusciel/teaching/Cauchy/Roscoff.pdf (retrieved on 2023-08-29).

[60] J. M. Lee. *Introduction to Riemannian Manifolds*. Second Edition. Graduate Texts in Mathematics 176. Cham, CH: Springer, 2018. 437 pp. ISBN: 978-3-319-91754-2. DOI: 10.1007/978-3-319-91755-9.

[61] K. Gödel. “An Example of a New Type of Cosmological Solutions of Einstein’s Field Equations of Gravitation”. In: *Reviews of Modern Physics* 21.3 (July 1949), pp. 447–450. DOI: 10.1103/RevModPhys.21.447.

[62] E. Minguzzi. “Lorentzian causality theory”. In: *Living Reviews in Relativity* 22.1, 3 (June 2019). DOI: 10.1007/s41114-019-0019-x.

[63] A. N. Bernal and M. Sánchez. “On Smooth Cauchy Hypersurfaces and Geroch’s Splitting Theorem”. In: *Communications in Mathematical Physics* 243.3 (Jan. 2003), pp. 461–470. DOI: 10.1007/s00220-003-0982-6. arXiv: gr-qc/0306108 [gr-qc].

[64] E. Minguzzi and M. Sanchez. “The causal hierarchy of spacetimes”. In: *Recent developments in pseudo-Riemannian geometry*. Ed. by H. Baum and D. Alekseevsky. ESI Lectures in Mathematics and Physics. Zurich, CH: European Mathematical Society, 2008, pp. 299–35. ISBN: 978-3-03719-051-7. arXiv: gr-qc/0609119.

[65] S. W. Hawking and G. F. R. Ellis. *The large scale structure of space-time*. Cambridge monographs on mathematical physics. Cambridge, U.K.: Cambridge University Press, 1973. ISBN: 0-521-09906-4. DOI: 10.1017/CBO9780511524646.

[66] R. Geroch. “Domain of Dependence”. In: *Journal of Mathematical Physics* 11.2 (Feb. 1970), pp. 437–449. DOI: 10.1063/1.1665157.

[67] É. Gourgoulhon. *3+1 Formalism in General Relativity. Bases of Numerical Relativity*. Lecture Notes in Physics 846. Berlin, DE: Springer, 2012. 294 pp. ISBN: 978-3-642-24525-1. DOI: 10.1007/978-3-642-24525-1.

[68] R. Arnowitt, S. Deser, and C. W. Misner. “Dynamical Structure and Definition of Energy in General Relativity”. In: *Physical Review* 116.5 (Dec. 1959), pp. 1322–1330. DOI: 10.1103/PhysRev.116.1322.

[69] L. D. Landau and E. M. Lifshitz. *The Classical Theory of Fields*. Fourth Revised English Edition. Course of Theoretical Physics 2. Oxford, UK: Pergamon Press, 1975. 402 pp. ISBN: 0-08-018176-7.

[70] J. D. Brown. “Elasticity theory in general relativity”. In: *Classical and Quantum Gravity* 38.8, 085017 (Apr. 2021). DOI: 10.1088/1361-6382/abe1ff. arXiv: 2004.03641 [gr-qc].

[71] R. J. Epp, R. B. Mann, and P. L. McGrath. “Rigid motion revisited: rigid quasilocal frames”. In: *Classical and Quantum Gravity* 26.3, 035015 (Feb. 2009). DOI: 10.1088/0264-9381/26/3/035015. arXiv: 0810.0072 [gr-qc].

[72] E. Poisson. *A Relativist’s Toolkit. The Mathematics of Black-Hole Mechanics*. Cambridge, UK: Cambridge University Press, 2004. 233 pp. ISBN: 978-0-521-83091-1.

[73] T. W. Baumgarte and S. L. Shapiro. *Numerical Relativity. Solving Einstein’s Equations on the Computer*. Cambridge, UK: Cambridge University Press, 2010. 698 pp. ISBN: 978-0-521-51407-1.

[74] T. W. Baumgarte and S. L. Shapiro. *Numerical Relativity: Starting from Scratch.* Cambridge, UK: Cambridge University Press, 2021. 220 pp. ISBN: 978-1-108-84411-6. DOI: 10.1017/9781108933445.

[75] C. W. Misner, K. S. Thorne, and J. A. Wheeler. *Gravitation.* San Francisco, US-C: W. H. Freeman, 1973. 1279 pp. ISBN: 0-7167-0334-3.

[76] P. T. Chruściel. *Elements of General Relativity.* Compact Textbooks in Mathematics. Cham, CH: Birkhäuser, 2019. 283 pp. ISBN: 978-3-030-28415-2. DOI: 10.1007/978-3-030-28416-9.

[77] M. L. Ruggiero and A. Tartaglia. "Gravitomagnetic effects". In: *Nuovo Cimento B Serie* 117.7 (July 2002), p. 743. arXiv: gr-qc/0207065.

[78] P. C. C. Freire et al. "The relativistic pulsar-white dwarf binary PSR J1738+0333 - II. The most stringent test of scalar-tensor gravity". In: MNRAS 423.4 (July 2012), pp. 3328–3343. DOI: 10.1111/j.1365-2966.2012.21253.x. arXiv: 1205.1450 [astro-ph.GA].

[79] C. M. Will. "The Confrontation between General Relativity and Experiment". In: *Living Reviews in Relativity* 17.1, 4 (Dec. 2014). DOI: 10.12942/lrr-2014-4. arXiv: 1403.7377 [gr-qc].

[80] E. Fermi. "Sopra i fenomeni che avvengono in vicinanza di una linea oraria. Nota I". In: *Rend. Mat. Acc. Lincei* 31 (1922), pp. 21–23.

[81] F. K. Manasse and C. W. Misner. "Fermi Normal Coordinates and Some Basic Concepts in Differential Geometry". In: *Journal of Mathematical Physics* 4.6 (June 1963), pp. 735–745. DOI: 10.1063/1.1724316.

[82] W.-T. Ni and M. Zimmermann. "Inertial and gravitational effects in the proper reference frame of an accelerated, rotating observer". In: Phys. Rev. D 17.6 (Mar. 1978), pp. 1473–1476. DOI: 10.1103/PhysRevD.17.1473.

[83] W.-Q. Li and W.-T. Ni. "Coupled inertial and gravitational effects in the proper reference frame of an accelerated rotating observer." In: *Journal of Mathematical Physics* 20 (Jan. 1979), pp. 1473–1480. DOI: 10.1063/1.524203.

[84] A. I. Nesterov. "Riemann normal coordinates, Fermi reference system and the geodesic deviation equation". In: *Classical and Quantum Gravity* 16.2 (Feb. 1999), pp. 465–477. DOI: 10.1088/0264-9381/16/2/011. arXiv: gr-qc/0010096.

[85] P. Delva and J. Geršl. "Theoretical Tools for Relativistic Gravimetry, Gradiometry and Chronometric Geodesy and Application to a Parameterized Post-Newtonian Metric". In: *Universe* 3.1, 24 (Mar. 2017). DOI: 10.3390/universe3010024.

[86] S. Weinberg. *Gravitation and Cosmology. Principles and Applications of the General Theory of Relativity.* New York, US-NY: John Wiley & Sons, Inc., 1972. 657 pp. ISBN: 0-471-92567-5.

[87] I. Ciufolini and J. A. Wheeler. *Gravitation and Inertia*. Princeton Series in Physics. Princeton, US-NJ: Princeton University Press, 1995. 498 pp. ISBN: 0-691-03323-4.

[88] W. Rindler. *Relativity. Special, General and Cosmological*. Oxford, UK: Oxford University Press, 2001. 428 pp. ISBN: 0-19-850836-0.

[89] J. Kerr. "A new relation between electricity and light: Dielectrified media birefringent". In: *The London, Edinburgh, and Dublin Philosophical Magazine and Journal of Science* 50.332 (1875), pp. 337–348. DOI: 10.1080/14786447508641302.

[90] J. Xu et al. "Experimental Observation of Non-Linear Mode Conversion in Few-Mode Fiber". In: *CLEO: 2015*. Optica Publishing Group, 2015, SM2L.3. DOI: 10.1364/CLEO_SI.2015.SM2L.3.

[91] R. T. Thompson. "Covariant electrodynamics in linear media: Optical metric". In: Phys. Rev. D 97.6, 065001 (Mar. 2018). DOI: 10.1103/PhysRevD.97.065001. arXiv: 1712.06872 [gr-qc].

[92] R. M. Wald. *Advanced Classical Electromagnetism*. Princeton, US-NJ: Princeton University Press, 2022. 229 pp. ISBN: 978-W0-691-22039-0.

[93] J. D. Jackson. *Classical Electrodynamics*. Third Edition. Hoboken, US-NJ: John Wiley & Sons, Inc., 1999. 808 pp. ISBN: 0-471-30932-X.

[94] T. B. Mieling. "On the influence of Earth's rotation on light propagation in waveguides". In: *Classical and Quantum Gravity* 37.22, 225001 (Nov. 2020). DOI: 10.1088/1361-6382/ababb2. arXiv: 1911.12156 [physics.optics].

[95] T. B. Mieling, P. T. Chruściel, and S. Palenta. "The electromagnetic field in gravitational wave interferometers". In: *Classical and Quantum Gravity* 38.21, 215004 (Nov. 2021). DOI: 10.1088/1361-6382/ac2270. arXiv: 2107.07727 [gr-qc].

[96] T. B. Mieling. "The response of optical fibres to gravitational waves". In: *Classical and Quantum Gravity* 38.15, 155006 (Aug. 2021). DOI: 10.1088/1361-6382/ac0b2f. arXiv: 2103.05289 [gr-qc].

[97] R. M. Wald. *General Relativity*. Chicago Lectures in Physics. US-IL: The University of Chicago Press, 1984. 491 pp. ISBN: 0-226-87033-2.

[98] R. Loudon. *The Quantum Theory of Light*. Oxford, UK: Oxford University Press, 2000. 438 pp. ISBN: 0-19-850177-3.

[99] C. Gerry and P. Knight. *Introductory Quantum Optics*. Cambridge, UK: Cambridge University Press, 2005. 317 pp. ISBN: 0-521-82035-9.

[100] L. Mandel and E. Wolf. *Optical coherence and quantum optics*. Cambridge, UK: Cambridge University Press, 1995. 1166 pp. ISBN: 978-0521-41711-2.

[101] W. Greiner and J. Reinhardt. *Field Quantization*. Berlin, DE: Springer, 1996. 440 pp. ISBN: 3-540-59179-6.

[102] C. Itzykson and J.-B. Zuber. *Quantum Field Theory*. Mineola, US-NY: Dover, 1980. 705 pp. ISBN: 0-486-44568-2.

[103] R. Ferrari, L. E. Picasso, and F. Strocchi. "Some remarks on local operators in quantum electrodynamics". In: *Communications in Mathematical Physics* 35.1 (Mar. 1974), pp. 25–38. DOI: 10.1007/BF01646452.

[104] F. Strocchi and A. S. Wightman. "Proof of the charge superselection rule in local relativistic quantum field theory". In: *Journal of Mathematical Physics* 15.12 (Dec. 1974), pp. 2198–2224. DOI: 10.1063/1.1666601. Corrected in Ref. [105].

[105] F. Strocchi and A. S. Wightman. "Erratum: Proof of the charge superselection rule in local relativistic quantum field theory". In: *Journal of Mathematical Physics* 17.10 (Oct. 1976), pp. 1930–1931. DOI: 10.1063/1.522818.

[106] J. Mandrysch. "The necessity of indefinite metric Hilbert spaces in covariant gauge formulations of QED". MSc thesis. Ludwig-Maximilians-Universität München, Technische Universität München, May 2019. 85 pp. URL: https://www.theorie.physik.uni-muenchen.de/TMP/theses/thesismandrysch.pdf (retrieved on 2023-08-29).

[107] N. D. Birrell and P. C. W. Davies. *Quantum fields in curved space*. Cambridge monographs on mathematical physics. Cambridge, UK: Cambridge University Press, 1982. 340 pp. ISBN: 0-521-27858-9.

[108] J. M. Jauch and K. M. Watson. "Phenomenological Quantum-Electrodynamics". In: *Physical Review* 74.8 (Oct. 1948), pp. 950–957. DOI: 10.1103/PhysRev.74.950.

[109] J. M. Jauch and K. M. Watson. "Phenomenological Quantum Electrodynamics. Part II. Interaction of the Field with Charges". In: *Physical Review* 74.10 (Nov. 1948), pp. 1485–1493. DOI: 10.1103/PhysRev.74.1485.

[110] K. M. Watson and J. M. Jauch. "Phenomenological Quantum Electrodynamics. Part III. Dispersion". In: *Physical Review* 75.8 (Apr. 1949), pp. 1249–1261. DOI: 10.1103/PhysRev.75.1249.

[111] T. G. Philbin. "Canonical quantization of macroscopic electromagnetism". In: *New Journal of Physics* 12.12, 123008 (Dec. 2010). DOI: 10.1088/1367-2630/12/12/123008. arXiv: 1009.5005 [quant-ph].

[112] X.-M. Bei and Z.-Z. Liu. "Electromagnetic Field Quantization in Time-Dependent Dielectric Media". Apr. 2011. arXiv: 1104.2453 [quant-ph].

[113] P. Longo. "Waveguide Quantum Optics: A Wave-Function Based Approach". Doctoral thesis. Karlsruher Institut für Technologie (KIT), 2012. 179 pp. DOI: 10.5445/IR/1000029038. URN: urn:nbn:de:swb:90-290389.

[114] A. Strohmaier. "The Classical and Quantum Photon Field for Non-compact Manifolds with Boundary and in Possibly Inhomogeneous Media". In: *Communications in Mathematical Physics* 387.3 (Nov. 2021), pp. 1441–1489. DOI: 10.1007/s00220-021-04218-4. arXiv: 2011.12601 [math-ph].

[115] M. Born and E. Wolf. *Principles of Optics. Electromagnetic Theory of Light Propagation, Interference and Diffraction of Light.* Reprint of the sixth edition 1980 (with corrections). Oxford, UK: Pergamon Press, 1987. 808 pp.

[116] H. Poeverlein. "Sommerfeld-Runge Law in Three and Four Dimensions". In: *Physical Review* 128.2 (Oct. 1962), pp. 956–964. DOI: 10.1103/PhysRev.128.956.

[117] T. B. Mieling. "The response of laser interferometric gravitational wave detectors beyond the eikonal equation". In: *Classical and Quantum Gravity* 38.17, 175007 (Sept. 2021). DOI: 10.1088/1361-6382/ac15db. arXiv: 2103.03802 [gr-qc].

[118] J. Ehlers. "Zum Übergang von der Wellenoptik zur geometrischen Optik in der allgemeinen Relativitätstheorie". In: *Zeitschrift für Naturforschung A* 22.9 (Sept. 1967), pp. 1328–1332. DOI: 10.1515/zna-1967-0906.

[119] V. Perlick. *Ray Optics, Fermat's Principle, and Applications to General Relativity.* Lecture Notes in Physics m61. Berlin, DE: Springer, 2000, p. 220. ISBN: 3-540-66898-5.

[120] C. Barceló, S. Liberati, and M. Visser. "Analogue Gravity". In: *Living Reviews in Relativity* 14.1, 3 (May 2011). DOI: 10.12942/lrr-2011-3.

[121] J. B. Keller. "Rays, waves and asymptotics". In: *Bulletin of the American mathematical society* 84.5 (1978), pp. 727–750.

[122] H. Römer. *Theoretical Optics. An Introduction.* Weinheim, DE: Wiley-VCH, 2005. 361 pp. ISBN: 3-527-40429-5.

[123] N. A. Lopez. "Metaplectic geometrical optics". PhD thesis. Princeton, US-NJ: Princeton University, 2022. arXiv: 2210.03188 [physics.optics]. URL: https://arks.princeton.edu/ark:/88435/dsp01bc386n43w.

[124] J.-L. Joly, G. Metivier, and J. Rauch. "Generic rigorous asymptotic expansions for weakly nonlinear multidimensional oscillatory waves". In: *Duke Mathematical Journal* 70.2 (1993), pp. 373–404. DOI: 10.1215/S0012-7094-93-07007-X.

[125] M. Kline. "An asymptotic solution of Maxwell's equations". In: *Communications on Pure and Applied Mathematics* 4.2-3 (1951), pp. 225–262. DOI: 10.1002/cpa.3160040203.

[126] J. B. Keller, R. M. Lewis, and B. D. Seckler. "Asymptotic solution of some diffraction problems". In: *Communications on Pure and Applied Mathematics* 9.2 (1956), pp. 207–265. DOI: 10.1002/cpa.3160090205.

[127] Y. A. Kravtsov and Y. I. Orlov. *Geometrical Optics of Inhomogeneous Media.* Vol. 6. Springer Series on Wave Phenomena. Berlin, DE: Springer, 1990. 312 pp. ISBN: 3-540-51944-0.

[128] M. J. Hadamard. "Sur les problèmes aux dérivées partielles et leur signification physique". In: *Princeton University Bulletin* 13.4 (1902), pp. 49–52.

[129] N. J. Popławski. “A Michelson interferometer in the field of a plane gravitational wave”. In: *Journal of Mathematical Physics* 47.7 (July 2006), p. 072501. DOI: 10.1063/1.2212670. arXiv: gr-qc/0503066.

[130] M. Rakhmanov. “On the round-trip time for a photon propagating in the field of a plane gravitational wave”. In: *Classical and Quantum Gravity* 26.15, 155010 (Aug. 2009). DOI: 10.1088/0264-9381/26/15/155010. arXiv: 1407.5376 [gr-qc].

[131] L. S. Finn. “Response of interferometric gravitational wave detectors”. In: Phys. Rev. D 79.2, 022002 (Jan. 2009). DOI: 10.1103/PhysRevD.79.022002. arXiv: 0810.4529 [gr-qc].

[132] M. J. Koop and L. S. Finn. “Physical response of light-time gravitational wave detectors”. In: Phys. Rev. D 90.6, 062002 (Sept. 2014). DOI: 10.1103/PhysRevD.90.062002. arXiv: 1310.2871 [gr-qc].

[133] A. Błaut. “Gauge independent response of a laser interferometer to gravitational waves”. In: *Classical and Quantum Gravity* 36.5, 055004 (Mar. 2019). DOI: 10.1088/1361-6382/ab01ad. arXiv: 1901.09956 [gr-qc].

[134] S. P. Kish and T. C. Ralph. “Quantum effects in rotating reference frames”. In: *AVS Quantum Science* 4.1, 011401 (Mar. 2022). DOI: 10.1116/5.0073436. arXiv: 2202.05381 [quant-ph].

[135] A. Khrennikov et al. “Quantization of propagating modes in optical fibres”. In: Phys. Scr 85.6, 065404 (June 2012). DOI: 10.1088/0031-8949/85/06/065404.

[136] A. Khrennikov et al. “On the quantization of the electromagnetic field of a layered dielectric waveguide”. In: *Quantum Theory: Reconsideration of Foundations 6*. Ed. by A. Khrennikov et al. Vol. 1508. American Institute of Physics Conference Series. Dec. 2012, pp. 285–299. DOI: 10.1063/1.4773140.

[137] A. Folacci. “Quantum field theory of p-forms in curved space-time”. In: *Journal of Mathematical Physics* 32.10 (Oct. 1991), pp. 2813–2827. DOI: 10.1063/1.529072.

[138] E. P. Furlani. “Quantization of the electromagnetic field on static space-times”. In: *Journal of Mathematical Physics* 36.3 (Mar. 1995), pp. 1063–1079. DOI: 10.1063/1.531106.

[139] M. J. Pfenning. “Quantization of the Maxwell field in curved spacetimes of arbitrary dimension”. In: *Classical and Quantum Gravity* 26.13, 135017 (July 2009). DOI: 10.1088/0264-9381/26/13/135017. arXiv: 0902.4887 [math-ph].

[140] C. Dappiaggi and B. Lang. “Quantization of Maxwell’s Equations on Curved Backgrounds and General Local Covariance”. In: *Letters in Mathematical Physics* 101.3 (Sept. 2012), pp. 265–287. DOI: 10.1007/s11005-012-0571-8. arXiv: 1104.1374 [gr-qc].

[141] K. Sanders, C. Dappiaggi, and T.-P. Hack. “Electromagnetism, Local Covariance, the Aharonov-Bohm Effect and Gauss’ Law”. In: *Communications in Mathematical Physics* 328.2 (June 2014), pp. 625–667. DOI: 10.1007/s00220-014-1989-x. arXiv: 1211.6420 [math-ph].

[142] F. Finster and A. Strohmaier. “Gupta-Bleuler Quantization of the Maxwell Field in Globally Hyperbolic Space-Times”. In: *Annales Henri Poincaré* 16.8 (Aug. 2015), pp. 1837–1868. DOI: 10.1007/s00023-014-0363-z. arXiv: 1307.1632 [math-ph].

[143] I. Białynicki-Birula and Z. Białynicki-Birula. *Quantum Electrodynamics*. First English edition. International series of monographs in natural philosophy 70. Warsaw, PL: Pergamon Press Ltd. and PWN – Polish Scientific Publishers, 1975. 548 pp. ISBN: 978-0-08-017188-3. DOI: 10.1016/C2013-0-10071-2.

[144] W. Vogel and D.-G. Welsch. *Quantum Optics*. Third, revised and extended edition. Weinheim, DE: Wiley-VCH, 2006. 508 pp. ISBN: 978-3-527-40507-7.

[145] S. Weinberg. *The Quantum Theory of Fields*. Vol. I: Foundations. Cambridge, UK: Cambridge University Press, 2005. 440 pp. ISBN: 978-0-521-67053-1.

[146] S. N. Gupta. “Theory of Longitudinal Photons in Quantum Electrodynamics”. In: *Proceedings of the Physical Society A* 63.7 (July 1950), pp. 681–691. DOI: 10.1088/0370-1298/63/7/301.

[147] K. Bleuler. “Eine neue Methode zur Behandlung der longitudinalen und skalaren Photonen”. In: *Helv. Phys. Acta* 23 (1950), pp. 567–586.

[148] C. Bär. “Green-Hyperbolic Operators on Globally Hyperbolic Spacetimes”. In: *Communications in Mathematical Physics* 333.3 (Feb. 2015), pp. 1585–1615. DOI: 10.1007/s00220-014-2097-7. arXiv: 1310.0738 [math-ph].

[149] R. M. Wald. *Quantum Field Theory in Curved Spacetime and Black Hole Thermodynamics*. Chicago Lectures in Physics. US-IL: The University of Chicago Press, 1994. 205 pp. ISBN: 0-226-87025-1.

[150] A. Ashtekar and A. Magnon. “Quantum Fields in Curved Space-Times”. In: *Proceedings of the Royal Society of London Series A* 346.1646 (Nov. 1975), pp. 375–394. DOI: 10.1098/rspa.1975.0181.

[151] H. Minkowski. “Die Grundgleichungen für die elektromagnetischen Vorgänge in bewegten Körpern”. In: *Nachrichten von der Gesellschaft der Wissenschaften zu Göttingen, Mathematisch-Physikalische Klasse* (1908), pp. 53–111. URL: https://eudml.org/doc/58707.

[152] M. Abraham. “Zur Elektrodynamik bewegter Körper”. In: *Rend. Circ. Matem. Palermo* 28 (1909), pp. 1–28. DOI: 10.1007/BF03018208.

[153] R. N. C. Pfeifer et al. “Colloquium: Momentum of an electromagnetic wave in dielectric media”. In: *Reviews of Modern Physics* 79.4 (Oct. 2007), pp. 1197–1216. DOI: 10.1103/RevModPhys.79.1197. arXiv: 0710.0461 [physics.class-ph].

[154] E. C. G. Stueckelberg von Breidenach. “La signification du temps propre en mécanique ondulatoire”. In: *Helvetica physica acta* 14.5-6 (1941), pp. 322–323. URL: https://archive-ouverte.unige.ch//unige:162057.

[155] R. P. Feynman. “Space-Time Approach to Non-Relativistic Quantum Mechanics”. In: *Reviews of Modern Physics* 20.2 (Apr. 1948), pp. 367–387. DOI: 10.1103/RevModPhys.20.367.

[156] R. J. Glauber. *Quantum Theory of Optical Coherence*. Weinheim, DE: Wiley-VCH, 2007. 639 pp. ISBN: 978-3-527-40687-6.

[157] D. Fursaev and D. Vassilevich. *Operators, Geometry and Quanta: Methods of Spectral Geometry in Quantum Field Theory*. Theoretical and Mathematical Physics. Dordrecht, NL: Springer, 2011. 286 pp. ISBN: 978-94-007-0204-2. DOI: 10.1007/978-94-007-0205-9.

[158] S. Hollands and R. M. Wald. “Quantum fields in curved spacetime”. In: Phys. Rep. 574 (Apr. 2015), pp. 1–35. DOI: 10.1016/j.physrep.2015.02.001. arXiv: 1401.2026 [gr-qc].

[159] I. Khavkine and V. Moretti. “Algebraic QFT in Curved Spacetime and Quasifree Hadamard States: An Introduction”. In: *Advances in Algebraic Quantum Field Theory*. Ed. by R. Brunetti et al. Cham, CH: Springer International Publishing, 2015, pp. 191–251. ISBN: 978-3-319-21353-8. DOI: 10.1007/978-3-319-21353-8_5.

[160] B. Romeo and K. Fredenhagen. “Quantum Field Theory on Curved Backgrounds”. In: *Quantum Field Theory on Curved Spacetimes*. Bär, Christian and Fredenhagen, Klaus. Lecture Notes in Physics 786. Berlin, DE: Springer, 2009. Chap. 5, pp. 129–155. DOI: 10.1007/978-3-642-02780-2_5.

[161] S. A. Fulling. *Aspects of Quantum Field Theory in Curved Space-time*. Vol. 17. London Mathematical Society Student Texts. Cambridge, UK: Cambridge University Press, 1989. 315 pp. ISBN: 0-521-34400-X.

[162] R. Geroch. “An approach to quantization of general relativity”. In: *Annals of Physics* 62.2 (Feb. 1971), pp. 582–589. DOI: 10.1016/0003-4916(71)90104-7.

[163] V. B. Berestetskii, E. M. Lifshitz, and L. P. Pitaevskii. *Quantum Electrodynamics*. Second Edition. Course of Theoretical Physics 4. Oxford, UK: Butterworth-Heinemann, 1982. 652 pp. ISBN: 978-0-7506-3371-0.

[164] M. D. Schwartz. *Quantum Field Theory and the Standard Model*. Cambridge, UK: Cambridge University Press, 2014. 850 pp. ISBN: 978-1-107-03473-0.

[165] J. Paczos et al. “Quantum time dilation in a gravitational field”. Apr. 2022. arXiv: 2204.10609 [quant-ph].

[166] R. J. Glauber. “Coherent and Incoherent States of the Radiation Field”. In: *Physical Review* 131.6 (Sept. 1963), pp. 2766–2788. DOI: 10.1103/PhysRev.131.2766.

[167] W. O. Kermack and W. H. McCrea. “On Professor Whittaker’s solution of differential equations by definite integrals: Part II: Applications of the methods of non-commutative Algebra”. In: *Proceedings of the Edinburgh Mathematical Society* 2.4 (1931), pp. 220–239.

[168] V. L. Ginzburg and V. P. Frolov. “Excitation and emission of a ‘detector’ in accelerated motion in a vacuum or in uniform motion at a velocity above the velocity of light in a medium”. In: *Soviet Journal of Experimental and Theoretical Physics Letters* 43 (Mar. 1986), pp. 339–342.

[169] V. L. Ginzburg. “Radiation by uniformly moving sources (Vavilov-Cherenkov effect, transition radiation, and other phenomena)”. In: *Physics Uspekhi* 39.10 (Oct. 1996), pp. 973–982. DOI: 10.1070/PU1996v039n10ABEH000171.

[170] A. Svidzinsky et al. “Unruh and Cherenkov Radiation from a Negative Frequency Perspective”. In: Phys. Rev. Lett. 126.6, 063603 (Feb. 2021). DOI: 10.1103/PhysRevLett.126.063603.

[171] J.-M. Liu. *Photonic Devices*. Cambridge, UK: Cambridge University Press, 2005. 1028 pp. ISBN: 978-0-521-55195-3.

[172] C. C. Davis. *Lasers and Electro-optics*. Second edition. Cambridge, UK: Cambridge University Press, 2014. 830 pp. ISBN: 978-0-521-86029-1.

[173] T. B. Mieling and M. A. Oancea. “Polarization transport in optical fibers beyond Rytov’s law”. In: *Physical Review Research* 5.2, 023140 (May 2023). DOI: 10.1103/PhysRevResearch.5.023140. arXiv: 2302.10540 [physics.optics].

[174] C. M. Bender and S. A. Orszag. *Advanced mathematical methods for scientists and engineers*. New York, US-NY: McGraw-Hill, 1978. 593 pp. ISBN: 0-07-004452-X.

[175] A. H. Nayfeh. *Perturbation Methods*. Wernheim, DE: Wiley-VCH, 2004. 425 pp. ISBN: 978-0-471-39917-9.

[176] O. R. Asfar and A. H. Nayfeh. “The application of the method of multiple scales to wave propagation in periodic structures”. In: *Siam Review* 25.4 (1983), pp. 455–480.

[177] M. Janowicz. “Method of multiple scales in quantum optics”. In: Phys. Rep. 375.5 (Feb. 2003), pp. 327–410. DOI: 10.1016/S0370-1573(02)00551-3.

[178] M. Spivak. *A Comprehensive Introduction to Differential Geometry*. Third ed. Vol. 2. Houston, US-TX: Publish or Perish Inc., 1999. 361 pp. ISBN: 0-914098-71-3.

[179] J. Lafuente and B. Salvador. “From the Fermi-Walker to the Cartan connection”. In: *Proceedings of the 19th Winter School ‘Geometry and Physics’*. Palermo: Circolo Matematico di Palermo, 2000, pp. 149–156. URL: https://eudml.org/doc/221070.

[180] M.-Y. Lai et al. “Electromagnetic wave propagating along a space curve”. In: Phys. Rev. A 97.3, 033843 (Mar. 2018). DOI: 10.1103/PhysRevA.97.033843. arXiv: 1802.04059 [physics.optics].

[181] M.-Y. Lai et al. “Geometrical phase and Hall effect associated with the transverse spin of light”. In: Phys. Rev. A 100.3, 033825 (Sept. 2019). DOI: 10.1103/PhysRevA.100.033825.

[182] Y.-L. Wang et al. “Geometric effects resulting from square and circular confinements for a particle constrained to a space curve”. In: Phys. Rev. A 97.4, 042108 (Apr. 2018). DOI: 10.1103/PhysRevA.97.042108. arXiv: 1711.05453 [quant-ph].

[183] R. Ulrich, S. C. Rashleigh, and W. Eickhoff. “Bending-induced birefringence in single-mode fibers”. In: *Optics Letters* 5.6 (June 1980), pp. 273–275. DOI: 10.1364/OL.5.000273.

[184] H. F. Taylor. “Bending effects in optical fibers”. In: *Journal of Lightwave Technology* 2 (Oct. 1984), p. 617. DOI: 10.1109/JLT.1984.1073659.

[185] H. Renner. “Bending losses of coated single-mode fibers: a simple approach”. In: *Journal of Lightwave Technology* 10.5 (May 1992), pp. 544–551. DOI: 10.1109/50.136086.

[186] M. V. Berry. “Interpreting the anholonomy of coiled light”. In: Nature 326 (Mar. 1987), pp. 277–278. DOI: 10.1038/326277a0.

[187] K. Okamoto. *Fundamentals of Optical Waveguides*. Second edition. Burlington, US-MA: Academic Press, 2006. 561 pp. ISBN: 978-0-12-525096-2.

[188] D. Gloge. “Weakly guiding fibers”. In: Appl. Opt. 10.10 (Oct. 1971), pp. 2252–2258. DOI: 10.1364/AO.10.002252.

[189] S. Rytov. “On transition from wave to geometrical optics”. In: *Dokl. Akad. Nauk SSSR*. Vol. 18. 2. 1938, pp. 263–266.

[190] V. Vladimirskii. “The rotation of a polarization plane for curved light ray”. In: *Dokl. Akad. Nauk SSSR*. Vol. 21. 1941, pp. 222–225.

[191] S. I. Vinitskiĭ et al. “Topological phases in quantum mechanics and polarization optics”. In: *Soviet Physics Uspekhi* 33.6 (June 1990), pp. 403–428. DOI: 10.1070/PU1990v033n06ABEH002598.

[192] J. N. Ross. “The rotation of the polarization in low birefringence monomode optical fibres due to geometric effects”. In: *Optical and Quantum Electronics* 16 (Sept. 1984), pp. 455–461.

[193] A. Tomita and R. Y. Chiao. “Observation of Berry’s topological phase by use of an optical fiber”. In: Phys. Rev. Lett. 57.8 (Aug. 1986), pp. 937–940. DOI: 10.1103/PhysRevLett.57.937.

[194] Y. Inoue and K. Michihiro. “A Method of Multiple Scales for Integral Equations”. In: *Journal of the Physical Society of Japan* 50.2 (Feb. 1981), p. 681. DOI: 10.1143/JPSJ.50.681.

[195] L. A. Skinner. “Asymptotic evaluation of integrals involving multiple scales”. In: *Journal of Mathematical Analysis and Applications* 89.1 (1982), pp. 203–211.

[196] U. Leonhardt. "Quantum physics of simple optical instruments". In: *Reports on Progress in Physics* 66.7 (July 2003), pp. 1207–1249. DOI: 10.1088/0034-4885/66/7/203. arXiv: quant-ph/0305007.

[197] Z. Y. Ou and L. Mandel. "Derivation of reciprocity relations for a beam splitter from energy balance". In: *American Journal of Physics* 57.1 (Jan. 1989), pp. 66–67. DOI: 10.1119/1.15873.

[198] A. Zeilinger. "General properties of lossless beam splitters in interferometry". In: *American Journal of Physics* 49.9 (Sept. 1981), pp. 882–883. DOI: 10.1119/1.12387.

[199] H. Fearn and R. Loudon. "Quantum theory of the lossless beam splitter". In: *Optics Communications* 64.6 (Dec. 1987), pp. 485–490. DOI: 10.1016/0030-4018(87)90275-6.

[200] C. K. Hong, Z. Y. Ou, and L. Mandel. "Measurement of subpicosecond time intervals between two photons by interference". In: Phys. Rev. Lett. 59.18 (Nov. 1987), pp. 2044–2046. DOI: 10.1103/PhysRevLett.59.2044.

[201] M. Toroš et al. "Generation of Entanglement from Mechanical Rotation". In: Phys. Rev. Lett. 129.26, 260401 (Dec. 2022). DOI: 10.1103/PhysRevLett.129.260401. arXiv: 2207.14371 [quant-ph].

[202] I. I. Shapiro. "Fourth Test of General Relativity". In: Phys. Rev. Lett. 13.26 (Dec. 1964), pp. 789–791. DOI: 10.1103/PhysRevLett.13.789.

[203] S. M. Barnett. "On single-photon and classical interference". In: Phys. Scr 97.11, 114004 (Nov. 2022). DOI: 10.1088/1402-4896/ac971a. arXiv: 2207.14632 [quant-ph].

[204] H. Lee, P. Kok, and J. P. Dowling. "A quantum Rosetta stone for interferometry". In: *Journal of Modern Optics* 49.14 (Jan. 2002), pp. 2325–2338. DOI: 10.1080/09500340210000011536. arXiv: quant-ph/0202133.

[205] A. Ashtekar and A. Magnon. "The Sagnac effect in general relativity". In: *Journal of Mathematical Physics* 16.2 (Feb. 1975), pp. 341–344. DOI: 10.1063/1.522521.

[206] J. Frauendiener. "Notes on the Sagnac effect in general relativity". In: *General Relativity and Gravitation* 50.11, 147 (Nov. 2018). DOI: 10.1007/s10714-018-2470-5. arXiv: 1808.07914 [gr-qc].

[207] H. C. Lefevre and H. J. Arditty. "Electromagnétisme des milieux diélectriques linéaires en rotation et application à la propagtation d'ondes guidées". In: Appl. Opt. 21.8 (Apr. 1982), pp. 1400–1409. DOI: 10.1364/AO.21.001400.

[208] G. Sagnac. "L'éther lumineux démontré par l'effet du vent relatif d'éther dans un interféromètre en rotation uniforme". In: *CR Acad. Sci.* 157 (1913), pp. 708–710.

[209] E. J. Post. "Sagnac Effect". In: *Reviews of Modern Physics* 39.2 (Apr. 1967), pp. 475–493. DOI: 10.1103/RevModPhys.39.475.

[210] R. Anderson, H. R. Bilger, and G. E. Stedman. "'Sagnac' effect: A century of Earth-rotated interferometers". In: *American Journal of Physics* 62.11 (Nov. 1994), pp. 975–985. DOI: 10.1119/1.17656.

[211] B. Culshaw. “The optical fibre Sagnac interferometer: an overview of its principles and applications”. In: *Measurement Science and Technology* 17.1 (Jan. 2006), R1–R16. DOI: 10.1088/0957-0233/17/1/R01.

[212] G. Bertocchi et al. “Single-photon Sagnac interferometer”. In: *Journal of Physics B Atomic Molecular Physics* 39.5 (Mar. 2006), pp. 1011–1016. DOI: 10.1088/0953-4075/39/5/001. arXiv: 1312.7754 [quant-ph].

[213] R. Silvestri et al. “Probing Earth’s rotation effect on two-photon entanglement”. In: *Optica Quantum 2.0 Conference and Exhibition*. Optica Publishing Group, 2023, QM2B.1. URL: https://opg.optica.org/abstract.cfm?URI=QUANTUM-2023-QM2B.1.

[214] A. D. V. Di Virgilio et al. “GINGER: A feasibility study”. In: *European Physical Journal Plus* 132.4, 157 (Apr. 2017). DOI: 10.1140/epjp/i2017-11452-6.

[215] S. Capozziello et al. “Constraining theories of gravity by GINGER experiment”. In: *European Physical Journal Plus* 136.4, 394 (Apr. 2021). DOI: 10.1140/epjp/s13360-021-01373-4. arXiv: 2103.15135 [gr-qc].

[216] A. D. V. Di Virgilio. “Status of the GINGER project”. Mar. 2023. arXiv: 2303.12572 [gr-qc].

[217] Y. Bonder and J. E. Herrera-Flores. “Measuring Relativistic Dragging with Quantum Interference”. May 2019. arXiv: 1905.02275 [gr-qc].

[218] C. W. Chou et al. “Optical Clocks and Relativity”. In: *Science* 329.5999 (Sept. 2010), p. 1630. DOI: 10.1126/science.1192720.

[219] T. Bothwell et al. “Resolving the gravitational redshift across a millimetre-scale atomic sample”. In: Nature 602.7897 (Feb. 2022), pp. 420–424. DOI: 10.1038/s41586-021-04349-7. arXiv: 2109.12238 [physics.atom-ph].

[220] M. Takamoto et al. “Test of general relativity by a pair of transportable optical lattice clocks”. In: *Nature Photonics* 14.7 (Apr. 2020), pp. 411–415. DOI: 10.1038/s41566-020-0619-8.

[221] S. Pallister et al. “A blueprint for a simultaneous test of quantum mechanics and general relativity in a space-based quantum optics experiment”. In: *EPJ Quantum Technology* 4.1 (2017), pp. 1–23. DOI: 10.1140/epjqt/s40507-017-0055-y. arXiv: 1611.01327.

[222] C. M. Natarajan, M. G. Tanner, and R. H. Hadfield. “Superconducting nanowire single-photon detectors: physics and applications”. In: *Superconductor Science Technology* 25.6, 063001 (June 2012). DOI: 10.1088/0953-2048/25/6/063001. arXiv: 1204.5560 [quant-ph].

[223] S. Hollands and R. M. Wald. “Local Wick Polynomials and Time Ordered Products of Quantum Fields in Curved Spacetime”. In: *Communications in Mathematical Physics* 223.2 (Jan. 2001), pp. 289–326. DOI: 10.1007/s002200100540. arXiv: gr-qc/0103074 [gr-qc].

[224] A. Strohmaier, R. Verch, and M. Wollenberg. “Microlocal analysis of quantum fields on curved space-times: Analytic wave front sets and Reeh–Schlieder theorems”. In: *Journal of Mathematical Physics* 43.11 (Nov. 2002), pp. 5514–5530. DOI: 10.1063/1.1506381. arXiv: math-ph/0202003 [math-ph].

[225] C. J. Fewster and R. Verch. “The necessity of the Hadamard condition”. In: *Classical and Quantum Gravity* 30.23, 235027 (Dec. 2013). DOI: 10.1088/0264-9381/30/23/235027. arXiv: 1307.5242 [gr-qc].

[226] V. Iyer and R. M. Wald. “Some properties of the Noether charge and a proposal for dynamical black hole entropy”. In: Phys. Rev. D 50.2 (July 1994), pp. 846–864. DOI: 10.1103/PhysRevD.50.846. arXiv: gr-qc/9403028.

Units and Conventions

This text uses geometric Lorentz–Heaviside units, in which the gravitational constant, G, the speed of light in vacuo, c, the vacuum permittivity, ε_0, and the vacuum permeability, μ_0, are set to unity:

$$G = c = \varepsilon_0 = \mu_0 = 1\,.$$

In this system of units, one has the following numerical values:

Earth's mass	$4.435 \times 10^{-3}\,\mathrm{m}\,,$
Earth's radius	$6.371 \times 10^{6}\,\mathrm{m}\,,$
Earth's angular momentum	$1.452 \times 10^{-2}\,\mathrm{m}^2\,,$
Standard gravity	$1.091 \times 10^{-16}\,\mathrm{m}^{-1}\,,$
Eötvös	$1.113 \times 10^{-26}\,\mathrm{m}^{-2}\,,$
Reduced Planck constant	$2.612 \times 10^{-70}\,\mathrm{m}^2\,.$

The metric signature is $(-,+,+,+)$, so that the Minkowski metric has the form

$$\eta = -\mathrm{d}t^2 + \mathrm{d}x^2 + \mathrm{d}y^2 + \mathrm{d}z^2\,.$$

The conventions for the curvature of any metric $g_{\mu\nu}$ are

$$\begin{aligned}
\Gamma^{\mu}{}_{\nu\rho} &= \tfrac{1}{2} g^{\mu\sigma}(\partial_\nu g_{\rho\sigma} + \partial_\rho g_{\nu\sigma} - \partial_\sigma g_{\nu\rho})\,,\\
R^{\mu}{}_{\nu\rho\sigma} &= \partial_\rho \Gamma^{\mu}{}_{\nu\sigma} - \partial_\sigma \Gamma^{\mu}{}_{\nu\rho} + \Gamma^{\mu}{}_{\lambda\rho}\Gamma^{\lambda}{}_{\nu\sigma} - \Gamma^{\mu}{}_{\lambda\sigma}\Gamma^{\lambda}{}_{\nu\rho}\,,\\
R_{\mu\nu} &= R^{\rho}{}_{\mu\rho\nu}\,,
\end{aligned}$$

and the Einstein field equations in the absence of a cosmological constant are

$$R_{\mu\nu} - \tfrac{1}{2} R\, g_{\mu\nu} = 8\pi T_{\mu\nu}\,.$$

In the Misner–Thorne–Wheeler classification of sign conventions [75], this corresponds to the $(+,+,+)$-convention.

Notation

$\mathbf{N}$	Natural numbers
$\mathbf{Z}$	Integers
$\mathbf{R}$	Real numbers
$\mathbf{C}$	Complex numbers
∂	Partial differentiation
$[\![f]\!]$	Jump of a function f
c.c.	Complex conjugate of preceding term
H.c.	Hermitian conjugate of preceding term

Tensors and matrices

$X_{(\mu\nu)}$	Symmetric part of $X_{\mu\nu}$
$X_{[\mu\nu]}$	Antisymmetric part of $X_{\mu\nu}$
ε_{ijk}	Three-dimensional Levi-Civita symbol with $\varepsilon_{123} = 1$
$\varepsilon_{\mu\nu\rho\sigma}$	Four-dimensional Levi-Civita symbol with $\varepsilon_{0123} = 1$
A^{T}	Transpose of a matrix A
$A^{\dagger}$	Adjoint of a matrix A
$\operatorname{tr} A$	Trace of a matrix A
$\operatorname{adj} A$	Adjugate of a matrix A
diag	Diagonal matrix

Special functions

J_m	Bessel function of the 1st kind
Y_m	Bessel function of the 2nd kind
I_m	Modified Bessel function of the 1st kind
K_m	Modified Bessel function of the 2nd kind

Differential geometry

$\mathscr{M}$	Four-dimensional manifold
$\mathscr{S}$	Three-dimensional manifold
ι	Immersion
Γ_μ	Gauss map
Γ^μ	Unit normal
$\theta^\mu{}_i$	Soldering form
$\mathrm{T}\mathscr{S}$	Tangent bundle of $\mathscr{S}$
$\mathrm{N}\mathscr{S}$	Normal bundle of $\mathscr{S}$

Mathematical operations

f^*	Pull-back along a map f
$\lrcorner$	Interior product
$\wedge$	Exterior product
d	Exterior derivative
$\mathfrak{L}$	Lie derivative
exp	Exponential map
$\Box$	d'Alembertian
Δ	Laplacian

Lagrangian field theory

$\mathbf{L}$	Lagrangian four-form
$\mathbf{E}$	Eulerian four-form
$\mathbf{\Pi}$	Momentum three-form
$Q_{\mathscr{K}}[\cdot,\cdot]$	Noether charge associated to Killing field $\mathscr{K}$
$\Omega(\cdot,\cdot)$	Symplectic product
$(\cdot \mid \cdot)$	Klein–Gordon product
$\{\cdot \mid \cdot\}$	Ashtekar–Magnon product
$\mathscr{H}$	Classical Hamiltonian
Δ	Pauli–Jordan distribution

Matter

$T_{\mu\nu}$	Energy-momentum tensor
μ	Energy density
p_i	Momentum density
σ_{ij}	Stress tensor
M	Total mass
J_i	Total angular momentum

Linearized gravity

$\eta_{\mu\nu}$	Minkowski metric
$h_{\mu\nu}$	Linear metric perturbation
GR	General theory of relativity
PN	Post-Newtonian approximation
PPN	Parameterized Post-Newtonian theory
ε_{PPN}	PPN expansion coefficient
α_{PPN}	PPN parameter equal to 0 in GR
γ_{PPN}	PPN parameter equal to 1 in GR
φ	Gravitational potential
g_i	Gravitational acceleration

Geometry of space-time

${}^{(4)}g_{\mu\nu}$	Metric tensor
${}^{(4)}\nabla_\mu$	Levi-Civita derivative
${}^{(4)}\Gamma^\mu{}_{\nu\rho}$	Connection coefficients
${}^{(4)}R^\mu{}_{\nu\rho\sigma}$	Curvature tensor
${}^{(4)}\epsilon_{\mu\nu\rho\sigma}$	Volume form

Geometry of space

${}^{(3)}g_{ij}$	Metric tensor
${}^{(3)}\nabla_i$	Levi-Civita derivative
${}^{(3)}K_{ij}$	Extrinsic curvature
${}^{(3)}\Gamma^i{}_{jk}$	Connection coefficients
${}^{(3)}R^i{}_{jkl}$	Curvature tensor
${}^{(3)}\epsilon_{ijk}$	Volume form

Geometry of foliations

Σ	Cauchy surface
t	Time function
X^μ	Foliation vector
ζ	Lapse function
ξ^i	Shift vector

Geometry of timelike curves

t	Proper-time
u^μ	Four-velocity
a^μ	Four-acceleration
${}^{(4)}\mathrm{D}_t$	Fermi–Walker derivative
$\mathfrak{e}^\mu_\alpha$	Adapted tetrad
Ω^μ	Tetrad rotation vector
$\ell_{\mu\nu}$	Landau–Lifshitz Metric

Geometry of spatial curves

s	Arc length (short distance scale)
ς	Long distance scale
ε	Slowness parameter
T^i	Unit tangent vector
ν^i	Normal vector
N^i	Unit normal vector
B^i	Binormal vector
κ	Curvature
τ	Torsion
${}^{(3)}\mathrm{D}_s$	Fermi–Walker derivative

Electromagnetism

A_μ	Gauge potential
$F_{\mu\nu}$	Field strength
$G^{\mu\nu}$	Excitation
$\chi^{\mu\nu\rho\sigma}$	Constitutive tensor
ε	Permittivity
μ	Permeability
n	Refractive index
η	Wave impedance
$\tilde{g}_{\mu\nu}$	Optical metric
$\bar{g}_{\mu\nu}$	Gordon's optical metric
χ	Gauge function

Quantum field theory

$\mathfrak{A}$	Algebra of basic observables
$\hat{\Phi}(A')$	Quantized potential $\hat{A}$, symplectically smeared by A'
$\hat{\mathfrak{X}}(\chi')$	Quantized gauge function $\hat{\chi}$, symplectically smeared by χ'
$\hat{\Psi}(F')$	Quantized field $\hat{F}$, symplectically smeared by F'
$\hat{a}(\cdot)$	Annihilation operator
$\hat{a}^\dagger(\cdot)$	Creation operator
$\hat{\mathscr{H}}$	Quantum Hamiltonian
$\mathfrak{K}$	Krein space
$\mathfrak{H}$	Hilbert space
$\mathfrak{Z}$	Space of physical states
$\mathfrak{B}$	Space of gauge states
$\lvert 0\rangle$	Ground state
$\lvert \mathrm{coh}(\cdot)\rangle$	Coherent state
$\hat{D}(\cdot)$	Displacement operator
$\hat{q}$, $\hat{p}$	Quadrature operators

Ray optics

Ψ	Time-dependent eikonal
ψ	Time-independent eikonal
k_μ	Wave covector
K^μ	Wave vector
$\mathscr{A}$	Optical amplitude
$\mathscr{I}$	Optical intensity
$\mathscr{J}_{\mu\nu}$	Optical polarization

Fiber optics

n_1, n_2	Refractive indices in the core and cladding
$\bar{n}$	Effective refractive index
Δ	Index contrast
ω	Optical frequency
β	Propagation constant
m	Azimuthal mode index
$\varkappa$	Radial mode index
U, W	Normalized transverse wave numbers
V	Normalized frequency
b	Normalized guide index
$\mathscr{E}_i$	Transverse electric field
$\mathscr{J}_i$	Jones vector
$\mathfrak{e}_b$, $\mathfrak{e}^b$	Complex frame and co-frame
H_m	Helmholtz operator
G_m	Green operator

Interferometry

u_{kij}	Transfer coefficients
$\mathscr{T}$	Transmission amplitude
$\mathscr{R}$	Reflection amplitude
$\mathscr{D}$	Delay operator
t^*	Delay time
ψ	Spectral distribution
σ	Spectral width
$\mathscr{V}$	Visibility